EXPERIMENTAL INVESTIGATION OF EPOXY-BASED FOAM COMPOSITES FOR BUOYANCY APPLICATIONS

A thesis Submitted for the degree of
Doctor of Engineering

Durban University of Technology
Faculty of Engineering and the Built Environment
Mechanical Engineering

By

AYODELE ABRAHAM AJAYI

(22176175)

Supervisor: Prof. TP Mohan

Co-Supervisor: Prof. K. Kanny

DECLARATION

I hereby affirm that I am the sole author of this thesis. It has never been submitted for another degree, and it isn't being submitted concurrently for any other degrees.
When information from other sources was used, it was acknowledged. I additionally state that the sole portion of this work that has been published has been in peer-reviewed articles, and they are listed under "Publications."

Signature of candidate **Date**: ...17.02.2025.....

Signature of Supervisor **Date**: 21.2.2025

Signature of Co-Supervisor **Date**: 21/2/2025

ACKNOWLEDGEMENTS

First and foremost, I would like to appreciate God Almighty, the owner of my life, my sustainer, the creator of heaven and earth, my Lord for divine grace and enablement giving to me during this academic journey.

I will like to appreciate my supervisors Prof. TP Mohan and Prof. K Kanny for their much-valued supervision, help, patience, encouragement and guidance which made this research work a success. I sincerely appreciate your collaborative efforts which gave this work a sensible direction.

I wish to appreciate the Durban University of Technology for giving me scholarship through Research and Postgraduate support office. My appreciation also goes to the staff of the Mechanical Engineering Department for their support all through my study, my fellow CRG members (past and present), and postgraduate students: Dr. Olusegun, Dr. Ajay, Dr. John, Dr. Joseph, Jali, Sumeshan, Kimen, Edwin and Ene. I cannot forget in a hurry the support I received from you all.

My gratitude goes to Pastor and Pastor(Mrs) Adejimi, Pastor and Mrs Tope Obafemi for your prayers, spiritual supports and assistance.

I also appreciate friends and brothers like Adedeji Adedayo, Engr. Kayode Awolola, Engr. Odeyemi Deji, Engr. Olaoye Akinghehin, Lanrewaju Adedayo, Jeremiah Adedeji, Dr. Elutunji, Cyril Edijike, Dr. Naheem Adesina, Dr. Ayorinde. I equally appreciate the mentorship role of Prof. Oluleke Oluwole, I so much value all our discussions, your counsels and guidance during the course of this study.

My heartfelt gratitude goes to my parents and siblings, Elder and Dcns Samuel Ajayi, Bunmi Ajayi and Seun Ajayi, the Olajire family-Mr&Mrs Akinloye Olajire, and my brother and sister in-laws.

Finally, my in-depth and heartfelt gratitude goes my sweetheart and my lovely wife Omotola Ajayi and my children Treasure and Gloria. Thank you for your love and understanding. Thanks for standing by me and without your support this wouldn’t have been a success. I love you all.

DEDICATION

This research work is dedicated to my God Almighty for His sustaining grace and mercy over my life. I also dedicate this work to my parents Elder & Dcns. Samuel Ajayi for their belief in me.

PUBLICATIONS

Some publications have resulted from this study which are in the form of peer-reviewed journal articles.

DHET South Africa accredited journal papers published

1. **A A Ajayi**, M Turup Pandurangan and K Kanny. Influence of hybridizing fillers on mechanical properties of foam composite panel. Journal of polymer engineering science (2023), volume 63, Issue 8, pg 2565-2577 doi:10.1002/pen.26396

2. **A.A. Ajayi**, K. Kanny, M.T. Pandurangan, V. Ramachandran, Thermal and Wettability Properties of Nanoclay-Filled Epoxy-Based Foam Composite as Lightweight Material, Journal of Materials Performance and Characterization, 12 (2023) 293-306. https://doi.org/10.1520/MPC20230085
3. **A A Ajayi**, M Turup Pandurangan and K Kanny Development of Epoxy-based sandwich composite panel with Hollow glass microspheres/Clay hybrid core and banana fiber facesheet for structural applications. Journal of Heliyon https://doi.org/10.1016/j.heliyon.2024.e30428

DHET South Africa accredited journal paper under revision

A A Ajayi, K Kanny, M Turup Pandurangan. Effect of surface modification on mechanical properties of hollow glass microspheres(HGM)-filled epoxy foam composites. (SPE Polymer)

Book chapter Submitted

1 **A.A Ajayi,** M. Turup Pandurangan, K. Kanny Chapter title: Synthetic Nanoclay: Synthesis and Physico-chemical characterization. Book title: Functionalized Nanoclays: Fundamental and Industrial Applications, Elsevier. Editor: Dr. Chaudhery Mustansar Hussain

Journal paper under preparation

1 A.A Ajayi, M. Turup Pandurangan, K. Kanny Numerical modelling of Flexural and Tensile behavior of foam composite panels

Target Journal: World Journal of Engineering

ABSTRACT

Selection of appropriate materials for composite design is very crucial in critical engineering applications such as aerospace, marine and automobile industries. This study focused on developing lightweight hybrid-filled foam composite panels with enhanced mechanical and thermal properties. Hollow glass microspheres (HGM) and nanoclay were the fillers used in the foam core. The HGM content was varied from 1wt.% to 3wt.% in foam composites panel while nanoclay content was varied from 1wt.% to 5wt.% in each of the HGM-filled series of foam composites panel, these foam composite panels were fabricated using a conventional resin casting method. These hybrid-filled foam panels were also reinforced with banana fibres as facesheet in the sandwich composites. Comprehensive characterization was carried out on the foam composite panels, this involve investigating their physical properties. The results obtained showed that tensile and flexural strength improved by 12% and 23.1% respectively with the infusion of hybrid fillers content of 3%wt.HGM+1%wt.clay and 1%wt.HGM+1%wt.clay into the epoxy when compared to neat epoxy. Thermal strength was optimum with infusion of 1%wt.HGM+5%wt.clay into the epoxy while the buoyancy results revealed that the sample with 3%wt. hollow glass microspheres concentration has the highest buoyancy due to the low density of the HGM used which is 0.19 g/cm^3 and because sample 3%wt.HGM has the highest concentration of HGM with the respect to series of samples considered in this study. Similar trend of improvement in mechanical properties and physical properties was observed when the fabricated hybrid-filled foam panels was used as core in the sandwich composites developed which resulted to 22.11% and 29.53% improvement as flexural strength and tensile strength while there was 32.26% improvement in the impact energy. Also, there was 8.61% reduction in the water uptake. Furthermore, the tensile and flexural results was validated numerically by using finite element method and abaqus® 6.13 software and this revealed that most of the modelled samples are stronger than the experimental tested samples with up to 9% increase from experimental values obtained because of limitation in some parameter estimation of the numerical model such as the thermal properties, perfect contact and linear failure criteria.

Since the improvement in mechanical and thermal properties has been established, the composite panels developed are suitable for applications in manufacturing ship propellers. Future studies aims to improve the fire retardation of sandwich composites for marine applications.

TABLE OF CONTENTS

LIST OF TABLES

LIST OF FIGURES

GLOSARY AND ACRONYMS

ASTM	American Standard Test Method
CFC	ceramic foam composites
CMC	Ceramics Matrix Composites
CTE	Coefficient of Thermal Expansion
DGEBA	Diglycidyl Ether of Bisphenol-A
DMA	Dynamic Mechanical Analysis
DTA	Differential Thermal Analysis
EP	Epoxy Resin
FRPC	Fiber Reinforced Polymer Composites
Fb	Buoyancy force
SFC	Sandwich foam composites
HFFCC	Hybrid filled foam composite core
HGM	Hollow Glass Microspheres
PP-g- MA	Polypropylene grafted maleic anhydride
MMC	Metal Matrix Composites
MMT	montmorillonite
MSFC	Metallic-based Syntactic Foam Composites
NaOH	Sodium hydroxide
NSSFC	nano-synthesized syntactic foam composites
PPC	Particulate Polymer Composites
PET	Polyethylene Terephthalate
PFC	polymer foam composites
PMC	Polymer Matrix Composites
SFC	Sandwich Foam Composites
SEM	Scanning Electron Microscopy
PVC	Polyvinyl Chloride
TEM	Transmission Electron Microscopy
TGA	Thermo-Gravimetric Analysis
UTM	Universal testing machine
WCA	Water contact angles
Clay	Nanoclay

LIST OF NOTATIONS

T_g	Transition Temperature	(^{0}C)
Vc	Volume of composite	(cm^3)
ɕ	density of composites	(g/cm^3)
D	percentage of water absorbed	(%)
W(f)	maximum water measured	(%)
W(i)	Initial water measured	(%)
Fb	Buoyancy force	(N)
V	Volume of submerged object	(m^3)
D	Density of the fluid	(Kg/m^3)
Fo	Force of gravity	(N/kg)
E_M	Bending modulus of elasticity	(GPa)
R	Crosshead motion	(mm/min)
L	Support span	(mm)
d	Thickness of the panel	(mm)
D	Mid-span deflection	(mm)
σf	Flexural stress	(MPa)
r	Strain	mm/mm
Pc	Sandwich composite porosity	(%)
Ɛf	Flexural strain	(mm/mm)
P	Load	(N)
L	Mid span length	(mm)
b	Specimen width	(mm)
d	Specimen thickness	(mm)
D	Midpoint deflection	(mm/mm)
IS	Impact strength	(Kj/m^2)
AE	Absorbed energy	(J)
T	Specimen thickness	(m)
W	Remaining width at notch	(m)

CHAPTER 1

1.1 Introduction

This study focused on developing and enhancing the properties of foam composite cores with hybrid fillers for industrial applications where lightweight materials with good mechanical properties are required. The hybrid-filled foam cores were made using hollow glass microspheres and nanoclay particles. Also, the hybrid-filled foam core was reinforced with banana fiber as a facesheet. The current development of epoxy-based sandwich foam composites with enhanced thermal and mechanical properties is one of the priority research areas surrounding sandwich foam composites made with hybrid core and biodegradable materials as facesheet. The aim was to broaden the range of applications of hybrid-filled foam cores and sandwich foam composite panels with natural fiber facesheet to include high-performance usage which is previously dominated by synthetic fiber-reinforced foam composites.

The foam composites and sandwich foam composites reinforced with synthetic fibres are currently the most used for applications requiring lightweight, good thermal, and mechanical properties[1-5]. The substitution of synthetic fiber with natural fiber in sandwich foam composites and single filler with hybrid filler in the foam cores in these applications tackles several issues related to synthetic fiber-reinforced foam composites, including toughness, stiffness, high production costs, and end-of-life waste disposal.

1.2 Background of the Study

The development and design of syntactic foam composites and sandwich foam reinforced with synthetic fibers as replacements to steel structures was a great achievement as it brought about improvements such as lightweight, resistance to corrosive substances, and high strength-to-low weight ratio. Many foam composites are becoming increasingly common in today's sectors due to their mechanical and thermal properties[6, 7]. Various metallic-based foam composites (MFC), polymer foam composites (PFC)[8], ceramic foam composites (CFC), nano-synthesized syntactic foam composites (NSSFC)[9, 10], and hybridized foam composites (HFC), and fiber reinforced foam composite (FRFC) are gaining popularity in the market [11, 12]. They are used in buoyancy applications, marine applications, and automotive applications such as drive shafts, gears, instrument panels, leaf springs, and automobile body interior panels because of their strong

hydrostatic and hygroscopic strength, elevated stiffness at low density, and ability to absorb impact.[13, 14].

The production and processing of these foam composites, as well as sandwich foam composites reinforced with synthetic fibres, are expensive and energy-intensive. The inability of sandwich composites reinforced with synthetic fibers to biodegrade presents another significant issue, making it difficult to dispose of them after usage. Strong evidence indicates that synthetic fiber-reinforced sandwich composites, play a major role in the world's waste issue [15-20]. It has been discovered that suggested initiatives like recycling, landfilling, and incineration have their difficulties in the quest for answers to the problems with synthetic fiber-reinforced sandwich composites. These difficulties include the high costs of recycling, landfill taxes, and the release of greenhouse gases during incineration. In light of this, a sandwich panel with a hybrid core and a facesheet made of natural fiber is anticipated to address the issue of the scarcity of sustainable materials in the automotive industry, marine industries. This will be a suitable replacement for metallic materials due to its stiffness, toughness, strong acoustic resistance, and thermal stability[21-24], for instance the propeller of ship because hybrid filled sandwich composite propellers are increasingly used in smaller boats, yachts, and high-speed vessels. These materials provide the required strength while being lighter than metal propellers. For structural applications, a hybrid-filled foam core that serves as the sandwich panel's core and is characterized for its physical, mechanical, structural, morphological, buoyancy, and water absorption properties is one of the many outcomes this study hopes to achieve based on low weight and high strength materials.

Furthermore, these proposed initiatives exclusively address sandwich foam composite panels and hybrid-filled foam cores, ignoring other issues related to typical polymer composites reinforced with synthetic fibers. Developing sustainable solutions centered around fiber-reinforced composites is the fundamental philosophical realignment that is required. This suggested using biodegradable ingredients to create a sandwich foam composite panel with a bio-base structure.

1.3 Problem Statement

Yung etal.[25] has previously prepared HGM–filled epoxy composites, with filler content ranging from 0 to 51.3 vol.%, these were prepared in order to modify the dielectric properties of the epoxy. The results showed that the dielectric constant (D_k) and dielectric loss (D_f) of the composites decreased simultaneously with increasing HGM content, which was critical for the

provision of superior high-frequency device performance but little improvement was observed in the thermal strength and tensile strength of the composites[25]. Qiao etal.[26] conducted research on lightweight epoxy foams, which are crucial for reducing weight in a variety of industries, including high-speed rail, shipbuilding, aircraft, and aviation. Using a template and moulding technique, they created a new lightweight epoxy foam with a macro-sized hollow structure by arranging hollow glass microspheres/epoxy resin (HGMs/EP) hollow spheres as filler and EP as a matrix[26]. Metallic foam, polymeric foam and phenolic foam have been previously used to develop sandwich panel which resulted in high fuel consumption [27].Also, different core materials such as nomax honeycomb, kraft honeycomb and syntactic foam have been hybridized with glass fiber face-sheet to produce sandwich composite material[28].However, hybridizing banana fiber facesheet with hybrid core has not been studied. Owing to the drawbacks associated with the existing foams with HGM filler such as that has also been in use previously as sandwich foam composites' core materials with synthetic fiber facesheet in terms of stiffness, toughness, and capacity to mitigate the environmental harm caused by synthetic fibers recyclability, it was inevitable to develop a novel buoyant hybrid filled foam core material with natural fiber facesheet, which will be beneficial in structural applications and reasonably cost-effective and environmentally friendly. Because of this, a novel hybrid-filled foam core material was developed which combines high strength, low density, and lightweight to make it widely usable.

Materials used in literature to create sandwich composites filled with hybrid foam core include, but are not limited to epoxy resin, hardener, synthetic fiber, foam core, poly-vinyl chloride PVC foam (R55), and polyurethane (PU) foam cores. [29, 30], metallic foam, polymeric foam, phenolic foam[31] , and polymer foams (DIAB) [34], ceramic foam, agglomerated cork [32], honeycomb (aramid and cellulose) [33, 34], 3-D integrated core [35], polyethylene terephthalate, etc.

However, there are certain drawbacks to using these foams as sandwich composites, which are illustrated in Figure 1.1

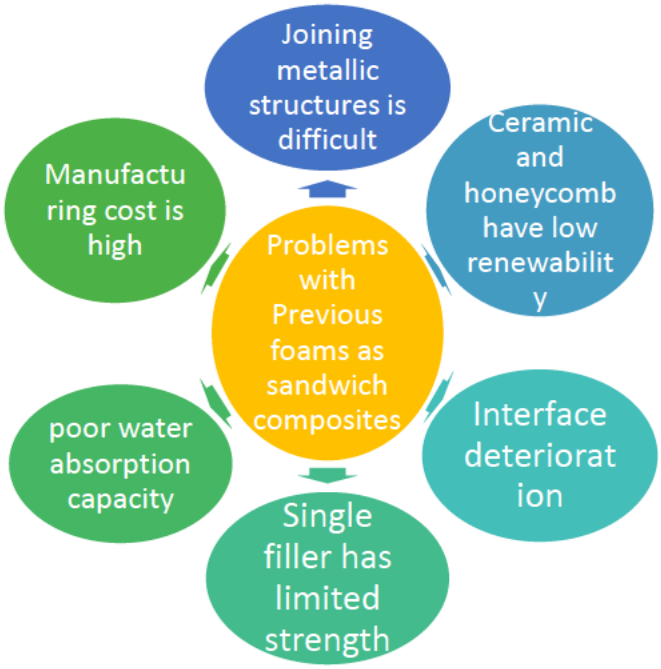

Figure 1.1: Problems with previous foam composites

1.4 Aim

- The goal of this research is to enhance the buoyancy and strengthen the sandwich panel using hollow glass microspheres and nanoclay as hybrid fillers in the foam core.

1.5 Objectives of the Study

1 To investigate the structural behavior of epoxy-based hybrid-filled foam composites using foam panels with different variations of HGM/Clay fillers

2 To fabricate/develop epoxy based sandwich composites panels with natural fiber (banana fiber) as facesheet

3 To conduct buoyancy test on the hybrid-filled epoxy-based sandwich foam panels developed

4 To simulate the epoxy-based foam cores developed

5 To validate the experimental tensile and flexural results with the numerical results of the foam composite panels

1.6 Assumptions

Data collection equipment, testing procedures, and instruments were pronounced valid and trustworthy based on their use and calibration time at the university and other institutions.

1.7 Scope of this Research

Although many natural fibers are available on the market, this study only used banana fiber since it is more readily available than other natural fibers at the time of this research effort. NaOH was used in this investigation to treat banana fibres despite the fact that many chemicals are used to surface treat natural plant fibres because. Additionally, because it can modify the chemical composition and enhance the interfacial interaction between the polymer matrix and natural fibres in composite materials[36-38]. This surface treatment can significantly enhance the mechanical and physical properties of the resulting composites. Although there were many different types of fillers in the market, only a hollow glass microsphere (HGM) and nanoclay were employed in this investigation.

1.8 Motivation

The growing global aviation and marine industries, coupled with the desire for lighter, more fuel-efficient aircraft, are driving the foam composites market's expansion. The manufacturing of more sophisticated materials and the launch of new goods by several significant aerospace industry players are what are fuelling the market's growth. There is a surge in growth in the aerospace foam market with the projection been displayed in Figure 1.2. It is growing increasingly as a result of advantageous government regulations in developing countries like China, India, and Brazil as well as a rise in bio-based foam composites in other parts of the world.

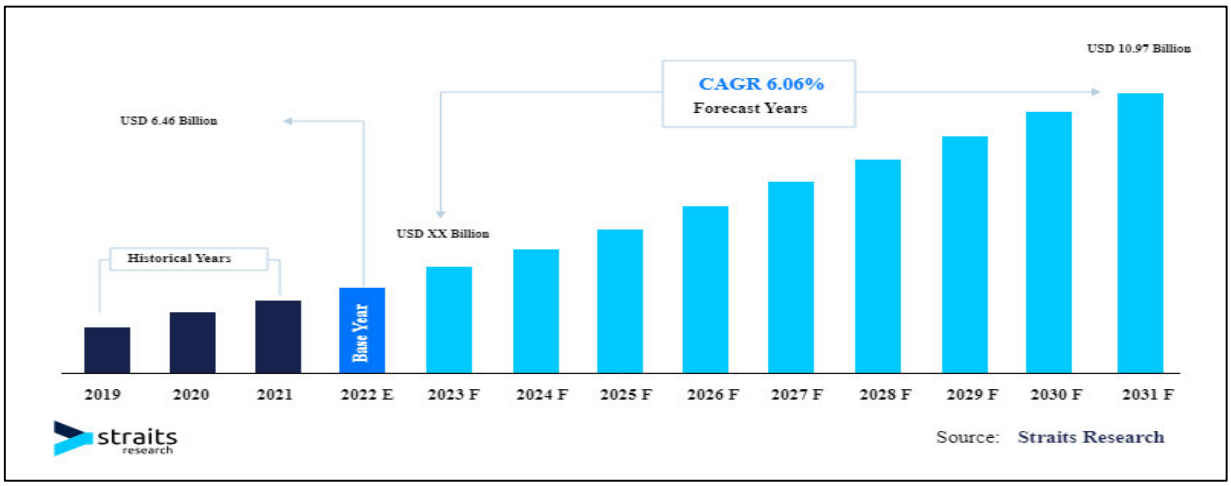

Figure 1.2: Foam composite market [39]

1.9 Justification

This research helps sustainability by developing partially biodegradable sandwich composites of low cost, light in weight, and made with a hybrid core. It also offers an industry for low-income countries whose people can begin producing natural fibers with little financial input. This research finding help in developing lightweight buoyant sandwich panels that are well-suited for marine and offshore applications and it also helps in enhancing the barrier properties of the sandwich panel by incorporating nanoclay as hybrid fillers in the foam core.

1.10 Contributions of the research work

This work contributes to the current body of knowledge in this field as follows;

• A unique hybrid-filled foam composite material was created for use in applications requiring low weight while maintaining high strength such as marine structures like propeller of ships. The material is distinctive and original due to the utilization of micron and nanoparticle materials such as HGM and nanoclay. The material is also unusual in that it is lightweight, and floats on water.

• Determines the optimal volume percent of hybrid fillers in foam cores intended for high-end applications.

• Establishes the theory behind the sandwich structure behavior of natural fiber-facesheet with hybrid core composites and their buoyancy response.

1.11 Structure of Thesis

This Thesis contains a total of nine (9) chapters, namely.

- Chapter One: This includes the introduction, background, problem statement, aim, objectives, assumptions, scope, justifications, contributions of the research work, and structure of the thesis
- Chapter Two: This includes a literature survey of composite materials, fiber-reinforced composites, foam composites, sandwich foam composites, fillers selected, Natural fibers, and modeling.
- Chapter Three: This includes the raw materials used in the study, the characterization methods used to determine mechanical, morphological, structural, and thermal

properties of hybrid filled foam composite core and sandwich foam composites, the step-by-step procedure of fabrication, mechanical testing conducted, and test configurations used method, and numerical response analysis method used in this study.

- Chapter Four: The influence of hybridizing fillers on the mechanical properties of foam composite panels is discussed in this chapter.
- Chapter Five: Thermal and Wettability Properties of Nanoclay-Filled Epoxy-Based Foam Composite as Lightweight Material are discussed in this chapter.
- Chapter Six: The development of an Epoxy-based sandwich composite panel with Hollow glass microspheres/Clay hybrid core and banana fiber facesheet for structural applications are discussed is this chapter.
- Chapter Seven: The effect of surface modification on mechanical properties of hollow glass microspheres (HGM)-filled epoxy foam composites is discussed in this chapter
- Chapter Eight: Modelling/Numerical Analysis was discussed in this chapter.
- Chapter Nine: This section is labeled general conclusions and recommendations, as well as future studies. The overall conclusion, recommendations, and proposals for future work are gathered from the full set of experiments, results observation, and discussion of future study directions.

CHAPTER 2

2.1 Introduction

The literature review covered topics such as composite materials, foam composite material kinds, qualities, and applications; sandwich foam composites, fiber-reinforced composites, natural fibers. Additionally, reviewed are hybrid-filled foam composite materials as well as various fillers that have been used in composite materials in the past. Also, modeling and different software packages that have been used for modeling in the past. The literature review provided a thorough grasp of the topic and indicated areas in need of further investigation.

2.2 Composite materials

Literature defines a composite in terms of a minimum of two distinctive phases or constituents in a material [40-44]. Hybrid composites result when at least two reinforcing materials are used [41, 45, 46]. The usage of composites is primarily driven by three factors: reduced weight, corrosion resistance, and part count [41]. Because of the low density of the polymers employed as matrices and reinforcing fillers, composites are lightweight materials. In the industrial sector, composites are very desirable and are replacing traditional materials like steel [41, 47]. Reducing the number of parts in an assembly, manufacturing, or inventory often results in savings that offset higher material costs [41, 47]. The primary criteria used to categorize composite materials are reinforcement, laminate configuration, and hybrid structure [41]. Unlike heterogeneous materials, which are composed of two microscopic elements with discrete phases and continuous or non-continuous layers, composite materials are composed of stronger fibers encircled by a weaker matrix substance. They are made up of at least two different components that work together to give a material certain properties that set it apart from its component parts [48]. In practical terms, the majority of composites are made up of a bulk substance called a matrix and some sort of reinforcement to increase the matrix's strength and stiffness; the reinforcement is typically in the form of fibers. Kamal [49] claims that because of their excellent corrosion resistance, light weight, flexibility, impact strength, fatigue strength, and other properties, composite materials are either being used or being researched as a potential replacement for metals and traditional materials in the aerospace, automotive, civil, mechanical, and other industries. Because of their excellent performance, composite materials are highly sought-after because of their high strength, high specific stiffness, and controlled anisotropy.

The special quality of composites is their capacity to carefully evaluate the matrix and filler to customize the final product towards a specific technical purpose. These qualities enable them to be beneficial for various applications [49].

2.2.1 Advantages of Composites

Composite materials can be used in many different ways and constructions because they can be made to meet certain functional requirements, such as the ones listed below [49] :

1. Aerospace and Aircraft: The aerospace industry makes considerable use of composite materials in the construction of several parts for satellites, gliders, galleys, trolleys, enclosures, ground support equipment, and containers, among other things.
2. Engineering: In engineering and business, composite materials are used for many different things. Some of these applications include fittings and assemblies, different enclosures, trays, bins, safety helmets, pallets, medical supplies, and equipment components.
3. Defense: Composite materials are used by the military industry to create a variety of products, including simulators, allied devices, rocketry and ballistics items, enclosures and containers, pipes and ducts, armor for soldiers, and shipping and transit containers.
4. Infrastructures: Composite materials are used to construct more durable infrastructure. These days, a broad range of infrastructure applications employ unique fiber-reinforced composite designs.
5. Electrical and Electronic Applications: Applications for electromagnetic composites include distribution posts and pylons, power poles, fuse tubes, ladders, cableways, transformer elements, insulators, circuit boards, generating and transmission parts, fittings and internal and exterior aerial parts.
6. Transportation: Composite materials are formed into engine and body panels for trucks, cars, buses, campers, and other vehicles, as well as various elements and components of vehicles; sea and land containers; railroad tracks and signals; traffic signs; seating; window coverings; and partitions, among other things.
7. Sports: Composite materials offer cutting-edge materials for both commercial modes of operation and the sports goods industry. Among other sporting products, composite materials are used to produce fishing rods, golf clubs, hockey sticks, bicycle supports, baseball bats, and marine hulls.

8. Maritime Applications: Composite materials find great use in window masks, buoys, boat accessories, subassemblies, and interior moldings and fittings for trawlers, workboats, ferries, and cruise ships, among other marine gear.
9. Building and Construction: Composite materials function better than wood or boards when it comes to making external and interior cladding, shutters, permanent and temporary formworks, ornamental and structural construction elements, fencing, walkways, etc.

2.2.2 Disadvantages of Composites

Although composite materials have many benefits, they also have certain inevitable drawbacks, some of which include [49]:

1. Manufacturing difficulties: The cost of producing high-quality composites increases when composite materials are made because of the technology involved.
2. The cost of producing consumer goods at competitive prices is significant. For example, producing general-purpose goods is not practical in the automobile and aerospace industries due to the high expense of operating machinery, tools, and other overhead.
3. There are limited, and often hard to assess, sources about the material economy and its operations.
4. Without a technology in place to allow for the competitive manufacture of goods, the full potential of composite materials cannot be realized.
5. Complex geometry, such as flat, flat with a curve, and flat with a curvature to the cone, presents a challenge for composite products.
6. High pressure is not a feasible way to achieve a high volume percent of fiber and lower the void content in products made of composite materials with intricate geometries.

2.3 Sandwich Foam Composite Panel:

The type of sandwich structure that is frequently utilized in numerous applications is sandwich foam composite panel, mostly due to its concept's suitability for lightweight structures. It consists of three layers: two thin stronger outer layers(factsheet) and a thicker, lightweight core material in between the facesheet as shown in Figure 2.1. The configuration offers combination of high strength and low weight making sandwich panels useful in variety of applications. However, fabricating epoxy-based sandwich with hybrid-filled core and banana fiber facesheet

has not been studied and this was critically looked into in the course of this study to satisfy the objective two of this study

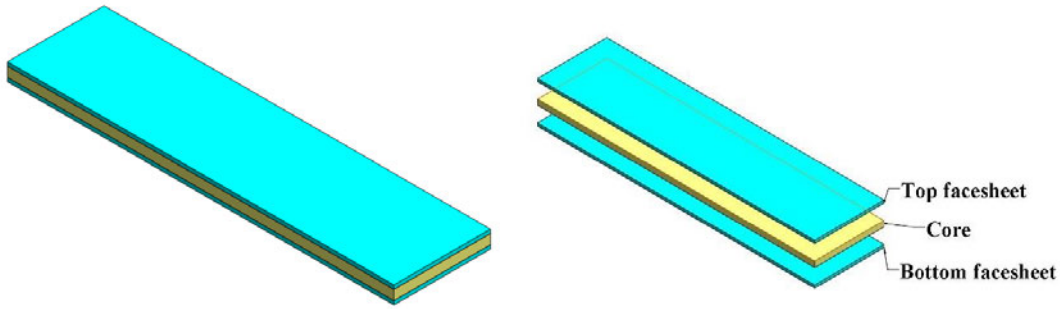

Figure 2.1: Schematic drawing of sandwich foam composite panel

2.3.1 Processing of Sandwich Foam Composite Panel

Sandwich foam composites are primarily processed in two ways: first, the face sheets are prepared, and then the face sheets and core are joined. The middle section of sandwich composites, known as the core, is determined by the applications and performance specifications. The core material, which is mechanically or adhesively bonded to the faces, must have low specific weight and sufficient shear stiffness to absorb applied shear stresses and distribute them over a wide region [50]. Three main types of popular core materials exist: Expanded, cellular high-density materials, low-density solid materials, and foams with both open and closed cell structures: Expanded high-density materials in web core, honeycomb, and corrugated form: Trusses and corrugated sheets. The most common types of cores include wood, polystyrene, polyurethane, PET, and polyvinyl chloride (PVC) foam cores. When hybrid-filled foam is used as the core material, it can save weight in marine applications, improve its stiffness, and improve the performance of sandwich structures, which are not often used[51].

The sandwich composites' skin, or face-sheet, is recognized for carrying the compressive, tensile, shear, and flexural strengths that act parallel to the sandwich panel. Meanwhile, the reinforcement and low specific weight of the core ensure sufficient shear stiffness to absorb applied shear forces. To maintain structural continuity throughout the depth of the sandwich panel, an adhesive is utilized to join the face sheets and the core. A sandwich composite

structure is effective when the combined weight of the facesheet and the core is about equal [30, 52].

2.3.2 Properties of Sandwich Foam Composite Panel:

Sandwich foam composites' characteristics are determined by the dimensions of the skins and core, as well as by their respective thicknesses and bonding strengths. The facesheets and the core are the two main parts of sandwich foam composites. The bending and in-plane loads are carried by the facesheets, while the core supplies compressive strength, flexural stiffness, and out-of-plane shear [53]. Sandwich structured composites are novel class of composite materials that have become quite popular due to their high specific strength and bending stiffness. Sandwich panels are well known for their exceptional durability and appropriateness in a wide range of applications in industries that include automotive, maritime, wind turbine, aerospace, railway systems, and structural applications.These materials are particularly well suited for usage in space, aviation, and marine applications due to their low density [54]. Two rigid panels, or face sheets, made of light materials are linked by a thick foam core to produce a sandwich composite. This is done to give the composite material low density and high bending stiffness. Over two decades have passed since the sandwich construction concept was first used, using various processing methods. Researchers have experimented with a variety of core and skin layers for sandwich panels in the past, but foam core is currently the most popular choice for composite sandwich panels due to its high bending rigidity, superior acoustic damping properties, better thermal insulation, and lighter weight [13, 55].

2.3.3 Advantages of Sandwich Foam Composite Panel

The following are a few advantages and applications of sandwich foam composites:

- The potential to customize qualities by selecting suitable constituent elements and their volume percentages.
- wide variety of readily available components for the core and skins
- Low-density results in weight savings.
- High bending stiffness
- Increased resistance to damage
- In-situ fabrication
- High ability to dampen vibrations.

- Low density leads to saving of weight.

Structural applications in aircraft, spacecraft, submarines, ships, and boats, surface transport vehicles, building materials, etc.

2.3.4 Disadvantages of Sandwich Foam Composite Panel:

The following are a few drawbacks of sandwich foam composites:

- Higher thickness of sandwich foam composite
- Increased preparation and processing costs
- challenging to join.
- Difficult to repair if damaged.

2.4 Foam Composite core

Since the filler and matrix have a distinct structure, foam composite core has many beneficial properties, such as a low coefficient of thermal expansion, a high strength-to-weight ratio, low density, excellent acoustic qualities, low moisture absorption, and strong resistance to hydrostatic pressure. Most of these unique properties are caused by a variety of factors, including as filler sizes, matrix types, volume fractions, void fractions, filler/matrix interfaces, and production conditions that allow for particular applications [56]. Because foam composite cores are lightweight, they are excellent material for underwater, floating, and maritime equipment. Additionally, they are excellent option for reinforcement since their mechanical properties outperform those of other foams with porosity in the matrix material. Their properties differ from those of simple foam composites when reinforced, and this is often accomplished using a matrix made of vinyl ester, epoxy, and phenolic resins [49, 57].

Furthermore, nanomaterials have been of recent advantages to the reinforced composite in science and technology, especially in the field of multiscale reinforced composites. The structure, physical, and morphological properties of nano and micro-scale reinforced foam composites manufactured with polymer matrix can be analyzed to identify the trend at which their properties might likely affect the design and the application of the composite. In this study, the micro filler (hollow glass microsphere) and nanofiller (nanoclay) materials are taken into consideration for use in the processing of the foam composite core as hybrid fillers and their structural behavior was studied in other to satisfy the objective one of this study. Due to the growing usage of various forms of reinforcement in foam composites, it is necessary to

comprehend the relationships between the structure and properties of these different types of reinforced foam composites in order to spot trends and create lightweight composites for engineering structures[54]. Foam composite cores as shown in Figure 2.2 can multi-function so that they can be used to perform different purposes and can be tailored for the specific application. For such applications to be unique, their properties such as tensile, flexural, impact, hardness, and thermal properties must be known. All these properties are considered and experimented with within this study.

The structural application of foam composite core is controlled by the density and volume fraction of the constituent materials by their mechanical properties. The tensile property of the foam composite core is responsible majorly for their structural applications most especially when reinforced with other materials such as warp-knitted spacer fabric (SF-WKSF) [58], carbon fabrics [59, 60], carbon nanofibers [61], glass-fiber/polymeric matrix [62-65], and resin impregnated paper honeycomb (RIPH) [28]. The compressive strength and modulus of foam composites vary generally with different types of foam composite core concerning their density, this can either be epoxy foam [2, 25, 66, 67], vinyl ester foams [68], polyetherimide (PEI) foam composites, magnesium alloy foam [69], cyanate ester foam [70], high-density polyethylene (HDPE) syntactic foams [71], A356 aluminum alloy syntactic foam [72] and more were studied in the literature.

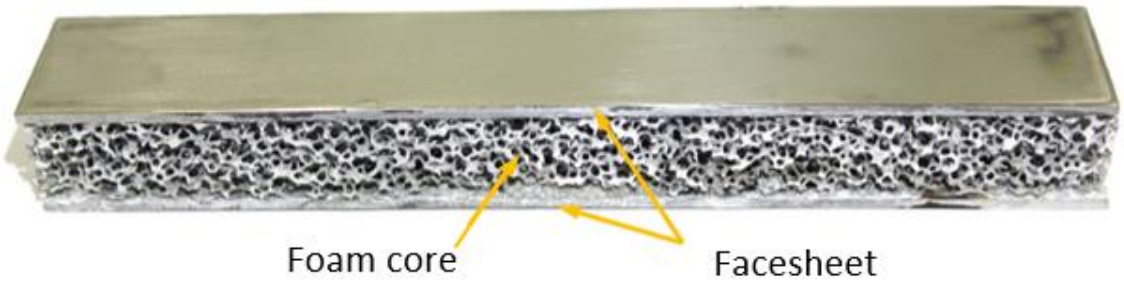

Figure 2.2: Sandwich panel showing foam core [73]

2.4.1 Applications of Foam Composite core

Foam composite core is a lightweight composite material that can be used in a variety of engineering industries or sectors. Some of these applications include:

1. Aircraft: Foam composite core finds application in fabrication of many components of aircraft which includes, fuselage, wing boxes, empennage boxes, control components, interior components, and exterior components, among other key structural components [42], Boeing

(Chicago, IL) and Airbus Americas (Herndon, VA) have both used foam composite as reinforcement in the hollow arrears within the aircraft [57].

2. In Helicopters: To ensure an aerodynamic profile and to act as a filler material to avoid profile distortion, foam composite is utilized on the helicopter blade. The blade is made up of an envelope or box. To manage the stiffness and torsion, the blade is formed by two shells under pressure.

3. Yoke rotor: This mechanical arrangement enables the blades to rotate and to move in small amplitude angular displacements while they are rotating [42].

4. Automobiles: Components utilized in the construction of automobiles, including the roof, doors, seat frames, side panels, hatchback doors, motor cap, headlamp supports, oil tanks, transmission shaft, and chassis sections, can be made with foam composites, etc.

5. In marine structures: foam composite's strong hydrostatic compressive strength and minimal moisture absorption make it ideally suited for buoyant behavior in the maritime environment. Foam composite is mostly used in marine structures, where it is used as blocks in the front and aft free-flood zones of Trelleborg Emerson & Cuming (TEC) and Trelleborg Offshore. [57].

6. Oil and gas industry: Pipelines carrying oil have been insulated using foam composite to enhance the thermal insulation properties.

7. Consumer Products: Foam composites have been used by the sports industry to make soccer balls. Adidas Inc. manufactured the 2006 World Cup ball out of polyurethane foam. The ball was able to go farther and along the exact trajectory because the foam composite layer assisted in promptly returning the ball to its spherical shape once it was kicked [57].

8. Furniture Industry: Polyvinylidene chloride saran microballoons combined with epoxy or polyester are used to create synthetic wood. The product accepts machine screws, nails, and staples and feels like real wood. Synthetic wood, as opposed to actual wood, is utilized in small boats and synthetic marble bathroom fittings like bathtubs since it is extremely resistant to moisture exposure [57].

9. Composite Tooling and Vacuum-Forming Plug Assists: Since foam composite is lightweight, easy to machine, and has low conductivity and thermal stability, it is utilized as tooling boards and plug aids for composite materials[57].

2.4.2 Disadvantages of Foam Composite Core

The primary drawback of foam composite core containing glass-based microspheres is that they are not recoverable due to their stiffness, brittleness, and susceptibility to damage when subjected to high strains [74].

2.4.3 Processing of Foam Composite Cores

Various researchers have used a variety of techniques in the past to create foam composites which include:

1. Extrusion Technique: To perform this technique, 5–10%wt of microballoons made of PE powder were allowed to pass through a heated zone in a laboratory for approximately one minute at a temperature of roughly 170^{o}C. Low-density polyethylene (PE), which has a melting point of 102^{o}C, was used as the matrix. Particle sizes for this technique range from 6 to 9um, with a starting temperature of 98–104^{o}C [75].

2. Firing Technique: By bonding the fillers using an inorganic binder solution comprising mono-aluminum phosphate and $Al(H_2PO_4)_3$ in water, the fire technique is carried out. To produce a complex hydrate and evaporate water, the solution is heated. When the temperature rises over 300 degrees Celsius, the hydrates break down into an amorphous material having the formula $Al_2O_3.3P_2O_5$. The mixture of the fillers/mono-aluminum slurries is then molded and vacuum-filtrated, dried at 50-90^{o}C, and heated for 24 hours at 230^{o}C. Thereafter, the foams are made by firing the fillers with spherical intergranular cavities for 3 hours at 600^{o}C [75].

3. Coating Technique: Foams can be produced using coating methods such as polymer precipitation, vacuum filtration, or resin coating. The slurry solution is vacuum filtered and washed on the filter, however, the resin coating causes unnecessary agglomeration due to a thin layer of the polymer. The coated spheres are subsequently vacuum-dried, yielding a molded powdery form of the discrete particles. Subsequently, the fillers coated by drying are pressed into the necessary volume using a mold charging process, and the mixture is allowed to cure at room temperature.

4. Stir Mixing Technique: This is the most common method of all the techniques which has been adopted by many researchers in the past for the fabrication of foam composites [56, 76-79]. This consists of mixing manually the fillers and the resin i.e., the filler and the matrix. The filler was added gradually into the matrix and gently stirred together to prevent the breakage of the fillers. This can be done in a beaker and the thorough mixture is poured into a pre-designed mold made either from steel, aluminum, copper, or plastic PVC materials. The mold can be in

any shape depending on the desired outlook of the foam composites to be produced. Mostly, a rectangular mold is used and then, the foam composite is machined to the desired shapes after curing. A new system of conservative mixers is used nowadays with the help of a stir mixing machine by using a glass rod and a magnetic bar which most time perform better. This method can be shaken manually for gelatinizing the starch as fillers are in the container. The conservative mixing method must be performed carefully to avoid filler breakage or container breakage. The desired quantity of fillers and the matrix resin to be mixed must be measured on a weighing scale inside a beaker. The mixture is then mixed thoroughly until a slurry solution is formed to remove or reduce the viscosity. This study also employed the use of stir mixing techniques because of their ability to control and give a better quality of the specimens. The degassing method was used to overcome the challenges of stir mixing and to ensure uniform/homogenous dispersion during the experiment. Molds of different shapes and sizes are designed for the fabrication of foam composite cores. Many researchers have used rectangular and cylindrical molds made from copper, steel, aluminum, and plastic PVC materials for compressive, tensile, and flexural test samples yielding excellent performance, according to specific test standards.

2.4.4 Properties of Foam Composites

The unique structure of foam composites between the filler and the binder gives rise to a number of advantageous characteristics, including low thermal expansion, high strength-to-weight ratio, low density, low moisture absorption, and strong hydrostatic pressure resistance. The majority of these unique properties are brought about by a number of variables, including the filler sizes, kind of binder utilized, volume fraction taken into account, void fraction, filler/matrix interface, and manufacturing conditions that permit unusual applications[56]. Because foam composites are lightweight, they are an excellent material for underwater, floating, and marine applications. Because of their superior mechanical properties over other foams with matrix material porosity, they are an excellent option for reinforcing.

When reinforced, their properties diverge from those of simple foam composite; a matrix, such as epoxy, phenolic, or vinyl ester resins, is typically used in this process[49, 57]. Recently, reinforced composites have benefited from nanomaterials in science and technology, particularly in the area of multiscale reinforced composites. It is possible to analyze the structure, morphological behavior, and physical attributes of nano- and micro-scale reinforced foam composites made of polymer matrix to determine the degree to which these properties are

likely to influence the composite's design and intended use. The usage of nanofiller (nanoclay) and microfiller (hollow glass microsphere) in the manufacturing of foam composites was considered in this work. Because different types of reinforcement have been used in foam composites more frequently, it is important to understand the structure and property correlations of the different types of reinforced syntactic foams in order to spot trends in the design of lightweight composites for engineering structures [57]. Foam composites have multiple uses and can be customized for a given application, making them multifunctional materials. Their tensile, flexural, hardness, impact, and thermal properties, among other attributes, must be understood for such applications to be distinct. This study, which was designed in response to other studies on similar topics in the literature, takes into account and experiments with all of these properties. The density and volume proportion of the component materials, along with their mechanical properties, determine how foam composites are used structurally.

2.4.4.1 Mechanical Properties

It is crucial to comprehend the operation of a composite panel by taking into account how well its mechanical properties can be applied. Contemporary engineering practice continuously stresses the material and many of the traditional designer approximations[80, 81]. An engineer takes the material's mechanical characteristics into account when recommending a certain material for a given application. The combination of reinforcement and matrix acts as a synergistic force to control the mechanical properties of a composite panel[82]

2.4.4.1.1 Hardness

Composite material's ability to withstand localized plastic deformation brought on by abrasion or mechanical indentation is measured by its hardness. Different composite materials have varying degrees of hardness; for instance, soft metals like sodium and metallic tin, wood, and common polymers are softer than strong metals like titanium and beryllium. Although strong intermolecular interactions are typically indicative of macroscopic hardness, there are various ways to quantify hardness because of the complexity of solid material behavior under force. Three types of hardness: rebound, indentation, and scratch [83]. The hardness of pure magnesium (Mg) increased steadily as HGM particles were added one at a time, according to Manakari *et al.* [83] study on the microhardness measurement of Mg and foam composite.

2.4.4.1.2 Tensile Strength

Tensile properties of foam composite quantify the longitudinal stress that the composite can bear without breaking or before breaking. Tensile properties are highly helpful in characterizing the behavior and failure mode of foam composite in structural core changes, particularly when it comes to its structural use for sandwich applications [55, 84].

Uniaxial strain alters the far less desired character of foam composite, leading to frequent brittle fracture. Depending on the kind of filler utilized, the tensile strength for uniaxial loading can range from 25 to 55% of the compressive strength; however, the modulus in tension is significantly smaller than the compressive modulus [66, 85].

The tensile strength of foam composite increases as the volume percentage of microballoons increases; this observation merely indicates that the microballoon content has a substantial impact on foam composite tensile strength[86]. It has also been studied how strong syntactic foam-reinforced materials can be tensed. The addition of nanofibers was found to improve the tensile properties according to research by Dimchev et al [87] and Colloca et al.[88] due to the matrix's function in fracturing under tensile stress within the composites.

2.4.4.1.3 Flexural Strength

A machine with a three- or four-point bend configuration device is used to perform flexural testing. A material's flexural strength, also known as bending strength or transverse rupture strength, is its maximum bending stress in the outermost layer of the foam composite, immediately preceding its yield point. On the convex or tension side of the foam composite panel, this is computed at the specimen's surface. The stress versus the deflection curve slope is used to get the flexural modulus of foam composite. The flexural modulus of foam composite is crucial because it establishes the strain energy release rate of the fracture specimen and allows the fracture test process to be validated using the specimen deflection and maximum load to failure[85].

The flexural properties of foam composite have been the subject of numerous investigations using various techniques, fillers, and matrices. Injection-molded cenosphere/HDPE was utilised by Bharath Kumar et al.[71] to investigate the surface treatment of the flexural properties of foam composite. The study demonstrates that as cenosphere content rises, foam composite's flexural strength does as well. Similarly, Doddamani et al. [89] investigated the flexural properties of foam composites using epoxy resin and functionally graded fly ash cenosphere. Furthermore, they utilized epoxy resin, HGM, and chopped strands of E-glass fibre. Additionally, Karthikeyan et

al. [90]investigated the impact of fibre reinforcement on the flexural behavior of syntactic foam. Twin-screw extruder was employed by Liang[91] to create a composite with hollow glass beads and an ABS matrix and their flexural properties was studied.
Additionally, in order to prevent the microballoons from breaking, Patil et al.[92] recently used the hand layup approach to investigate the behaviour of hybrid HGM/fly ash cenosphere filled vinyl ester foam composite. In this investigation, the same hand layup approach was used.

2.4.4.1.4 Impact Strength

In order to determine the foam composite's fracture resistance, a Houndsfield impact tester is often utilized, and the test is carried out at room temperature. The impact test of composite materials has not received much research. The impact stiffness of the repaired composite was consistently higher than that of the unrepaired composite, according to Jefferson Andrew et al. [93]. This indicates that the bonding between the composite materials is well-suited for withstanding impacts. Additionally, sandwich panels including an aluminium honeycomb core and carbon epoxy shells were the subject of an investigation by Davies et al.[94]. Since the impactor severely caused the skin's rear face to debond, the studied panel was a greater energy absorbent than the thin skins.
Furthermore, in a separate study, Patil et al.[92] found that the absorbed impact energy in vinyl ester matrix syntactic foam increases with an increase in the wall thickness of HGM and decreases inversely with the volume percentage of HGM. According to impact tests, foam composite typically has good rigidity and can withstand impacts

2.4.4.2 Thermal Properties

Understanding the thermal characteristics of composite materials is essential to comprehending how well they function in a variety of applications, especially those in which temperature changes play a significant role, such as maritime and aircraft applications[95]. The thermal properties to be studied includes:

2.4.4.2.1 Thermal Conductivity

A material's capacity to conduct heat is gauged by its thermal conductivity. It is commonly stated in watts per meter-kelvin (W/m·K) and is symbolized by the sign k. Heat may be transferred efficiently by materials with high thermal conductivity, such as metals

(such as copper and aluminium), whereas insulators, such as wood and rubber, have low thermal conductivity.

Important elements influencing thermal conductivity consist of:

- Material composition: the thermal conductivities of various materials vary naturally
- Temperature: the temperature can affect the thermal conductivity of many materials
- Phase: The thermal conductivities of solids, liquids, and gases vary; solids usually conduct heat more effectively than liquids or gases.
- Microstructure: How quickly heat is transported through a material can be influenced by the arrangement and bonding of atoms.

2.4.4.2.2 Coefficient of thermal expansion(CTE)

A material's capacity to expand or contract in response to temperature changes is expressed in terms of its CTE. The fractional change in length (or volume) per degree change in temperature is what it is commonly represented as, and its symbol is α. Usually, the units are stated in either Kelvin (K) or degrees Celsius (°C).[96]

2.4.4.2.3 Specific heat capacity

The quantity of heat energy needed to raise a unit mass of a substance's temperature by one degree Celsius (or one Kelvin) is known as its specific heat capacity, also just denoted as specific heat. Units of measurement for it are usually joules per kilogramme per degree Celsius (J/kg·°C) or joules per kilogramme per Kelvin (J/kg·K). It is represented by the symbol C.

2.4.4.2.4 Dynamic Mechanical Analysis(DMA)

The advanced method known as DMA is used to examine how materials behave mechanically under different frequency and temperature conditions. Understanding a material's viscoelastic behavior—which is essential for comprehending how materials behave in practical applications—means measuring the material's response to deformation under oscillatory stress.[97]

Essential concepts

- Viscoelasticity: DMA evaluates how materials respond to stress by displaying both viscous and elastic properties. This is especially crucial for complicated materials like polymers.

- Storage Modulus (E'): Indicates the material's elastic response and the amount of energy stored when the material is distorted.
- Loss modulus (E"): This is viscous response which indicates how much energy is lost as heat during deformation.
- Damping Ratio (tan δ): The material's energy dissipation is indicated by this ratio, which compares the loss to the storage modulus. Greater damping and less energy storage are indicated by a higher tan δ

2.4.4.2.5 Thermogravimetric analysis(TGA)

A method called TGA is used to calculate how much a material's mass changes when it is heated, cooled, or kept at a constant temperature. This technique offers insightful information about the compositional changes and thermal stability of materials[98]. The essential parameters to the noted are:

- Weight Change Measurement: Usually conducted in a controlled environment (such as air, nitrogen, or argon), TGA determines a sample's mass as a function of temperature or time.
- Thermal Stability: The findings can reveal the temperatures at which a substance liquefies, disintegrates, or experiences other chemical transformations.
- Analyses Stages:
  - Decomposition: Mass loss as a result of thermal breakdown or disintegration.
  - Evaporation: Mass loss brought on by volatile components escaping.
  - Oxidation: Reactions with oxygen cause mass changes.

2.4.4.3 Morphological properties

At high magnifications, Scanning Electron Microscopy (SEM) is a powerful tool for analyzing the composition and surface morphology of materials. It collects data about the material and creates finely detailed images using concentrated electron beams.[99]
Important Composite Morphology Aspects are:

- Matrix and Strengthening:

  -Matrix: Usually a polymer and this continuous phase is what secures the reinforcement material in place.

-Reinforcement: Discrete materials (plates, fibres, or particles) that provide something rigidity and strength. Aramid, carbon, and glass fibres are examples of common reinforcements

- Interface: Stress transfer and overall performance depend on the interface between the reinforcement and matrix. The mechanical characteristics and load distribution are enhanced by a well-bonded contact
- Distribution and Orientation: The mechanical characteristics can be greatly affected by the distribution and orientation of reinforcing fibres or particles. As an illustration, randomly orientated fibres might have isotropic qualities

2.4.4.4 Physical properties

This section discusses the physical properties of foam composites, including density, buoyancy, water contact angle, and water absorption, as they impact the composite material's behaviour.

2.4.4.4.1 Density

To comprehend a composite panel's attributes and performance qualities, its density must be measured. Density affects a material's general behaviour, thermal conductivity, and mechanical strength.

2.4.4.4.2 Buoyancy

An upward force applied by a fluid against the weight of an item partially or fully submerged is known as buoyancy or upthrust. Variations in a fluid's density under the influence of gravity give birth to buoyancy force, which causes a variety of significant phenomena in numerous fields of fluid mechanics. The buoyancy force exerted on an item is directly proportional to its volume; that is, the larger the weight of the submerged solid object, the greater the buoyancy force acting on it [100]. Ren & colleagues [101] created buoyant material using SiO_2 and hollow glass microspheres and investigated its properties for use in high-temperature resistance applications. Because ships and boats are built to maximise buoyancy by optimising the form and volume of the hull to displace enough water, ensuring they float and retain stability, this feature is extremely important for marine applications. Because they offer the required strength without being overly heavy, materials like steel are frequently utilised for larger ships and fibreglass or aluminium for smaller boats[102] but in this study, hollow glass microspheres and nanoclay

particles were used to fabricate the panels and their buoyancy level was tested which justifies the objective three of this study.

2.4.4.4.3 Water Absorption

A technique to assess syntactic foam's ability in an aquatic environment is water absorption. The water concentration gradient is thought to cause water to stay in a single free phase and enter the resin. Foam composite panel may swell and become plasticized as a result of water absorption[103]. Water can permeate the materials in multiple directions under most circumstances. Since the coefficient of diffusivity generally changes with direction, edge effects can become significant and ought to be taken into account in any analysis of foam composite structures' water uptake that exposes many surfaces to water diffusion. It is also important to remember that water seeping into resin matrix composites might alter their mechanical characteristics. According to Tagliavia et al.[104], foam composite panel can be absorbed into water in a variety of environments, including freshwater, saltwater, and deionized water at room temperature. According to Gupta and Woldesenbet [105], the attenuation coefficient of foam composite panel might vary due to changes in its density and mechanical properties caused by moisture or water absorption.

2.4.4.4.4 Water Contact angle

Measurements of the water contact angle on composite panels reveal important details about how wettable and hydrophobic their surface is. The angle that forms at the interface of a liquid (such as water), a solid (the composite panel), and the vapour phase is known as the contact angle. Understanding how surfaces interact with liquids and how this affects characteristics like adhesion, staining, and corrosion resistance is made possible by this crucial parameter. Essential parameters to be noted while measuring contact angle are:

- Definition: The angle formed by the tangent to the liquid surface at the contact point and the solid surface is known as the contact angle(θ).
- Wettability:

-Hydrophilic Surface: A surface is deemed hydrophilic(ater-attracting) if its θ value is less than 90°.

- Hydrophobic Surface: A hydrophobic (water-repelling) surface is one where $\theta > 90°$.

-Superhydrophobic Surface: Extreme water repellency is displayed on the surface if $\theta > 150°$.

2.5 Review of the Material Selection

2.5.1 Hollow Glass Microspheres

Glass bubbles, also known as hollow glass microspheres or microballoons, are made mostly of a borosilicate-soda lime glass blend and possess great heat and chemical resistance along with low density. The usual thickness of the glass microsphere walls is 10% of the sphere's diameter. Nowadays, a wide variety of spherical microparticles with diameters ranging from 5µm to 180µm and densities ranging from as low as 0.06g/c3 to as high as 0.8g/c3 are accessible. The walls' thickness determines the crush strength of hollow spheres, and as could be assumed, the crush strength rises with sphere density. The chemically stable, noncombustible, nonporous, lightweight hollow glass spheres offer good water resistance. These characteristics are used in deep-sea oil drilling equipment and submersible hulls, when other types of foam would break. Syntactic foams made of hollow spheres made of other materials have different characteristics. For instance, light syntactic aluminum foam can be produced using ceramic balloons. [106]
There are also glass microspheres that are hollow and coated with conductive materials. While maintaining the weight-saving advantage of hollow-core low-density materials, spherical particles with strong conductivity and shielding capabilities are produced via conductive coating with a customized thickness. These conductive microbubbles have great potential uses in biology, electronics, medical devices, military applications, and other specialized fields.

2.5.1.1 Synthesis and Production of Hollow Glass Microspheres

Microspheres are spherical particles that fall into one of two categories: hollow or solid [107]. It is possible to create hollow and solid microspheres from glass, ceramics, carbon, or plastic. According to Watkins and Prado [108] and Bobkova et al. [109], because soda-lime glass has a low melting point and is chemically inert, it is commonly used to manufacture solid glass microspheres. Glass microspheres can be produced using a variety of techniques, and the chosen production method will determine the product's characteristics. Glass microspheres were treated by Watkins and Prado using the in Flame Spherodization Method (IFSM), which involved feeding irregularly shaped glass particles into a flame that was hotter than the vitreous temperature (Tg). The microspheres were gathered after passing through the cool region of the flame into a cyclone system that collected all of the spheroid particles [108]. Understanding the principles of dispersion was essential to comprehend the potential for handling and combining HGM. Simple, forceful mixing of materials with extremely tiny (often microscopic) particles

can lead to complications because the materials retain mechanical, molecular, and/or electrical connections after mixing [110].

2.5.1.2 Application of Hollow Glass Microspheres

Hollow glass spheres have several uses in thermal insulation because of their great strength, low density, and chemical resistance. As was already mentioned, one method of energy conservation in drilling and extraction was the use of glass hollow spheres. Application and mixing are made easier when microspheres are used in composite components [111]. The ball-bearing effect improves flow and lowers viscosity in resin mixtures, which makes them easier to process and leads to quicker cycle times, greater machinability, and cost savings. The spherical, smooth shape of microspheres allows for efficient packing and even dispersion. Microspheres can be used in the majority of extrusion and injection molding procedures used in the manufacture of thermoset and thermoplastic polymers. The ability to integrate seamlessly into compounds makes them appropriate for a variety of industrial processes, including casting and spraying.

To lighten and prolong resin, hollow glass microspheres are utilized in the paint, abrasive, automotive, automotive aircraft, construction, explosive, marine, and sporting goods industries[112]

2.5.2 Nanoclay

Layered silicate mineral nanoparticles make up nanoclays. They are divided into several classes, such as montmorillonite, bentonite, kaolinite, hectorite, and halloysite, according to their chemical makeup and nanoparticle form. Because of their exceptional engineering properties such as better thermal behavior, high fatigue endurance, stiffness, high specific strength, high damping, and low density, innovative polymer/nanoclay composites have seen the birth of novel applications[113, 114]. About 75–80% of polymer/nanoclay composites are used in the automotive, aerospace, and packaging industries.The adoption of nanoclay filler as the second filler in this study was due to the above-mentioned characteristics of nanoclay, which is one of the research's emphasis areas[115]. Additionally, the high aspect ratio of nanoclay particles creates a tortuous path for gases and liquids, which significantly reduced moisture permeability and gas diffusion. This makes the composite produced more resistant to moisture absorption, chemical infiltration, and environmental degradation. Additionally, the improved barrier

properties of nanoclay contributed to the improvement in the moisture absorption rate of the panels produced from this study[116, 117].

2.5.2.1 Overview of Nanoclay

An essential type of layered aluminosilicate is nanoclays. [118-120]. Typically, platelet sizes fall between 10 and 100 nm. Nanoclays can be created artificially, but they also occur naturally. The constituent nanolayers of nanoclays are either $[AlO_3(OH)_3]^6$ octahedra or SiO_4^{4-} tetrahedra. Van der Waals forces are commonly used to stack the layered nanosheets of aluminosilicate together. Ions between the platelets have been ensnared by the stacked nanosheets. The structural, morphological, mechanical, thermal, and barrier properties of the nanoclay-based nanostructures are remarkable because the nanoclays' unique nano-scale structure has made them useful as nanofillers in polymeric matrices to create nanomaterials. [121, 122] Alkyl cations are often used to treat layered silicates to create organoclays, which increase the inorganic nanoclays' compatibility with organic polymers [123], and mechanical robustness, thermal stability, and flame resistance are all properties of polymer/nanoclay nanocomposites.

They also consist of tiny crystals of mixed metallic ions that are obtained through a hydrothermal process from alkaline volcanic ash [124]. Clay nanoparticles can also come from waste products from mining and mineral processing [125]. Phyllosilicates, such as the hydrous silicates of aluminum, magnesium, iron, and zinc, constitute the primary basis for clays [124]. Microscopically, clays appear in a platelet fashion with layers consisting of silica (SiO_2) and alumina (Al_2O_3) [124]. The clay families include [124]:

• kaolinite/kaolin family with chemical formula $Al_2[Si_2O_5](OH)_4$

• The family Halloysite, which exhibits a tube-shaped structure and an empirical formula $Al_2Si_2O_5(OH)_4.2H_2O$

• MMT family which combines many minerals and has a large quantity of SiO_2 and a small quantity of Al_2O_3

• laponite family which is a synthetic clay and its chemical structure is $Na^{+0.7}[(Si_8Mg_{5.5}\ Li_{0.3})O_{20}(OH)_4]^{-0.7}$

• layered double hydroxide clays which are referred to as hydrotalcite with a large amount of water with chemical structure $[M^{2+}{}_{(1-x)} + M^{3+}{}_{(x)}\ (OH)_2]X^+\ (An^-)_{x/n}\cdot mH_2O$.

2.5.2.2 Synthesis of Nanoclay

Many methods, including solution-blending, melt-blending, and in-situ polymerization, can be used to create nanoclay. The homogeneous dispersion of nanoclay in the polymer matrix is a crucial step in the production of polymer/nanoclay composites. Because of its low viscosity and powerful agitation power, the solution-blending method frequently produces a larger dispersion of clay layers in the polymer matrix than melt blending. On the other hand, melt blending is seen to be both ecologically benign and industrially feasible, with significant economic potential[126]. The reason the in-situ polymerization procedure is so common in synthesis is that it produces uniform dispersion and can be adjusted by changing the polymerization parameters [127]. Recently, several innovative synthesis techniques have been developed to create polymer/nanoclay composites with distinctive characteristics.

2.5.2.3 Application of Nanoclay

Nanoclay has recently discovered several new area of applications due to its exceptional technical properties. These includes, packaging, aerospace, and automotive, where 1–10% of nanoclay particles are utilised. This is because it is commonly used as reinforcement in polymer matrix composites, which improve mechanical, thermal, and anticorrosion properties. Entrepreneurs have invested billions of dollars in developing novel synthetic nanoclay materials [128, 129].

2.5.3 Fibers

Fibres with high modulus, strength, and stiffness are frequently used as reinforcement in the fabrication of composites[41, 130, 131].

The preferential orientation of the molecules makes them significantly more potent than their bulk counterparts. Their covering, a substance called size, serves to prevent moisture absorption while shielding them from potential harm that would arise from coming into contact with other fibers or equipment [132]. A measure of the linear density (grams per 1000 m) of fibers, filaments, tows, and yarns, "Tex" is frequently used to describe fibers. The choice of fiber type to be used as reinforcement is a trade-off among considerations such as mechanical properties, environmental properties, and cost [133]. The fibers employed in the reinforcement can be synthetic or natural, or a combination of the two in the case of some hybrid composites. The functions of fibers are described in Figure 2.3

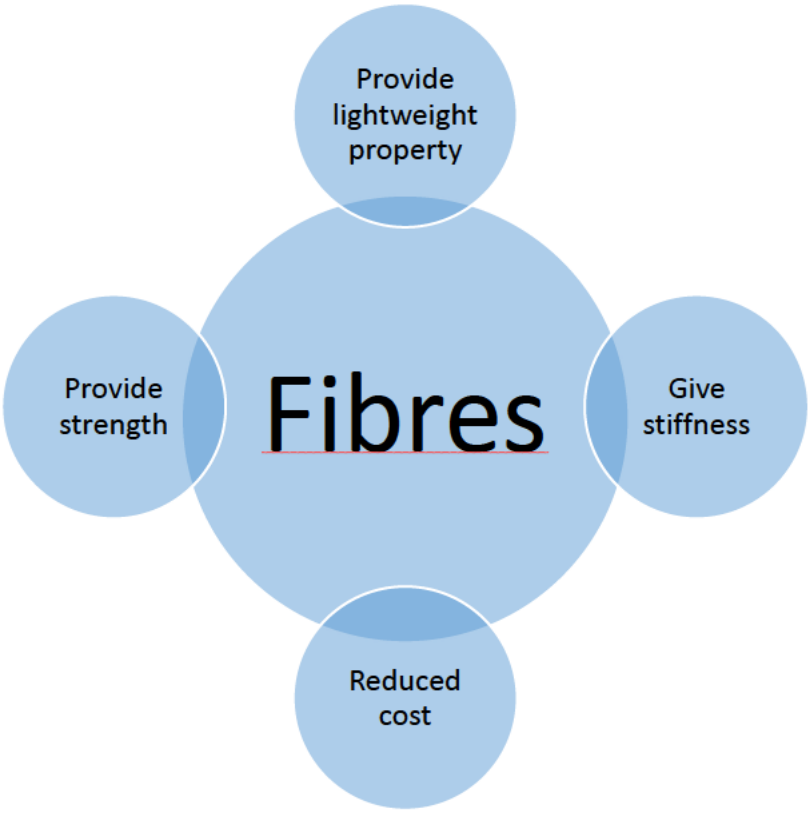

Figure 2.3: Functions of fibers in composites

2.5.3.1 Synthetic Fibres

These are artificial (man-made) fibers and are the most often used reinforcing fibers in composite materials reinforced with fibers. Synthetic fibres commonly used as reinforcement in composites include glass fibre, carbon fibre, and aramid fibre[47, 133-135]. When it comes to polymer reinforcement applications, glass fibers are at the forefront. Roughly 90% of all fiber-reinforced polymer composites are made of glass fibers [134]. One fairly common type of glass is called electrical glass grade, or e-glass. There are various sorts of glass fibers, such as A-glass, an alkali glass type, C-glass, a chemical resistant glass type, and R-glass (S-glass), a high-strength glass type [134]. Carbon fiber is extremely strong and has the highest strength and modulus properties [134]. Carbon fibers are moisture-independent and retain their tensile strength even at high temperatures[134]. Aramid fibers are used in applications that require high strength, high impact resistance, and lightweight. Kevlar is the most often utilized aramid fiber in the production of high-impact fiber-reinforced composites [134]. Several synthetic fibers that have been used as reinforcement materials include silica, quartz, boron, ceramic, basalt, and metallic fibers.[47, 133, 135]. Literature suggests that they have certain disadvantages despite their excellent mechanical properties[136-139]. The main issues with synthetic fibers are shown in Figure 2.4.

Figure 2.4: Synthetic fibers with associated problems

• They are not environmentally friendly and non-biodegradable, which puts safe disposal of used materials at risk.

• Fibers are often expensive due to the need for a large investment in processing and production equipment.

• They require expert labor during raw material extraction and processing into finished products. This suggests that there is a need to invest in the human capital development of qualified employees to handle synthetic fiber production processes, as opposed to natural fiber production, where low-level skills are required.

• Production expenses are increased by the high energy needed for processing and manufacturing. Additionally, developing nations with energy problems should not use them.

• They originate from nonrenewable petroleum resources, and as these resources are running low, it is imperative that we find alternatives.

• They possess manufacturing and extraction processes that harm the environment. Among the many ways that petroleum mining contributes to environmental deterioration is through the

production of contaminants that end up in the environment, both toxic and non-toxic. Additionally, the industry's emissions of greenhouse gases and byproducts such as volatile organic compounds damage the environment.

• They are usually landfilled after use due to their low capacity for recycling. Because landfill space is scarce everywhere and costs are high, this presents a dilemma. Because incinerating something releases toxic fumes, it is not a viable alternative.

2.5.3.2 Natural Fibres

Fibers that arise naturally are known as natural fibers. They are categorized as plant, animal, or mineral fibers because they originate from different parts of plants, animals, or minerals. Animal fibers are composed of proteins like keratin and collagen, while plant fibers are naturally cellulosic [140, 141]. Figure 2.5 shows the categories of natural fibers.

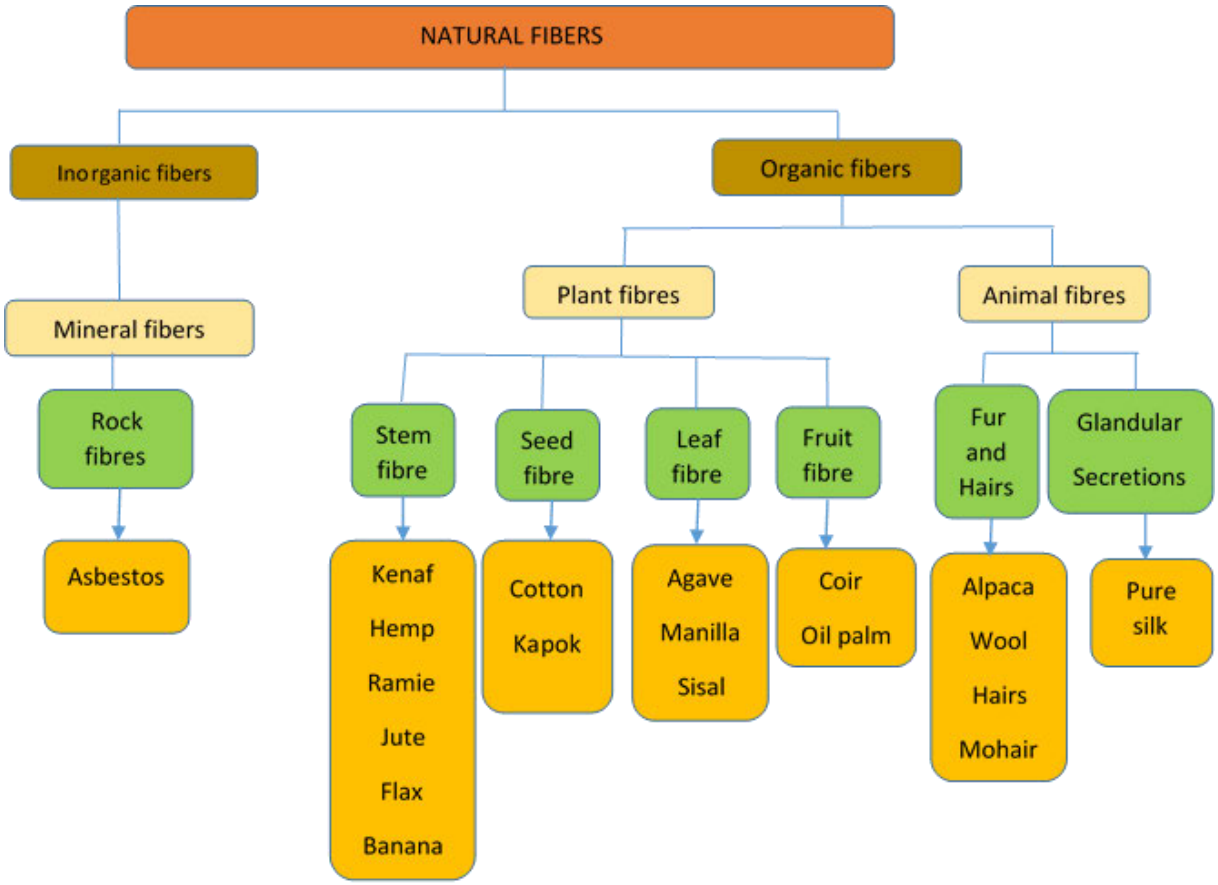

Figure 2.5: Classification of Natural fibers

The most common natural fibre used in composite reinforcement is plant fibre[140]. The most common and viable sustainable fibers for use as reinforcement in composites include flax, banana, hemp, jute, sisal, kenaf, and coir[140, 142]. For this reason, companies using plant fibers as reinforcing materials need to know annual production data and producing countries. Table 2.1 shows natural fibers' annual production, costs, and largest producers.

Table 2.1: World annual production of selected natural fibers, cost and largest producers [140, 143-150]

Fiber Producers	**Species**	**Production (10^3 tons)**	**Cost ($/Kg)**	**Largest**
Banana	Musa indica	200	0.81	India and Brazil
Kenaf	Hibiscus Cannabinus	970	0.38	USA, India, South Africa & Bangladesh
Coir	Cocos nucifera	100	0.50	India & Sri Lanka
Pina	Ananas comosus	74	0.10	Philippines, India, Thailand & Indonesia
Sisal	Agave sisalana	378	0.65	Brazil & Tanzania
Cotton	Gossypium	2500	1.5-2	SriLanka & India
Hemp	Cannabis Sativa	214	1.55	China, Philippines, and France
Jute	Corchorus Capsularis	2500	0.90	Bangladesh, India, and China
Ramie	Boehmeria nivea	100	1.52	India, Brazil, Philippines & China
Flax	Linum Usitatissimum	830	3.11	Belgium, Canada, And France

Developing nations profit socially and economically from the production and use of natural fibers. The living conditions of low-income workers and small-scale farmers are improved and supported by starting plant cultivation for the production of natural fiber. For instance, the Indian jute industry directly employs around 260,000 people and raises the standard of living for about 4 million families. [150]. In 2008, a similar situation existed in Bangladesh, where 2.5 million people worked in jute processing facilities and approximately 750,000 farmers were engaged in the production of jute plants [150]. These situations highlight the benefits of growing plants for the production of natural fiber and owning mills for the processing of natural fiber. Living standards rise and the unemployment rate declines nationally.

Unlike artificial fibers like carbon, glass, and aramid fibers, which are not biodegradable, natural fibers are environmentally safe [151]. They come from abundant renewable sources, like self-renewing plants and plants cultivated by humans, in large quantities. The main energy source needed to produce natural fiber is solar energy. They don't increase the strain on the country's power infrastructure, which keeps the demand for energy from rising steadily. Because natural fibers can be obtained for less money than synthetic fibers, they are more affordable. In contrast to the manufacture of synthetic fiber, which calls for expensive equipment and large investments, the creation of natural fiber requires less expensive equipment. Compared to the creation of synthetic fibers, less skill is needed in the process of producing natural fibers. Therefore, developing nations might simply produce them. Because they have substantially lower densities than synthetic fibers, natural fibers can aid in weight loss more than synthetic fibers do. The density of natural fibers ranges from as low as 1.20 g/cm^3 to as high as 1.5 g/cm^3 whilst that of E-glass and carbon fibers are 1.8 g/cm^3 and 2.1 g/cm^3, respectively [152]. According to the literature, the modulus-to-weight ratio of some natural fibers is greater than that of some synthetic fibers, such as E-glass fibers [152]. This suggests that natural fibers like these could compete with E-glass in designs where stiffness is crucial [152]. Because plants utilize carbon dioxide during photosynthesis and release oxygen, their growth lowers their carbon footprint. This ultimately lowers greenhouse gas emissions and hence global warming. Understanding natural fibers' chemical and mechanical properties is essential when working with them. The natural fibers found in plants are lignocellulosic, consisting of cellulose, hemicellulose, lignin, pectin, and waxes [145, 150]. Table 2.5 shows the chemical

compositional status of selected natural fibers and the quantities of the different components. Table 2.5 Chemical compositional status of selected natural fibers.

The bulk of the chemical components of natural plant fibers, which are lignocellulosic in origin, include cellulose (-cellulose), hemicelluloses, and lignin.[151, 153, 154]. Natural plant fibers also contain ash, pectin, waxes, and moisture content. Because the cellulose component is strong and stiff, the fiber surface is covered in many hydroxyl (-OH) groups, which gives the fibers their intrinsic hydrophilicity.[151, 153, 155, 156]. It is composed of a lengthy chain of anhydroglucose polymer units that are linked together to create microfibrils. [151, 153]. Figure 2.15 shows the cellulose structure.

The -OH groups facilitate both intramolecular hydrogen bonding inside the macromolecule and intermolecular hydrogen bonding between airborne hydroxyl groups and other cellulose macromolecules [151].

All natural plant fibers are composed primarily of cellulose, which is found as fibrils throughout the length of the fiber [153]. In addition to increasing tensile and flexural strength, cellulose also increases stiffness, inflexibility, and rigidity [153, 157]. The natural plant fiber's ability to reinforce itself depends on the kind and crystallinity of its cellulose [153]. Natural plant fibres' mechanical properties are determined by cellulose. Another non-cellulose material called hemicellulose serves as a matrix for cellulose microfibrils. It is very hydrophilic, hydrolysing in acids and soluble in alkali[153, 155, 158]. It improves the fiber's ability to absorb water [154]. Lignin is a three-dimensional complex hydrocarbon copolymer composed of aliphatic and aromatic constituents that are insoluble in many solvents and cannot be decomposed into monomeric components [153, 158]. It is amorphous and extremely hydrophobic, and it gives plants stiffness [153, 158]. Hydroxyl, carbonyl, and methoxyl groups have been discovered in lignin.[153 158]. Lignin is a thermoplastic polymeric component with melting and glass transition temperatures (Tg) of 170 and 90 degrees Celsius, respectively [153]. Although acids do not hydrolyze lignin, it is soluble in hot alkali, rapidly condensable in phenol, and easily oxidizable. [153]. It is difficult to separate lignin from plant fibers [159]. Hetero polysaccharides, or pectins, are what give plant fibers their flexibility. They typically contain a range of alcohol.[153, 159]. The complex structure of pectin is usually caused by the cross-linking of arabinose sugars and calcium ionic components with its side chains [157]. Pectins are the most hydrophilic natural plant fiber constituents due to the presence of carboxylic groups, which makes them particularly vulnerable to fungus invasion [160]. Wax is composed of various kinds of alcohols[153, 158]. Elimination of non-cellulosic components

including waxes, lignin, hemicellulose, and pectins alters the mechanical properties of natural plant fibers and their ability to form interfacial bonds with matrix elements [161].

However, natural fibers are not without flaws. Some of the main issues with natural fibres are depicted in Figure 2.6.

Figure 2.6: Problem associated with natural fibers

The properties of natural fibers can vary or be inconsistent. Their physical characteristics vary depending on the farming region, weather, soil type, and harvesting season [162]. Another big issue is how easily natural fibers can degrade and how little resistance they have to microbial attack. This is an issue for storing materials for an extended period, transporting fibers, especially via ships, and creating composites [162]. Nonetheless, the advantages of biodegradability include sensitivity to microbial attack and rotting fragility. Processing temperatures are impacted by the limited or poor heat stability of natural fibers. The majority of natural plant fibers degrade at temperatures higher than 200 degrees Celsius, which is the optimum processing temperature [162]. The chemical and physical structures of the fibers are altered by heat. Depolymerization, dehydration, oxidation, decarboxylation, hydrolysis, and recrystallization are a few possible changes[162]. In this study, banana fiber was used because is environmentally safe and possess good mechanical and thermal properties

2.5.3.2.1 Banana Fibre

In South-east Asia, the Malaysian-Indonesian region is home to banana plants, which are endemic to the Musa family. Worldwide, countries with tropical and subtropical climates generate large amounts of bananas and have an abundance of natural resources [163-165]. The banana plant is among the most useful plants on the planet. Nearly every component of this plant, including the fruit, peel, leaves, stalk, pseudo-stem, and inflorescence (flower), is edible[165, 166]. They are used as fibers, thickeners, organic fertilizers, colorants, flavorings, sources of macro- and micronutrients, livestock feed, and bioactive chemicals, among other uses both linked to and unrelated to food [166]. The banana leaf is widely utilized in food processing, food aesthetics, food packaging, and other related fields (in some countries, such as Indonesia). The banana fruit is one of the most widely consumed fruits and a staple of many diets due to its high nutritional value [166], as a result, it gains value as a commodity globally. Additionally, research has been done on the use of banana pseudo-stems as filler, textile fibre, pulp and paper, or structural reinforcement in composite materials[167-170]. Furthermore, every part of the banana plant has some additional medicinal benefits. For example, people with diabetes, pneumonia, diarrhea, and ulcers can prepare and eat the flower. The pseudo-stem sap of bananas can be administered externally to bites and stings or eaten internally. The young leaf can be applied as a poultice on inflamed skin. Certain countries also employ the roots, ashes from leaves, peels, and seeds for medicinal purposes[171]. Bananas as shown in Figure 2.7 are currently the world's fourth-most important fruit crop in terms of production. Global banana fruit production is estimated to be 72.5 million tons per year [165]. Once ripe, the fruit can be eaten raw or processed to make a variety of goods, including as flour, ice cream bread, smoothies, dried fruit, and so on. [172] Another option is to prepare the flower bud into a meal. Abaca (Musa textiles) is the most well-known species of banana plant used for its fiber. In contrast to the most popular banana, which is a member of the Musa acuminate species, its fibre is extremely prominent within the leaf fibre group [172]. A picture of a banana tree and its various sections can be found in Figure 2.5. The pseudo-stem is the part of the banana plant that transports and supplies nutrients from the soil to the fruits. Since the banana plant cannot bear more banana fruit, this pseudo-stem will be chopped and converted into waste biomass once the banana fruit is fully ripe and collected[163, 173, 174]. For every tons of bananas that are harvested, roughly 100 kg of rotten fruit are rejected, and about 4 tons of biomass waste (leaf, pseudo-stem, rotten fruit, peel, fruit-bunch-stem, rhizome, etc.) are produced. Consequently, for each cycle of banana fruit production, four times as much biomass waste is produced[174]. An

estimated 220 tons of biomass waste might be produced by a single hectare of banana farming, according to additional literature[174]. Typically, farmers burn these wastes or dispose of them in lakes and rivers. If not correctly managed, the trash from banana trees can harm the environment [174]. This agricultural waste is thought to have more sensible uses, such as serving as a supply of cellulose fiber for future projects [175]. A portion of the banana plant called the pseudo-stem resembles a trunk and is made up of tightly wrapped leaf sheaths that enclose up to 25 fragile leaf cores. When these leaf sheaths are fully developed, they separate from the stem and become identifiable banana leaves. With its base where the leaf sheaths begin, the banana plant can reach a height of 7.5 meters, and some of its inner leaves are roughly the same length as the tree. On the outside, on the other hand, the later-growing leaves are smaller. Leaf widths on bananas can get as large as thirty centimetres[176].

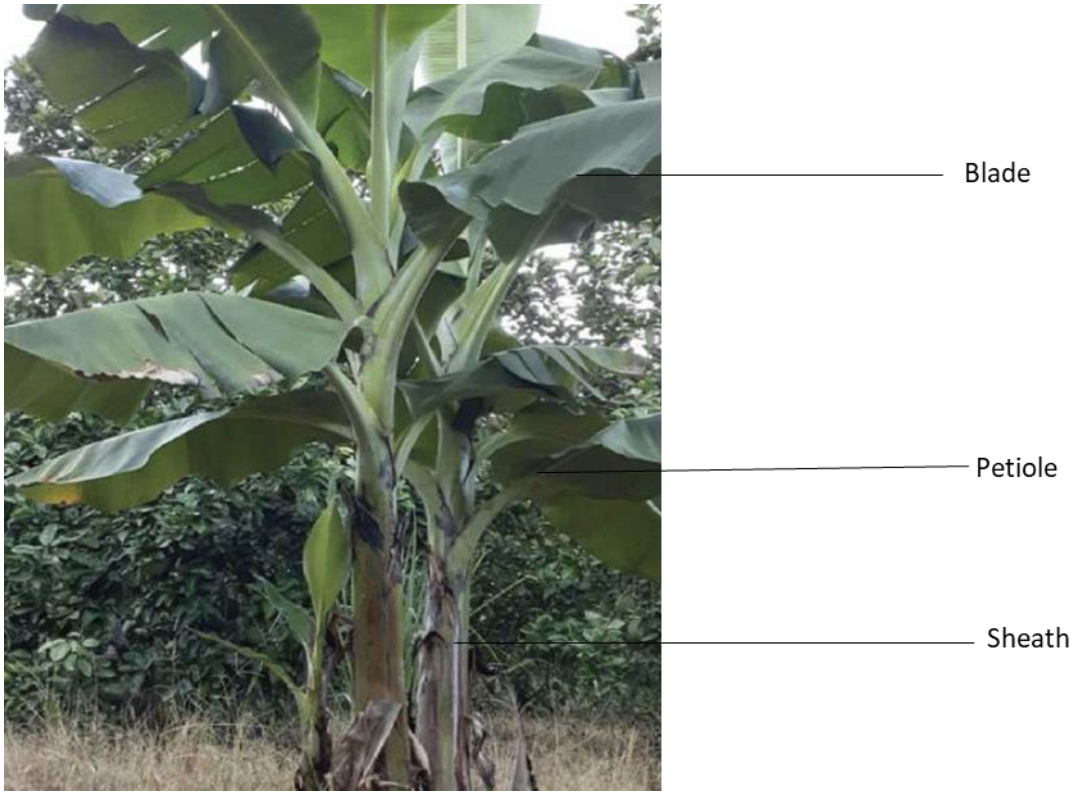

Figure 2.7: Banana tree

2.5.3.2.1.1 Extraction of Banana Fibres

Banana pseudo-stem leaf fibre extraction can be facilitated with the use of a decorticator machine. This device removes wood, grain, bark, and skin. The process of extraction commences as soon as the pseudo-stem's leaves are cut. The typical method in practice is a combination of scraping and water retting. In the initial stage, referred to as tuxing, the fibre

bundles are isolated from the other components. Manual or mechanical methods can be used to perform tattooing[177]. The leaves are removed from the sliced pseudo-stems. After inserting a knife at the butt end between the outer and middle layers, the outer portion of the leaf shaft is firmly grabbed and pulled out. The fibre bundles created by the tuxing process were around 5-8 cm broad, or the length of the leaf. The second step after the tuxing operation is to remove the gum or non-fibrous tissue and any leftover items inside the fibres[176]. The fibres also go through a rigorous washing and drying procedure. Both skill and patience are essential for these treatments. In general, there are merely 11 outer leaf sheaths on the banana pseudo-stem that can be removed to extract the fibres. It is discovered that the inside sheaths' fibres are weak and brittle, making it challenging to remove them[178] .

2.5.3.2.1.2 Characteristics of Banana Fibers

In addition to its many other qualities, banana fiber has unique physical and chemical features that contribute to its high quality.

1. Banana fiber resembles ramie and bamboo fiber in appearance, although it is finer and spinnable than both of them.
2. The three components of banana fiber are cellulose, hemicellulose, and lignin.
3. The fiber is quite strong.
4. The elongation is smaller.
5. It seems relatively sparkly, depending on how the extraction and spinning processes were carried out.
6. It is lightweight.
7. It has a high capacity to absorb moisture. It quickly both absorbs and releases moisture.
8. Because it is environmentally benign and biodegradable, it can be categorised as eco-friendly fibre.
9. Its average fineness is 2400Nm.
10. It is possible to spin it using nearly every technique, including ring, open-end, bast fiber, and semi-worsted spinning, among others.

2.5.3.2.1.3 Applications of Banana Fiber

Banana fiber had very little use in the past; it was mostly used to make ropes, mats, and other composite materials [179, 180]. But as environmental consciousness and the need for sustainable materials have increased, banana fibre has been more widely known for all of its advantages and is now being used in a variety of different industries, such as the home furnishings, aerospace, automotive, and apparel sectors[180]. However, it has been used in Japan to make traditional clothing like kimonos and kamishimo since the Edo era (1600–1868). Because it's comfortable and lightweight, many continue to choose it for their summer wardrobe.
Banana fibre is also used to make purses, tablecloths, curtains, neckties, and other delicate products. Rugs made from banana silk yarn fibres are quite popular all over the world.[181-183].

2.5.3.2.1.4 Surface Modification of Banana Fiber

Although banana fibers are more affordable, less dense, recyclable, and abundant in nature than synthetic fibers, they do have certain drawbacks of their own, including a tendency to absorb moisture, quality fluctuations, thermal instability, and wettability [184-186]. The hemicellulose is primarily responsible for the ability to absorb moisture. Furthermore, the hydrophilicity of lignocellulosic biofiber rather than the hydrophobicity of resin causes poor interfacial bonding at the fiber-matrix interface, which diminishes the mechanical properties of natural fibre composites[187]. Strong interfacial bonding results in poor stress transfer between the fibre and matrix, which reduces the mechanical strength of natural fibre composites, as Wang et al.[188] had researched. Furthermore, the reactive functional groups at the surface are hidden by pectin and waxes, which further hides the interaction with the matrix. The process of altering the surface characteristics of unprocessed natural fibers by applying different physical and chemical treatments results in a decrease in the fiber's absorption of moisture and an increase in the interfacial bonding between the fibre and the resin. boosts the mechanical strengths of natural fibre composites[187]. The following are a few typical surface modification methods:

2.5.3.2.1.4.1 Physical methods

The physical surface characteristics of the fibre are changed by physical treatment techniques in order to improve the connection between the fibre and matrix. Nevertheless, there is no chemical structural change at the fiber's surface [189]. The following are the most often utilized physical treatment techniques.

2.5.3.2.1.4.1.1 Plasma treatment

One type of electric discharge is plasma therapy, which balances the concentrations of positive and negative particles in the ionized gas inside the tube based on macroscopic volume and duration [190]. One efficient technique for physically altering a surface is plasma treatment. More than chemical modification techniques, plasma treatment has been demonstrated to improve the fiber-matrix's thermal resistance and interfacial strength [191]. The process of plasma treatment increases the fibers' hydrophobicity [192]. Thermal and non-thermal plasma treatments are the two types of plasma treatment. Either air pressure or vacuum can be used for the plasma therapy [190]. Other well-liked surface treatment techniques for the physical treatment of fibre surfaces include corona treatment and cold plasma.

2.5.3.2.1.4.1.2 **Ultrasound modification**

The process of ultrasound treatment involves breaking down saccharides using ultrasonic vibration. The primary components of lignocellulosic fibres, cellulose and hemicellulose, allow natural fibres to absorb water[187]. Saccharide breakdown is facilitated by the use of ultrasonic therapy to natural fibre [193]. The removal of lignin, pectin, hemicelluloses, and other surface contaminants by ultrasound treatment at varying temperatures strengthens the fiber-matrix adhesion in composites. Additionally, compared to untreated fibers, the composites have demonstrated greater thermal stability and less moisture absorption [194]. Chang et al. [195] claims that combining chemical treatment with ultrasonic assistance yields better results than utilising chemical treatment alone.

2.5.3.2.1.4.1.3 **Ultraviolet modification** or **UV modification**

Another method that has been suggested for altering the surface of banana fibers is ultraviolet modification. The chemical composition and mechanical characteristics of banana fibre are altered by UV treatment. It is discovered that the fiber's UV treatment greatly increased its tensile strength and young's modulus values [196]. Abdullah Al Kafi et al's research [197] indicates that composite tensile strength, impact strength, tensile modulus, and impact modulus values were higher for UV-treated fibres. According to M.M. Rahman et al. [198] , the UV pre-treatment of the fibre increased its tensile capabilities because of the "inter-cross linking" that UV radiation causes between the cellulose molecules in the fiber's adjacent molecules.

2.5.3.2.1.4.2 **Chemical methods**

It has been demonstrated that chemical treatment methods increase the interfacial adhesion between the fibre and matrix and reduce the amount of water that the fibres absorb[199]. The success of chemical treatment techniques in improving fibre matrix compatibility, fibre fitness, and fibre strength in natural fiber reinforced composites(NFRCs) has varied depending on the chemical reagent used [200]. For the purpose of improving mechanical interlocking and bridging the hydrophilic features of cellulosic fibre with the hydrophilic plastic matrix employing bifunctional molecules with intermediate properties, chemical treatment procedures are usually employed to remove lignin and wax from the fiber's surface[201]. Poor adhesion between fibre and matrix is one of the main issues with NFRCs, and this is mostly because of the fiber's hydrophilic nature and the matrix's hydrophobic nature. Poor adhesion is caused by the polar natures of the matrix and fibre[200]. However, if the surface properties of the fibre are specifically altered to improve interfacial bonding, high interfacial adhesion can be attained. This might potentially be achieved by chemically modifying the surface properties of fibres through chemical grafting, chemical coating, and chemical coupling of fibres with suitable additives that contain desirable functional groups[187]. Improved adhesion between the lignocellulosic fibre and the matrix results from chemical treatment of the fibre[202]. For thermoset matrices, altering the fibre by a variety of chemical processes has been proposed and implemented[203, 204]. The most effective method to increase fibre matrix adherence has been demonstrated to be the application of alkali treatment in conjunction with other coupling agents such as titanates and silanes[202, 204-207]. Before, a number of different approaches were taken to increase integrity. While the physical method concentrates on surface roughening, the chemical process results in changes to the crystal structure and increases compatibility by reducing the hydrophilicity of the fibre and isolating weak areas like lignin and hemicelluloses from it[137, 190]. It is also evident that the treatment's concentration and duration have a significant impact on the fiber's properties[208]. Chemical treatment procedures are those types of modification that entail altering the chemical structure of the fibre surface by a chemical reagent reaction. In this study, alkali treatment was used.

2.5.3.2.1.4.2.1 **Alkali treatment**

Natural fibres can have their surface properties altered chemically by applying an alkali or NaOH treatment, which has been demonstrated to be very successful in improving the mechanical properties of composites made of natural fibres[199]. The process of alkylation

enhances the interfacial adhesion between the matrix and fibre[209]. Thus, improving the stress transfer [210]. The fiber's thermal properties are improved by alkylation because it eliminates wax layers and surface impurities[211].

Fiber-OH+NaOH ⟶ Fiber-O-Na+H_2O

Natural fibres are treated chemically by being immersed in a solution containing a known concentration of NaOH for a set period of time at a steady temperature. The alkaline treatment aids in removing lignin, hemicellulose, waxes, and oils from the fibre surface to promote improved bonding between the fibre and resin[212]. When fibre is treated with NaOH, the fibre cell membrane swells, forming an amorphous area on crystalline cellulose. Alkylation decreases the fibers' propensity to absorb water by breaking down alkali sensitive hydrogen bonds and forming new reactive hydrogen bonds[213, 214]. It is possible to argue that the elimination of micro voids results in a more uniform fibre surface and improved bonding. Furthermore, a rise in aspect ratio following a decrease in diameter enhances stress transmission[215]. On the other hand, above-average alkali concentration produces delignification in excess, weakening fibre, and should be rigorously avoided[188, 200]. Therefore, mercerisation, alkylation, or alkyl treatment is a useful technique for boosting the strengths of composites made of banana fibres[216-218].

2.5.3.2.1.4.2.2 **Silane treatment**

During the silane treatment process, silane bonds to the fibre surface through a number of stages, including condensation and hydrolysis. When humidity and hydrolysable alkoxy groups are present, silane changes into silanol, which then combines with cellulose hydroxyl to improve fiber-matrix adhesion and increase the fiber's strength[200, 219]. By means of Siloxane Bridge, a chemical connection can be formed between the resin and the cellulose fibre surface thanks to the composition of silane coupling agents, which are bifunctional siloxane molecules. Moreover, it supplies the hydrocarbon chains that prevent fibres from expanding into the matrix [188]. According to

Valadez-Gonzalez et al. [220] , composites treated with silane performed better in mechanical tests than composites treated with mercerisation. Seki [221] investigated the effects of silane treatment on the bending behaviour of composites made of jute, polyester, and epoxy.

2.5.3.2.1.4.2.3 **Acetylation** or **acetyl treatment**

Cellulosic fibres are plasticised via the well-known "esterification method" of acetylating natural fibres. Acetyl groups take the place of the OH group at the fibre surface's cell walls after chemical treatment‘‘acetic anhydride (CH_3-C (=O)-O-C(=O)–CH_3)”. The fibre surface cell walls' hydroxyl groups are removed and replaced with acetyl groups by the chemical modification process using acetic acid. The fibres become hydrophobic due to this change in chemical makeup, which improves their compatibility with hydrophobic polymer matrix[222].

2.5.3.2.1.4.2.4 **Benzoylation** or **benzyl treatment**

Benzoyl chloride is the main reagent used in benzoylation treatment. When a benzoyl group is added to the fibre, its hydrophilic character decreases and it becomes more compatible with hydrophobic matrix[38].

2.6 Numerical Modeling

The mechanical characteristics of foam composites made of epoxy can be determined through a variety of experimental verifications and by using numerous mechanical models included in software programs like Abaqus, ANSYS, CIRCLY, ASTRAN, STRAND, and many more.
[223]. When predicting experimental outcomes, numerical modeling is employed; it is more economical and time-efficient than conducting actual research. During the composite production process, modeling helps engineers feel less stressed [47, 224, 225]. After the model is developed and validated, it can be used for simulation to observe how the composite behaves under different condition[226, 227], this simulation was performed in this study which satisfy the objectives four and five of the current study. In particular, in areas such as sandwich panel constructions where numerous materials were involved, the micromechanical model can be utilized to anticipate the optimal mix of constituent materials to be used for composite manufacture and to meet design considerations for the materials. These models can provide insights into the basic workings of reinforcement. The foam composite is simulated in to forecast its distress performance using the mechanical reaction models included in software programs like Abaqus.

2.6.1 Finite Element Analysis

FEM describes an indirect identification method that uses eigenfrequencies and experimental examination of a composite plate specimen to forecast the mechanical properties of composites. Madke and Chowdhury[228] have employed corresponding numerical eigenvalue analysis and optimization methods to model debonding during interphase to analyze fiber-matrix debonding. Both the surface between the fiber and the matrix, known as the interface, and the zone in the matrix phase known as the interphase, which has a limited thickness and is influenced by fiber, are thought to be bonded and have a thickness of zero. And using (ABAQUS) as a computational program for modeling and simulating. Lisle et al. [229] utilized the ANSYS program's finite element approach to estimate bending stress and forecast the gear teeth design on the ANSYS workbench.

The mechanical strength of glass fiber/resin polyester, glass fiber/resin epoxy, and glass fiber/PVC foam under tensile loading conditions was investigated by Shohel et al. [230] in ANSYS and ANSYS ACP. Their study has demonstrated that glass fiber bonded with resin epoxy composite has a higher life cycle and high stress-bearing capacity compared to glass fiber/resin polyester and glass fiber/PVC foam. Faizan and Gangwar [231] prepared the car roof panel made of carbon fibre-reinforced polymer composite material and tested its mechanical strength.

Furthermore, FEM is more accurate than the multilayer elastic approach and can handle complex loading situations, including static, dynamic, and spatially distributed forms.

The application of FEM to solve any problem consists of three separate stages, as shown in Figure 2.8.

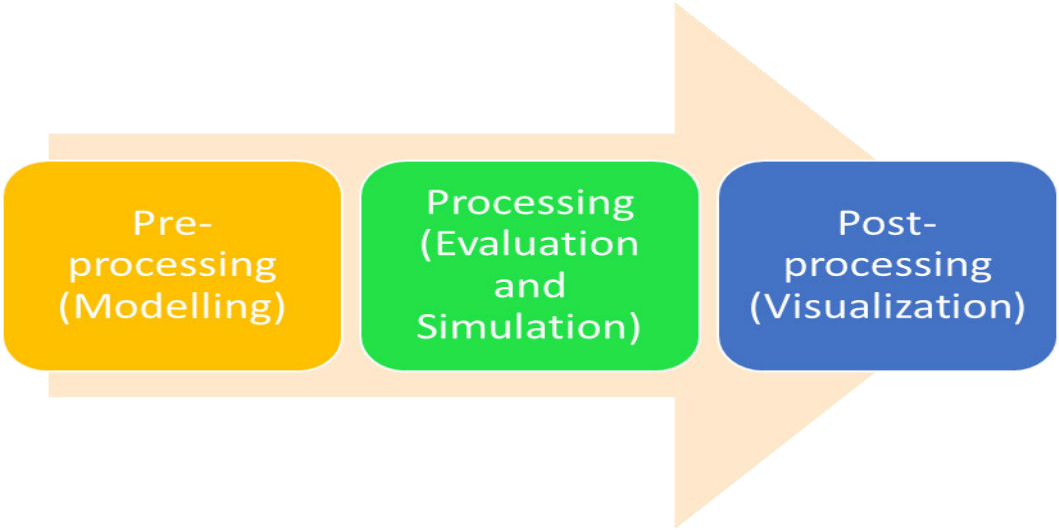

Figure 2.8: FEM application stages (Abaqus 2013)

2.7 Summary of the Review:

Based on the information presented in this chapter, it is clear that sandwich composites and hybrid-filled foam cores are most useful in various marine applications especially for fabrication of ship propellers and hulls because their combination of mechanical and thermal properties are more beneficial to marine industries than nomax honeycomb, kraft honeycomb and syntactic foam which have been in use previously. Therefore, we present a method through which our research study takes into account using two fillers for the processing of hybrid-filled foam cores. Furthermore, Chapter 3 discusses in detail the materials, methods, and processing techniques adopted in this study to fabricate hybrid-filled foam composite core and sandwich foam composite panel.

CHAPTER THREE

3.1 Materials, Manufacturing and Methods

3.1.1 Introduction

The materials, equipment, and techniques used in this work are covered in this chapter. Testing, testing standards, characterizations and analyses performed in this work are also discussed in this chapter. The Figure 3.1 shows the summary of experimental design carried out in this work.

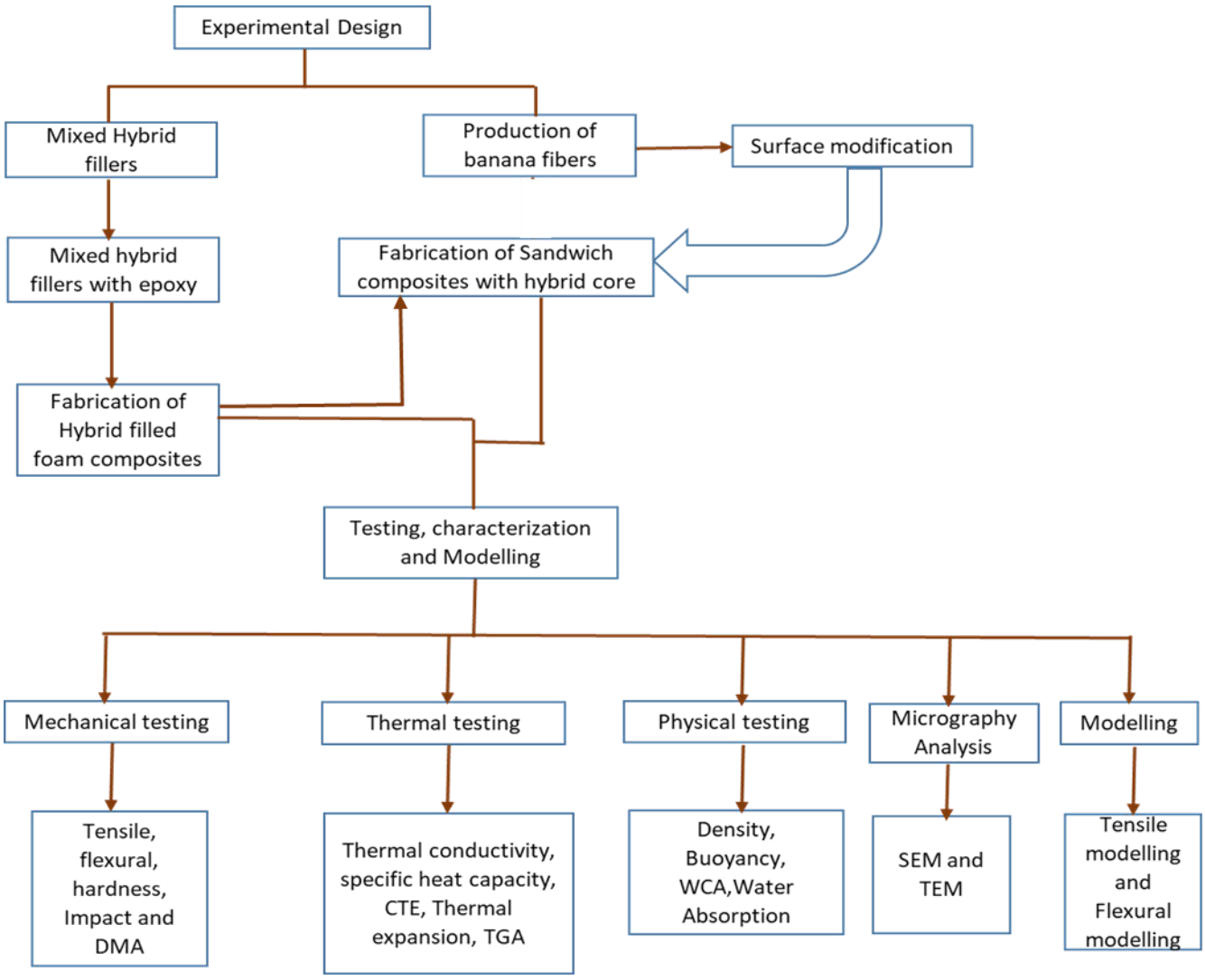

Figure 3.1: Experimental design Summary

3.1.1.1 Materials

Table 3.1 shows the properties of the hollow glass microsphere (HGM) and nanoclay specifications from the manufacturer.

Table 3.1:Hollow glass microspheres(HGM) and Nanoclay specifications from the manufacturer

Materials	Appearance	True density g/cm^3	Particle size µm
HGM-7019	White Powder	0.19	5-150
Nanoclay-25A	Cream powder	0.19	2-13

The materials utilized to create hybrid-filled foam composites (HFFC) are listed in Table 3.2.

Table 3.2: Materials that were used for fabrication of hybrid-filled foam composite (HFFC)

Materials	Supplier
Diglycidyl ether of bisphenol „A‟ (DGEBA) epoxy resin (LR 30)	AMT Composite, Durban. South Africa
Cycloaliphatic amine-based hardener (LH30)	AMT Composite, Durban. South Africa
Cloisite® 25A clay was natural montmorillonite (MMT) USA.	Southern Clay Products, Inc., USA.
Hollow glass micro balloons (HGM 7019)	AMT Composite, Durban. South Africa

Table 3.3 shows the materials that were used for the fabrication of the sandwich foam composite.

Table 3.3: Materials for SFCs

Materials	Supplier
Diglycidyl ether of bisphenol „A‟ (DGEBA) epoxy resin (LR 30)	AMT Composite, Durban. South Africa
Cycloaliphatic amine-based hardener (LH30)	AMT Composite, Durban. South Africa

Cloisite® 25A clay was natural montmorillonite (MMT)	Southern Clay Products, Inc., USA.
Hollow glass micro balloons (HGM 7019)	AMT Composite, Durban. South Africa
Banana fibers	Reddcolt Enterprises in India

Table 3.4: Materials used for HGM-filled foam composite with compatibilizer

Materials	Supplier
Diglycidyl ether of bisphenol „A" (DGEBA) epoxy resin (LR 30)	AMT Composite, Durban. South Africa
Cycloaliphatic amine-based hardener (LH30)	AMT Composite, Durban. South Africa
Hollow glass micro balloons (HGM 7019)	AMT Composite, Durban South Africa
Maleic anhydride grafted polypropylene (MA-g- PP)	VladaChem Gmbh Germany 76316, Malsch, Bruhruckstra, 14a

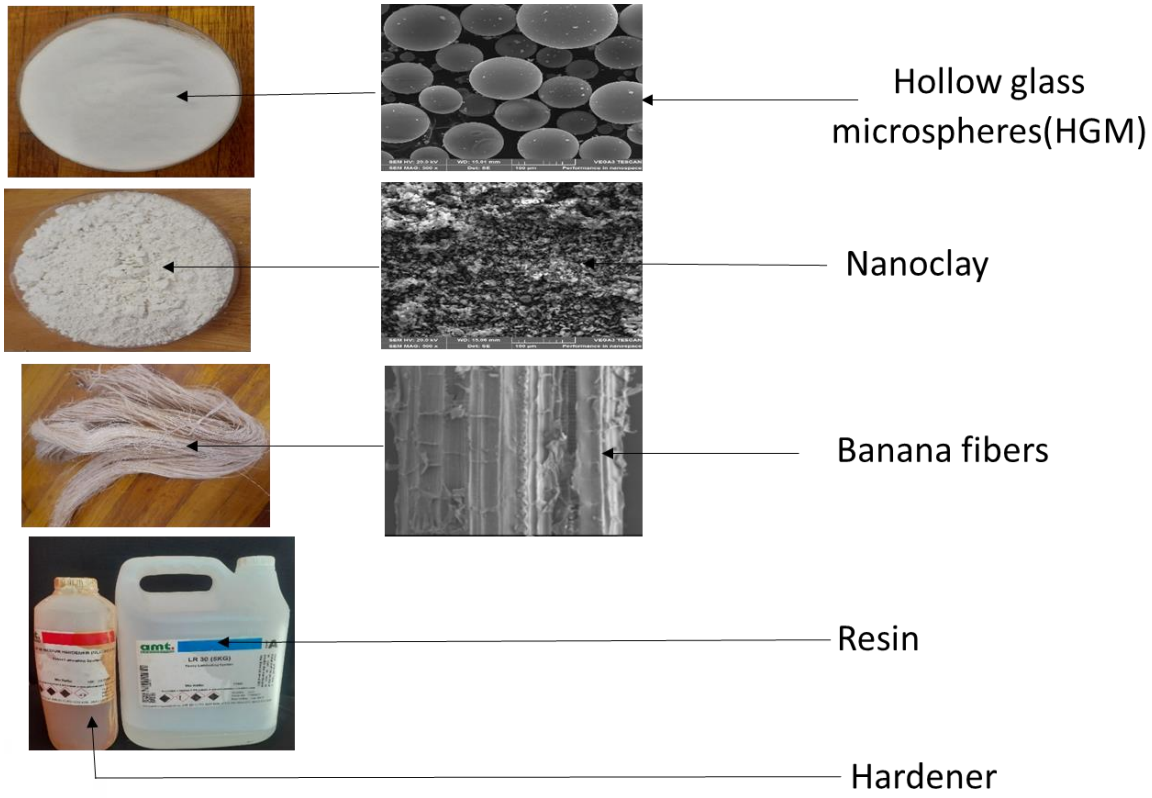

Figure 3.2: Figure 3.2:Materials for hybrid-filled foam cores and sandwich composite

Table 3.5: Densities of constituent materials used for sandwich composites

Constituent Materials	Density(g/cm^3)
Banana fibre [x]	1.20
Matrix resin [y]	1.13
Sandwich composite [x]	1.157
HGM [y]	0.19
Clay [y]	0.19

[x] Calculated

[y] As received from the supplier

3.1.1.2 Fabrication Methods of Foam Composite Core with Sandwich Foam Composite

3.1.1.2.1 Fabrication of Hybrid filled Foam Composite core

The epoxy-based foam panel was produced by weighing epoxy resin into a beaker as shown in Figure 3.3 and heating it to 60 degrees to decrease the resin's viscosity and ease the addition and mixing of hollow glass microspheres with nanoclay. To create a homogeneous mixture, epoxy resin, HGM, and nanoclay were combined using a magnetic stirrer running at 500 RPM for 60 minutes. As directed by the manufacturer, 10:20 was the weight ratio of epoxy resin to hardener in a calibrated beaker. After that, HGM with nanoclay was added according to the volume fraction for each sample preparation. The volume of HGM varied from 1-3%, while nanoclay also varied from 1-5% for each of the HGM-filled series. The selection of the lower percentage of these fillers were considered because of Strength and Stiffness; while hollow glass microspheres reduce the density and contribute to buoyancy**,** they can also reduce the strength and stiffness of the composite. At higher percentages, the microspheres may not provide sufficient reinforcement, leading to lower tensile strength**,** flexural strength, and modulus. A lower percentage helps maintain the structural integrity of the composite while a lower percentage of nanoclay ensures compatibility with other fillers and also ensures that it does not interfere with the synergy between different reinforcements or disrupt the overall composite matrix. The mixture prepared was poured into a silicon mold. To make removing the foam composite panel from the silicon mold easier, silicon grease was applied to the mold's

surface before filling it. After the foam panel had cured for 24 hours at room temperature, tensile, flexural, and impact test samples were cut from it using a cutting grinder equipped with fine-grit abrasives to ensure a flawless cut while reducing surface damage. Also, it should be noted that when the concentration of HGM and nanoclay is high, it will affect the curing time but it will not affect the degree of curing due to exothermic heat. Exothermic heat will influence the curing of epoxy more strongly and accelerate its curing process in proportion to its thickness.

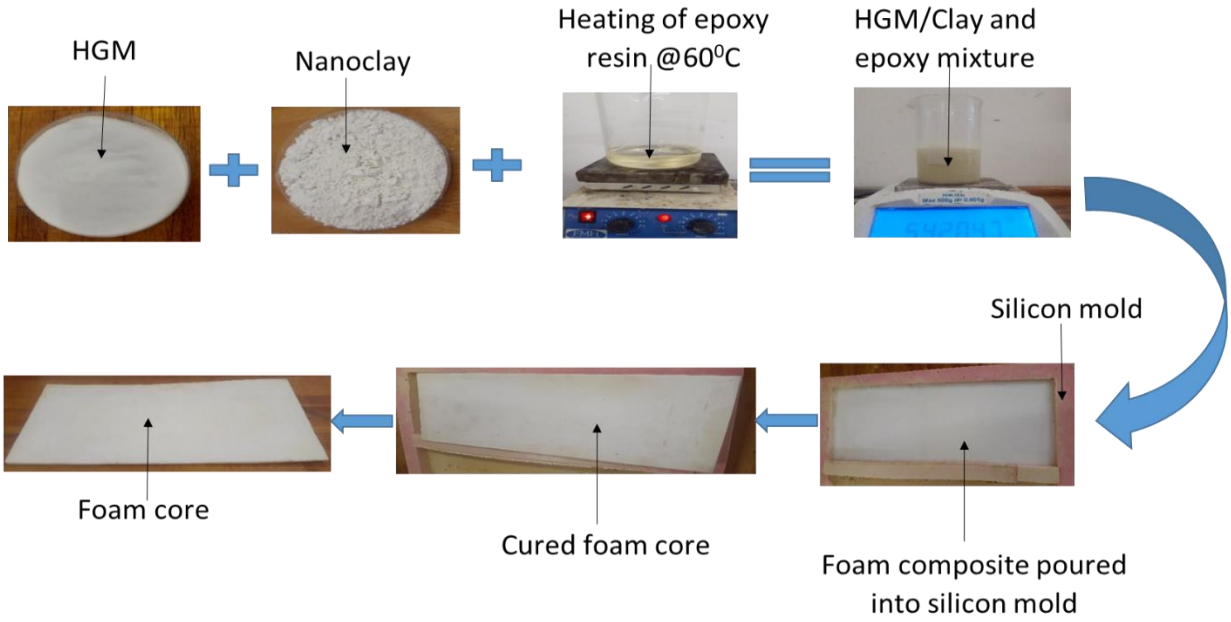

Figure 3.3: Manufacturing process of hybrid filled foam core

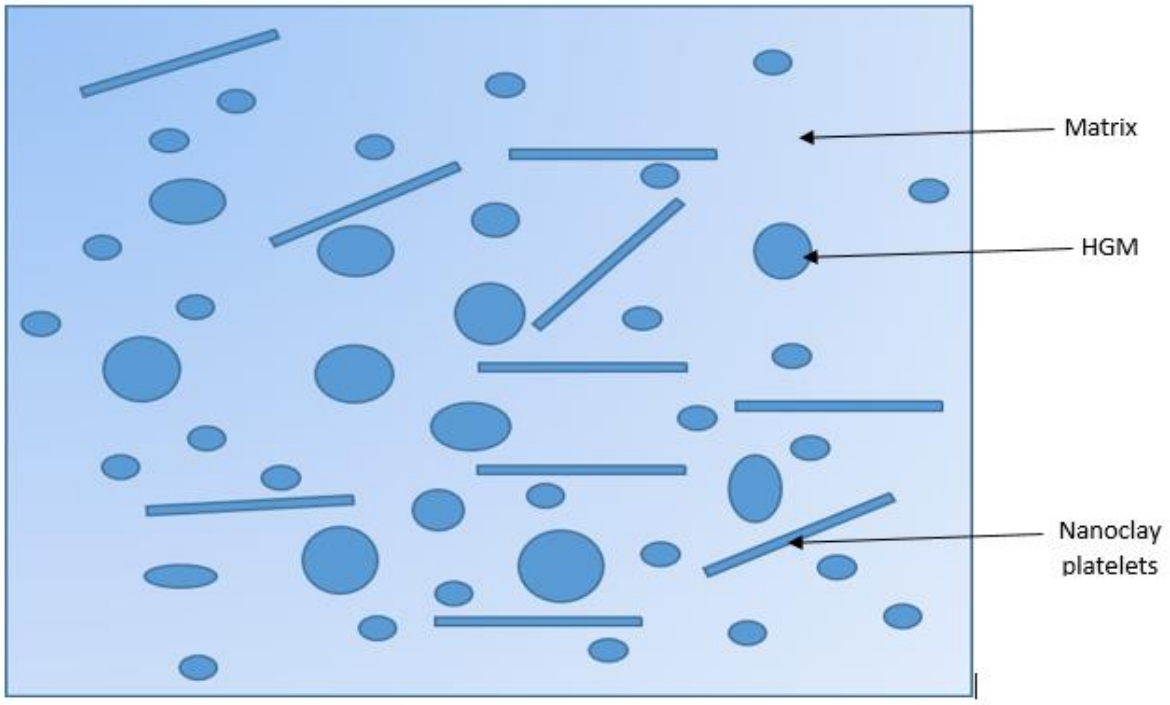

Figure 3.4: Schematic diagram showing the HGM/Clay and Matrix structures in the foam composite

3.1.1.2.2 Surface modification of banana fibers

Unidirectional fibers were used in this work because unidirectional fibers align all the fibers in a single direction, making them stronger and stiffer in that direction[232, 233]. This is especially important for fabrication of marine structures like ship propeller where high strength and stiffness is required. Also, unidirectional fibers provide efficient load transfer along the fiber direction. Since the fibers are aligned, they can efficiently bear the load and resist tensile, compressive, and shear forces along their axis[234, 235]. Literature reported that modification of fibers brings about positive effects that improve interfacial adhesion [36, 37, 137, 236-238]. Chemical modification was chosen in this work among all other available fiber modification techniques. This is because chemical modification is relatively cheap and easily performed [161]. Sodium hydroxide (NaOH) was used as the surface modification chemical as seen in Figure 3.6 due to its ability to alter the chemical structure and improve the interfacial bonding between the natural fibers/fillers and polymer matrix in foam composite materials[239, 240]. This surface treatment can significantly enhance the mechanical and physical properties of the resulting composites. Additionaly, NaOH treatment can increase the fiber's hydrophilicity by opening up the fiber surface and introducing additional hydroxyl groups. The increased hydrophilicity improves the wetting of fibers by the polymer matrix, leading to better fiber-matrix adhesion. This can also

improve the durability of the composite, especially in moisture-prone applications. The chemical treatment conditions used in this work were selected based on literature [37, 238, 241-245]. The banana fibers were in dry state before the surface modification because water is considered a contaminant most of the time[246]. However, it has been proven that, thanks to its unique structure and physicochemical properties, water might lead to particular interactions like polarity[247], hydrogen bonding[248], hydrophobic effects[249], and trans-phase interactions[250]; therefore, it determines the reaction course[246]. Drying of treated banana fibers was done at room temperature for 7 days.

3.1.1.2.3 Fabrication of sandwich foam composites with hybrid core (SFCHC):

The production of sandwich panel with banana fiber facesheets and the HGM/Clay hybrid core method includes the production of unidirectional banana fiber laying up, surface modification of the fibers, and the actual fabrication of the sandwich foam panel.

Production of sandwich panels was made using a banana fibers facesheet. Before the composite was put into the mould, the banana fibres were first evenly aligned in a single direction to prevent misalignment. Then, they were completely soaked with resin to prevent weak points.

. The fiber length was an average of 30 mm. A standard hand lay-up technique is used to create the sandwich composite panels, and then a moderate compression molding operation is performed. It was created by sandwiching the hybrid-filled core between the sandwich composites' top and bottom face sheets as seen in Figure 3.6. By varying the volume fraction loading of fillers in the hybrid core, nine groups of sandwich composite samples were produced. Table 3.6 shows the identification of the hybrid core composition in the sandwich composite while in chapter 6, Table 6.1 shows the experimental density and theoretical densities of the sandwich composites developed for this study. Figure 3.5 depicts a schematic representation of sandwich composite production. The hybrid core was inserted as needed between the top and bottom facesheets of the sandwich composites. Banana fibers were prepared in a unidirectional method with (14.68g) by weight and 1.2mm thickness each as top and lower facesheet. The selection of 1.2 mm thickness for each of the facesheets and 14.68 g weight in the facesheet design can be justified based on a combination of structural performance**,** the expected panel properties**,** weight optimization**,** thermal resistance, and manufacturing considerations for ship propeller and hull in marine structures. This thickness offers a balance of mechanical strength and protection, while the weight aligns with performance and cost-effectiveness goals, ensuring the composite meets application-specific requirements, particularly in industries such as

aerospace, automotive, and high-performance structural components. The size of the panel created for each sample was $300\times 140 \times 5.4mm^3$. The angle for overlaying the facesheet was $0^0/90^0$ for all the sandwich composites. A± 0.01mm discrepancy in facesheet thickness was discovered, which can be explained by undulation during the fiber laying up process. For quick and easy removal of the sandwich composite material, wax was applied on the surface of the mold. By using a gradual mixing method and a spatula to gently push any bubbles that might have formed to the surface during composite preparation, care was taken to prevent the formation of air bubbles during the preparation process.

Careful control of material handling, processing conditions. For efficient bonding, epoxy adhesive was used and thereafter a 50Kg load made of mild steel material was applied from the top, but before then a flat sheet plate made of neat epoxy material was placed on the panel for even distributions of resin in the facesheet of the sandwich panel, and the mold was then allowed to cure at room temperature for 48 hours. After 48 hours, the samples were removed from the mold and post-cured in a 70°C oven for 4 hours before cutting into the required size for tensile, flexural, impact, and water uptake tests with specifications according to their respective ASTM standards and tested accordingly. Each sandwich composite formulation was tested with three samples.

Table 3.6: Designation and detailed composition of the sandwich panel

Sandwich Composite notation	Composition
EPF	Filler(0%)+Epoxy(100%)
1HF	HGM(1%)+ Clay(0%)+Epoxy(99%)
1H1CF	HGM(1%)+ Clay(1%)+Epoxy(98%)
1H3CF	HGM(1%)+ Clay(3%)+Epoxy(96%)
1H5CF	HGM(1%)+ Clay(5%)+Epoxy(94%)
3HF	HGM(3%)+ Clay(0%)+Epoxy(97%)
3H1CF	HGM(3%)+ Clay(1%)+Epoxy(96%)
3H3CF	HGM(3%)+ Clay(3%)+Epoxy(94%)
3H5CF	HGM(3%)+ Clay(5%)+Epoxy(92%)

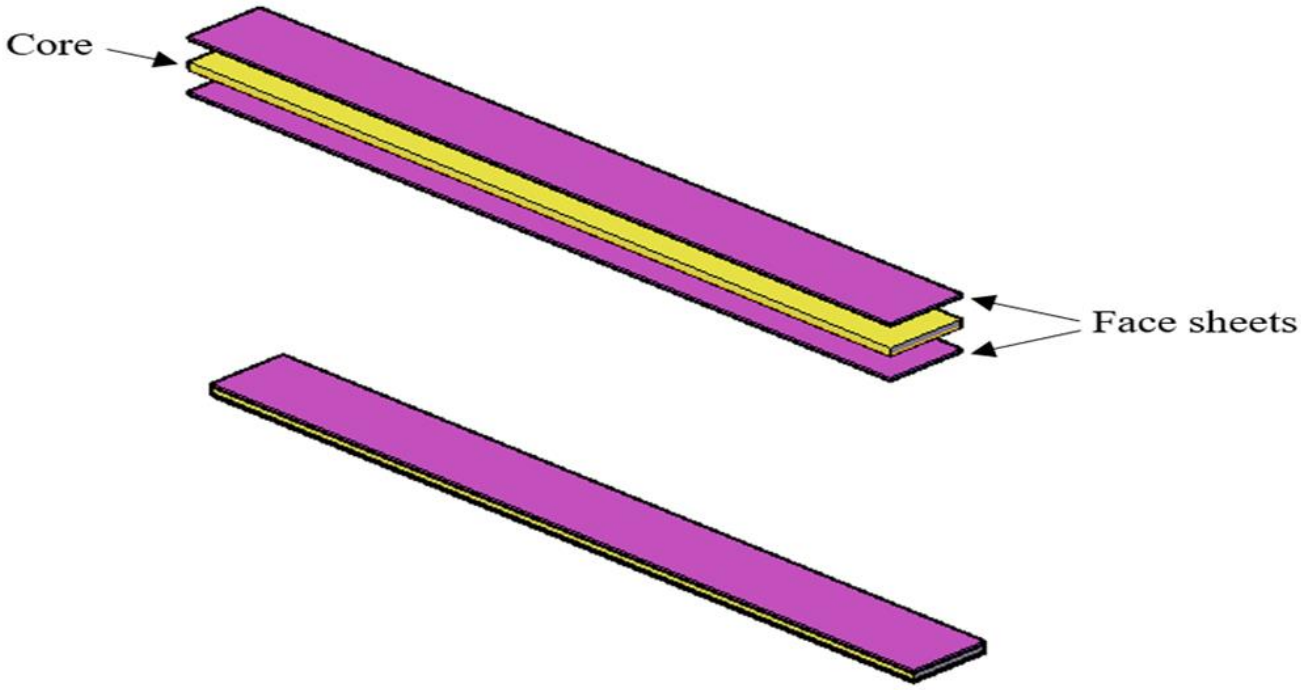

Figure 3.5: Figure 3.5: Schematic illustration of Sandwich composite panel

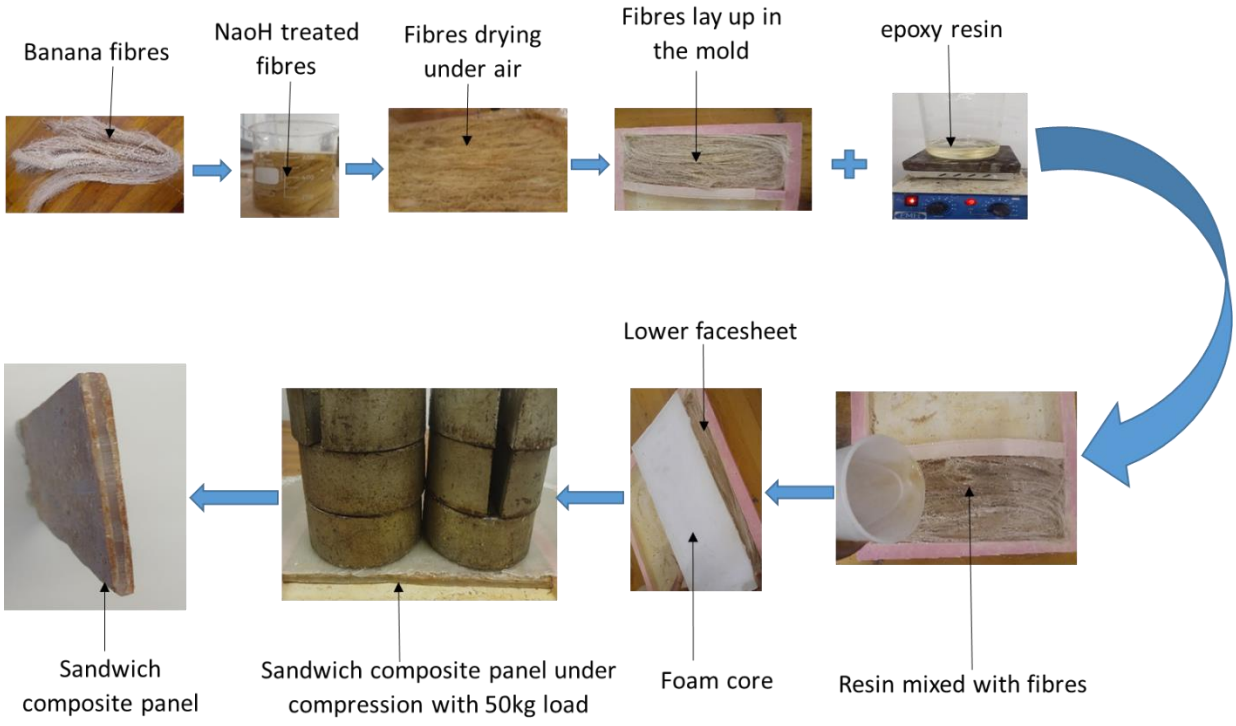

Figure 3.6: Fabrication sequence of sandwich composite panels

3.1.1.2.4 Fabrication of Foam composites with compatibilizer

The foam composites were created by using a hand lay-up casting method. [251]. The procedure has been reported in our earlier work [252]. Table 3.7 shows the composite foam formulations of HGM and PP-g-MA. The volume by weight of HGM varied from 0% wt. to 5%wt. The uniform mixture prepared as shown in Figure 3.7 was poured into the silicon mold. Silicon grease was applied to the surface of silicon mold before pouring it into the silicon mold so that the foam panel could be removed with ease. [253]. The foam panel was allowed to cure for a full day at room temperature following curing, and after that, samples for mechanical properties and water contact angle tests were cut from the foam composite panel with the use of cutting grinder with fine-grit abrasives so as to obtain smooth cut by minimizing surface damage.

3.1.1.2.4.1 Surface modification of HGM filler with compatibilizer

HGM fillers were placed in a vacuum drying box, it was dried for 24 hours at 80^0C. The HGM were then added to a (3:1) combination of ethanol and water with polypropylene-grafted maleic anhydride (PP-g-MA) (3%). This mixture was then heated to 75^0C, washed with distilled water, and dried under vacuum at 80^0C. This process was carried out for attaching hydroxyl groups on the surface of the HGMs for successful subsequent reaction. After that, a volume fraction of modified HGM (1%, 3%, and 5%) was added to epoxy resin. The mixture was heated to 70^0C and stirred for six hours using a magnetic stirrer. A hardener was subsequently added to the mixture. After that, the mixture was put into a mold and allowed to cure for a whole day. At 70^0C, post-heat treatment was carried out for four hours.

Table 3.7: Foam composite sample formulation with HGM and PP-g-MA content

Samples	Epoxy resin(wt.%)	HGM(wt.%)	PP-g-MA(wt.%)
Neat epoxy	100	0	0
1% wt.HGM	99	1	0
1%wt.HGM+ PP-g-MA	96	1	3
3% wt.HGM	97	3	0
3%wt.HGM+ PP-g-MA	94	3	3
5% wt.HGM	95	5	0

5%wt.HGM+ PP-g-MA	92	5	3

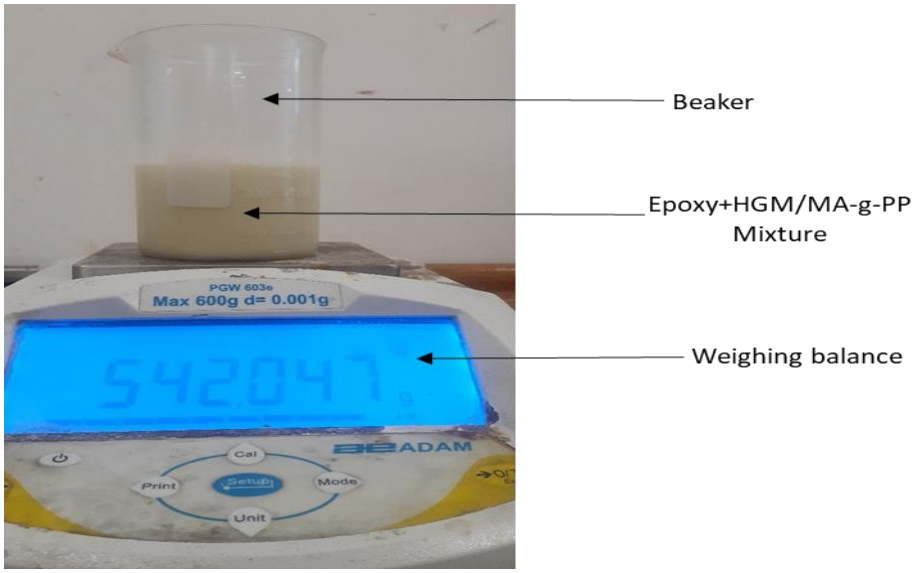

Figure 3.7: HGM-filled foam composite mixed with PP-g-MA

Table 3.8:Lists of Characterization Techniques Performed in the study

Microscopy analysis	Purpose of the test
Scanning electron microscopy(SEM)	Determination of distribution of particles, porosity and defects within the samples produced and also fracture surface of the samples produced
Transmission electron microscopy(TEM)	To reveal details about the microstructure of including defects and phase distribution

Mechanical test	Purpose of testing
Tensile test	To determine the maximum tensile stress that a panel can bear before failing or cracking.
Flexural test	To measure the force required to bend the samples and to determine its resistance to stiffness
Impact test	To determine the impact resistance and performance of the panel to sudden mechanical stress
Hardness	To measure the panel's resistance to indentation or penetration

Physical test	Purpose of the test
Water contact angle(WCA)	Measure the samples wetting behavior and surface interactions with water
Buoyancy	Measure the floating behavior of the panels
Water absorption	Determination of the panel's resistance to water uptake
Density	To determine the mass per unit volume of the panel

Thermal tests	Purpose
Thermogravimetric analysis(TGA)	Determination of the thermal stability of the panels by monitoring their weight loss or gain as a function of temperature
Dynamic mechanical analysis(DMA)	This is to study the viscoelastic properties of panels as a function of temperature, frequency, or time
Coefficient of thermal expansion(CTE)	To quantify how a panel's dimensions change in response to changes in temperature
Specific heat capacity	To the determine the panel's ability to store and release thermal energy per unit mass when subjected to temperature changes
Thermal conductivity	To determine/quantify how the panel conducts heat

3.1.1.3 Characterizations of foam Composite

3.1.1.3.1 Physical Property

The physical properties of HFFC such as density, water contact angle, water absorption and buoyancy were carried out because they affect the functionality of the composite material

3.1.1.3.1.1 Density

Theoretical density can be achieved concerning weight fraction based on the rule of the mixture and was calculated with the equation below. In contrast, the experimental density was calculated using a specimen specification of 25×25×12.5mm^3, according to Ajayi et al.[254]. Four specimens were prepared from the foam composite panel, and the mean results were recorded

$$\mathfrak{c}_{th} = \left(\left(\frac{W_{fH}}{\mathfrak{c}_{fH}} \right) + \left(\frac{W_{fC}}{\mathfrak{c}_{fC}} \right) + \left(\frac{W_m}{\mathfrak{c}_m} \right) \right)^{-1} \quad [3.1]$$

The volume fraction percentage of voids (Vv) in the foam panel is calculated by equation (ii) below:

$$V_v = \frac{\mathfrak{c}_{th} - \mathfrak{c}_e}{\mathfrak{c}_{th}} X\ 100 \quad [3.2]$$

$\mathfrak{c}_{th}$ = theoretical density

$\mathfrak{c}_e$ = experimental density

W_{fH} = weight fraction of HGM filler

W_m = weight fraction of matrix

$\mathfrak{c}_{fH}$ = corresponding density of the HGM filler

$\mathfrak{c}_m$ = corresponding density of the matrix

W_{fC}= weight fraction of nanoclay filler

$\mathfrak{c}_{fC}$= corresponding density of the nanoclay filler

3.1.1.3.1.2 Water Contact Angle (WCA)

To determine the surface hydrophobicity of hybrid filled foam composites, contact angle experiments are typically performed. By measuring the contact angles of specific liquids on the epoxy-based foam composites, it is often possible to evaluate the interactions (interfacial energy difference) between fillers and the polymer matrix. To evaluate the wetting behavior of foam composite panels, the DropMeter A-100 contact angle system (Maist Vision Inspection & Measurement Co. Ltd.) was utilized for the water contact angle experiment, which was carried out utilizing the sisal drop method[255]. The foam composite panels (60 mm × 10 mm × 3 mm) were put on a rectangular glass slide, and droplets of deionized water were dropped at five different locations on the foam composite panel's surface using a micro syringe of 25μL. The water contact angle was determined by measuring the contact angles at room temperature and calculating the mean of the obtained values.

3.1.1.3.1.3 Water Absorption Capacity of Hybrid filled foam Cores (HFFC) and Sandwich foam composites (SFC).

The maximum percentage of water absorption for the manufactured HFFCs and SFCs was investigated under ASTM D570-98 standard. The samples were completely submerged in the distilled water and were taken out from the water after 24 h of immersion. Then the samples were weighted after all the water of the surface was removed with a clean dry cloth. This procedure was regularly repeated at an exposure of 24,48,72,96,120,144,336 and 720 hours. The water-absorption percentage is calculated using the following equation 3.3

$$\% \text{ water absorbed (D)} = \frac{(\text{wet weight } (W_f) - \text{dry weight (Wi)})}{\text{Dry weight (Wi)}} \times 100 \qquad [3.3]$$

For this study, the maximum weight gained W(s) was measured at saturated water absorption, or when the variance in weight acquired after 7 days (168 hours) is less than 0.1%. W(i) is the initial measurement made after the specimens were submerged in the distilled water for more than 24 hours. At the hybrid-filled foam cores' maximum moisture absorption, the diffusion coefficient W(d) is written as

$$W(d) = W(s) - M(i) \qquad [3.4]$$

3.1.1.3.1.4 Buoyancy Force Determination of HFFCs and SFCs:

The upward force that a fluid exerts in opposition to an object's weight when it is partially or completely submerged is known as buoyancy. The samples of neat epoxy, HFFCs, and SFCs were immersed in a 400 ml test tube filled with water according to research by Afolabi and Nergaard etal. [256, 257]. For accurate comparison, the submerged HFFCs and SFCs had the same weight. The experimental result related to the buoyancy of the sandwich has been published[258]. In the water-filled test tube depicted in Figure 3.8, three specimens each were immersed. Variations in the fluid's density under gravity give rise to the force of buoyancy. The buoyant force is determined by the Equation 3.15:

$$Fb = Vo \times D \times Fg \qquad [3.5]$$

where Fb (N) is the buoyancy force acting on the object, Vo (m^3) is the volume of the submerged object, D (Kg/m^3) is the density of the fluid the object is submerged in, and Fg is the force of gravity

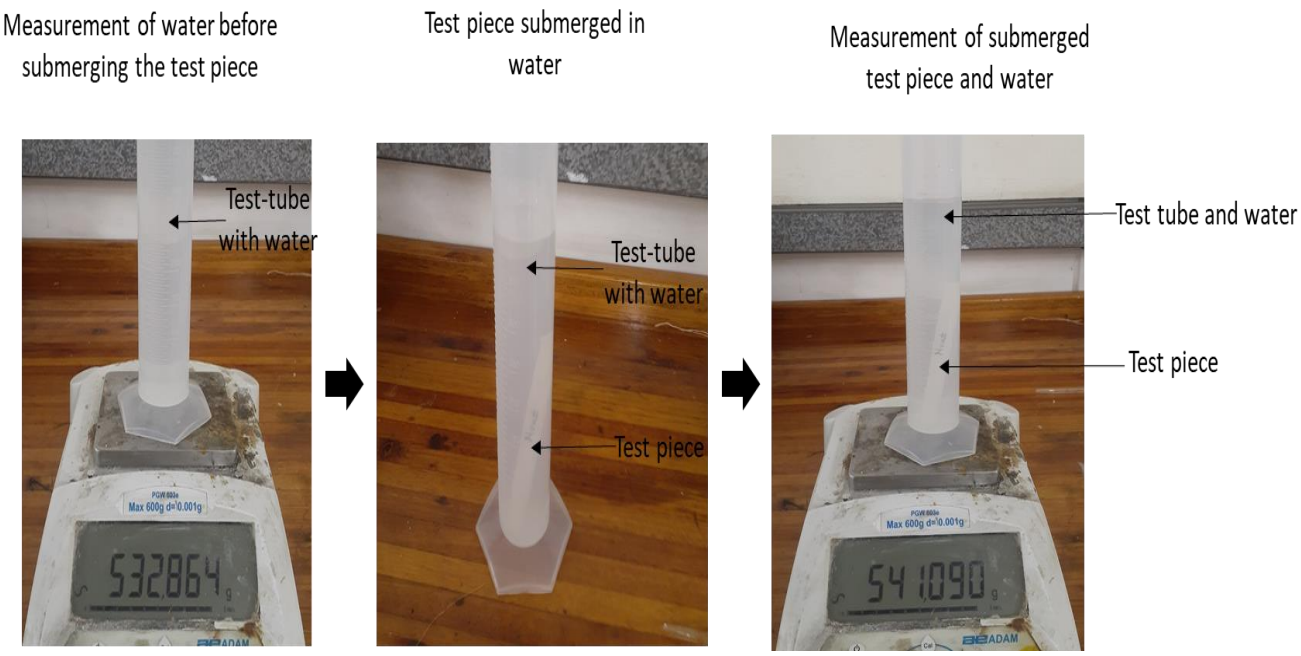

Figure 3.8: Buoyancy measurement procedure for HFFCs and SFCs

3.1.1.3.1.5 Thermal Conductivity, Coefficient of Thermal Expansion(CTE) and Thermal Expansion

For each of the new hybrid filled foam composites, thermal conductivity testing was done. The Unitherm Model 2022 is used to measure the thermal conductivity of the developed composites. According to the ASTM E-1530 Standard, the tests are conducted. One polished surface, controlled at a different temperature than the other, holds a sample of the material being tested under a uniform compressive load. To create an axial temperature differential in the stack, heat moves through the sample from the higher to the lower surface. Once thermal equilibrium is reached, the output from the heat flow transducer and the temperature differential across the sample are monitored. After that, the thermal conductivity is computed using these values and the sample thickness. The experimental results related to this study have been published[259]

Using a Perkin Elmer DSC-7 Thermal Mechanical Analyzer, the glass transition temperature and the composites' coefficient of thermal expansion are determined. During the measurement, the specimen is heated from 30°C to 150°C at a heating rate of 5°C/min. For each measurement, two heating scans are used. The purpose of the initial heating scan is to get rid of any potential internal tension and moisture that might have been created during the sample preparation and curing procedures. The material's Tg and CTE are ascertained using the second heating scan.

3.1.1.3.1.6 Thermogravimetric Analysis (TGA)

The thermal decomposition behavior of the hybrid-filled foam composite was analyzed using a thermogravimetric analyzer (TGA). This was performed on a combined differential scanning calorimeter and thermogravimetric analyzer, model SDT Q600 V20.9. ASTM E 1131 – 08 was followed in performing the thermal decomposition analysis [260]. Specimens were heated at a rate of 10 °C/min in the presence of nitrogen that was flowing at 100 ml/min from a temperature of 20 °C to 600 °C.

3.1.1.3.1.7 Dynamic mechanical analysis

Dynamic mechanical analysis (DMA) of the foam composite panels was conducted on a dynamic mechanical analyzer (DMA) Q800 V21.2. The tests were carried out according to ASTM D4065-01 [261]. DMA was done in three-point bending mode on a support span of length 50mm at a frequency of 1Hz and amplitude of 20 µm. The heating temperature was ramped from 25 ^{0}C (room temperature) to 80 ^{0}C at a rate of 3 0C/min. Specimen dimensions of 60 mm x 10 mm x 3 mm were used and three specimens were tested per sample. The glass transition temperatures (Tg) were determined from the midpoint of the loss modulus peak and tandelta peak based on literature [262-265].

3.1.1.3.2 Basic mechanical testing

Basic mechanical testing of the specimens fabricated in this work consist of hardness test, impact test, tensile strength testing, and testing for flexural properties. The interaction between the reinforcement and the matrix determines an HFFC's mechanical properties rather than the reinforcement acting alone. The following variables, among several others, are anticipated to affect an HFFC's mechanical performance:

• wettability and interfacial bonding,
• the volume fraction of the fillers,
• thermal stability,
• dispersion of the fillers in the matrix,
• fiber orientation,
• the crystallinity of the matrix
• the density of the filler material of HFFCs generally possesses good stiffness and tensile characteristics.

3.1.1.3.2.1 Impact

Using a Hounsfield Balance Impact Tester made by Tensometer Ltd., Croydon, England, Charpy tests were carried out at room temperature to ascertain the impact resistance of sandwich foam composite panels and fabricated hybrid-filled foam composite panels. As per ASTM D6110-10, the Hounsfield Balance Impact Machine features a three-point calibration device. [266]. The test specimens' geometric dimensions were measured and they were cut from foam panels to measure 50 x 10 x 3 mm^3. This technique allowed for fluctuation in the specimen's width for varying materials, whether brittle or ductile. The impact values should represent the width specified in the specification, which encompasses the measurable. The impact breadth is 6 mm by the width area in all specimens due to a notch that is 4 mm deep in the middle of the section opposite the impact part. Figure 3.9 revealed the experimental set-up for the V- notch Charpy test. For every foam panel formation, five specimens were evaluated, and the impact velocity was roughly 6.7 m/s. The following formula was used to determine energy absorption based on the average values that were gathered.

$$IS = \frac{AE}{TW} \qquad [3.6]$$

IS: impact strength (kj/m^2)

AE: absorbed energy (Joule)

T: specimen thickness (m)

W: Remaining width at notch (m)

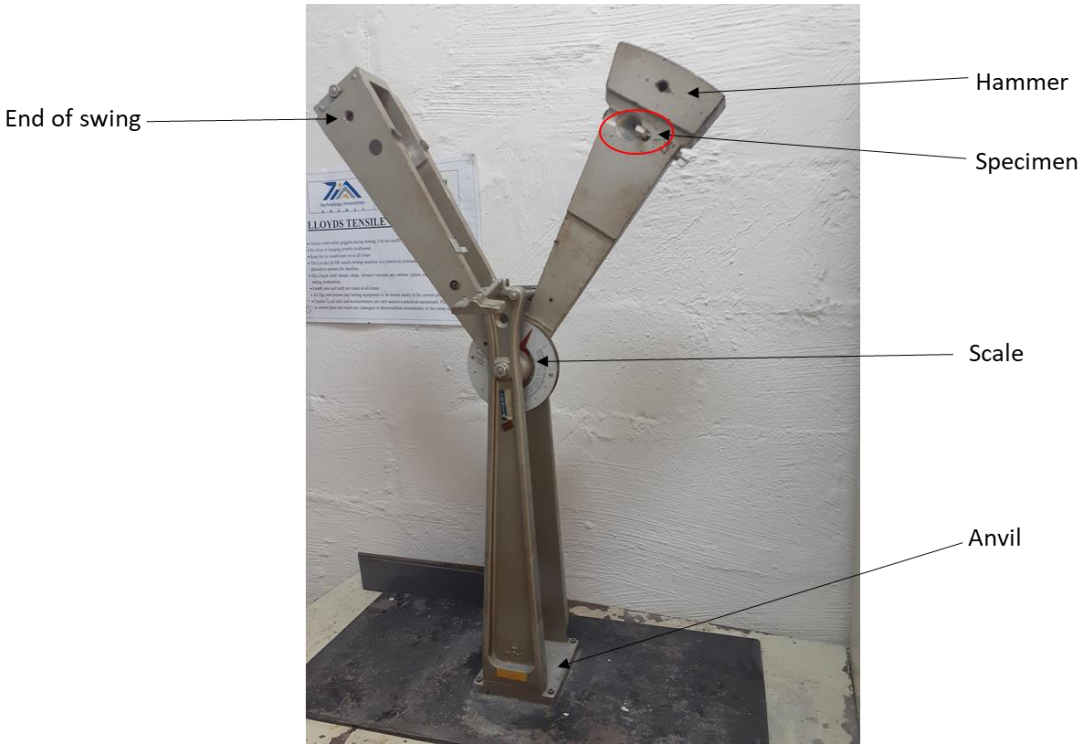

Figure 3.9: Hybrid-filled foam composite sample under impact test

3.1.1.3.2.2 Hardness

The foam composite panel's hardness was ascertained using a Barber Colman Barcol impressor hardness tester, which is appropriate for testing both individual specimens and manufactured products for production control. The ASTM D 2583 test standard specification was followed for conducting the hardness test [267]. As seen in Figure 3.10, the hardness test measures the depth of the indenter tip penetration to determine a material's indentation hardness. Specimens' hardness was measured using the Barcol impressor (model GYZJ-934-1) hardness tester, which is frequently used for composite materials. This impresser features an intender, or hardened steel truncated cone, angled at 260 degrees and with a 0.157 mm diameter flat point. Fitted into a hollow spindle, this was secured in place with a spring-loaded plunger. To balance on the testing specimen surface, it additionally features an indenter leg. Placing the Barcol impressor indenter point parallel to the sample plate was done, following Figure 3.10. To record the maximum value on the dial indicator, a consistent downward push was manually applied until it reached that point. A graphical depiction was created by taking the mean value of twenty indentation values that were randomly selected from samples.

Figure 3.10: Figure 3.10: Barcol hardness test being conducted on hybrid filled foam composite core's surface

3.1.1.3.2.3 Tensile strength testing

Testing for the tensile strength of the foam composite was performed following ASTM D3039 [268]. The tests were conducted on a universal testing machine (UTM), Model: MTS Criterion Model 43, and computer-controlled by MTS Suite software. The machine has a capacity 30 kN (in both the tension and compression modes), a sensitivity of 2.214 mV/V, and data acquisition rate of 10 Hz. The crosshead speed was 2 mm/min. The length, width and thickness of the foam composite specimens for tensile strength tests were 250, 25, and 3 mm, respectively. The gauge length was 150 mm. Five specimens were tested for each of the foam composite samples and relevant calculations on mean tensile strength values, strain at break, and Young's modulus were done. Figure 3.11 demonstrates how the specimens were mounted on the UTM machine.

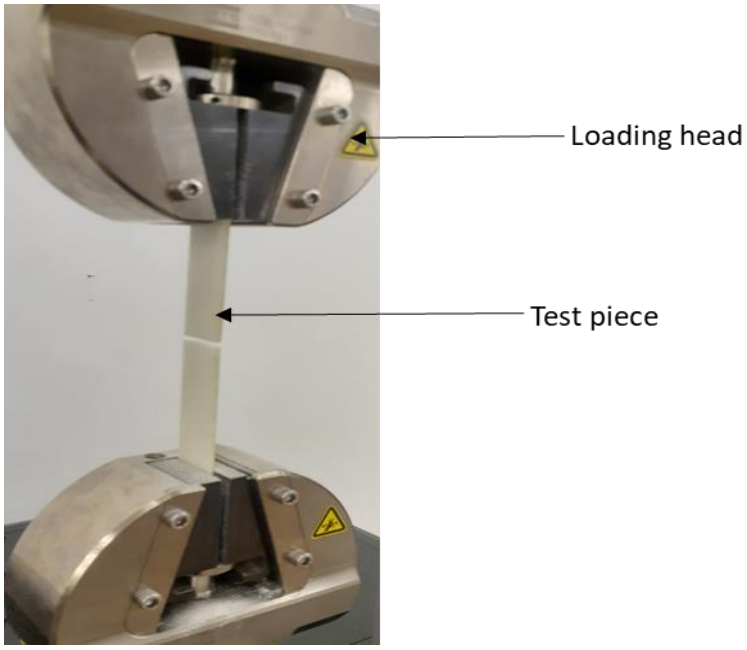

Figure 3.11: Hybrid-filled foam composite sample under tensile test

3.1.1.3.2.4 Flexural tests

The sandwich composite panels and hybrid-filled foam composite panels underwent flexural testing to evaluate their stiffness and strength. A three-point bending flexure test was performed following ASTM D790-03 test standard [269]. As illustrated in Figure 3.12, the technique made use of a supported beam with a center loading support span and a span-to-thickness ratio of 16:1.

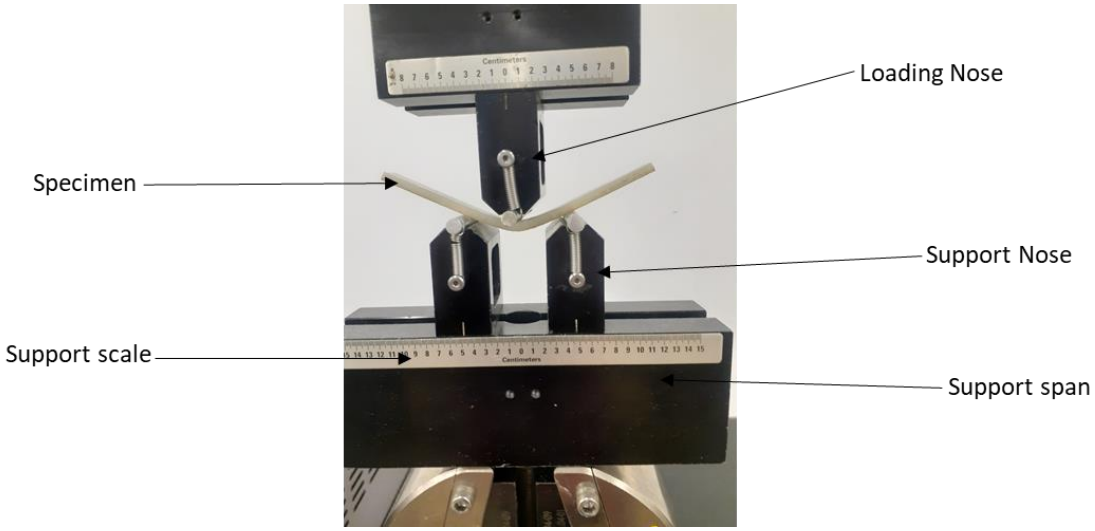

Figure 3.12: Three-point bending test of hybrid-filled foam composite specimen on a simply supported beam

The nominal thickness was 3 mm, width was 12.7 mm and the span length was 48 mm. The total length of each specimen was 128 mm. The foam composite specimens were deflected until they ruptured in the outer surface and in instances where rupture was not going to be achieved, the test would be stopped when a maximum strain of 5% was reached. The rate of straining was 0.01 mm/mm/min. Each foam composite sample was tested five times, and the average flexural strength and modulus values were determined. The rate of crosshead motion was calculated using Equation 3.7 [269] and set on the machine

$$R = \frac{XL^2}{6d} \quad [3.7]$$

Where:

R is the rate of crosshead motion (in mm/min),

L is the support span (in mm),

d is the thickness of the panel in mm,

X is the rate of straining of the outer exterior (in mm/mm/min) and it is taken as 0.01.

Using Equation 3.7, the rate of crosshead motion to be used during the tests was 1.3 mm/min. The tests were conducted in a displacement control mode. The test was to be terminated when the maximum strain experienced by the outer (exterior) surface of the foam composite specimen had reached 0.05 mm/mm and the deflection at which this strain occurs is calculated using Equation 3.8

$$D = \frac{rL^2}{6d} \quad [3.8]$$

where:

D is the mid-span deflection (in mm),

r is the strain in mm/mm and is taken as 0.05,

L is the support span (in mm),

and d is the thickness (depth) of the specimen in mm.

Using Equation 3.8, the mid-span deflection was 6.4 mm. Flexural stress (σf) was calculated using Equation 3.9 [269]:

$$\sigma f = \frac{3PL^2}{bd^2} \quad [3.9]$$

where;

σf is the stress (in MPa) at the exterior surface at the mid-span of the specimen

P is the load (in N) at a given point on the load versus deflection curve

L is the support span (in mm)

b is the specimen width (in mm)

d is the thickness (depth) of the specimen (in mm)

Flexural strain (εf) was calculated using Equation 15 [269] :

$$Ɛf = \frac{6Dd}{L^2} \quad [3.10]$$

Where,

Ɛf is the flexural strain in the exterior surface (mm/mm)

D is the maximum deflection of the center of the specimen (mm)

d is the thickness (depth) in mm

L is the support span in mm.

The modulus of elasticity, EM (tangent modulus of elasticity) is determined using Equation 3.11[269] :

$$E_M = \frac{L^3 m}{4bd^3} \quad [3.11]$$

where,

E_M is the bending modulus of elasticity (MPa),

L is the support span in mm,

b is the specimen width in mm,

d is the thickness (depth) in mm, and

m is the gradient of the initial straight-line portion of the load versus deflection curve, with the unit's N/mm of deflection.

3.1.1.3.3 Morphological Properties

3.1.1.3.3.1 Scanning Electron Microscopy (SEM)

It was used to study the microstructure of HGM, nanoclay, hybrid-filled foam cores, and sandwich foam composites using a Zeiss EVO 1 HD 15 Oxford instrument X-max scanning electron microscope (SEM). Before SEM (Carl Zeiss) observation, the specimen was gold coated for the flow of electrons using a Quorum Q 150R ES machine for 6 minutes.

3.1.1.3.3.2 Transmission Electron Microscopy

The transmission electron microscopy resolution performed on the foam composite was used to transmit the bean of electrons of the hollow glass microscope to form an image. The image was formed because of the interaction between the electrons and the foam composite, and was examined with the aid of a higher resolution transmission electron microscopy (HR-TEM) Joel 2100, from Japan.

3.1.1.3.4 Sandwich Foam Composites

3.5.2.1 Density Measurement The density of the sandwich foam composite was measured to track physical changes in hybrid-filled foam samples and sandwich composites. The measured density was calculated according to ASTM C271-94 [270]. Since density is equal to mass/volume in Equation 3.12 Therefore, volume is equal to mass/density in Equation. 3.13. Then the volume of the sandwich composite was calculated by adding the volumes of all the constituent materials together using Equation 3.14.

$$ɕ = m/v \quad [3.12]$$

$$v = m/ɕ \quad [3.13]$$

$$Vs = Vf + VH + Vcl + Vm \quad [3.14]$$

where Vs, Vf, VH, Vcl, and Vm are the sandwich composite volume, banana fiber volume, HGM volume, clay volume, and matrix resin volume respectively (cm^3). The volume fraction of each constituent material is then calculated using Equation. 3.15

$$ɕ = m/v \quad [3.15]$$

where V is the volume fraction.

$$Vc = V_H + V_{cl} + V_f + V_m \quad [3.16]$$

The sandwich composite density is therefore calculated using Equation 3.17

$$ɕ_C = ɕ_H V_H + ɕ_{cl} V_{cl} + ɕ_f V_f + ɕ_m V_m \quad [3.17]$$

The percentage difference between the measured and theoretical density is taken as the matrix porosity (void) content using Equation 3.18.

$$Pc = \frac{ɕ_{th} - ɕ_e}{ɕ_{th}} X\ 100 \quad [3.18]$$

Where Pc is the sandwich composite porosity, ɛth is the theoretical density, and $ɛ_e$ is the experimental density.

3.1.2 Numerical Response Analysis

3.1.2.1 Geometry of Foam Composite Mix Samples

Since its highly accurate results indicate that the epoxy-based foam composite samples modelled in Abaqus software possess the most probable inclusive simulation of the actual problem, 3D modeling of the samples is part of this study. When composite structures are exposed to service loads, numerical response analysis provides a comprehensive and clear method for calculating the reaction rate of the structures.

The samples were modeled following the experimental sample dimensions measuring 250mm×25mm×3mm in length, width, and thickness for tensile and 150mm×14mm×3mm in length, width, and thickness for flexural was modeled

3.1.2.2 Model Description

A micromechanical model was used to predict the mechanical properties of the model composite based on the properties of its constituents and by considering the filler distribution as random and constant. For a completely random distribution of fillers, the distribution function is constant, as the distribution is assumed equal in all directions.

$$Ec = Vf(\frac{16}{45}Ef + 2Em)\frac{8}{9}Em$$

Where Ec is the elastic modulus of the composite, Ef is the elastic modulus of the filler, Em is the elastic modulus of the matrix, and Vf is the volume fraction of the filler. The invariant properties of composites defined by Tsai and Pagano[271] were used along with Puck's micromechanics formulation to develop equation[272] .For predicting the breaking strength of the composite, the equation by Piggott was used as a good approximation. In his fiber theory, Piggott considered for the elastic and plastic effects in the matrix.

Thus, for composites having fillers/fibers which are random in 3D, the suggested an upper strength is,

$$\sigma c = \frac{1}{5}\sigma f Vf + \sigma m Vm$$

Where σc, σf, σm, stand for the tensile strengths of the composite, the filler, and the matrix while Vf and Vm represent the volume fractions for the filler and the matrix and these are required as an input data for defining the material in ABAQUS.

b. Model geometry development

1. Part development

The composite specimen considered in this study is assumed isotropic for hybrid-filled foam core only. Therefore, a uniform material model was used in this work. Accordingly, the composites were developed with ABAQUS based on experimental sample dimensions measuring 250mm×25mm×3mm in length, width, and thickness for tensile and 150mm×14mm×3mm in length, width, and thickness for flexural was modeled

2. Assembly

The finite element method (FEM) was used to model the crack location.

3. Property definition

Section creation and section assignment are other procedures to be completed under the property definition module

4. Step

A basic concept in ABAQUS is the division of the problematic history into steps. In its simplest form, a step can be just a static analysis, in ABAQUS/Standard, of a load change from one magnitude to another. This process can be imitated with the constant rate of loading (CRL) type of the tensile testing machines. The step definition includes the type of analysis to be performed and optional history data, such as loads, boundary conditions, and output requests. ABAQUS has two measures of time in a simulation. The first is the total time, which increases throughout all general steps and is the accumulation of the total step time from each general step.

5. Load and boundary conditions (BCs)

After specifying the steps in which the loads and BCs become active, the prescribed conditions of loads and BCs, which are step-dependent, must be specified. After defining the steps in the analysis, three boundary conditions were created:

- The first BC (BC1) locates the specimen as a cell and constrains the 1, 3, 4, 5, and 6 degrees of freedom and allows the 2nd degree of freedom, which is the load to be applied only in the Y direction as a distributed load. This BC allows the distributed load to be applied in the Y direction
- For, the 3rd BC, a surface traction load was applied on the upper surface of the specimen to assign a distributed tensile load on the top face of the model composite. The load is applied during the general analysis step.
- On the third BC (BC3), the 1, 3, 4, 5, and 6 degrees of freedom will be set zero and finally the BC should be modified, the 2nd degree of freedom (U2) activated, and the

value of the distributed force shall be set. The force applied will be in the form of stress as it is applied on the surface.

6. Mesh

A free meshing technique was used for seeding the part instance and applying the mesh to the instance. This technique was used because the whole part is not partitioned into cells for easy and convenient application of the crack initiation and growth.

7. Job

With the Job module, a job is created, submitted for analysis, and its progress can be monitored. If there is no error in the previous steps performed, the submitted job will be completed successfully and the output will be prompted for the visualization module, which will be discussed in the results section. Several jobs have been run by varying the crack location and five outcomes were selected for better simulation and comparison of the five experimental tests

3.1.2.3 Material Characterization of Foam Composite Mix Samples

The samples of foam panel mix may have any one of the following three types of model characteristics: viscoelastic, elastic, or visco-elastoplastic. However, because of the non-convergence of the elastic model, this study considers the viscoelastic model. The laboratory (tensile and flexural test) results for samples in terms of stress and strain were plotted in MATLAB software using the curve fitting tool to obtain the Prony series values which helps in the non-linear material characterization of the samples through equation 3.19. It is worth noting that R square values for each of the mixes have a good correlation ranging from 0.97 to 0.99. The results Prony series and other material characterization used to effectively model and simulate foam composite mix samples in Abaqus (Table 3.8)

$$G'(\omega) = (Ge) + \frac{£iGi\omega^2\tau i^2}{1+\omega^2\tau i^2} \quad [3.19]$$

Table 3.9: Material characterization and Dimensionless Prony series coefficients input in Abaqus® for the foam composite mixture

Neat Epoxy					Density
Young Modulus	969.63	Poisson Ratio	0.280	1130	
Term	g_i	k_i	τ_i		R^2
1	0.2492	-	0.04406		**0.98919**
2	0.2071	-	1.221		
A (1%wt.HGM)					
Young Modulus	679.44	Poisson Ratio	0.278	1120	
1	0.2719	-	0.04101		**0.98951**
2	0.2258	-	1.115		
B (1%wt.HGM+1%wt.Clay)					
Young Modulus	651.39	Poisson Ratio	0.278	1110	
1	0.4142	-	0.02853		**0.99188**
2	0.3049	-	0.681		
C (1%wt.HGM+3%wt.Clay)					
Young Modulus	729.51	Poisson Ratio	0.276	1092	
1	0.3178		0.03618		**0.98997**
2	0.2559		0.9455		
D (1%wt.HGM+5%wt.Clay)					
Young Modulus	1202.6	Poisson Ratio	0.274	1073	
1	0.3741		0.07007		**0.97637**
2	0.1963		3.265		
E (3%wt.HGM)					
Young Modulus	525.67	Poisson Ratio	0.278	1099	
1	0.3191		0.03527		**0.99005**

2	0.2618		0.9137		
F (3%wt.HGM+1%wt.Clay)					
Young Modulus	768.01	Poisson Ratio	0.277	1090	
1	0.2597		0.04265		**0.98933**
2	0.2157		1.172		
G (3%wt.HGM+3%wt.Clay)					
Young Modulus	621.1	Poisson Ratio	0.275	1071	
1	0.3588		0.0322		**0.99065**
2	0.2868		0.8071		
H (3%wt.HGM+5%wt.Clay)					
Young Modulus	778.34	Poisson Ratio	0.279	1052	
1	0.2713		0.04111		**0.9895**
2	0.2252		1.118		

3.1.2.4 Boundary Conditioning, Interaction and Loading

To simulate the real experimental boundary condition, the boundary condition was chosen. Thus, both ends of the samples in terms of length were restrained from moving not only in the transversal, horizontal, and vertical direction but also no rotation allowed (i.e. the degree of freedom 1, 2, and 3) against the supports. The purpose of the fixation was to stop any displacement or rotation that could be brought on by the load's acceleration and velocity.

Furthermore, all foam composite samples meshing size control size were 0.5 and modeled using the 8-node continuum three-dimensional brick element (C3D8R) with reduced order numerical integration available in Abaqus® (6.13). C3D8R element has the capability of representing large deformation, geometric, and material nonlinearity [273]. Instead of the commonly used random mesh, sweep mesh was used for samples. On the other hand, the supports in the model were modeled as discrete rigid elements: 4-node 3-D bilinear rigid quadrilateral (R3D4). A standard load of 30 KN as in the load capacity of the universal testing machine(UTM) that was used in the experiment was applied to the sample perpendicularly at the middle length of the sample for flexural while that of the tensile was pulled apart at both ends. The experimental

results in this study have been published[254]. The contact area between the load and the sample was fixed in all direction apart from the vertical directions and all analysis are run as a visco-analyses procedure type available in Abaqus.

CHAPTER 4: INFLUENCE OF HYBRIDIZING FILLERS ON MECHANICAL PROPERTIES OF FOAM COMPOSITE PANEL

4.1 Introduction

This chapter presents discussion of the journal paper titled “Influence of hybridizing fillers on mechanical properties of foam composite panel’’, by Ayodele Abraham Ajayi, Turup Pandurangan Mohan, and Krishnan Kanny published in the Journal of Polymer Engineering Science (2023), volume 63, Issue 8, pages 2565-2577. This paper focused on enhancing the mechanical properties of epoxy-based foam composites by hybridizing HGM with clay nanoparticles.

4.1.1 Objectives of the journal paper

The major objectives of this journal paper were to:

• To fabricate novel HGM/nanoclay hybrid foam composites with improved mechanical properties.

• To investigate the efficacy of hybridizing HGM and clay nanoparticles in enhancing the mechanical performance of the epoxy-based foam composites.

• To determine the optimum HGM/clay particle content.

• To determine the interfacial bonding and microstructure characteristics of the hybrid HGM/clay epoxy-based foam composites.

4.1.2 Summary of the mechanical properties of hybrid filled foam composites.

Materials designed to combine excellent mechanical properties with low density are used to make foam composite panels, which are filled with hybrid fillers. By mixing hollow glass microspheres (HGM) with nanoclay, this work aims to enhance the mechanical properties of foam composite panels made of epoxy and hybridised fillers. The HGM content was varied from 1 wt.% to 3 wt.% in foam composite panels, while nanoclay content was varied from 1 wt.% to 5 wt.% in each of the HGM-filled series of foam composites panels, this foam composite panel was developed by employing a traditional resin casting technique. The mechanical properties such as tensile strength, impact strength, hardness, and flexural strength of the prepared hybrid-filled foam composite panels were determined and compared with the

neat epoxy. It was found that the hybrid-filled foam composite panels exhibited improved mechanical properties than the neat epoxy. Excellent interfacial adhesion between the hybrid fillers and the matrix was the reason for these enhanced properties. The enhanced mechanical properties may indicate that this material is appropriate for use in sectors requiring lightweight materials with strong mechanical properties. This study showed a new area of synthetic foam development research by enhancing mechanical properties using hybrid-filled.

4.1.2.1 Tensile Strength

Figure 4.1 shows how the percentage of HGM/nanoclay loading affects the mechanical characteristics of the foam composite panel. When the proportion of HGM in the foam composite panel was increased, it was found that the panel's tensile strength improved at that point and then reduced when the percentage of nanoclay in the foam composite grew. When the concentration of hybrid fillers HGM/nanoclay was at 3wt.%HGM+1wt.%Clay, there was a good synergy between HGM/nanoclay and matrix. When the foam composite was subjected to a load, the matrix and filler interface could absorb energy effectively[274, 275] so the tensile strength of the foam composite was increased. Nevertheless, due to the higher loading of fillers which could not effectively withstand stress delivered from the matrix because of the decrease in matrix material, this later brought about a lower thickness of the interfacial layer [66, 276]. Concurrently, the volume fraction of the foam composite's non-penetration areas and internal voids grew due to the cluster effect and the filler particles' close proximity[277, 278]. When the load was applied to the material, the filler was likely to detach from the matrix (Figure 4.1) until the foam composite was destroyed. In addition, Figure 4.1 shows that the foam composite's elongation at the breaking load decreased as the filler content increased. This occurred because adding the filler particles increased the hardness of the foam composite panel. Furthermore, the material broke before it yielded at rapid tensile loading rates.

The Neat epoxy exhibited a much greater tensile strain at failure compared to the filled materials, suggesting that the unfilled epoxy possessed superior ductility than the filled materials. The increased number of voids found in the foam composites as a result of the filler percentage applied was the cause of this performance. High loading of HGM can cause agglomeration which can lead to reduced pulling strength and stress resistance in the foam composites [91, 279]. Moreover, the decrease in the pulling strength of foam composites may be caused by the poor interfacial bond between the matrix and fillers as a result of the high loading of hybrid filled [280, 281]. However, the improvement in tensile strength observed in this study was

a result of good interfacial adhesion between the matrix and fillers in the foam composites. Furthermore, N. Gupta et al. and Barbosa A et al. [275, 282] published findings that are similar to the current study, when a slight increase in filler concentration results in an increase in tensile strength. The influence of excellent interfacial adhesion between the matrix and the HGM/nanoclay has been revealed via the fracture surfaces in Figure 3.

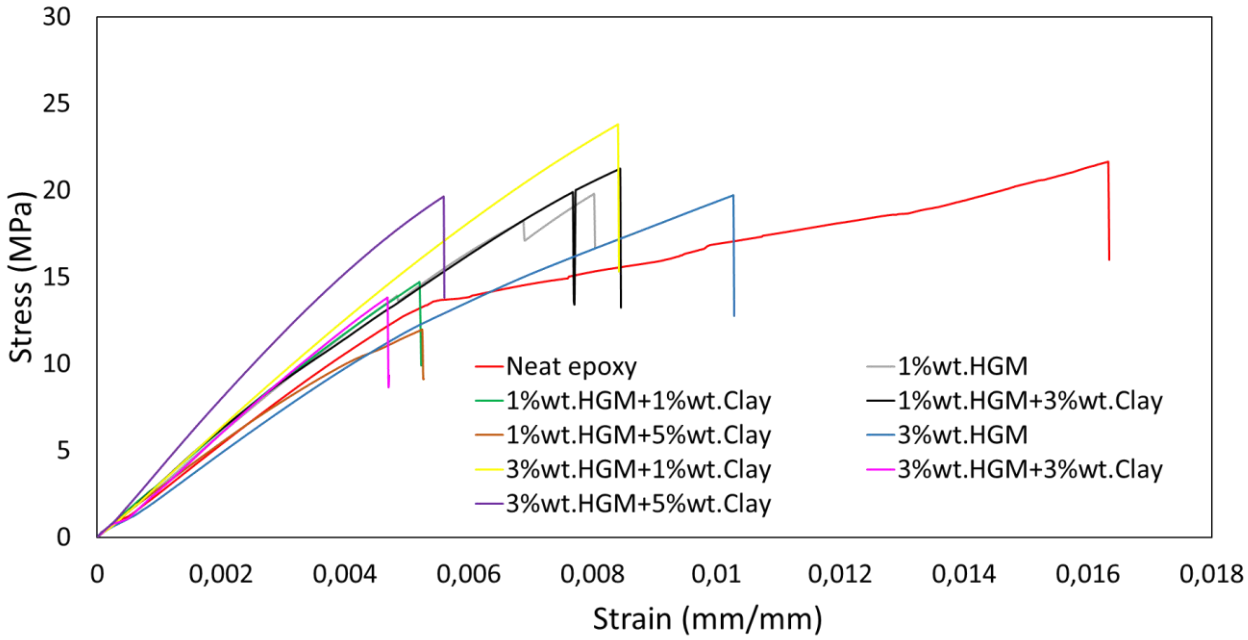

Figure 4.1: Tensile strength of Neat and HGM/Clay foam composite

4.1.2.2 Tensile Modulus

Figure 4.2 shows the tensile modulus of the hybrid foam composite series. It was noticed that the tensile modulus of composites increased with a corresponding increase in filler loading. These results align with the study by Gupta et al.[282] and Raju et al.[276], which reported that foam composites have elevated Young's modulus in different percentage concentrations of filler than neat epoxy. However, it was noticed that the tensile modulus at 1wt.%HGM+3wt.%Clay declined due to high agglomeration between the hybrid fillers and the matrix as a consequence of mixing, which triggered quick brittle failure at that point. Because of the intrinsic characteristics of hollow glass microspheres and their impact on the overall composite structure, the measured decreased tensile modulus value resulted from changes in the matrix-filler interaction at very low amounts of HGM. Additionally, because to the microspheres' low

rigidity, poor adhesion to the polymer matrix at an only 1% concentration, and propensity to interfere with load transmission and matrix continuity.

On ther other hand, the improved modulus can also be attributed to the softening improvement effect of HGM/Clay fillers in the foam composites since HGM and nanoclay have higher modulus properties than neat epoxy.

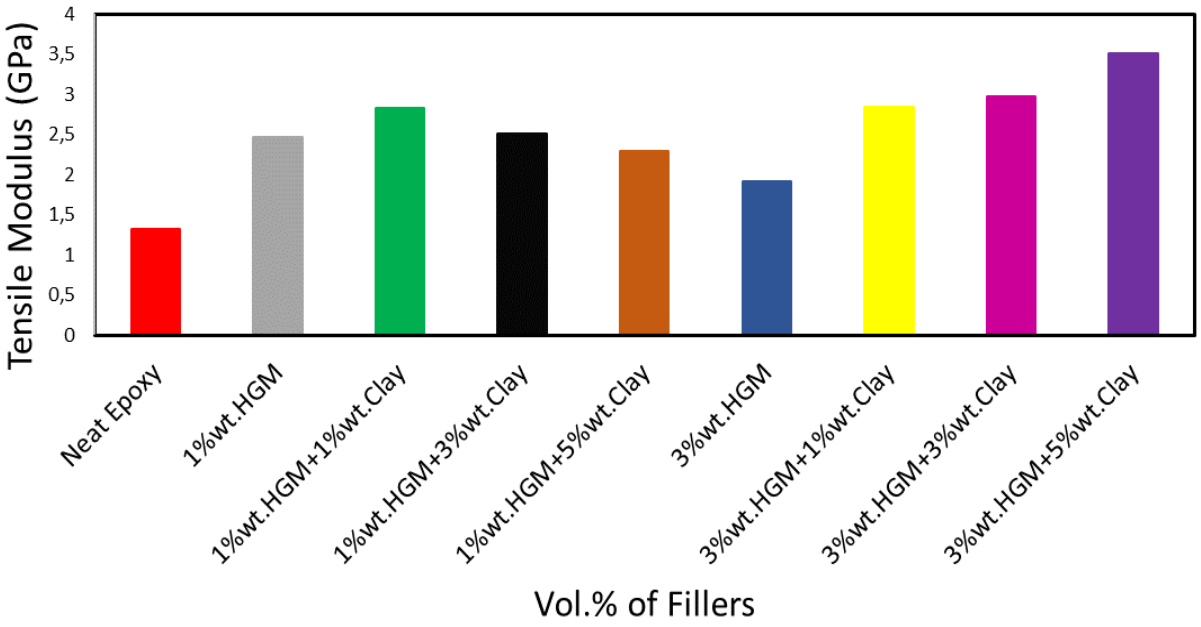

Figure 4.2:Tensile modulus versus Vol.% of filler

Table 4.1: Tensile properties of Foam composite panels

Materials	UTS (MPa)	Modulus (GPa)	Strain (mm/mm)	Specific Strength (MPa/g.cm^3)	Specific Modulus (GPa/g.cm^3)
Neat Epoxy	21.23 ± 2.5	1.32 ± 0.08	0.0163	19.538	1.195
1wt.% HGM	19.71 ± 2.6	2.47 ± 0.15	0.00798	18.559	2.326
1wt.% HGM+1wt.% Clay	14.73 ± 2.3	2.83 ± 0.17	0.0052	14.042	2.698

1wt.% HGM+3wt. % Clay	21.59 ± 2.49	2.51 ± 0.15	0.0084	20.238	2.451
1wt.% HGM+5wt. % Clay	11.93 ± 1.49	2.30 ± 0.14	0.0052	11.906	2.295
3wt.% HGM	19.67 ± 2.52	1.92 ± 0.12	0.01024	19.247	1.879
3wt.% HGM+1wt. % Clay	23.77 ± 1.29	2.84 ± 0.17	0.00836	23.488	2.806
3wt.% HGM+3wt. % Clay	13.64 ± 1.76	2.97 ± 0.18	0.0046	13.764	2.997
3wt.% HGM+5wt. % Clay	19.61 ± 1.83	3.51 ± 0.21	0.00558	20.196	3.615

4.1.2.3 Morphology Structure of Fractured Foam Panel

The morphology of tensile fractured samples of foam composites was examined under a scanning electron microscope (SEM) which is as shown in Figures 4.3(a-i).

Figure 4.3a shows the fractured surface of neat epoxy and rough plateaus micrograph on neat epoxy, indicating a brittle fracture. Meanwhile, Figure 4.3(b-i) represents the tensile fractured micrograph of foam composites with homogeneous HGM/nanoclay particle distribution. In Figure 4.3(f, h, i), a substantial cluster between the particles of the fillers and the matrix was observed in the micrograph. This cluster happened because of air entrapped in the process of mixing fillers with resin, which is obvious on the surface of the morphological structures by the tiny particles. In essence, these air bubbles are holes in the foam composite panel. Since air is not thick and does not interact effectively with light in SEM imaging techniques, these spaces will appear as dark patches in a micrograph image. The micrograph's dark patches or poor contrast regions may be signs of air bubbles that were trapped in the foam composite during

production. Typically, the bubbles are empty spaces rather than solid particles that lower the composite's density and mechanical integrity.

Nevertheless, the homogenous distribution of HGM/nanoclay in the matrix was not affected. In Figure 4.3(b,c,e,g), ductile fracture occurs due to good adhesion, enhanced cross-linking network, and improved interface interaction between the HGM/nanoclay and epoxy resin [277, 279]. Uneven surface morphology with debris, deboned particles, and the fractured surface was observed, which is likely to be due to ductile fracture under loading conditions and resulted in high flexural strength and tensile strength. This also suggests compatibility between the hybrid fillers and matrix, which resulted in increased impact resistance at moderate loading of the fillers. On the other hand, in Figure 4.3d, there was an increase in the debris on its surface, which was a result of the percentage of nanoclay in the foam composites, which makes it exhibit ductile fracture, which is in line with the idea that during tensile stress, the adhesive force holding the nanoclay and epoxy matrix together diminishes, reducing their flexural strength.

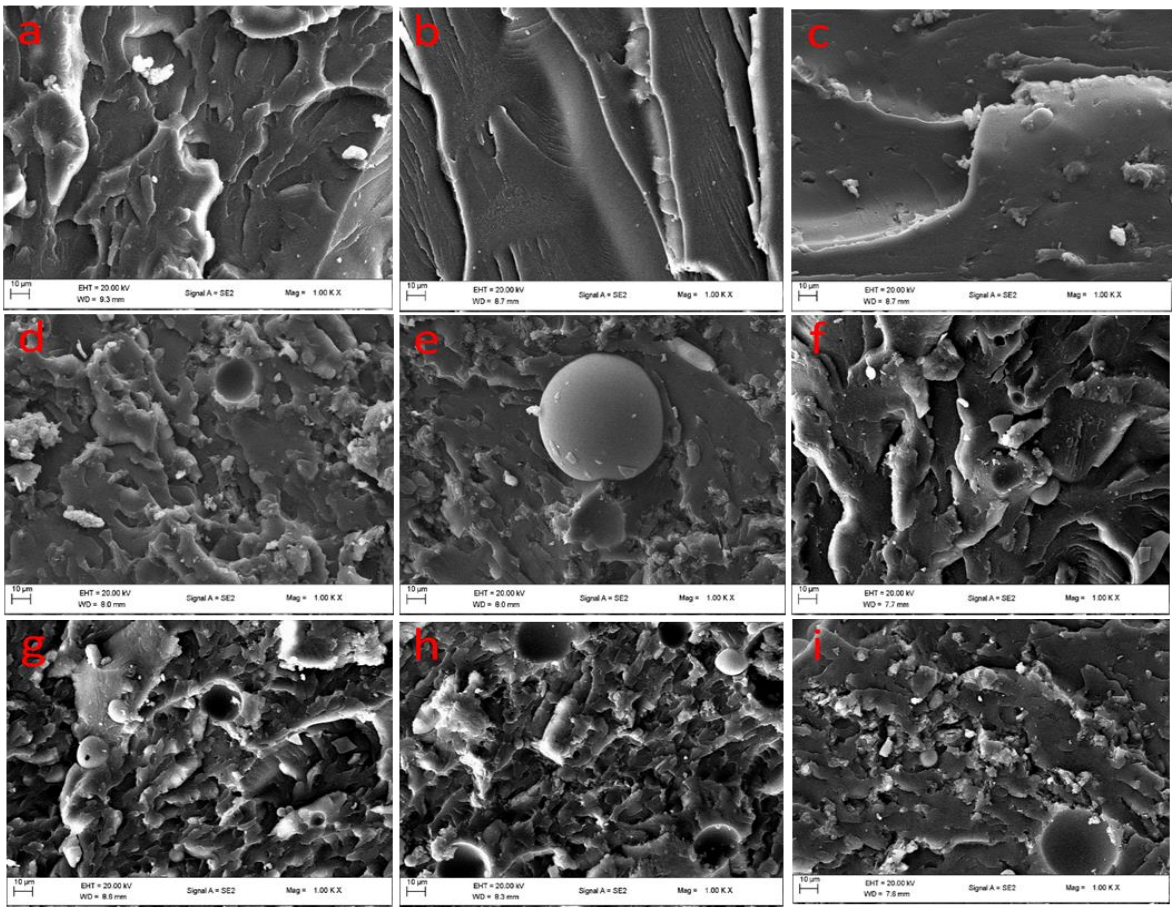

Figure 4.3: SEM image of Tensile fracture surfaces (a) Neat epoxy (b) 1%wt.HGM (c) 1% wt.HGM+1%wt. Clay (d) 1%wt.HGM+3%wt.Clay (e) 1%wt.HGM+5%wt.Clay (f) 3%wt.HGM (g) 3%wt.HGM+1%wt.Clay (h) 3%wt.HGM+3%wt.Clay (i) 3%wt.HGM+5%wt.Clay

4.1.2.4 Dispersion Characteristics of Hybrid-filled Foam Composite Panel - Transmission Electron Microscopy (TEM)

The clustered particles of hollow glass microspheres and nanoclay are visible in the TEM image, distributed throughout the hybrid-filled foam composite at every volume fraction. This dispersion of HGM/clay filler in the HFFC was investigated using transmission electron microscopy (TEM). The TEM images of HFFC at varying volume fractions of HGM/Clay in the matrix for the heterogeneous form are displayed in Figure 4.4 (a-i). As the concentration rose from Figure 4a–4i, the HGM/Clay filler was distributed unevenly across the matrix. This, particularly with the large loading volume fractions, had an impact on the HFFC's mechanical properties and raised the level of porosity in the matrix. Neat epoxy, 1wt.% HGM and 1wt.% HGM+1wt.%Clay shows little agglomeration of the HGM/Clay due to lower concentration. As shown in figures 4d through 4i, the agglomeration grew as the concentration rose with much clustering and percolation of fillers at 3wt.%HGM+3wt.%Clay and 3wt.%HGM+5wt.%Clay

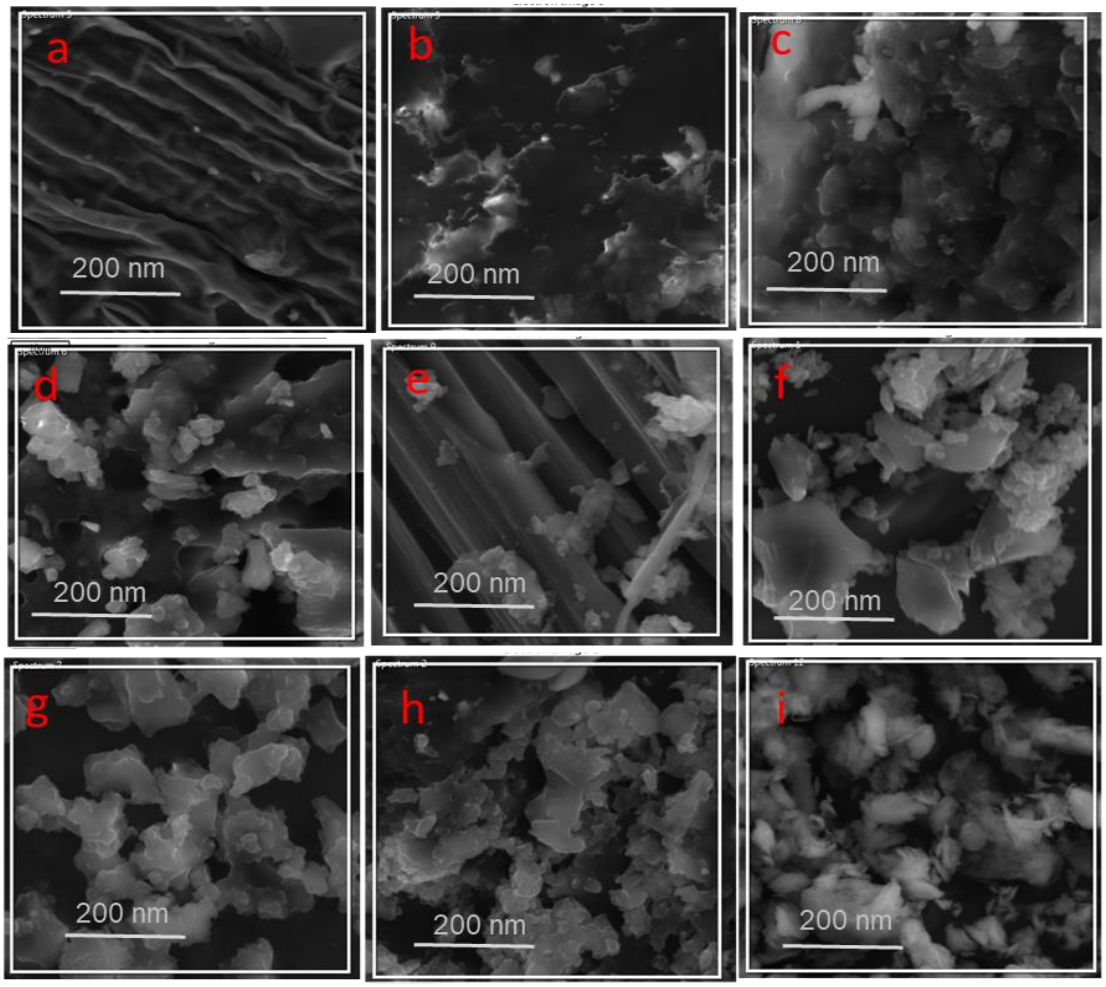

Figure 4.4: TEM of HFFC at (a) Neat epoxy (b) 1%wt.HGM (C)1%wt.HGM+1%wt.Clay (d) 1%wt.HGM+3%wt.Clay (e) 1%wt.HGM+5%wt.Clay (f) 3%wt.HGM (g) 3%wt.HGM+1%wt.Clay (h) 3%wt.HGM+3%wt.Clay (i) 3%wt.HGM+5%wt.Clay

4.1.2.5 Flexural Properties

Flexural tests were performed to evaluate the strength and stiffness of neat epoxy and HGM/Clay foam composite panels. Figure 4.5 explains the behavior of the foam composite panel at different loading of HGM/nanoclay filler concentrations together with the neat epoxy. It was observed that some specimens are brittle and crack after getting to the highest yield stress. The hybrid-filled foam composite panels possess better bending capacity than the neat epoxy except for 3%HGM, 3wt.%HGM+3wt.%Clay, and 3wt.%HGM+5wt.%Clay composition which has lower stress values. This occurrence is possible because of the weak interaction of fillers with the matrix during the process of mixing, causing early cracks and lowering the strain of the samples. Besides, this could have occurred because of debonding and matrix cracking of the samples which could have led to early reduction in the failure strain in Figure 4.5. The highest stress value was achieved at 1wt.%HGM+1wt.%Clay due to low filler concentration. This can be related to adding a smaller quantity of HGM and nanoclay, giving better matrix dispersion during the mixing process, and resulting in high strength and stiffness [277, 283]. It was also observed that even though the tension experiments indicated that the unfilled Neat epoxy would have much better ductility than the filled epoxies, the beam bending tests indicated that the 3wt.%HGM+1wt.%Clay + Epoxy would have the best ductility (strain to failure). This may be due to the formation of a solid epoxy skin on the surfaces of the beam samples.

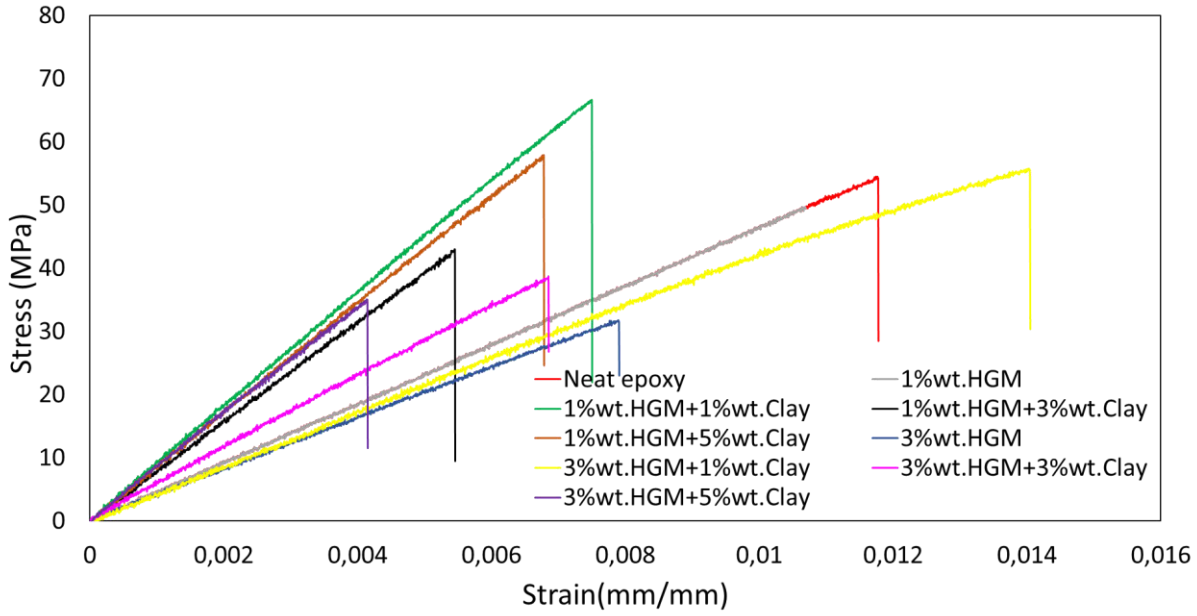

Figure 4.5: Flexural stress versus strain curve of neat and HGM/Clay foam composite material.

Table 4.2: Flexural Properties of Neat and HGM/Clay foam composites.

Materials	Flexural Strength (MPa)	Modulus(GPa)	Strain(mm/mm)
Neat Epoxy	54.1±0.04	4.59±0.005	0.01175
1wt.%HGM	61.61±0.10	5.81±0.009	0.01069
1wt.%HGM+1%wt.Clay	66.21±0.09	8.70± 0.010	0.007484
1wt.%HGM+3wt.%Clay	42.53±0.06	7.90± 0.010	0.0054
1wt.%HGM+5wt.%Clay	57.25±0.08	8.44± 0.02	0.0068
3wt.%HGM	31.50±0.02	3.99± 0.003	0.0079
3wt.%HGM+1wt.%Clay	55.48±0.15	3.96± 0.015	0.0140
3wt.%HGM+3wt.%Clay	38.50±0.13	5.68±0.02	0.0068
3wt.%HGM+5wt.%Clay	34.30±0.05	8.17± 0.01	0.00411

4.1.2.6 Impact Properties

The impact strength for neat epoxy and fortified foam composite panels is shown in table 4.3, Improvement in strength is noticed for foam composite panels with up to 3wt.%HGM in each sample formulation and a decrease in the impact resistance at 1wt.%HGM+1wt.%Clay, 1wt.%HGM+3wt.%Clay, and 3wt.%HGM+5wt.%Clay. This shows that adding a higher concentration of HGM filler than nanoclay fillers improves the impact strength of the epoxy of the foam composite panel. The increase in impact strength can be ascribed to the homogenous dispersion of the hybrid fillers bringing about a coordinated bond that improves the energy-absorbing capacity of the foam composite. Agglomeration brought on by greater weight percentages may produce a decrease in impact strength for a higher concentration of nanoclay in the constituent.

Table 4.3: Impact fracture strength of neat and HGM/Clay foam Composite materials.

Materials	Impact Strength(KJ/mm)
Neat Epoxy	108 ± 3.6
1wt.%HGM	117 ± 4.2
1wt.%HGM+1wt.%Clay	105 ± 3.7
1wt.%HGM+ 3wt.%Clay	105 ± 3.9
1wt.%HGM+5wt.%Clay	110 ± 3.9
3wt.%HGM	113 ± 4.1
3wt.%HGM+1wt.%Clay	109 ± 3.9
3wt.%HGM+3wt.%Clay	139 ± 5.2
3wt.%HGM+5wt.%Clay	107 ± 3.8

4.1.2.7 Density.

In Table 4.4 below, it was observed that the density calculated theoretically from the weight fraction does not equal the experimentally measured density due to the presence of void and pore during the experimental process that cannot be wholly avoided. This performance was due to voids in the foam panel because of hybrid fillers. It was observed that more voids and pores were found in the panel with a higher concentration of nanoclay and higher HGM. Also, as fillers keep increasing, a corresponding decrease in density was observed

Table 4.4: Theoretical and experimental densities of foam composite panel along with the corresponding volume fraction of voids

Percentage(%) of Filler Concentration	Theoretical Density of Foam panels (g/cm^3)	Experimental Density of Foam panels (g/cm^3)	Void Fraction(%)
0	1.130	1.105	2.21
1wt.%HGM	1.120	1.062	5.18
1wt.%HGM+1wt.%Clay	1.110	1.049	5.50
1wt.%HGM+3wt.%Clay	1.092	1.024	6.23
1wt.%HGM+5wt.%Clay	1.073	1.002	6.61
3wt.%HGM	1.099	1.022	6.88

3wt.%HGM+1wt.%Clay	1.090	1.012	6.15
3wt.%HGM+3wt.%Clay	1.071	0.991	7.47
3wt.%HGM+5wt.%Clay	1.052	0.971	7.70

One important component that determines the properties of foam panels is the density of a foam composite material, which is dependent on the corresponding mix of strengthening and matrix materials. The amount of pores is the primary reason for the difference between the values obtained from experimental density and values obtained from theoretical density when calculated. Some of the mechanical qualities are significantly impacted by the existence of pores, which in turn impacts how well the foam panel performs in real-time applications. A good foam composite panel should have fewer pores, although the complete absence of pores cannot be achieved in the fabrication of foam panels mainly through the hand lay-up method.

4.1.2.8 Hardness

The hardness values of neat epoxy and hybrid-filled foam composite panels are shown in Figure 4.6. The hybrid fillers primarily influenced the hardness values obtained. An increase in the filler weight% of nanoclay in each constituent of HGM in the matrix increases its hardness due to its increase in wear resistance, as revealed in Figure 4.6. An increase in surface hardness means that the foam composite panel's wear and scratch resistance will increase, these are very vital properties in service which results obtained from this work by using hybridized filler have enhanced the foam composite panel's resistance to wear and scratch, which is similar to what was reported by Nzioka et al. [284]. The filler content can vary for applications requiring different hardness levels to achieve desired results.

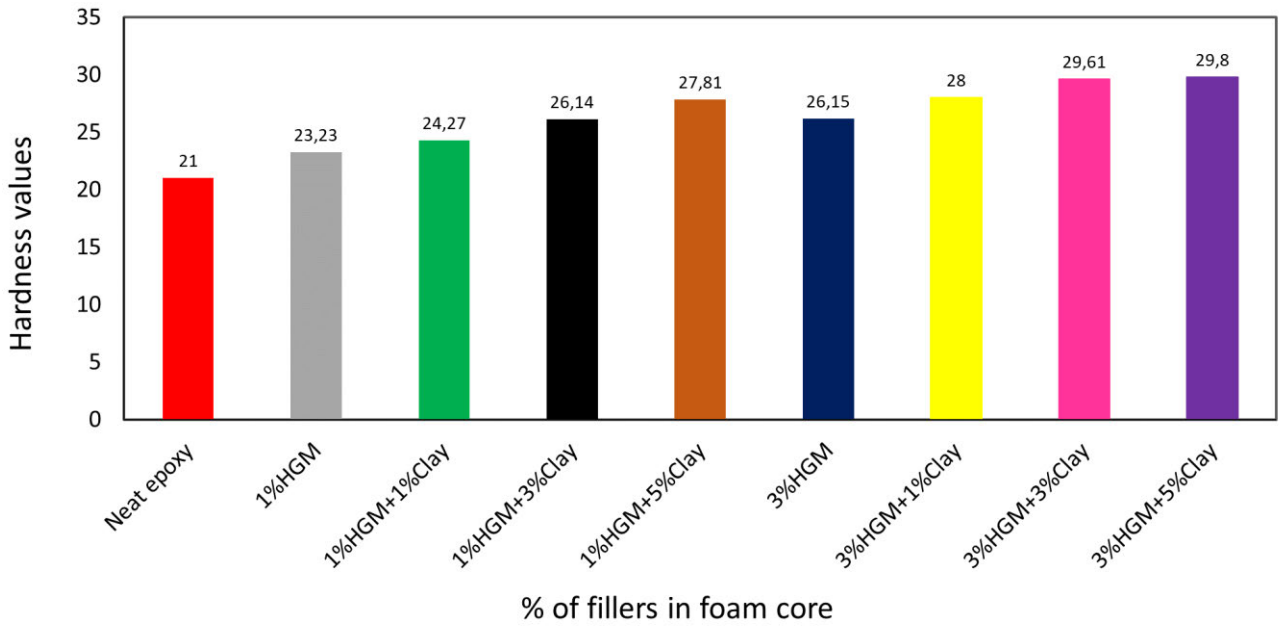

Figure 4.6: Hardness properties of foam panels infused with mixed fillers

4.1.2.9 Dynamic Mechanical Analysis (DMA)

Storage modulus estimates the energy stored in the yielding portion of the foam panel. In Figure 4.7a, an increase in the storage modulus peak was noticed in 3wt.%HGM+3wt.%Clay when compared to neat epoxy. Nevertheless, the loss modulus which estimates the energy lost as heat under the deformation of foam panel showed varieties of trends in the neat epoxy and hybrid foam composite material[283, 285] . It was observed in Figure 4.7b that the addition of nanoclay as a second filler into foam composite caused an increase of loss modulus at the glass transition temperature (Tg) which was more visible at hybrid foam composite with 3wt.%HGM+3wt.%Clay loading. A higher peak value of 347.7MPa was observed in the loss modulus peak which was more than the neat epoxy value and other foam composite samples. Figure 4.7c reveals the damping factor (Tan δ), which measures the impact and elastic characteristics of the hybrid-filled foam composites, maximum height is near to the energy dissipation of hybrid foam composites. One can approximate the glass transition temperature (Tg) of hybrid foam composites by examining Tan δ's peak temperature. Figure 4.7c evaluates how the hybrid foam composites' tan delta (δ) varies for the homogeneous HGM/nanoclay. The Tg was obtained from the peak of tan δ at a temperature above 65^0C, which rose across various compositions up to 80^0C. The epoxy resin and HGM surrounding the nanoclay undergo a high Tg because the clay acts as a thermal barrier in the medium of the soft segment. This shows the effectiveness of nanoclay as a second filler. Tan δ Tg values reduced with an increase in the

concentration of nanoclay in hybrid foam composite materials. It is not amazing that no significant increase occurred in tan δ Tg values of the hybrid foam composite materials; this has also been previously reported [284, 286]. The increase in the loss modulus's Tg value suggests that nanoclay functions as a catalyst in the medium, causing the polymer to exhibit a high viscous response as energy is released. It was demonstrated that using nanoclay as a second filler for strengthening is justified.

Table 4.5: DMA properties of foam panel

Materials	Storage modulus Peak(MPa)	Storage modulus Tg(^{0}C)	Loss modulus Peak (MPa)	Loss modulus Tg(^{0}C)	Tan δ Peak	Tanδ Tg(^{0}C)
Neat Epoxy	1895	60	196	66	1.27	80
1wt.%HGM	1313	60	145.7	66	1.013	80
1wt.%HGM+1wt.%Clay	1805	60	196	66	1.076	70
1wt.%HGM+3wt.%Clay	1648	60	234	68	1.141	78
1wt.%HGM+5wt.%Clay	1599	60	227.4	66	1.041	75
3wt.%HGM	1204	60	167.7	66	0.953	78
3wt.%HGM+1wt.%Clay	1552	60	189.7	66	1.035	75
3wt.%HGM+3wt.%Clay	2421	60	347.7	68	1.133	75
3wt.%HGM+5wt.%Clay	1547	60	172	66	1.099	80

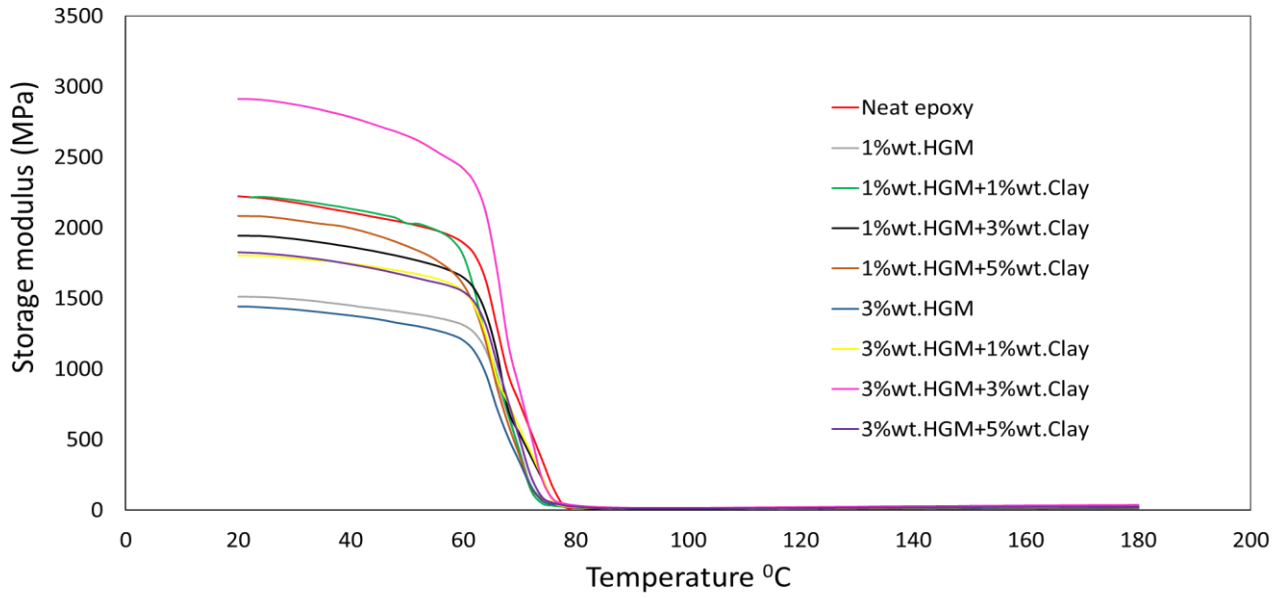

Figure 4.7: Storage modulus of foam panels against temperatures

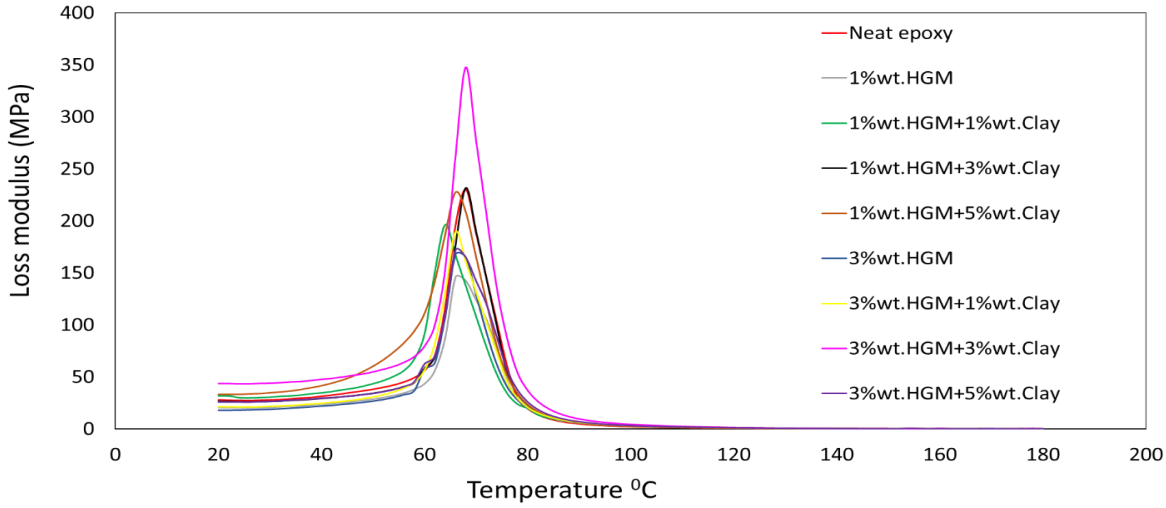

Figure 4.8: Loss modulus of foam panels against temperatures

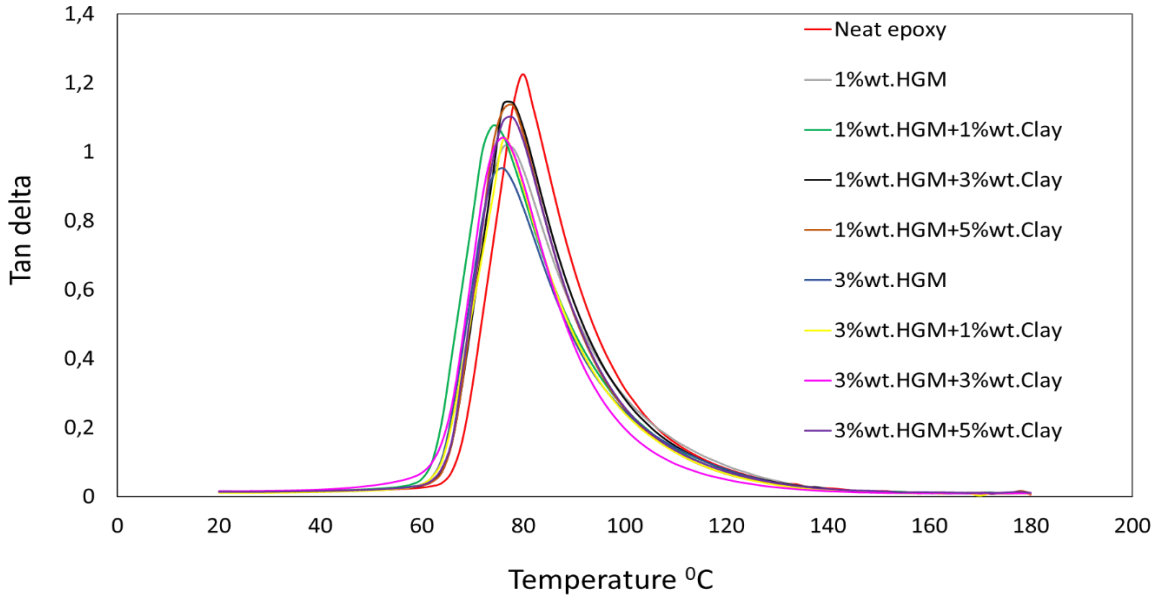

Figure 4.9: Tan delta of Foam panels against temperatures

4.1.3 Conclusion.

A hybrid epoxy-based foam composite comprising HGM, nanoclay, and epoxy resin was developed. The influence of HGM/clay on the mechanical properties of foam composites was investigated. The HGM content was varied from 1wt.% to 3wt.% in foam composites while

nanoclay content was varied from 1wt.% to 5wt.% in each of the HGM-filled series of foam composites.

The results of the hybrid filled foam composite panel showed superior and improved tensile strength, young modulus, flexural strength, hardness values, and impact strength of 23MPa, 3.5GPa, 66.21MPa, 29.8 and139KJ/mm when compared with neat epoxy and other samples filled with only HGM filler and also there was reduced strain to failure under uniaxial tension with addition of filler. This was achieved because of excellent interfacial adhesion between the hybrid fillers and the matrix and also because of the unique nanometer-size dispersion of the layered silicates of nanoclay which arrested initiation and propagation of micro cracks.

Therefore, improved properties of hybrid-filled epoxy-based foam composites suggest materials suitable for marine and aerospace applications. The potential future direction of this research could be a surface modification of fillers and to study their interfacial properties.

CHAPTER 5: THERMAL AND WETTABILITY BEHAVIOR OF HGM/NANOCLAY FILLED FOAM COMPOSITE

5.1 Introduction

This chapter presents discussion of the journal paper titled "Thermal and wettability properties of nanoclay-filled epoxy-based foam composites as lightweight materials'', by Ayodele Abraham Ajayi, Turup Pandurangan Mohan, Krishnan Kanny, and Raman Velmurugan published in the journal of Material performance and Characterization (2023), volume 12, Issue 1, pages 293-306. This paper focused on enhancing the thermal behavior of epoxy-based foam composites by hybridizing HGM with clay nanoparticles.

5.1.1 Objectives of the journal paper

The major objectives of this journal paper were to:

• To fabricate novel HGM/nanoclay hybrid foam composites with improved thermal performance and better resistance to water absorption.

• To investigate the efficacy of different HGM and clay nanoparticle contents in enhancing the thermal performance of the epoxy-based foam composites.

• To determine the optimum HGM/clay nanoparticle content.

5.1.2 Summary of Thermal and Wettability Properties of Nanoclay-filled Epoxy-based Foam Composite

In this work, hollow glass microspheres (HGM) and clay are infused to improve the wettability and thermal properties of epoxy-based foam composite materials using hybridised fillers. These foam composite materials were created using a traditional resin casting process. The HGM concentration ranged from 1% wt to 5% wt, whereas the clay content varied from 1% wt to 5% wt in each of the HGM-filled series of foam composite materials. The thermal properties of hybrid-filled foam composite materials were examined and contrasted with neat epoxy and epoxy foam materials. These properties included thermal conductivity, thermal expansion, coefficient of thermal expansion, specific heat capacity, water contact angles, and percentage of water absorption. Because of the good chemical reactions and great interfacial adhesion between the fillers and matrix, it was discovered that hybrid-filled foam composite materials

demonstrated better thermal properties than neat epoxy material. These enhanced thermal properties may indicate that this material is appropriate for use in sectors requiring lightweight materials with favourable thermal properties. By using hybrid fillers to improve thermal properties, this opens up new research opportunities in the field of foam composite fabrication.

5.1.2.1 Thermal Conductivity

To safeguard passengers against thermal and acoustic stresses, insulating materials should have thermal conductivity values ranging from 0.030 to 0.840 W/(m×k) [287]. Low thermal conductivities of HGM and clay are beneficial in effectively enhancing the thermal behavior of the foam composite panel.

Figure 5.1 illustrates how foam composite materials infused with HGM and clay behave in terms of heat conductivity. The neat epoxy has a thermal conductivity of 3.54 W/(m×k) at 120^0C. It was observed in all foam composite compositions that thermal conductivity reduces when the temperature rises and likewise, the thermal conductivity decreases as the concentration of HGM and nanoclay increases in each sample formulation which could be attributed to the ability of HGM to effectively absorb moisture and also when nanoclay is added to epoxy, it fills the holes in its structure and shifts the atoms' orientation [288] in which as a result of this, heat flow is hindered. Additionally, the inclusion of HGM causes the composites' thermal conductivity to sharply fall since the HGM contains a rare gas or vacuum with very poor thermal conductivity [289]. However, clay filler has a lower thermal conductivity of 0.11 W/mK which is lower than HGM filler, which has a thermal conductivity of 0.183 W/mK, the foam composite material with a higher concentration of clay showed the lowest thermal conductivity. As a result, the composite's overall thermal conductivity decreased when nanoclay was added as a hybrid filler. Thermal conductivity decreased from 3.73 W/m×K to 0.333 W/m×K for 1%wt.HGM+5%wt.Clay weight fraction composition. These composites are intended for use in thermal applications and can be used as the core material for sandwich composites. The composites can also be utilized to make electronic equipment casings that need to dissipate heat generated by operating electrical gadgets to the outside and cabin insulation for airplane interiors.

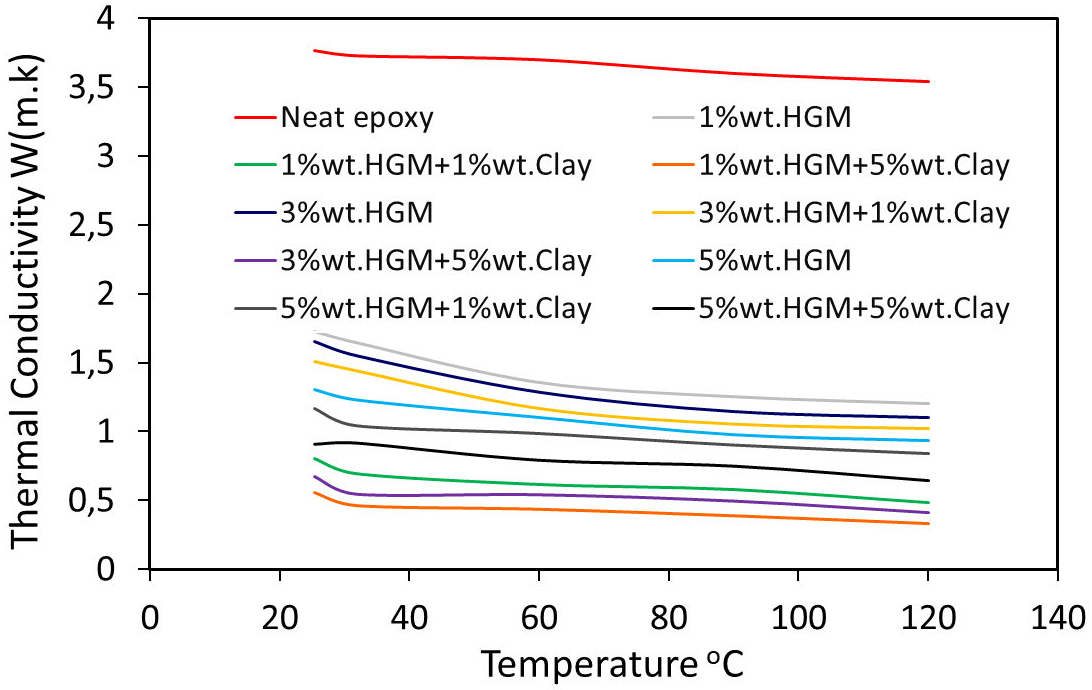

Figure 5.1: Thermal Conductivity of Neat Epoxy with HGM/Clay foam composite material

5.1.2.2 Specific Heat Capacity

The influence of hybrid fillers on the specific heat capacity of the foam composites was investigated in Fig. 5.2

It was observed that the addition of fillers into the epoxy matrix led to an increase in specific heat capacity for the composite materials in all the selected temperature ranges. For the neat epoxy, the specific heat capacity was 0.92J/Kg^{0}C at 120^{0}C, and the addition of hybrid filler up to 5%HGM+5%Clay enhanced the specific heat capacity of the composite material but it was observed that composite material with 1%HGM+5%Clay has the highest specific heat capacity of 2.297J/Kg^{0}C due to higher concentration of nanoclay in this formulation because the material's insulation increases as the concentration of nanoclay in it increases. The reason is the high heat capacity of nanoclay due to the presence of silicate in it which after mixing it with epoxy and HGM raised the composite's specific heat capacity. As observed across various selected temperature ranges, the specific heat capacity of each sample of foam composites keeps increasing as the temperature increases because as the material heats up, the average kinetic energy of the molecules increases in which collisions provide enough energy to allow rotation, which adds to internal energy and boosts the specific heat capacity [290].

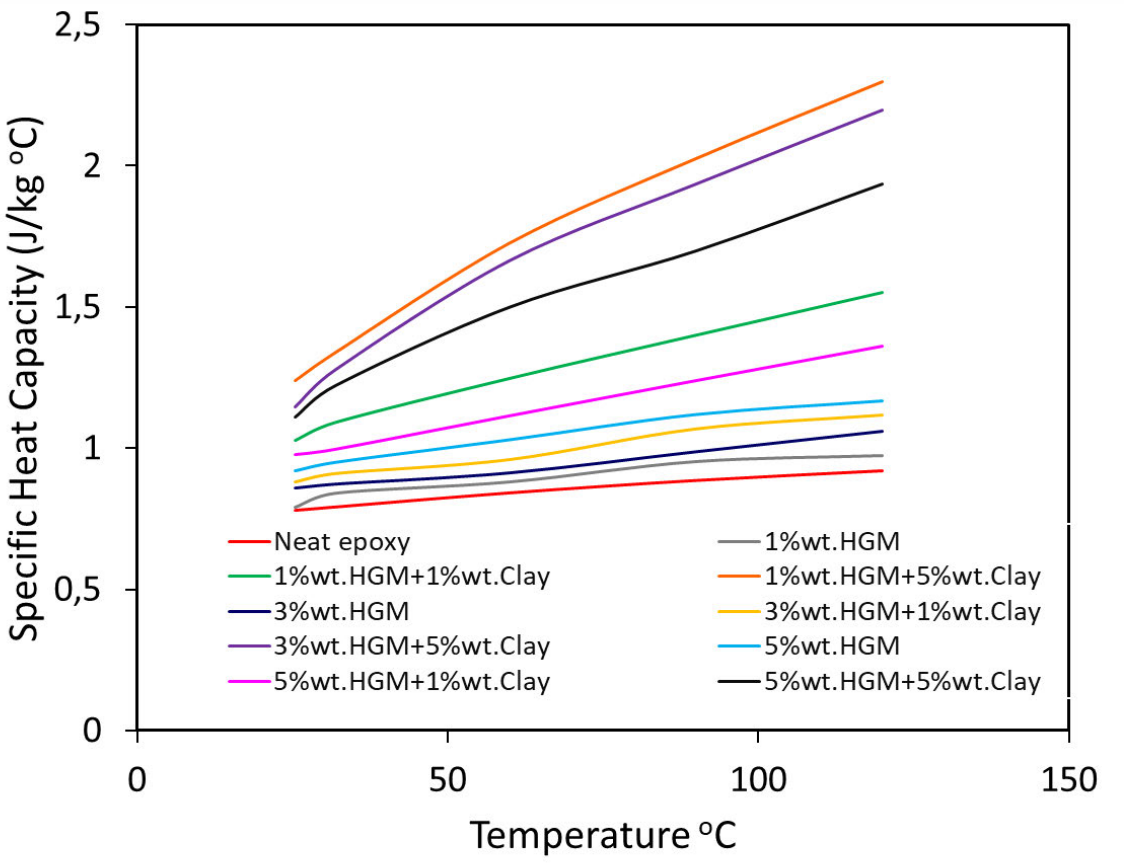

Figure 5.2: Specific heat capacity of Neat Epoxy and HGM/Clay foam composite material

5.1.2.3 Thermal Expansion

Fig. 5.3 reveals the thermal expansion of foam composite infused with hybrid fillers and this measures the thermal stability of foam composite materials considered in this study. It was discovered that the thermal expansion varied with temperature changes. However, it was discovered in this study that the rate of thermal expansion decreases as the concentration of nanoclay increases in the hybrid-filled foam composites because nanoclay contains iron, and hydroxide ions which enhances the thermal stability as seen in Figure 5.3.

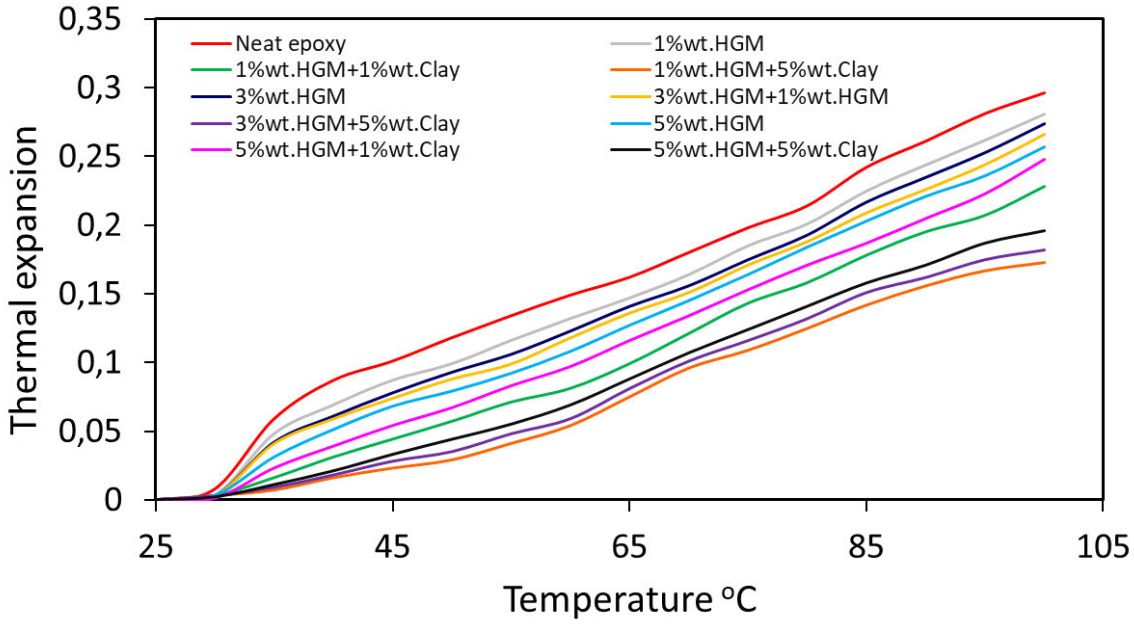

Figure 5.3: Thermal Expansion of Neat Epoxy and HGM/Clay Foam composite material Thermal Expansion

5.1.2.4 Coefficient of thermal expansion(CTE)

The coefficient of thermal expansion (CTE) indicates how the size of a material changes as the temperature changes. Specifically, it is a measurement of the little change in size per degree change in temperature under constant pressure. Thermo-Mechanical Analyzer (TMA) was used to calculate the coefficient of thermal expansion. CTE for neat and different compositions was found to be 1.08×10^{-4} (K^{-1}), 0.0001 (K^{-1}), 7.88×10^{-5} (K^{-1}), 6.77×10^{-5} (K^{-1}), 9.81×10^{-5} (K^{-1}), 9.07×10^{-5} (K^{-1}), 7.03×10^{-5} (K^{-1}), 9.31×10^{-5} (K^{-1}), 8.64×10^{-5} (K^{-1}) and 7.22×10^{-5} (K^{-1}) and as seen in Fig.5.4 in which decrease was observed in CTE. This indicates that heat is absorbed by the hollow glass microspheres in the epoxy network structure, acting as a heat sink for the composite materials. The hollow glass microspheres prevent heat from diffusing throughout the epoxy and filler mixture and prevent the epoxy resins' surface cross-linking. The presence of nanoclay particles is ascribed to a much higher reduction of CTE because nanoclay has a very low coefficient of thermal expansion but epoxy, on the other hand, has a higher CTE value. When the composites are exposed to higher temperatures, the silica in nanoclay aids in preventing the material from expanding.

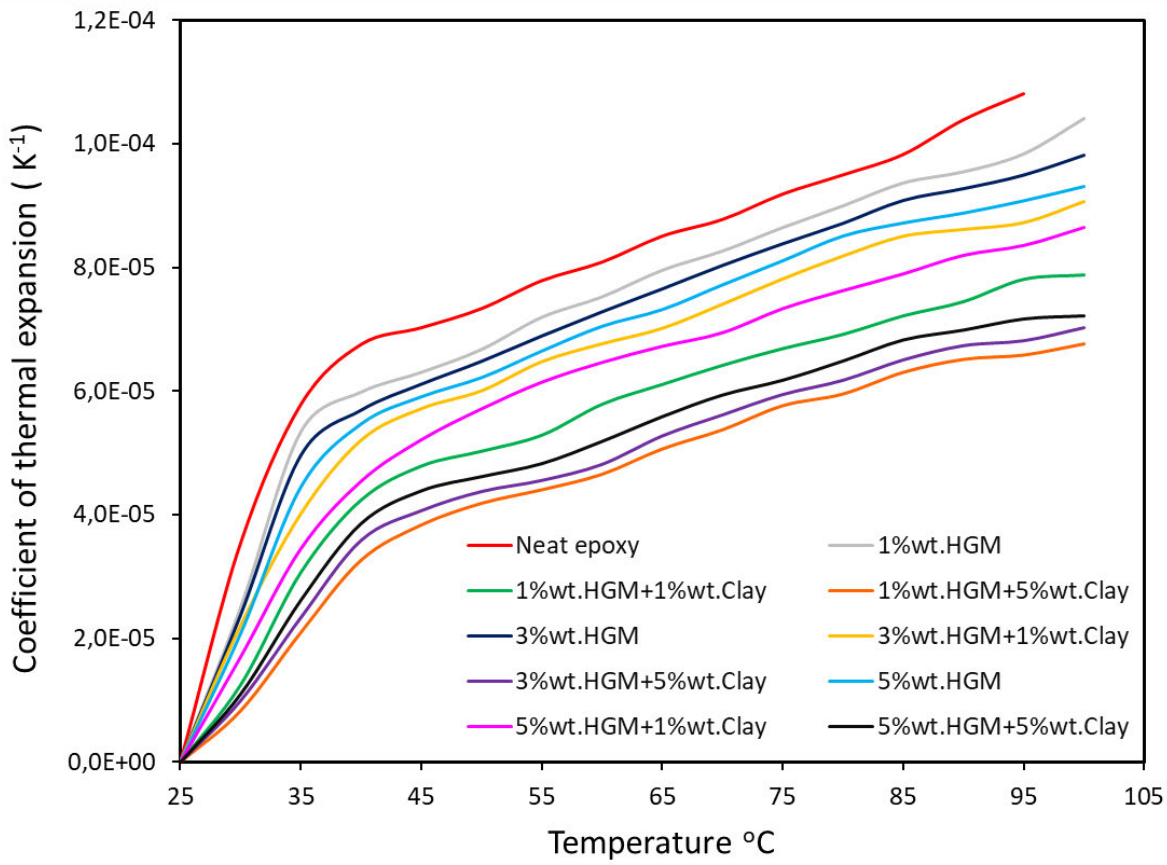

Figure 5.4: CTE of Neat epoxy and HGM/Clay filled foam composite material

5.1.2.5 Thermal Gravimetric Analysis(TGA)

Figure 5.5 shows the thermo-gravimetric analysis (TGA) for the HFFC and neat epoxy resin. The effect of hollow glass microsphere and nanoclay in pure epoxy resin on thermal stability was analyzed by comparing the weight loss as a function of temperature. Figure 5.5 begins to lose weight gradually after 170^0 until 320^0 followed by major decomposition between 320^0 and 470^0 and the remaining inorganic components after 470^0. It was observed that neat epoxy has the lowest weight % at maximum decomposition and it can be seen that HFFC has thermal stability more than neat epoxy. This suggested that adding HGM and nanoclay as hybrid fillers could increase the epoxy resin's thermal stability. The low molecular weight of the HFFCs may potentially be caused by inadequate cross-linking of the filler molecules' functional group during covalent bonding with the matrix.

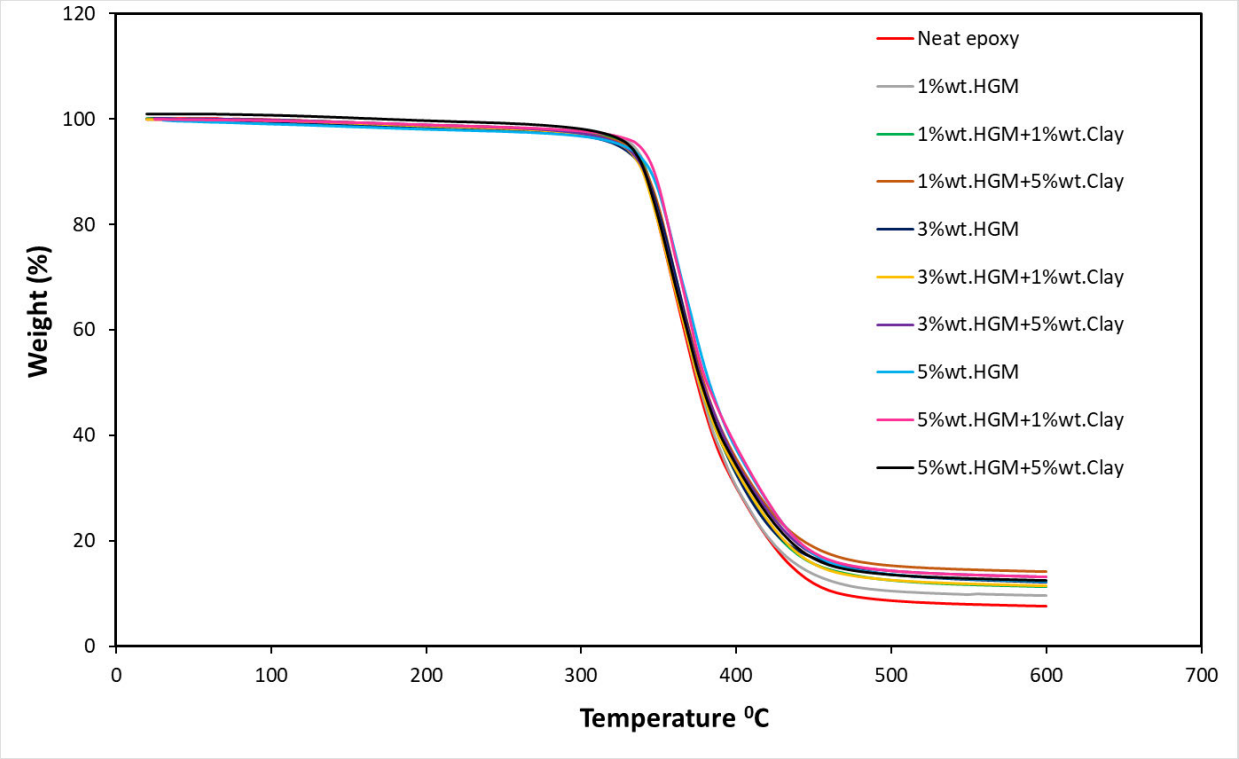

Figure 5.5: TGA analysis of Neat Epoxy and HGM/Clay filled foam composite material

5.1.2.6 Water Contact Angle(WCA).

The WCA is a crucial indication of the hydrophilicity and hydrophobicity of materials since it primarily relates to the surface microstructure and surface chemical characteristics [291]. For the same material, the rougher the surface, the lower the contact angle. The contact angle test was used to analyze the wettability behavior of neat epoxy and HGM/clay-filled foam composite materials. According to Klein N S et al. and Xiong B et al.[292, 293], a surface is considered hydrophilic when the static water contact angle θ is less than 90^0 and hydrophobic when θ is greater than 90^0. Figure 5.6 illustrates how the surface became more hydrophilic following the addition of filler, which may have been caused by the samples' rough surfaces. Since the water contact angle of the water droplets on the surface of the foam composites changes concerning concentration of fillers. A summary of the water's contact angle with the foam composite panel surface is provided in Table 5.1. Every foam composite sample used in this investigation demonstrated hydrophilic behaviour, demonstrating their affinity for water.

However, the study revealed that foam composite 5%wt.HGM displayed an average contact angle of 49.2 which is because water invades the interface layer of HGM and epoxy resin of HGM and the pores, this may cause damage to the HGM at higher concentrations while foam composite 1%wt.HGM+5%wt.Clay with the highest concentration of nanoclay displayed an

average contact angle of 73.74 because clay contains silicon-oxygen (SiO_4) tetrahedron bilayers with deep-rooted octahedral layers of aluminum and iron which can resist moisture and shows that, as opposed to neat epoxy and other foam composites, the composite exhibits a markedly different hydrophilic behaviour as seen in Figure 5.6.

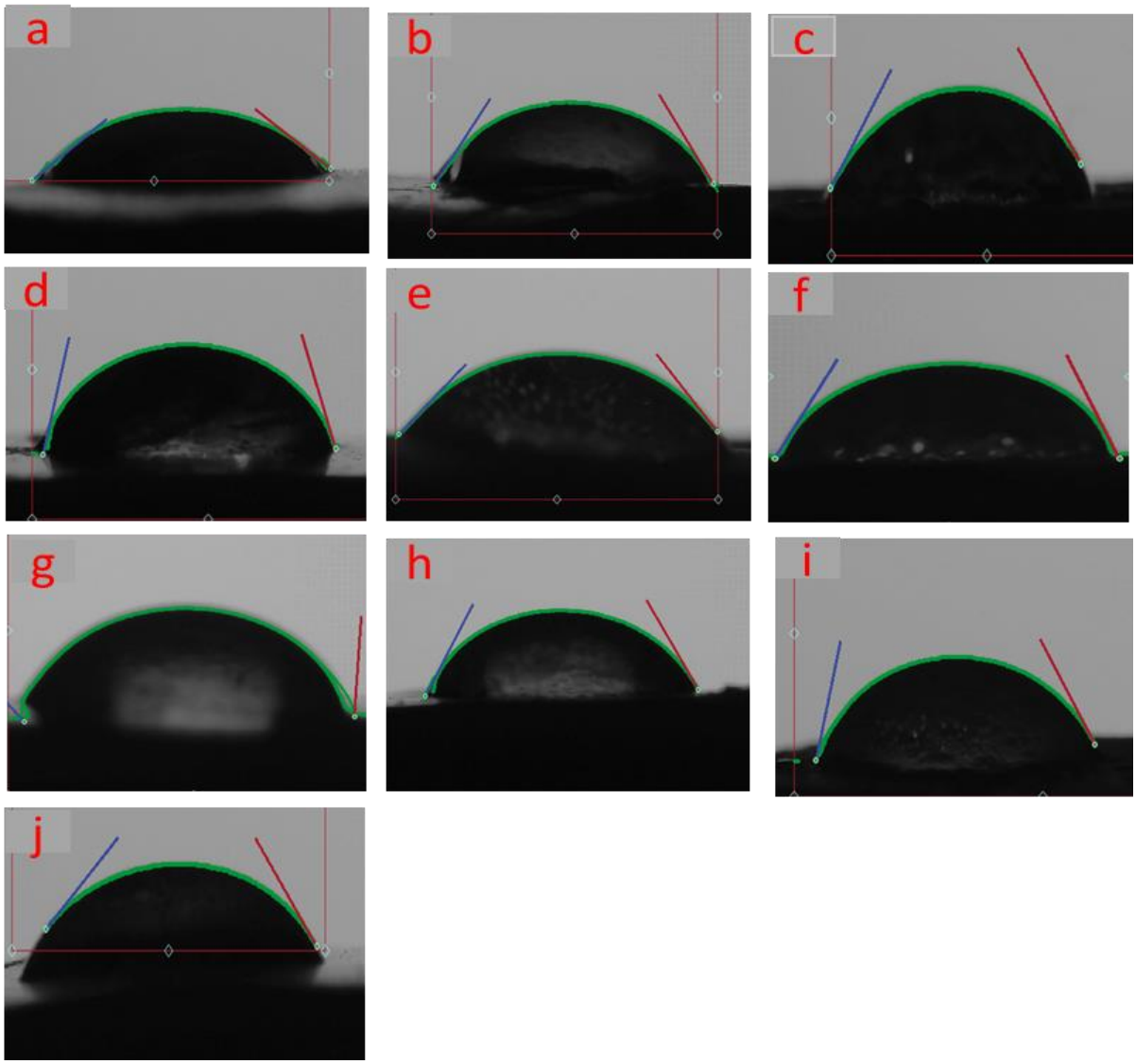

Figure 5.6: Images of WCA of (a) Neat epoxy (b) 1%wt.HGM (c) 1%wt.HGM+1%wt.Clay (d) 1%wt.HGM+5%wt.Clay (e) 3%wt.HGM (f) 3%wt.HGM+1%wt.Clay (g) 3%wt.HGM+5%wt.Clay (h) 5%wt.HGM (i) 5%wt.HGM+1%wt.Clay (j) 5% wt.HGM+5%wt.Clay

Table 5.1: Water contact angles of foam composite materials.

Materials	Water contact angles(WCA) θ^0
Neat epoxy	33.39 ± 1.598
Epoxy+1%wt.HGM	52.79 ± 0.634
Epoxy+1%wt.HGM+1%wt.Clay	64.23 ± 0.589
Epoxy+1%wt.HGM+5%wt.Clay	73.74 ± 0.592
Epoxy+3%wt.HGM	51.03 ± 0.564
Epoxy+3%wt.HGM+1%wt.Clay	58.941± 0.825
Epoxy+3%wt.HGM+5%wt.Clay	71.635± 0.575
Epoxy+5%wt.HGM	49.42 ± 0.634
Epoxy+5%wt.HGM+1%wt.Clay	57.52 ± 1.652
Epoxy+5%wt.HGM+5%wt.Clay	69.02 ± 0.286

5.1.2.7 Water absorption

Figure 5.7 reveals the percentage of water absorption of the foam composites at each volume fraction of fillers relative to the basic epoxy matrix. By taking into account the material's surface and subsurface characteristics as well as its internal porosity, the water absorption of foam composites can be characterized in a variety of ways. Moisture entrapped in the surface pore occurs before the sample's real diffusion occurs when submerged in water. Surface entrapment of this kind cannot provide the precise computation required for the diffusivity of the composite material, hence it is irrelevant in explaining the matrix material water diffusion mechanism [104]. Any epoxy-based foam composite submerged in a marine environment will absorb some water; nevertheless, to preserve the material and prevent material degradation, the foam composite material must have a low water absorption rate. When compared to pure epoxy, it has been discovered that the inclusion of HGM generally lowers the modified composite's water absorption. This phenomenon can be explained by the filler's superior barrier qualities [294]. Similarly, the water-repellent characteristics of the nanoclay incorporated into the epoxy-based composite aid in more effectively lowering the rate of water absorption [295].

The same time range was considered for all the foam composite compositions and the neat epoxy since the samples in Fig. 5.7 were immersed in water all at once and remained there for

the specified amount of time. The first wet measurement was performed after 24 hours, and the last time that was taken into account was 720 hours. All of the samples have an increasing percentage of water absorption intake with time as a result of their prolonged stay in the water, which reflects their varying densities. Following a 24-hour period, 5HGM absorbs the maximum amount of water which is 0.108%. The results show that 5HGM is more capable of absorbing moisture than clay; after 48 hours, it has the highest percentage of water absorption (0.152%), followed by 5HGM+1Clay (0138%). By observation, 1HGM+5Clay shows the lowest value of percentage of water absorption among the foam composites after 720 hours which is 0.508 % while neat epoxy shows the highest percentage of water absorption after 720 hours which is 0.606%. The neat epoxy sample's highest percentage of water absorption shows that it has a more porous matrix than other foam composites, allowing for the absorption of more water.

Thus, the hybrid-filled foam composites proved to be an effective solution for improving the foam composite's resistance to water.

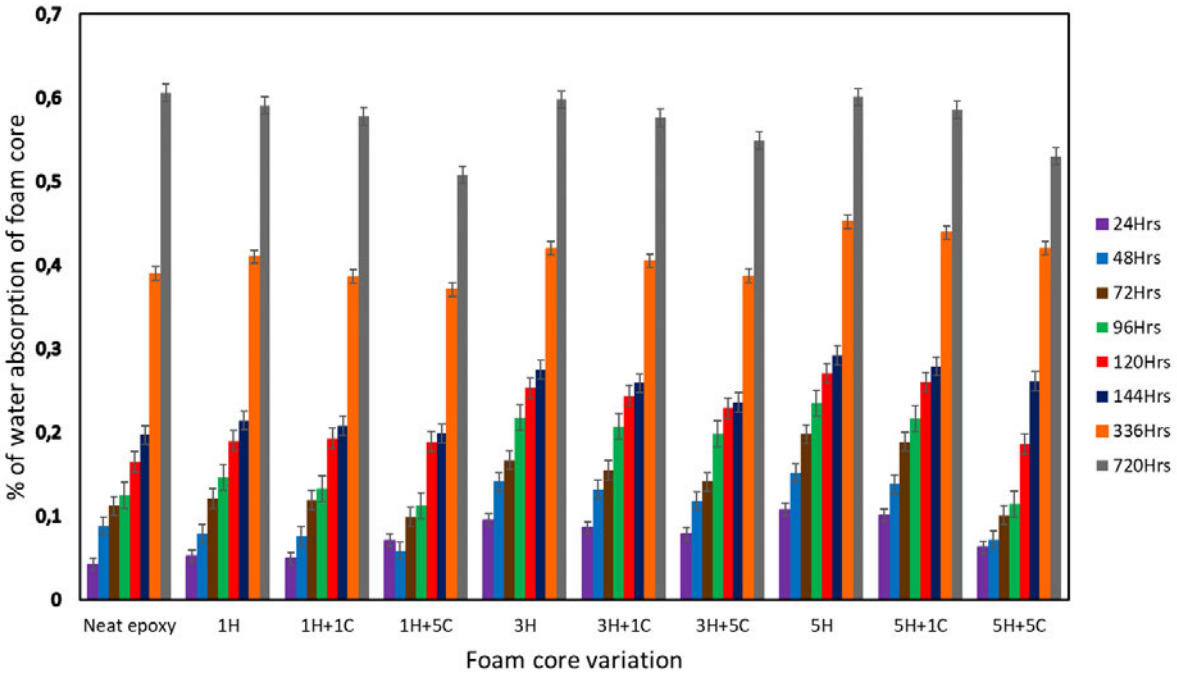

Figure 5.7: Percentage of Water Absorption of Neat and hybrid filled foam composites Percentage of Water Absorption of Neat and hybrid filled Foam Composites

5.1.2.8 Buoyancy Behavior of Hybrid-filled Foam Composites

The buoyancy force (Fb) of the hybrid-filled foam composites is displayed in Figure 5.8. The Neat had the lowest Fb of 0.0.0556N and the highest Fb of 0.0891N in the foam composite 5H. It was also noticed that there was a decrease in Fb as concentration on nanoclay is increased in each of the HGM-filled series of the hybrid-filled foam composites which turns to reduce the floating capacity of the foam composites which could be because of the nano-silicate layer features in nanoclay which does not enhance the floating behavior of the composite like the hollow spheres feature of HGM and its low density that enhances the floating capacity of the composites. Because 5H had a larger proportion of HGM than any other foam composite, it produced the greatest Fb that was discovered there. According to this research, the foam composite that produced more Fb has a higher buoyancy force than other foam composites filled with hybrid fillers when submerged in liquid.

.

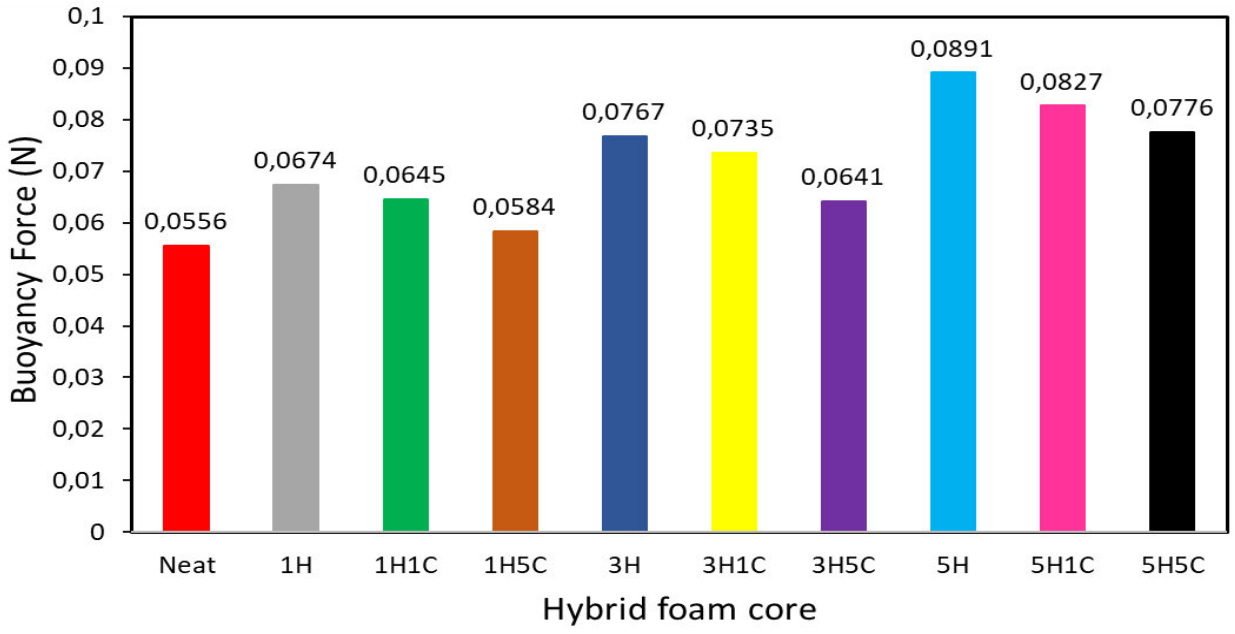

Figure 5.8: Buoyancy force of Neat and hybrid-filled foam composites

5.1.2.9 Surface Morphology of Foam Composite Material.

Using a scanning electron microscope (SEM), images of the foam composite materials' surface were taken in order to study their morphology, filler distribution, surface flaws, filler and matrix interaction of the tested composites[296, 297]. Morphology images of the hybrid filled foam composites prepared are presented in Figure 5.9 which shows dispersion of HGM and clay

particles in epoxy resin are uniform and had a certain degree of combination with each other. Figure 5.9(e, g, h, j) shows that the fillers were not closely combined resulting in more voids when compared with other foam composites additionally, the inclusion of HGM will cause bubbles to create pores and voids at greater concentrations. However, Figures 5.9(c&d) revealed a rough surface with fewer voids resulting in better thermal properties than other foam composites. In addition, the hybrid fillers prepared in this work by mixing HGM and clay in epoxy resin with different particle sizes produce a closer overlap between fillers and matrix which resulted in obtaining a better thermal conductivity.

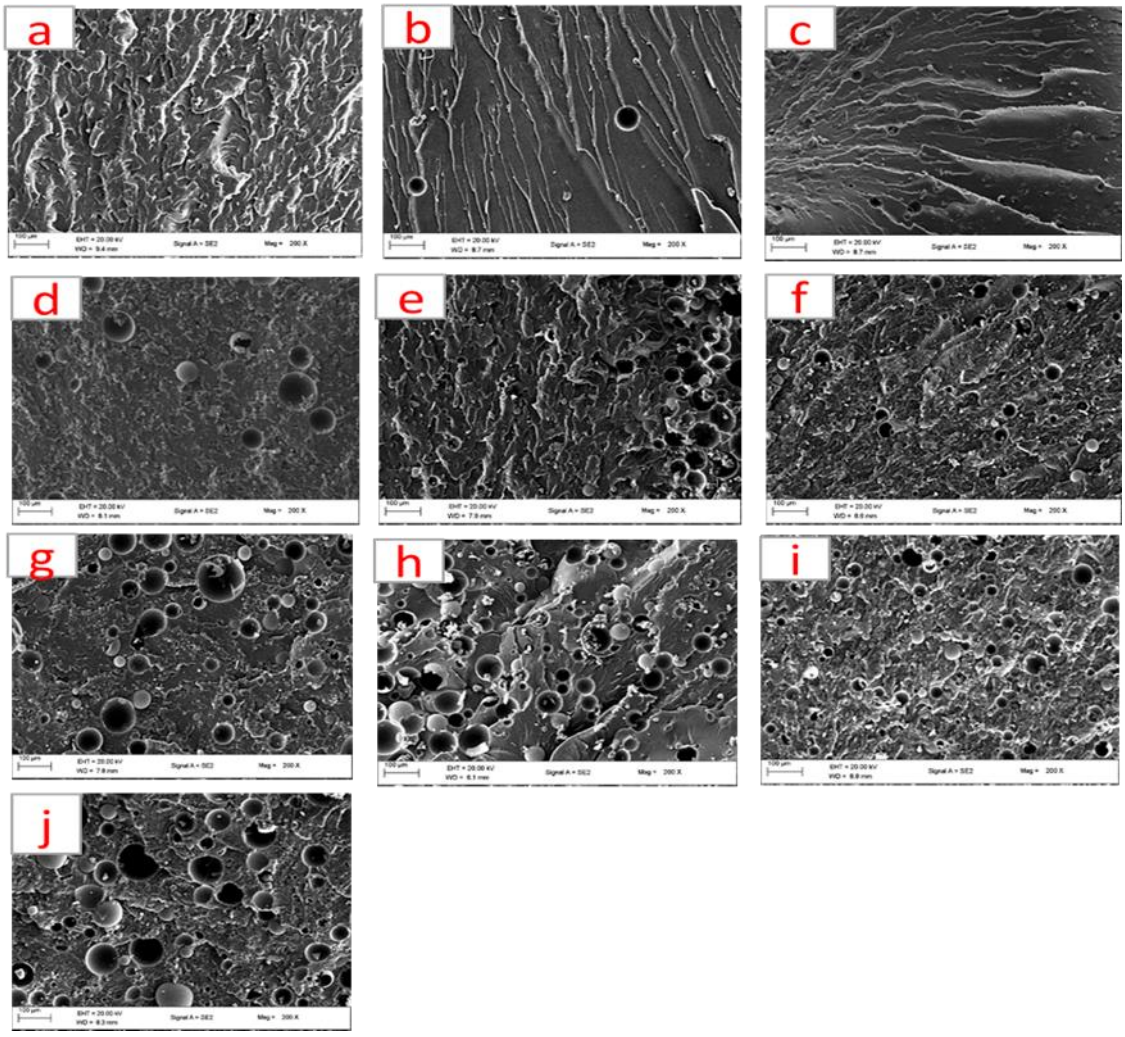

Figure 5.9: SEM images of Neat and hybrid-filled foam composites

5.1.3 Conclusion

By mixing HGM and clay with epoxy resin, the epoxy-based foam composite materials were successfully modified by employing hybrid fillers. The traditional resin casting procedure was utilized to create epoxy-based foam composites infused with varied volume fractions of HGM/clay. In foam composites, the HGM content was adjusted between 1% and 5% of the total weight, and in each HGM-filled series of foam composites, the clay content was adjusted between 1% and 5% on the total weight. The changes in properties of epoxy-based foam composite material as introducing HGM/clay fillers showed that the presence of hybrid fillers led to a decrease in thermal conductivity and an increase in specific heat capacity of the composite material due to nanometer-size dispersion of the layered silicates of clay in the matrix. The thermal expansion of the foam composite decreased from 0.296 to 0.173 for a sample containing 1%wt.HGM+5%wt.Clay. The coefficient of thermal expansion decreased from 1.08×10^{-4} (K^{-1}) to 6.77×10^{-5}(K^{-1}), while water contact angles increased from 33.39^0 to 73.74^0 as compared to the neat epoxy sample. A significant decrease in thermal conductivity was also seen for the foam composites containing a hybrid filler 1%wt.HGM+5%wt.Clay with a decrease from 3.73 W/m*K to 0.33 W/m*K. As compared to neat epoxy samples and other hybrid-filled foam composites, the foam composite containing 1%wt.HGM+5%wt.Clay of a hybrid filler shows better results.

Therefore, improved thermal properties of epoxy-based foam composite material could suggest that this material can find application in marine and aerospace industries.

CHAPTER 6: DEVELOPMENT OF EPOXY-BASED SANDWICH COMPOSITE PANEL WITH HOLLOW GLASS MICROSPHERES/CLAY HYBRID CORE AND BANANA FIBER FACESHEET FOR STRUCTURAL APPLICATIONS

6.1 Introduction

This chapter presents discussion of the journal paper titled ‘’Development of Epoxy-based sandwich composite panel with Hollow Glass Microspheres/Clay Hybrid core and banana fiber facesheet for Structural Applications’’, by Ayodele Abraham Ajayi, Mohan Turup Pandurangan and Kanny Krishnan published in the Journal of Heliyon (2024), Volume 10, Issue 9, pages 1-16. The paper focused on characterizing the performance of Sandwich Composite Panels reinforced with HGM/Clay hybrid core and banana facesheet exposed to various core loading conditions.

6.1.1 Objectives of the journal paper

The major objectives of this journal paper are

- To fabricate a lightweight sandwich panel with a hybrid core and banana facesheet with improved mechanical properties for structural applications
- To determine the water absorption rate of the sandwich panel
- To determine the mechanical performance of the sandwich panel.
- To determine the buoyancy behavior of the sandwich panel.
- To investigate the efficacy of different nanoclay particle contents in enhancing the water absorption resistance of the sandwich composite panel

6.1.2 Summary of the journal paper

Banana fibres were prepared in a unidirectional manner for the facesheet, and the sandwich composite panels were created using a conventional resin casting method. The HGM content of the core ranged from 1 weight percent to 3 weight percent in the sandwich composites panel, while the nanoclay content of the core varied from 1 weight percent to 5 weight percent in each

of the HGM-filled series of the sandwich composite panel. The mechanical, water absorption, and buoyancy behaviour were all carefully examined in this study, and the results showed that sandwich composites with hybrid core formulation and facesheets made of banana fibre performed better than sandwich composites without hybrid core formulation. This indicates that the strength of banana fibre with epoxy resin is restricted when it is used without a hybrid core. However, when HGM and clay particles are combined as the hybrid core, the performance improves due to the excellent interfacial adhesion between the hybrid core and the matrix. The enhanced mechanical characteristics may indicate that this material can find use in sectors requiring sandwich constructions that are both lightweight and mechanically sound. This work demonstrated a novel approach to sandwich structure construction by utilising hybrid core and banana fibres to improve mechanical properties.

6.1.2.1 Density of Sandwich composites

The density of sandwich composite is determined by the relative quantity of matrix and reinforcing elements, and this is one of the very critical factors defining composites' qualities. The inclusion of voids in the sandwich composites accounts for the disparity in theoretical and experimental densities. As a result, determining the percentage of voids in the prepared samples of sandwich composites becomes critical. Table 6.1 shows the theoretical and experimental densities, as well as the volume proportion of voids in the sandwich composites with the hybrid core. Sandwich composite had more voids, which were attributed to poor filler bonding or fiber/matrix bonding and, ultimately to the epoxy matrix not completely wetting the banana fiber. The content of voids in sandwich composites is determined by the behavior of the hybrid cores with facesheet due to particle concentration of fillers in the hybrid core and also because natural fibers have lumens in their cellular structure that behave as voids, implying that such fiber naturally transports these spaces. Thus, it may contribute to an increase in void content in the sandwich composite [298]. The density of the core as observed in Table 4.4 play a key role in determining the overall density of the sandwich panel because of the hybridization of HGM with nanoclay in the core and as the concentration of HGM increases in each of the formulation, it makes the sandwich panel to be more buoyant as observed in Table 6.1

Table 6.1: The experimental density of sandwich composites with hybrid core

Composite notation	Theoretical density (g/cm^3)	Experimental density (g/cm^3)	Porosity(%)
EPF	1.157	0.997	3.797
1HF	1.102	0.994	9.800
1H1CF	1.091	0.987	9.532
1H3CF	1.032	0.946	8.333
1H5CF	0.978	0.916	6.339
3HF	1.060	0.962	9.245
3H1CF	1.032	0.981	4.942
3H3CF	0.978	0.903	7.669
3H5CF	0.931	0.880	5.477

6.1.2.2 Tensile Properties of Sandwich Composites

Determining the tensile properties is crucial because it offers details about different tensile characteristics (elastic limit, tensile strength, modulus of elasticity, etc.), and understanding how composite materials react to applied forces in tension is crucial because it offers details about the materials' ability to withstand tension. Since each composite has unique tensile characteristics, tensile tests are carried out to comprehend how various composites behave [299]. The tensile strength and specific tensile strength of sandwich composites are depicted in Figure 6.1 with the effect of hybrid core loading on the tensile strength of sandwich composites. Varying tensile strength results were observed in the composites, this performance was a result of the amount of voids observed in the sandwich composites due to the percentage of hybrid filler added in the core which is similar to results obtained by Basheer A. et al.[300] and also because natural fibers have lumens in their cellular structure that behave as voids, implying that such fiber naturally transports these spaces but the highest tensile strength was observed in 3H1CF which is 30.31MPa with 3%HGM+1%Clay of hybrid core loading with banana fiber facesheet. This is because the fillers in the hybrid core provide reinforcement, allowing stress to flow from the matrix to the fillers. The sandwich composites containing 3H3CF hybrid core loading show a decrease in tensile properties which could be because of the filler packing or filler loading in the core as well as insufficiently rich epoxy areas. Furthermore, the possibility of fiber entanglements and filler agglomeration occurs in the sandwich composite, resulting in

a reduction in stress transfer between the matrix and the fiber/filler. Similar results were reported by Boopaan et al.[301] for fiber-reinforced sandwich composites. Porosity and cavities affect the matrix-dominated characteristics like tensile, the flexural strength. Additionally, as shown in Figures 6.1 and 6.2, the density values of the sandwich composites were utilized to normalize the tensile strength and tensile modulus, producing specific tensile strength and specific tensile modulus. Due to the volume percentage of fillers employed in the construction of the hybrid core, this has little impact on the material. It was also observed that the specific tensile strength and specific tensile modulus are higher than the tensile strength and tensile modulus in all the composites because of their strength-to-weight ratio.

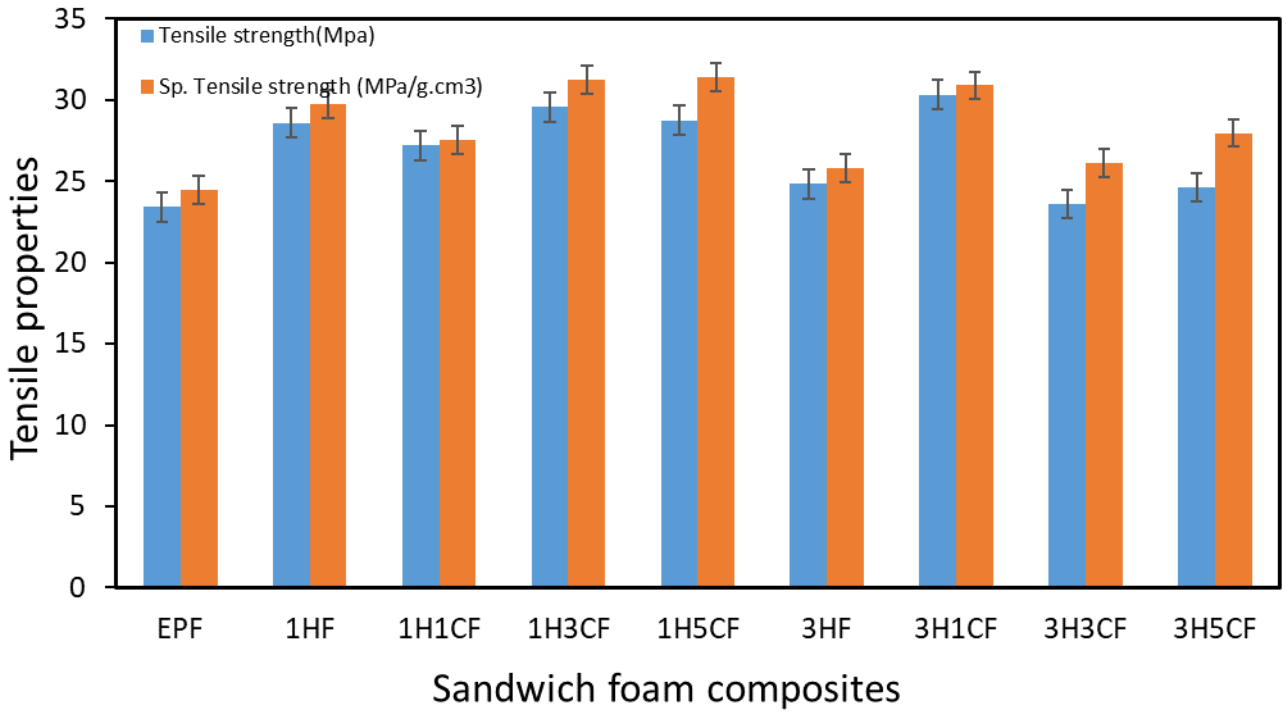

Figure 6.1: Tensile strength of sandwich composites with hybrid core

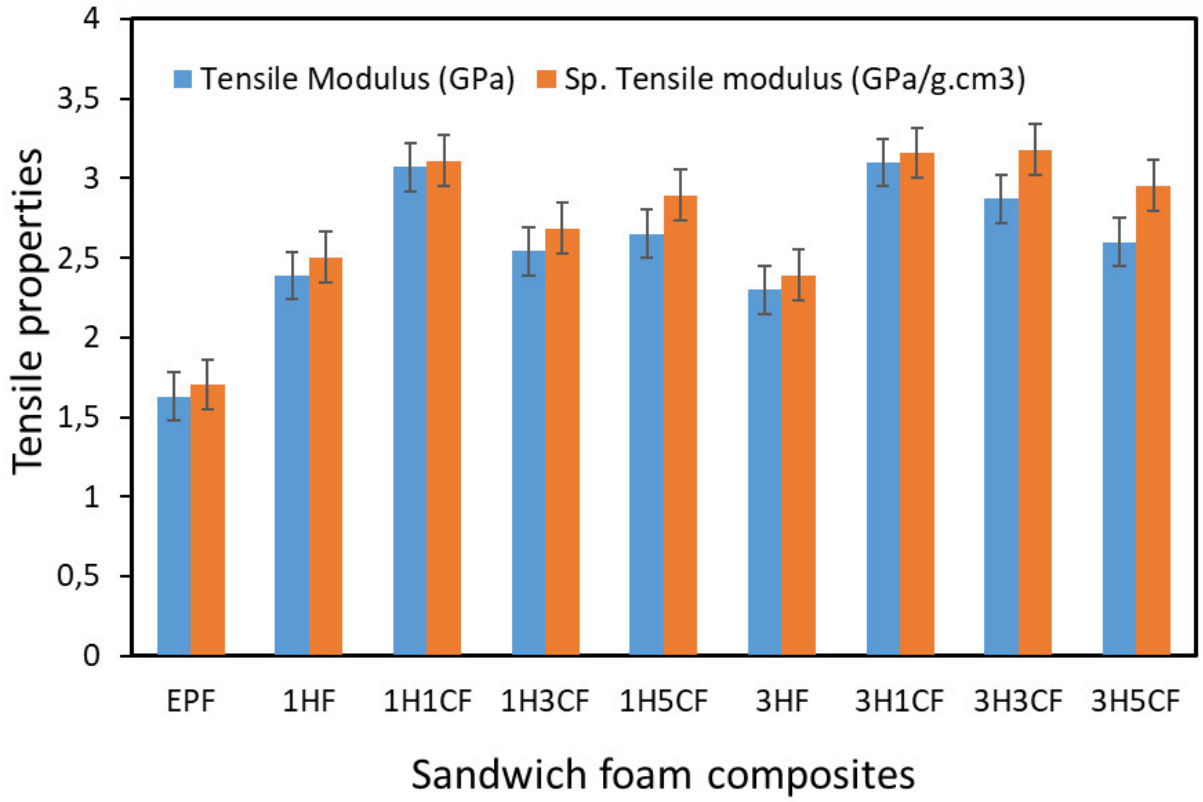

Figure 6.2: Tensile modulus of sandwich composite with hybrid core

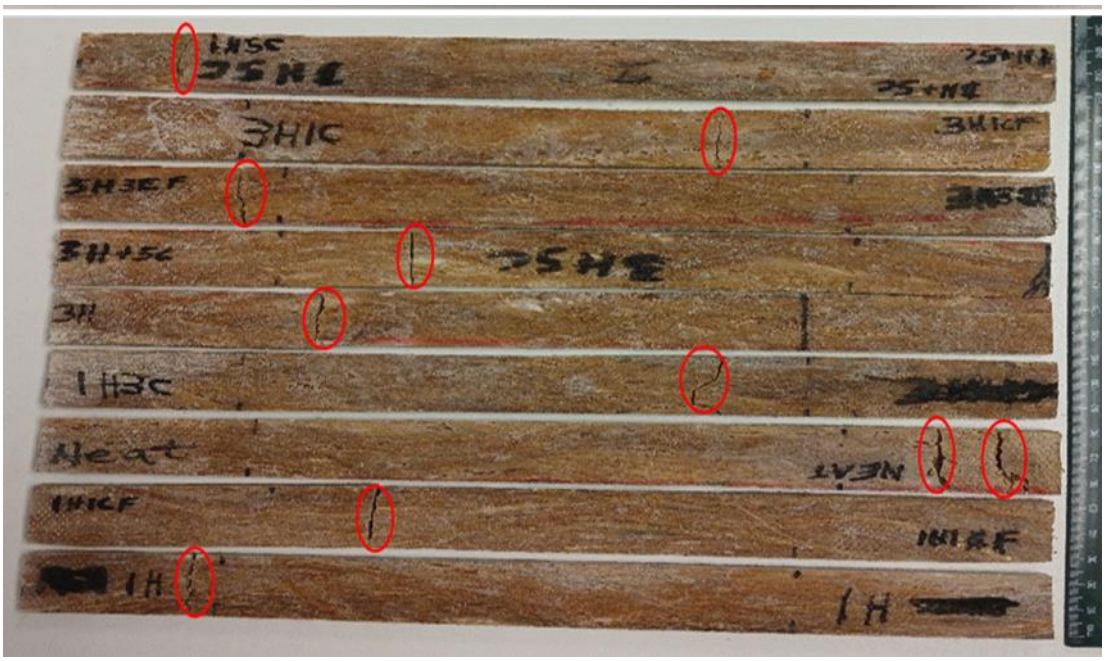

Figure 6.3: Tensile samples of sandwich composites filled with hybrid core after fracture

6.1.2.3 Flexural Properties

Figures 6.6 and 6.7 show a summary of the flexural test 3-point bending findings which shows the graphs of the nine sandwich composite sequences. As can be seen in Figures 6.6 and 6.7, the flexural strength and flexural modulus were normalized using the sandwich composites' density values to get the specific flexural strength and specific flexural modulus. Due to the volume percentage of fillers employed in the construction of the hybrid core, this has little impact on the material. It was also observed that the specific flexural strength and specific flexural modulus are higher than the flexural strength and flexural modulus in all the composites because of their strength-to-weight ratio. The flexural strength of samples 3H3CF and 3H5CF decreases as the percentage of hollow glass microspheres increases because of their brittleness, which may make the sandwich composite panel less resistant to bending or flexural stresses. In contrast, nanoclay particles increase the flexural strength by enhancing the panel's stiffness, providing reinforcement at the nanoscale level, and improving the stress transfer between the matrix and fillers. Figures 6.4&6.5 display the average flexural performance of the sandwich structures, with the main form of failure observed at the lower face sheet undergoing tension as seen in Figure 6.5. It is worth noting that while the improved performance of sandwich structures with hybrid core may be due to the concentration of filler used in the core, the samples with hybrid core consist of slightly denser cores compared to the samples with virgin core as shown in Table 1. Figure 6.6 compares the flexural strength of the nine sandwich composites, 67.79 MPa strength level at 1H1CF was observed and this represents the influence of the combined effect of hybrid core and banana fiber skin to increase strength. The differences in maximum flexural values are related to each sample's capacity to bear the bending force. A high degree of flexural strength at 1H1CF demonstrates the ability of the hybrid core in the sandwich structures to absorb more applied shear pressure than the HGM-filled core sandwich structure which is similar to work done by Pandey et al. [302]. This is due to the good bonding structure that exists between the facesheets and the hybrid core when the loads are carried together [303]. A significant correlation was detected between the strength values and the maximum flexural modulus, which was observed at 1H1CF. This suggests a strong link between the face sheets and the core. The rising sequence for flexural strength and modulus is > 1H1CF> 1HF>1H5CF>3H1CF >EPF>3H3CF>3H5CF>1H3CF, with a percentage increase of over 18.11% and 16.07% in terms of flexural strength and modulus, respectively. It was also determined that the bending strength exceeded the tensile strength, which corresponds to the Leguillon et al.[304] investigations when they stated that the bending strength of the sandwich

composite panel was larger than the tensile strength. Overall, the sandwich composite structures using hybrid cores demonstrated better improvement in flexural properties, with 1H1CF showing an average flexural strength of 67.80 MPa, and 1H3CF showing a flexural modulus of 8.74 GPa.

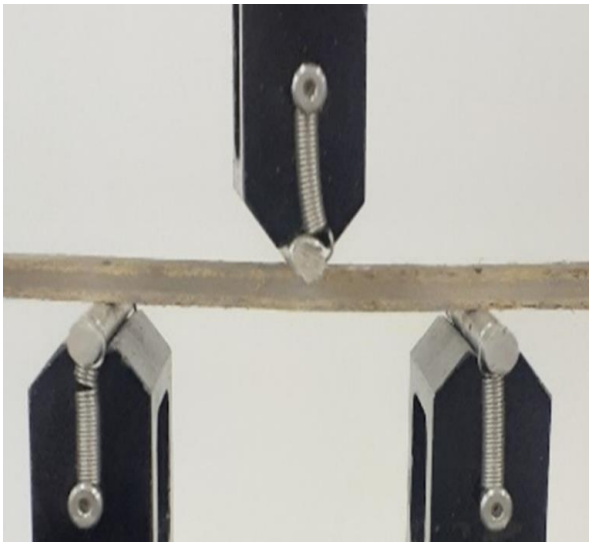

Figure 6.4: Flexural test set up showing sample before fracture

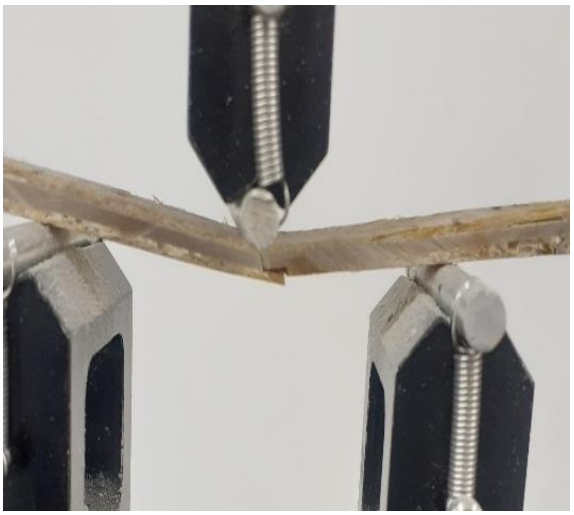

Figure 6.5: Flexural test set up showing sample after fracture

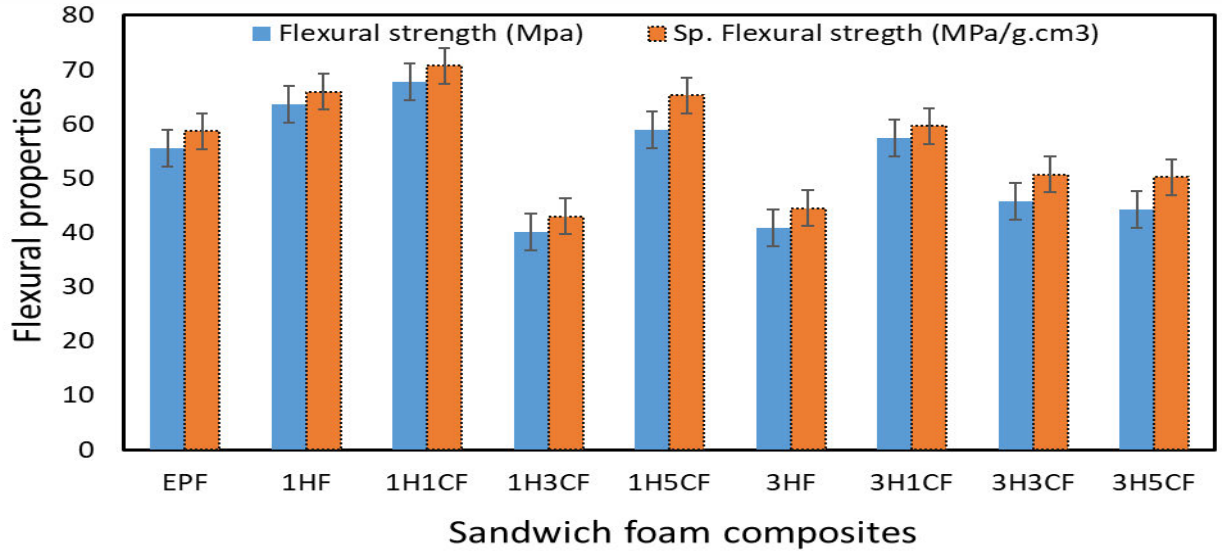

Figure 6.6: Flexural strength of sandwich composites filled with hybrid core

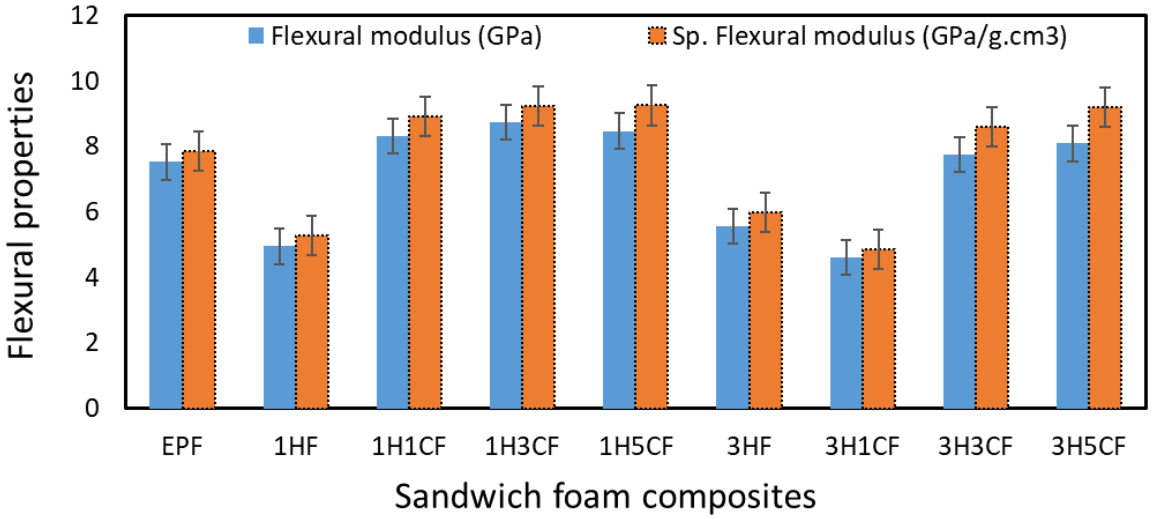

Figure 6.7: Flexural modulus of sandwich composite filled with hybrid core

6.1.2.4 Impact Properties of Sandwich Composites

Impact tests are used to measure a material's toughness. The toughness of a material is a measure of its capacity to absorb energy during plastic deformation. Figure 6.8 depicts the effects of filler/fiber loading on sandwich composites' impact energy. The impact energy of the sandwich composites filled with HGM core is found to be lesser than the sandwich composite panels filled with the hybrid core. Fractures in the specimen begin with crack propagation caused by a lack of a high level of adhesion between the facesheets and the core, following that,

fiber breakage, matrix fracture, and pull-out ensue. The findings of the experiments revealed that using a hybrid core in sandwich composite material increases the bonding capability and this results in increased impact strength. The greatest amount of impact energy value of 168.1KJ was achieved for the sandwich composite at 3H3CF of hybrid core loading. A similar pattern of increasing impact strength value with increasing filler/fiber loading was also reported by Cabral et al. and Eyvazian et al. in their studies. [305-307]. The increase in impact strength with increasing filler concentration in hybrid core loading could be attributed to more energy being required to break the connection between the interlaced filler/fiber bundles [308].

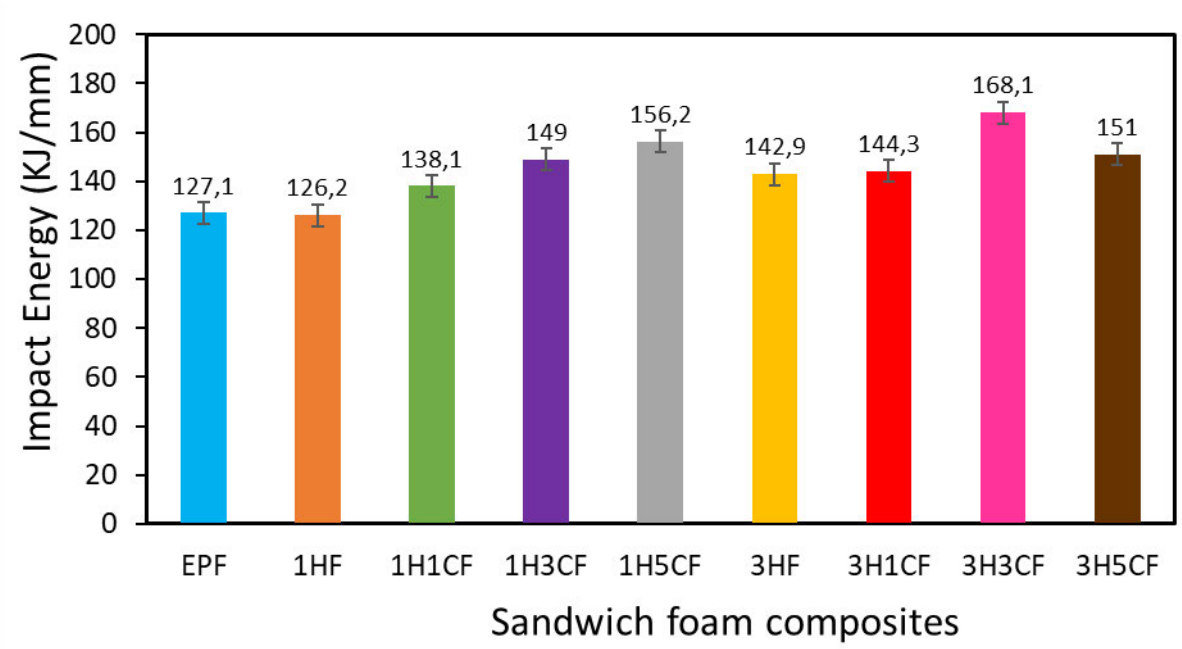

Figure 6.8: Impact strength of sandwich composites with hybrid core

6.1.2.5 Surface Morphology

Following the tensile test, the surface properties of the sandwich composite material were investigated using a scanning electron microscope (SEM). Figure 6.9(a-i) shows a micrograph of a tensile test broken specimen of the sandwich composite materials. Using scanning electron microscopy (SEM), the microstructural pattern of the tensile cracked specimens on each composite during testing was characterized for sandwich composite materials with different hybrid core formulations. The shattered fibers and distributed fillers in Figures 6.9b, 6.9d, and 6.9g exhibit improved load-bearing and reduced agglomeration as a result of the strong link between the facesheets and hybrid core which was also revealed in the tensile and impact strength of the panel as observed in Figures 6.2 and 6.8. The sandwich composites' strength and

modulus improved as a result. Clustered fillers with a rough surface that led to early breakage and low strength values were seen in Figures 6.9e, 6.9f, and 6.9h which corresponds to result of the flexural strength as seen in Figure 6.7. This might occur as a result of their independent load-bearing before the core fracture [309]. Additionally, Figures 6.9c and 6.9i showed the tensile cracked fibers, indicating increased load bearing because of the strong link between the hybrid core and facesheets. As a result, the sandwich composites experienced an improvement in modulus and strength.

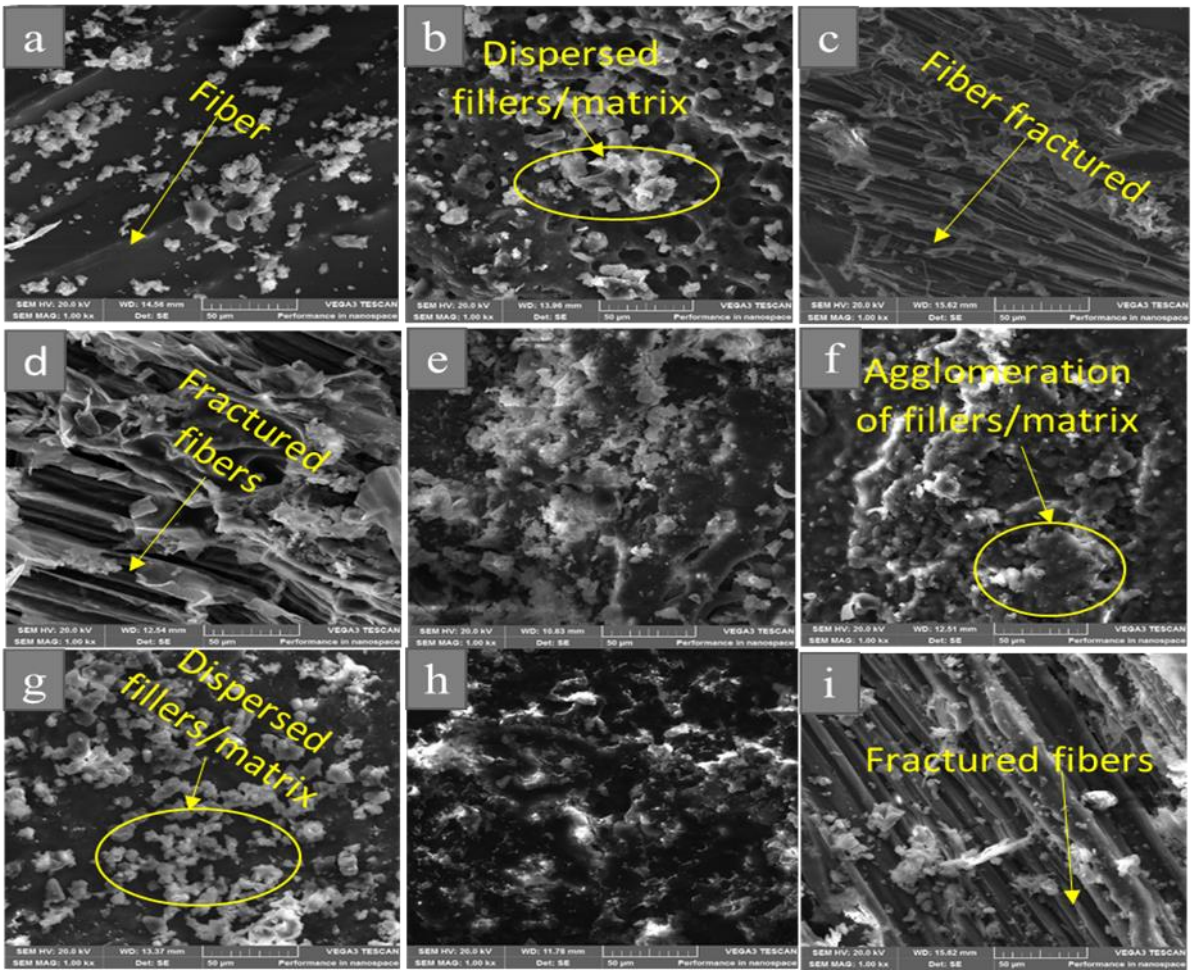

Figure 6.9: SEM image of the tensile fracture surface of sandwich composite for (a) EPF (b) 1HF (c) 1H1CF (d) 1H3CF (e) 1H5CF (f) 3HF (g) 3H1CF (h) 3H3CF (i) 3H5CF

6.1.2.6 Water Absorption Behavior of Sandwich Composites

The water absorption capacity of sandwich composites as a function of immersion time is shown in Figure 6.10. It shows the hourly percentage of water absorption. It is evident that for about six days, the absorption behaviour increases gradually with the length of immersion. The graph shows that sandwich composites with HGM cores absorb water much more quickly than sandwich composites with hybrid cores. This is because water penetrates the pores and the

interface layer of HGM and epoxy resin, potentially causing more damage to the HGM at higher concentration. Given that the hybrid core contains nanoclay, which contains silicon-oxygen (SiO4) tetrahedron bilayers with deeply rooted octahedral layers of aluminium and iron that can withstand moisture, the sandwich composites with the hybrid core exhibit a maximum absorption of 4.54%, whereas the sandwich composites with the HGM core that has no nanoclay exhibit 8.61% and this is similar to result reported by Nemati Giv et al. [310] on water absorption behavior of composites filled with nanoclay.

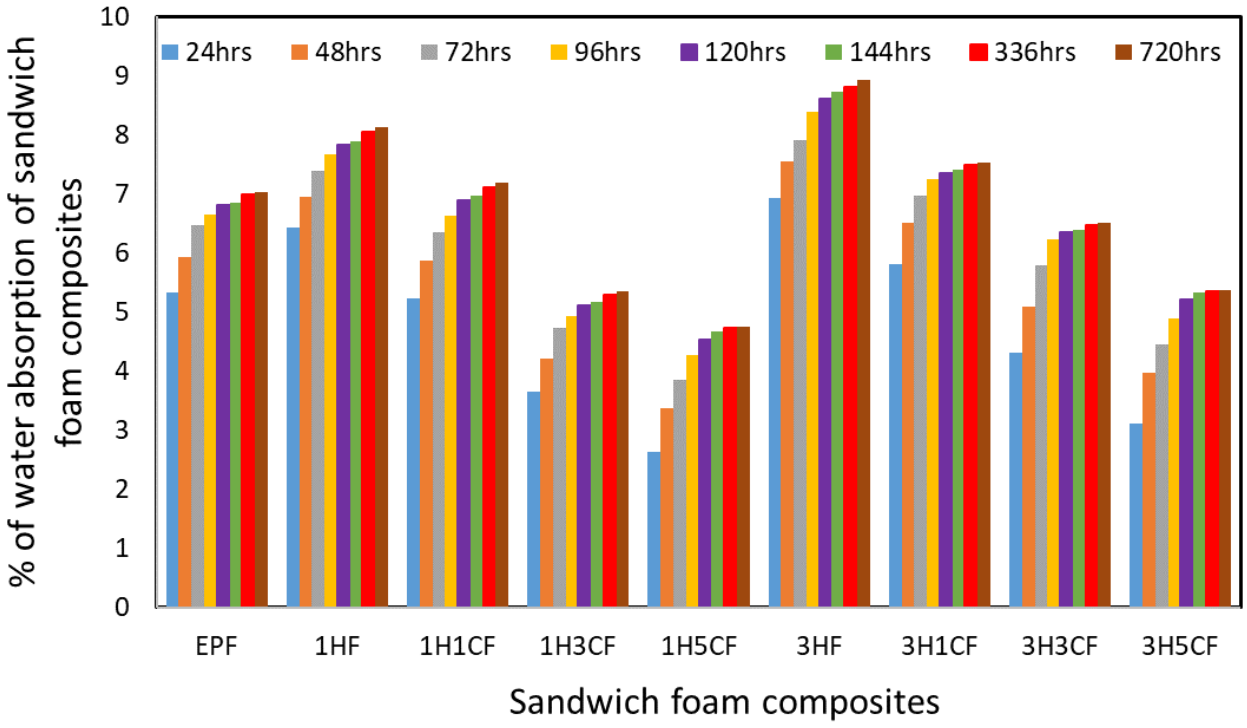

Figure 6.10: Percentage of Water Absorption of sandwich composites with hybrid core

6.1.2.7 Water Contact Angle.

The contact angle test was used to analyze the wettability behavior of the sandwich composite materials filled with the hybrid core. The contact angle of water on the transverse surface of sandwich composite panels is summarized in Table 6.2. According to Klein N S et al. and Xiong B et al.[292, 293], a surface is considered hydrophilic when the static water contact angle θ is less than 90^0 and hydrophobic when θ is greater than 90^0. In this study, all the sandwich composite samples exhibited hydrophilic behavior, indicating their affinity for water because of their natural use as the facesheet. However, the study revealed that sandwich composite 1H5CF with the highest concentration of nanoclay displays an average contact angle of 62.13

indicating a significant change in the hydrophilic behavior of the sandwich composite panel when compared to other samples of sandwich composite as seen in Figure 6.11. This behavior justifies the reason why the sandwich composite sample 1H5CF exhibits the lowest percentage of water absorption in Fig.6.6 due to the concentration of nanoclay in the hybrid core.

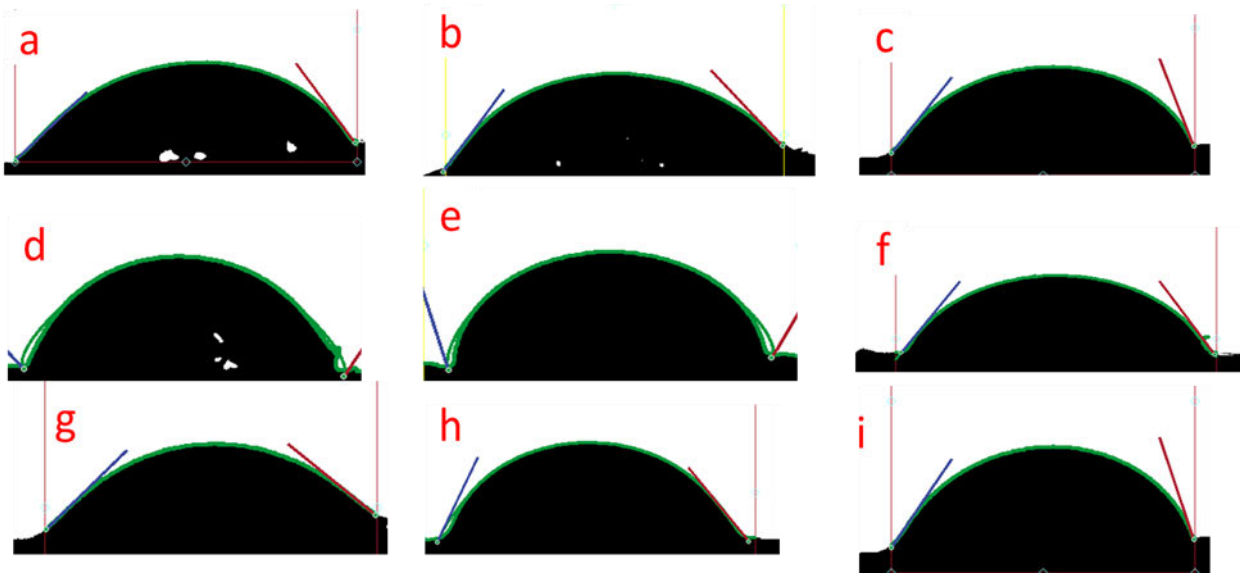

Figure 6.11: Images of WCA of (a)EPF (b) 1HF (c) 1H1CF (d) 1H3CF (e) 1H5CF (f) 3HF (g) 3H1CF (h) 3H3CF (i) 3H5CF

Table 6.2: Water contact angles of sandwich composite panels.

Materials	Water contact angles(WCA) θ^0
EPF	47.41 ±0.43
1HF	37.55 ± 0.39
1H1CF	45.17 ± 2.13
1H3CF	58.22 ± 0.87
1H5CF	62.03 ± 0.34
3HF	33.87 ± 1.85
3H1CF	41.47 ±3.31
3H3CF	52.74 ±0.63
3H5CF	56.67 ± 2.74

6.1.2.8 Buoyancy Behaviour of Sandwich Composites

The buoyancy force (Fb) of the sandwich composites is displayed in Figure 6.12. The 1H3CF had the lowest Fb of 0.102N, while the 3HF had the highest Fb of 0.147N. The maximum Fb found at 3HF may have resulted from its higher concentration of HGM than any other sandwich composite, suggesting that when submerged in fluid, it has a better buoyancy force than other sandwich composites because it has more Fb for an up-thrust to float than other sandwich composites filled with hybrid core. Additionally, 1H3CF will sink more quickly when submerged due to the high cellulose content of the banana fibres used as the face sheet and the concentration of nanoclay in the core. However, when a hybrid core containing a higher concentration of HGM is added to the sandwich composite, the low density of the fillers in the hybrid core can enhance the sandwich composites' floating capacity.

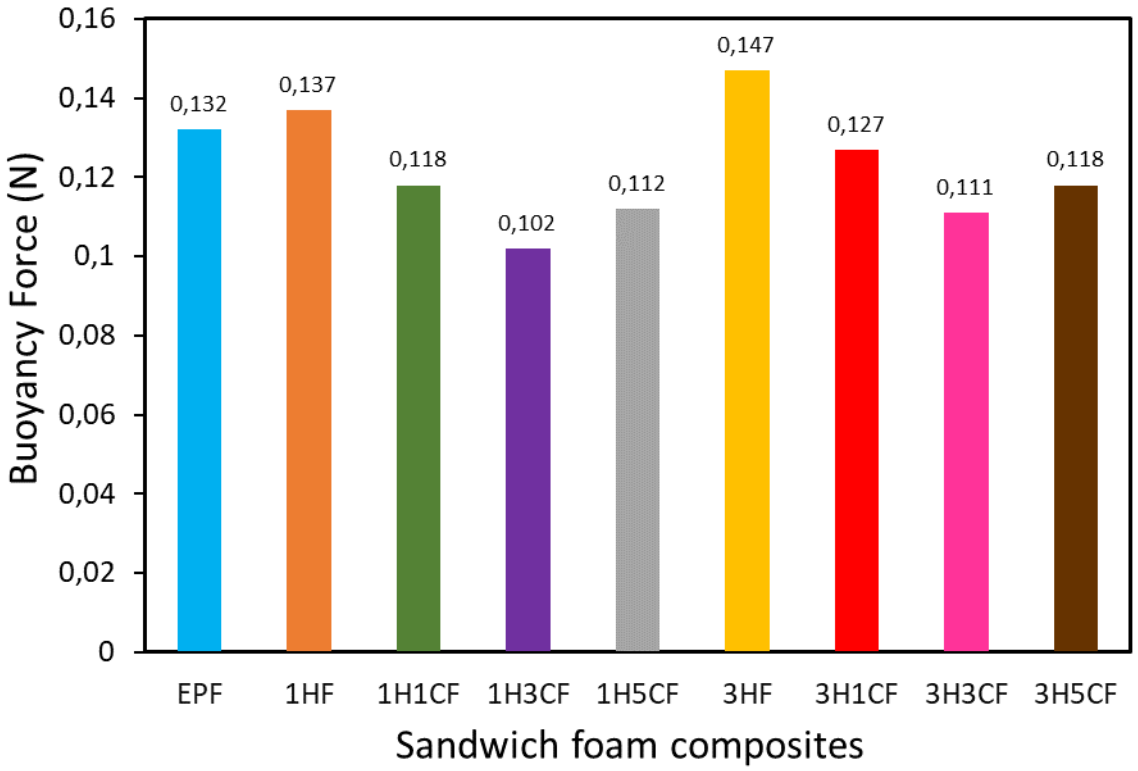

Figure 6.12: Buoyancy Force (N) of hybrid-filled Sandwich Composites

6.1.2.9 Strength-to-weight ratio

The strength-to-weight ratio of the hybrid core refers to the relationship between the weight of a sandwich composite structure and the amount of weight it can support before collapsing.

Sandwich composite structures are known for having an exceptional strength-to-weight ratio, due to their density, which provides a balance between structural integrity and material usage. It was observed that the use of HGM and nanoclay as hybrid core enhanced the sandwich constructions' strength-to-weight ratio in tensile strength and flexural strength. Strength-to-weight characteristics of the sandwich structures, as seen in Figures 6.1, 6.2, 6.6, and 6.7, undergoing tensile and flexural have improved with the addition of a hybrid core in the sandwich respectively.

6.1.3 Conclusion

In conclusion, the study demonstrates the feasibility of using hybrid core materials with banana fiber facesheet in a sandwich composite structure. The use of natural fiber at the facesheet provides a sustainable alternative to traditional structures made of non-environmentally friendly materials. The combined effect of HGM and nanoclay in the hybrid core enhanced the tensile strength, flexural strength, and impact resistance of the structures while reducing water uptake. The combined effect of HGM and nanoclay in the hybrid core enhanced the flexural strength and tensile strength by 22.11% and 29.53%, respectively. The sandwich composite structures with 3H3CF absorbed 32.26% more impact energy than other remaining samples with different hybrid core loading. The sandwich composite structure with a hybrid core showed improved tensile strength while reducing moisture uptake, making them a promising option for use in various applications, including aerospace, automotive, and marine industries. The sandwich structure with hybrid core showed a tensile strength that was 6.05% higher than those sandwich composites using solely HGM core and was found to be hydrophobic, leading to a reduction of 8.61% in water uptake compared to solely HGM core and this is a significant because it gives the basis for comparison between sandwich panels with hybrid fillers in the core and sandwich panels with only HGM filler in the core. In summary, this study highlights the potential of using banana fiber as a facesheet with a hybrid core for sandwich composite offers desirable properties while being environmentally friendly, providing a valuable contribution to the growing body of research in sustainable materials for sandwich composite structures

CHAPTER 7: EFFECT OF SURFACE MODIFICATION ON MECHANICAL PROPERTIES OF HOLLOW GLASS MICROSPHERES(HGM)-FILLED EPOXY FOAM COMPOSITES

7.1 Introduction:

This chapter discussed the journal paper tittled "Effect of surface modification on mechanical properties of hollow glass microspheres (HGM)-filled epoxy foam composites" by Ayodele Abraham Ajayi, Mohan Turup Pandurangan and Kanny Krishnan submitted to Journal of SPE Polymer (Accepted with correction).
The paper focused on characterizing the mechanical performance of foam composite panel with surface modification of HGM.

7.1.1 Objectives of the journal paper

The major objectives of this journal paper

- To fabricate lightweight foam composite panel with hollow glass microspheres and compatibilizers
- To determine the influence of surface modification on HGM filler
- To compare the mechanical properties of HGM-filled foam composite with compatibilizer.
- To investigate the efficacy of surface modification in enhancing the mechanical properties of foam composite panel

7.1.2 Summary

This work focuses on comparing the mechanical properties of epoxy-based foam composite panels with modified fillers by using polypropylene-grafted maleic anhydride (PP-g-MA) as compatibilizer to modify the surface of the filler so as to enhance its mechanical properties. Foam composite panels were made by conventional resin casting, with the HGM content ranging from 1 to 5 weight percent. The PP-g-MA content was 3 weight percent in each of the modified HGM-filled series of foam composite panels. The prepared epoxy-based foam composite panels with compatibilizer modification were tested for mechanical properties like

tensile strength, impact strength, hardness, and flexural strength. The results were compared to neat epoxy and foam composite panels without compatibilizer modification.

It was found that the epoxy based foam composite panels that were modified with compatibilizer exhibited improved mechanical properties than the epoxy based foam composites that were not modified and the neat epoxy. The superior interfacial connection between the fillers and the matrix was the reason of these enhanced properties. Given its better mechanical properties, this material might be a good fit for applications requiring lightweight materials with strong mechanical properties. This work demonstrated a new field of study in synthetic foam production by employing modified HGM to improve mechanical qualities.

7.1.2.1 Surface Morphology of Foam Composite(SEM)

The microstructure of the composite is depicted in Figures 7.1(a,b,d,f) without the compatibilizer PP-g-MA. The broken surface is extremely clean in the absence of PP-g-MA, and the shattering of hollow glass microspheres suggests that there was insufficient interaction between the filler surface and the matrix. A hollow glass microsphere was incorporated into the polymer matrix without exhibiting any notable indications of a strong connection. The composite's microstructure with PP-g-MA acting as a compatibilizer is depicted in Figures 7.1(c,e,g). The hollow glass microspheres were evenly distributed throughout the polymer matrix, as the image illustrates. The primary cause of this is improved stress transmission at the interface due to better bonding between the polymer matrix and the reinforcements.

.

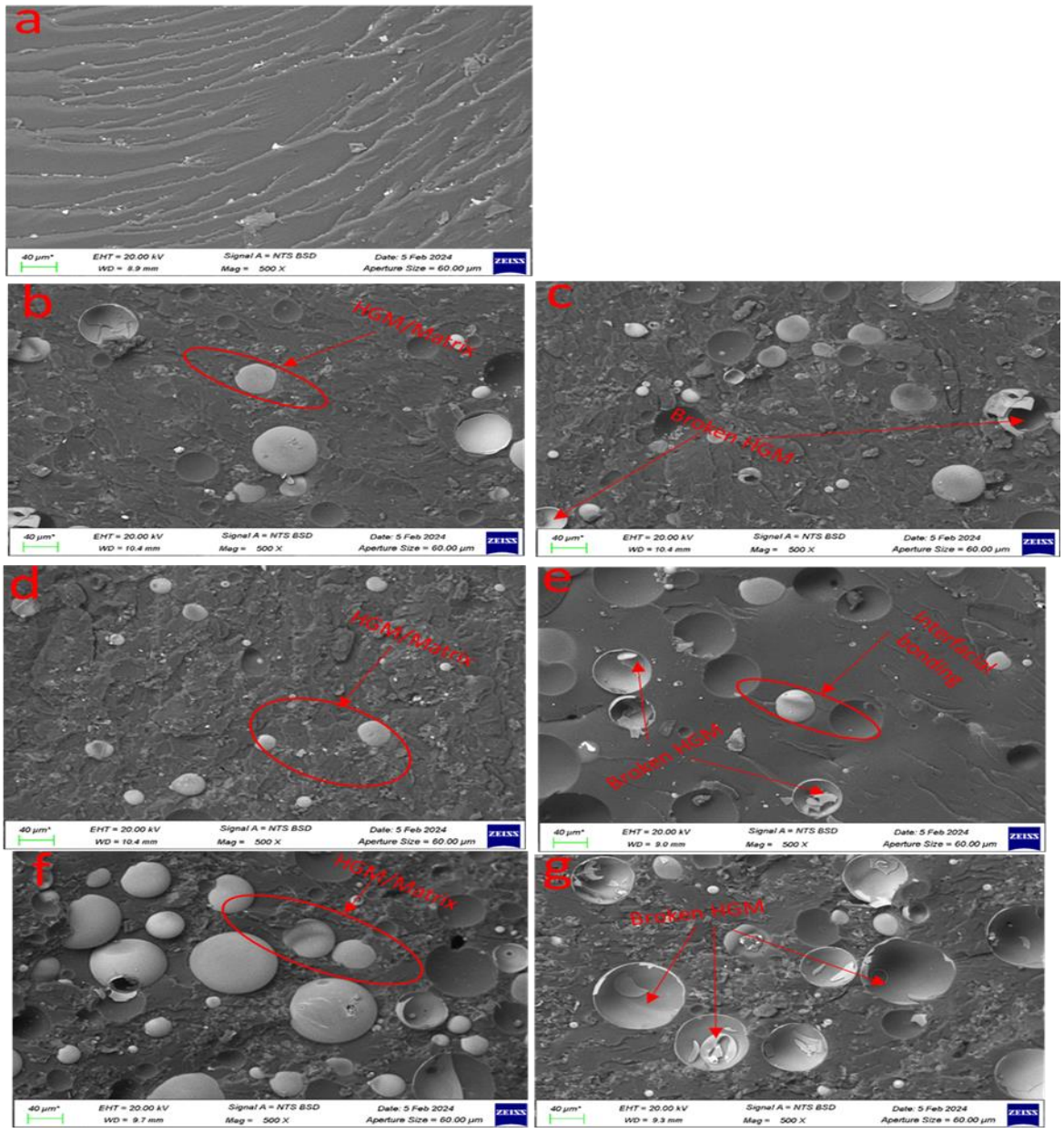

Figure 7.1: SEM images of Neat and HGM-filled foam composites (a) Neat epoxy (b) 1%wt.HGM (c) 1%wt.HGM+PP-g-MA (d) 3%wt.HGM (e) 3%wt.HGM+PP-g-MA (f) 5%wt.HGM (g) 5%wt.HGM+PP-g-MA

7.1.2.2 Density

Also in Table 7.1, it was observed that the density calculated theoretically from the weight fraction does not equal the experimentally measured density due to the presence of void and pore during the experimental process that cannot be wholly avoided. This performance was due to voids in the panel because of filler. Also, as PP-g-MA compatibilizer was introduced into the filler, there was a decrease in the density. This implies that the foam composites with

compatibilizer may find application where lightweight materials are required because of its reduced weight.

A foam composite material's density depends on the corresponding proportion of matrix materials and compatibilizers, which is a critical factor in determining foam panels' properties. The amount of pores is the primary reason for the difference between the values obtained from experimental density and values obtained from theoretical density when calculated. Some of the mechanical properties are significantly impacted by the existence of pores, which in turn impacts how well the foam panel performs in real-time applications. A good foam composite panel should have fewer pores, although the complete absence of pores cannot be achieved in the fabrication of foam panels mainly through the hand lay-up method.

Table 7.1: Foam composite Sample formulation with HGM and PP-g-MA content

HGM-filled Samples	Theoretical density(g/cm^3)	Experimental density(g/cm^3)	Void fraction (%)
Neat epoxy	1.130	1.046	7.434
1%wt.HGM	1.120	1.015	9.375
1%wt.HGM+PP-g-MA	0.958	0.897	6.367
3%wt.HGM	1.099	0.983	10.55
3%wt.HGM+PP-g-MA	0.981	0.908	7.441
5%wt.HGM	1.027	0.897	12.658
5%wt.HGM+PP-g-MA	0.847	0.789	6.848

7.1.2.3 Water Contact Angle

The WCA is a crucial indication of the hydrophilicity and hydrophobicity of materials since it primarily relates to the surface microstructure and surface chemical characteristics [291]. The contact angle decreases with increasing surface roughness for the same material. Figure 7.2 illustrates how the hydrophobic behavior of the HGM-filled foam composites following filler surface modification may be examined by the measurement of water contact angle and contrasted with the HGM-filled foam composites prior to filler surface modification. All of the

foam composite panels that didn't have their filler modified were found to demonstrate hydrophilic behavior, which is consistent with the findings from our previous studies [311]. In contrast, foam composites that had filler surfaces modified showed hydrophobic behavior because of their water-repelling properties. Additionally, the research showed that the foam composite 5%wt.HGM showed an average contact angle of 35.28, as shown in table 7.2. This is because water infiltrates the pores of the HGM and epoxy resin interface layer, potentially causing damage to the HGM at higher HGM filler concentrations.

.

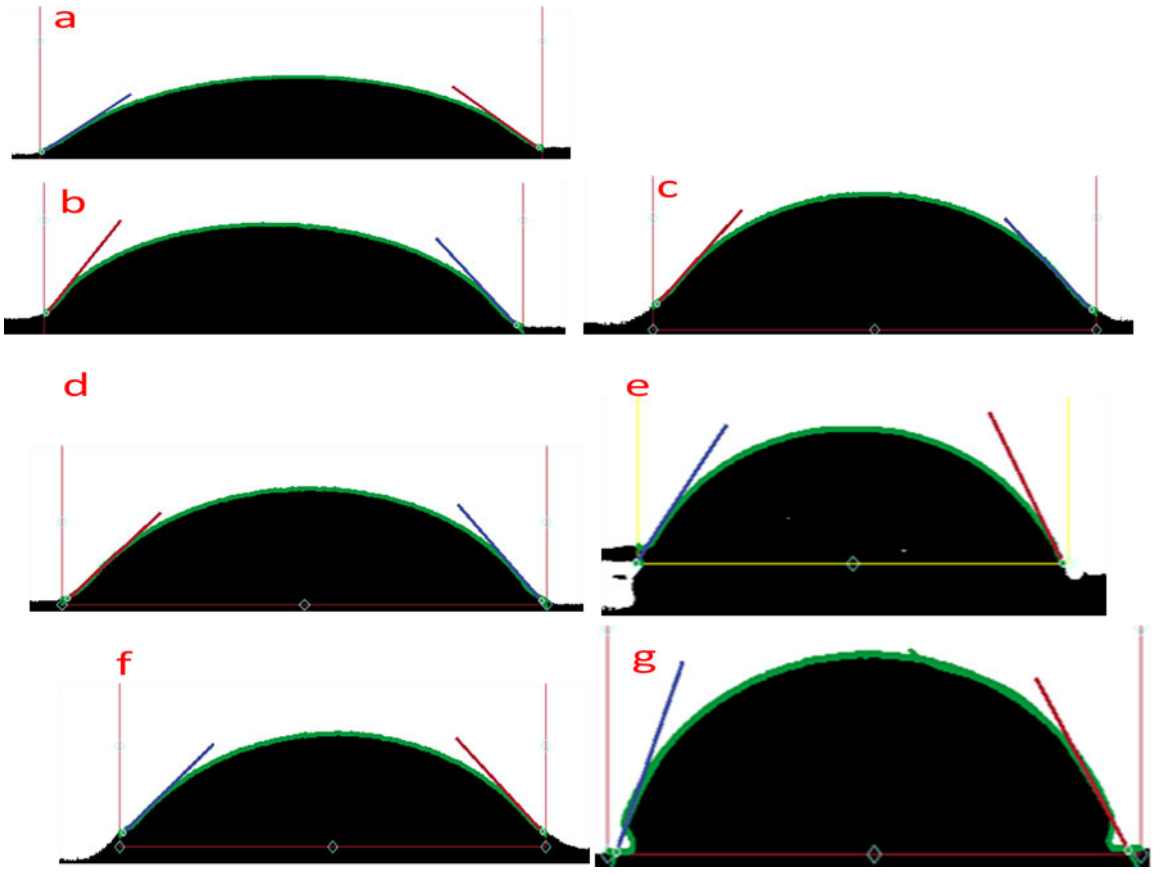

Figure 7.2: Images of WCA of (a) Neat epoxy (b) 1%wt.HGM (c) 1%wt.HGM+PP-g-MA (d) 3%wt.HGM (e) 3%wt.HGM+PP-g-MA(f) 5%wt.HGM (g) 5%wt.HGM+PP-g-MA

Table 7.2: Water contact angles of foam composite materials.

Materials	Water contact angles(WCA) θ^0
Neat epoxy	33.4 ± 2.0
1%wt.HGM	52.8 ± 0.8
1%wt.HGM+PP-g-MA	64.1 ± 0.7
3%wt.HGM	51.1 ± 1.6
3%wt.HGM+PP-g-MA	98.1 ± 0.7
5%wt.HGM	49.7± 1.6
5%wt.HGM+PP-g-MA	109.6± 0.6

7.1.2.4 Tensile Strength

Figure 7.3 displays the tensile strength of foam composites filled with HGM and PP-g-MA. The material's stiffness under axial loading is precisely measured by the Young's modulus. [312]. The tensile strength and young modulus are increased by the addition of PP-g-MA. The epoxy-based foam composite with 5wt%HGM and PP-g-MA had the maximum tensile strength, measuring 29.87 MPa. When the weight fraction of HGM increases, the percentage increase in tensile strength relative to the neat increases from 1, 3, and 5% wt. as 0.88%, 5.57% and 16.35% respectively and likewise each of the modified HGM-filled foam composites increased with the percentage of improvements as 20.20%, 27.06% and 45.31% which is an indication that the HGM-filled foam composite panels with compatibilizer possess better resistance capacity to breaking under tension than the HGM-filled foam composite panels without compatibilizer which is similar to previous findings on PP-g-MA studies [313-316]. Yet, lower tensile strength values at foam composites without the inclusion of PP-g-MA were ascribed to non-homogeneous reinforcement distribution in the matrix, resulting in the production of HGM agglomerates, which is consistent with the findings of Li et al [281] .

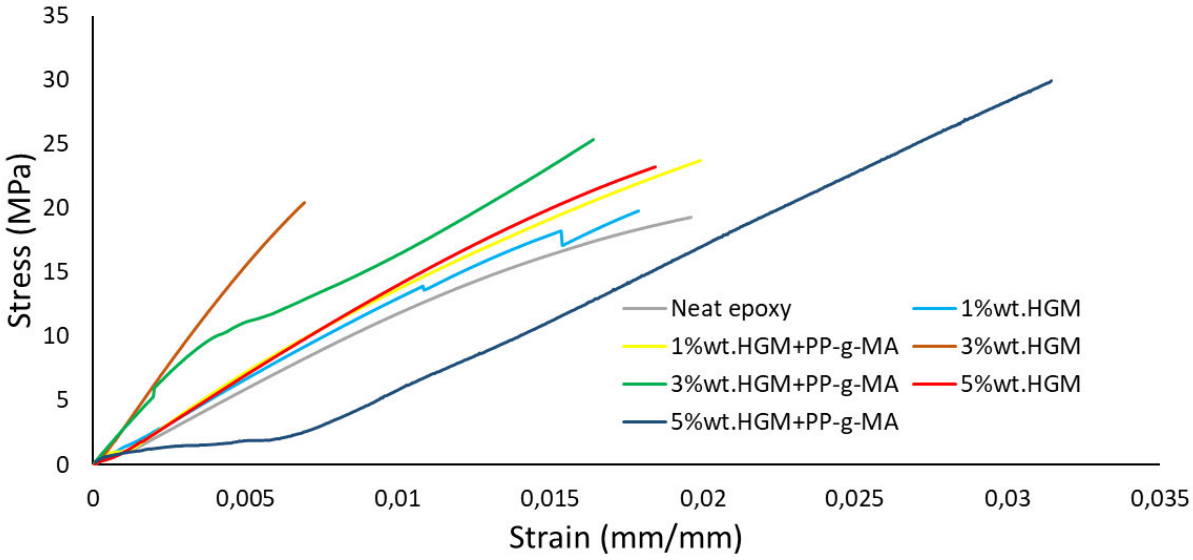

Figure 7.3: Tensile strength of Neat Epoxy and HGM-filled foam composite

7.1.2.5 Tensile Modulus

The HGM-filled foam composites series' tensile modulus is displayed in Figure 7.4. The findings showed that the tensile modulus rose in all HGM-filled foam composites; however, the tensile modulus rose even more in each HGM-filled series of foam composite after compatibilizer was added. This could be due to the filler's improved softening effect with compatibilizer, as well as better reinforcement distribution in the matrix, both of which work together to increase the stiffness of the composite. This aligns with the general pattern of outcomes documented by Sombatsompop N. et al. and Risite H et al.[316, 317]. As the weight proportion rises from 1, 3 and 5% weight, so does the tensile modulus percentage increases as 60.71%, 93.60%, 104.29% respectively

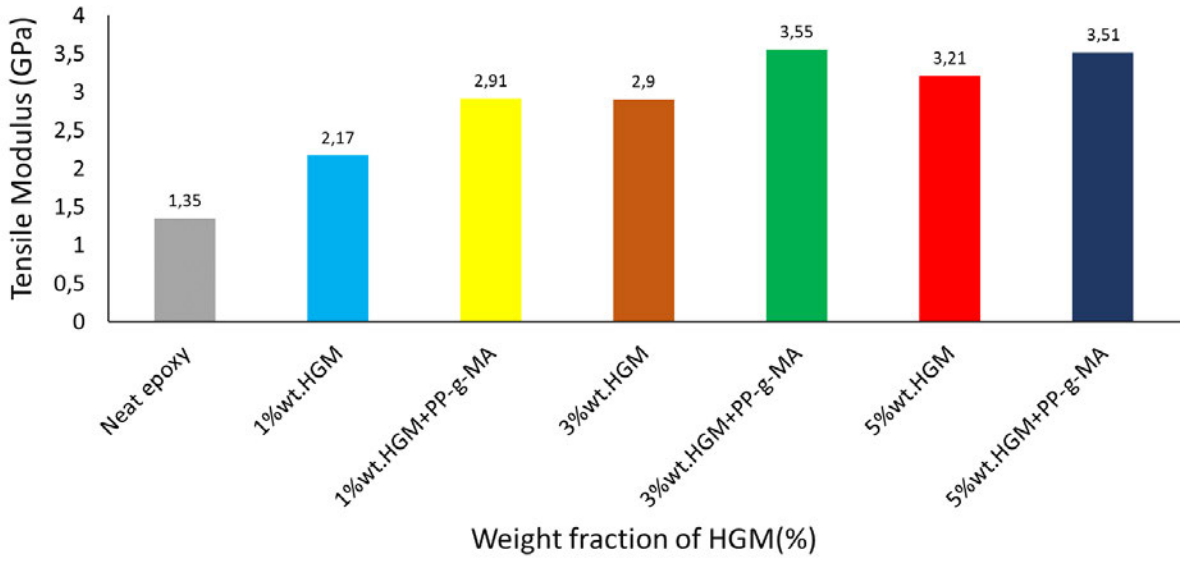

Figure 7.4: Tensile modulus of Neat epoxy and HGM-filled foam composite

7.1.2.6 Flexural Strength

To determine the strength and stiffness of both modified and unmodified HGM-filled foam composite panels, flexural tests were conducted. The figure 7.5 explains the behavior of the foam composite panel at different loading of HGM filler concentrations together with the neat epoxy. When HGM filler is added, and as the filler content rises, the foam composites' overall flexural strength increases. However, the flexural strength increases more when the HGM was modified in each of HGM-filled foam composites.

This suggests that adding HGM filler to an epoxy matrix can increase its strength. Similarly, adding surface treatment to HGM filler can increase its strength. The weight fraction of HGM in foam composites increases in direct proportion to the increase in strength. The tensile strength reaches its maximum strength at the 5%wt.HGM weight fraction of HGM, corresponding to the highest flexural strength of 81.3 MPa at that weight fraction. This can be attributed to reduced agglomeration and strong intramolecular bonding during the composite mixing. With a rising weight fraction of HGM from 1, 3, and 5% wt., the percentage increase in flexural strength relative to the neat epoxy increases as 2.58%, 11.50% and 27.76% respectively and likewise each of the modified HGM-filled foam composites increased with the percentage of improvements as 17.20%, 19.85% and 31.33% which is an indication that the HGM-filled foam composite panels with compatibilizer possess better bending capacity than the HGM-filled foam composite panels without compatibilizer. It can also be said that surface

treatment of HGM with compatibilizer can give better matrix dispersion during the mixing process, and resulting in high strength and stiffness. Additionally, the enhanced matrix and interfacial properties brought about by the inclusion of HGM and the HGM's surface treatment may be responsible for the improvement in flexural properties.

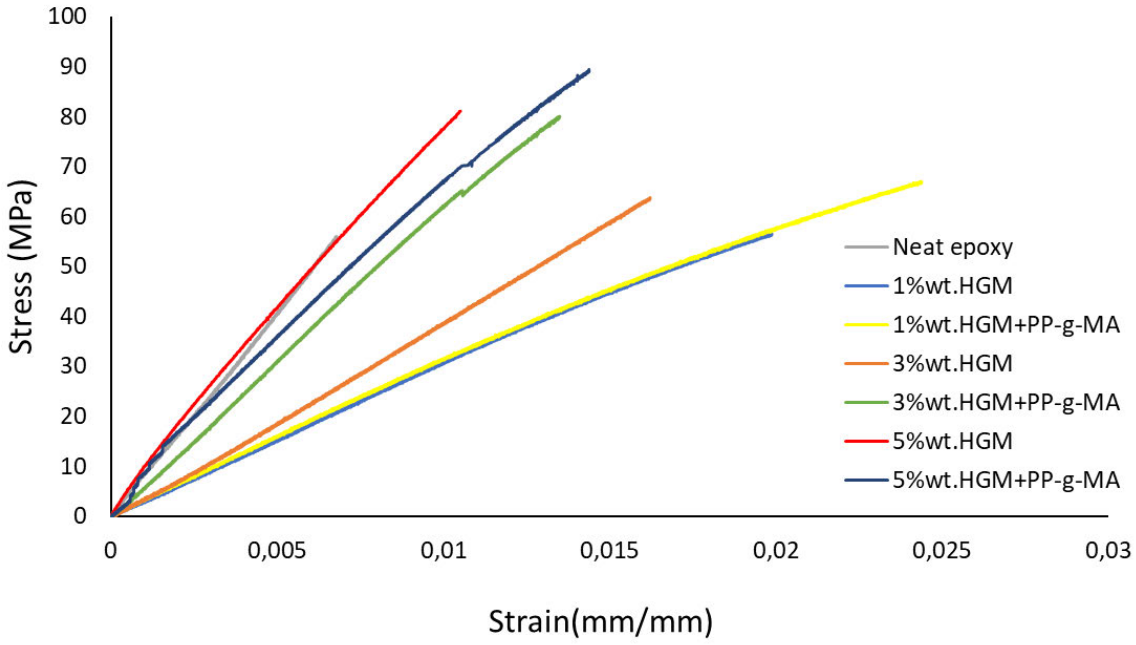

Figure 7.5: Flexural strength of Neat epoxy and HGM-filled foam composites

7.1.2.7 Hardness

Figure 7.6 shows the hardness values of HGM-filled foam composite, pure epoxy, and foam composite with and without compatibilizer. The hardness values obtained were predominantly influenced by the compatibilizer; as Figure 7.6 illustrates, the addition of PP-g-MA to the foam composites resulted in a decrease in hardness. The resistance of the foam composite panel to wear and scratches will decrease with a decrease in surface hardness. These are extremely important properties in service, and the results of this work by using compatibilizer to modify the filler have a negative influence on the resistance of the foam composite panel to wear and scratches.

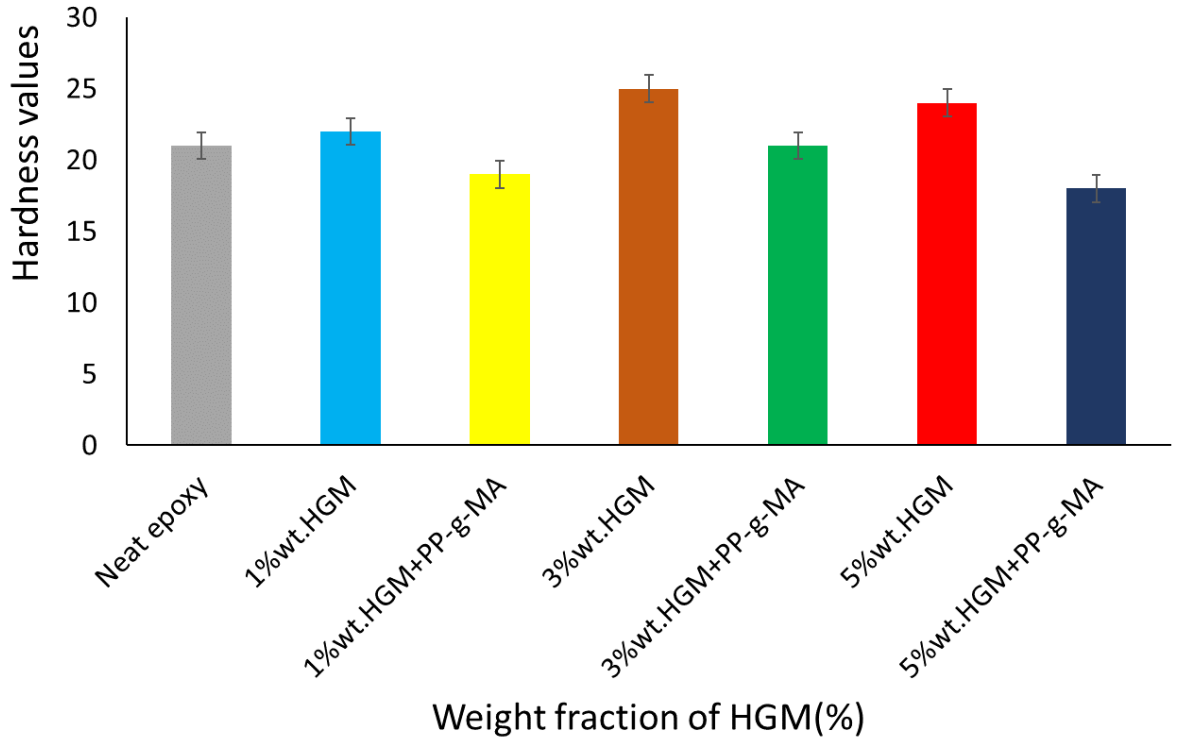

Figure 7.6: Hardness properties of Neat epoxy and HGM-filled foam composite panels

A decrease in surface hardness means that the foam composite panel's wear and scratch resistance will decrease, these are very vital properties in service which results obtained from this work by using compatibilizer has negative influence on the foam composite panel's resistance to wear and scratch, which is similar to what was reported by

7.1.2.8 Impact Strength

The impact strength for neat epoxy, HGM-filled composites with PP-g-MA and without PP-g-MA is shown in Figure 7.7. All foam composite compositions have impact strengths greater than neat epoxy, and the percentage of increase in strength rise with increasing HGM filler concentration. Since there is less agglomeration and greater dispersion with the epoxy matrix, it may be believed that a lower percentage of HGM filler below 10%wt. fraction can better absorb impact strength. This is consistent with our earlier research[252]. Also, increase in impact strength was noticed when HGM was modified in each HGM-filled foam composites which could be ascribed to the homogenous dispersion of the compatibilizer bringing about a coordinated bond that improves the energy-absorbing capacity of the foam composite, thereby adhering to the same general pattern as the flexural and tensile strengths. This demonstrates consistency in the results, indicating a positive reaction between the matrix, compatibilizer, and HGM filler mix that is consistent with the findings reported by Eker et al.[312]

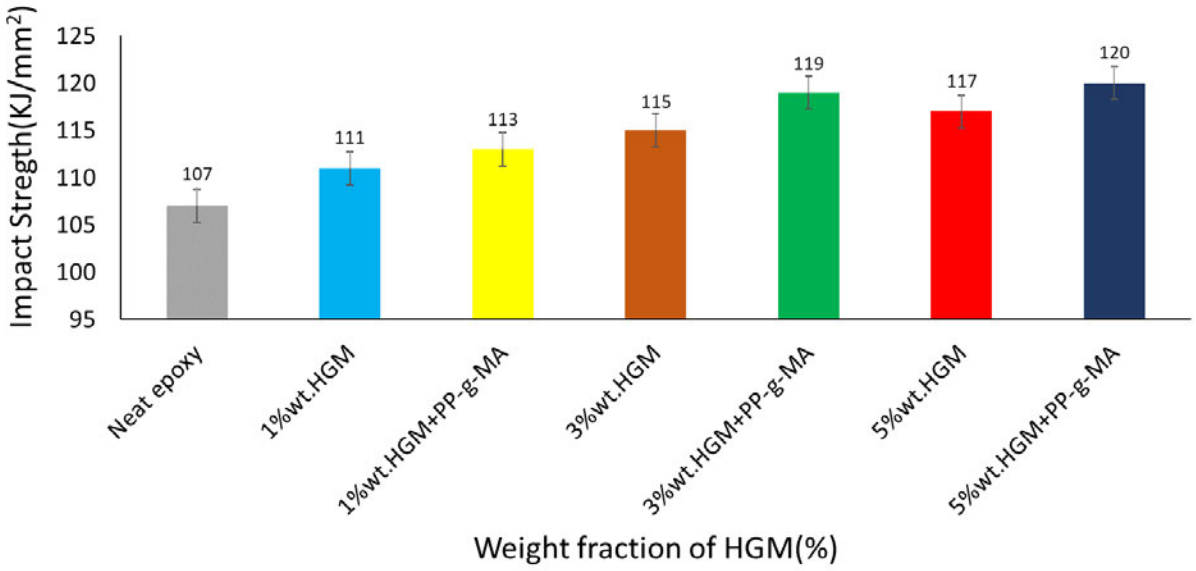

Figure 7.7: Impact properties of Neat epoxy and HGM-filled foam composite panels

7.1.2.9 Dynamic Mechanical Analysis (DMA)

Storage modulus estimates the energy stored in the yielding portion of the foam panel. In Figure 7.8, an increase in the storage modulus peak was noticed in 5wt.%HGM+PP-g-MA when compared to neat epoxy and other foam composite panels. Nevertheless, the loss modulus which estimates the energy lost at heat per cycle under the deformation of foam panel showed varieties of trends in the neat epoxy and other HGM-filled foam composite materials [318, 319]. Figure 7.9 shows that adding PP-g-MA as a compatibilizer for surface treating fillers in foam composites increased the loss modulus at the glass transition temperature (Tg). This effect was more pronounced in the foam composite with compatibilizer when the filler loading was 5wt.%HGM+PP-g-MA. The loss modulus peak showed a greater peak value of 278.8MPa, surpassing both the clean epoxy value and other foam composite samples.

Storage modulus estimates the energy stored in the yielding portion of the foam panel. In Figure 7.8, an increase in the storage modulus peak was noticed in 5wt.%HGM+PP-g-MA when compared to neat epoxy and other foam composite panels. Nevertheless, the loss modulus which estimates the energy lost at heat per cycle under the deformation of foam panel showed varieties of trends in the neat epoxy and other HGM-filled foam composite materials [318-320] .

It was observed in Figure 7.9 that the addition PP-g-MA as compatibilizer for surface treatment of fillers in the foam composites caused an increase of loss modulus at the glass transition temperature (Tg) which was more visible at foam composite with compatibilizer when it was

5wt.%HGM+PP-g-MA filler loading. A higher peak value of 247.5MPa was observed in the loss modulus peak which was more than the neat epoxy value and other foam composite samples. Because of the reduced density and void content as well as the good interaction and interfacial bonding between the modified HGM and the matrix, the storage and loss modulus values are better than those of neat epoxy resin. As the temperature rose, the void rate of the composites reduced as a result of the air bubbles degassing during the manufacturing of the composites, which is consistent with previous findings by Sankaran *et al.* [64] and Ghamsari *et al.* [67]

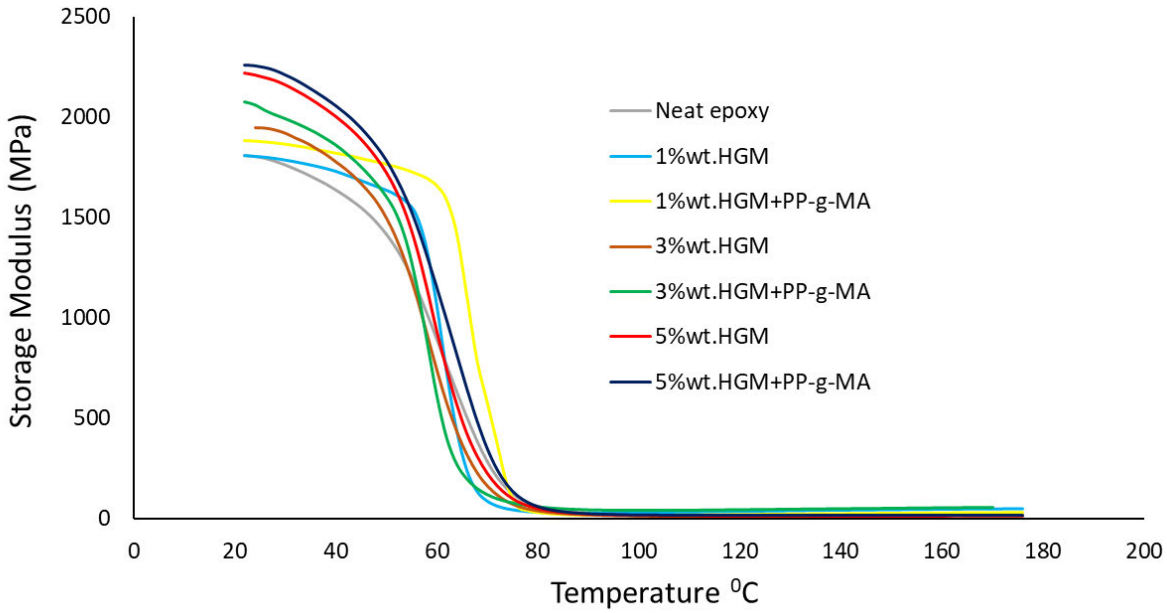

Figure 7.8: Storage modulus of foam panels against temperatures

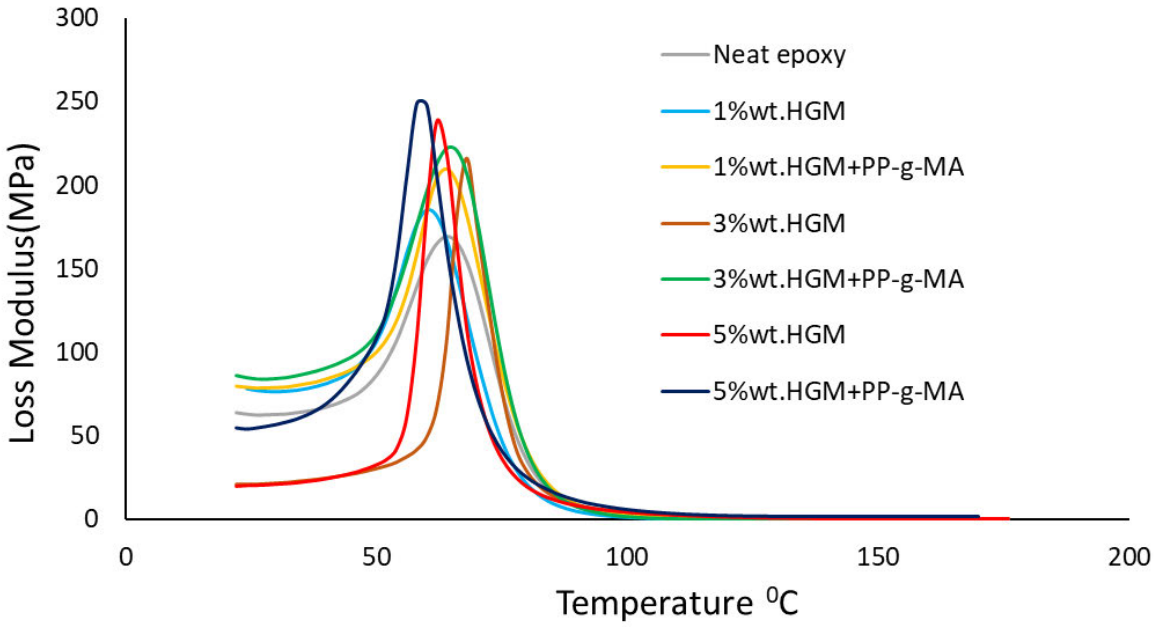

Figure 7.9: Loss modulus of foam panels against temperatures

7.1.3 Conclusion

Epoxy-based foam composite HGM filler, PP-g-MA compatibilizer, and epoxy resin was developed. The influence of modifying the HGM filler with PP-g-MA compatibilizer on the mechanical properties of foam composites was investigated. The HGM content was varied from 1 wt.% to 5 wt.% in foam composites while PP-g-MA content was fixed to be 3 wt.% in each of the modified HGM filler in the foam composites.

The results of the foam composite panels with modified filler foam showed better and improved tensile strength, young modulus, flexural strength, of 28.06MPa, 2.75GPa, and 134.8MPa but there was decrease in hardness values and impact strength when compared with neat epoxy and other samples filled with only HGM filler without surface modification. Outstanding interfacial adhesion between the HGM filler and the matrix allowed for this to happen. Therefore, improved properties of HGM-filled epoxy-based foam composites suggest materials suitable for marine and aerospace applications. The potential future direction of this research could be to study the interfacial properties of hybrid fillers.

CHAPTER 8: NUMERICAL/MODELLING ANALYSIS

8.1 Introduction

This chapter examine numerical analysis related to tensile and flexural strength. Moreover, Abaqus software simulation and modelling of the experimental work was demonstrated in order to assess the reliability of the acquired results.

8.2 Modelling and Simulation

Data entry for each sample formulation as collected from the experimental work is the initial step in the simulating process and data entry and flow chart is represented by step module in Figure 8.1. Additionally, the Representative Volume Element (RVE) method was used when entering data for a composite material.

8.2.1 Modelling of Samples

In order to create the model simulation for tensile and flexural samples, boundary conditions were included after the Abaqus geometry part was completed in order to compute the results using Finite Element Analysis and this was earlier explained under section 3.1.2.

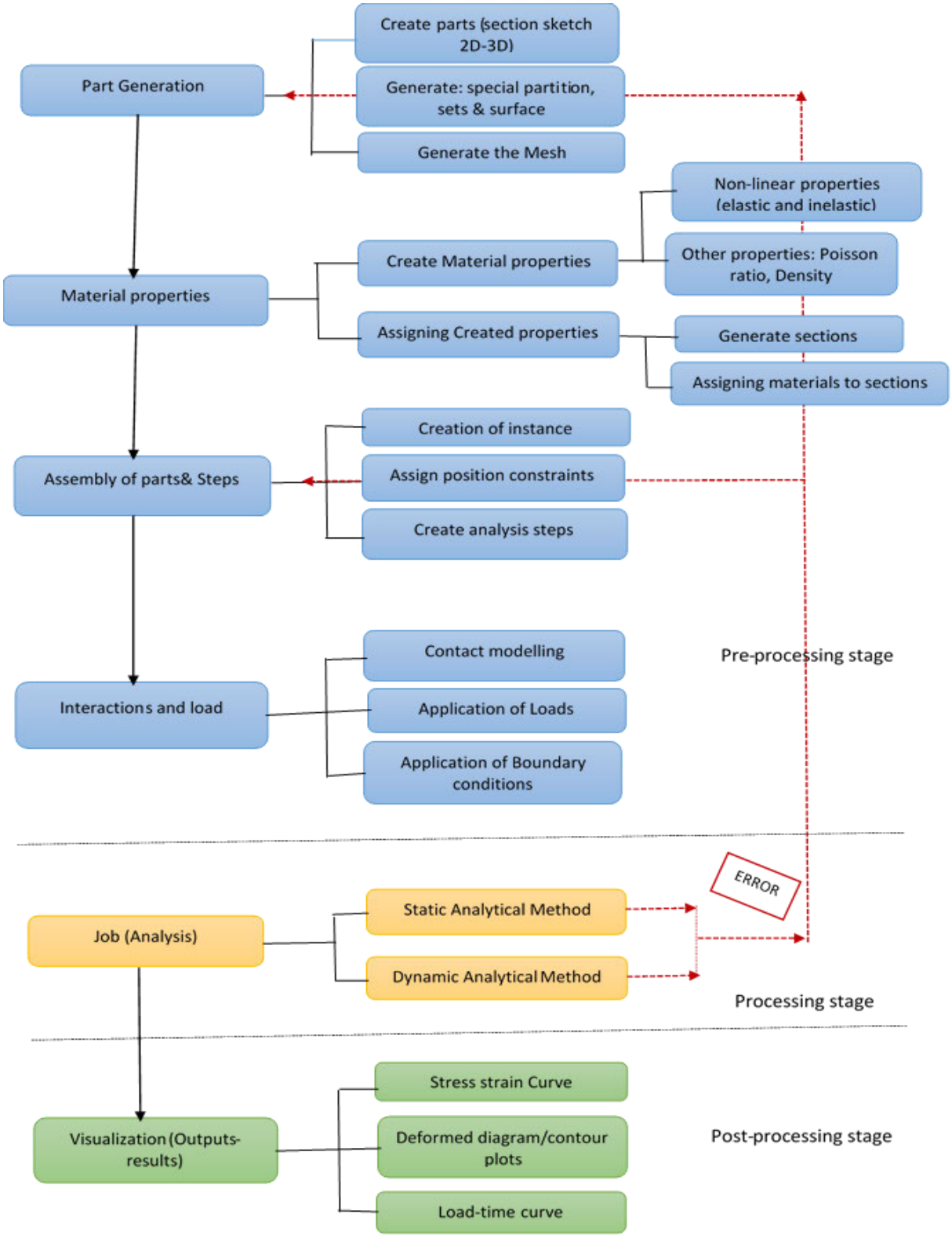

Figure 8.1: General steps for the development of flexible hybrid foam composite panel (Abaqus®/CAE usage)

8.2.1.1 Modelling of Tensile and flexural Samples

There is no predetermined order in which to model a member in Abaqus®/CAE; nonetheless, in any FEM analysis, the input (geometrically speaking) is fundamentally considered first. The load module and interactions were used to define the interface in line with the previously created stages in the step module since the foam composite shows a range of mechanical contact interactions, as illustrated in Figure 8.1. In an effort to depict the foam panel's on-site state, the load determines the transmitted load and boundary condition.

Finally, the foam panel model built is submitted, analysed, and monitored using the Abaqus task module. The visualisation module then displays the results.

When utilising Abaqus® software, each module was carefully examined to avert mistakes and alerts. Additionally, the stress and bending strength were determined using the velocity rate for tensile and flexural strength. Figure 8.2 represent modelled tensile sample while Figure 8.3 and 8.4 represent the flexural sample after meshing and when in bending position

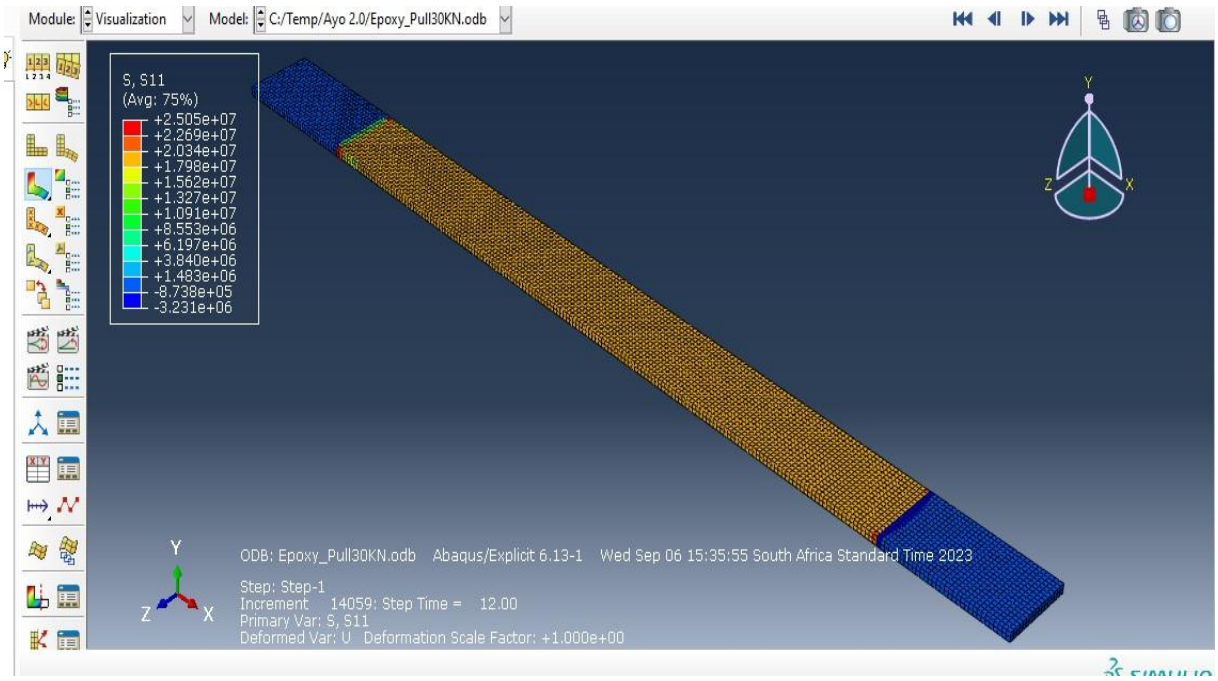

Figure 8.2: Simulation of Tensile samples

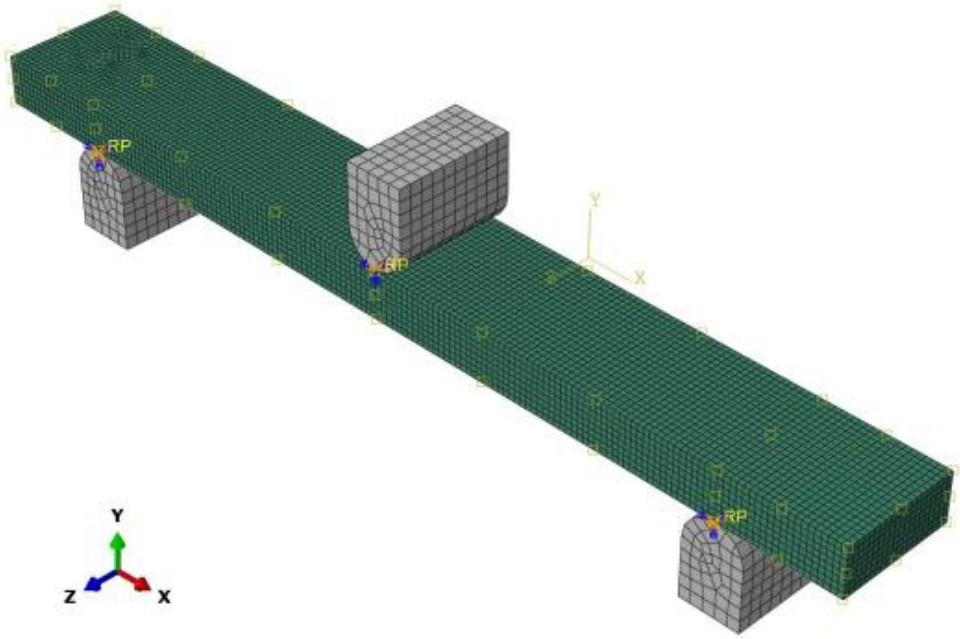

Figure 8.3: Mesh of flexural sample

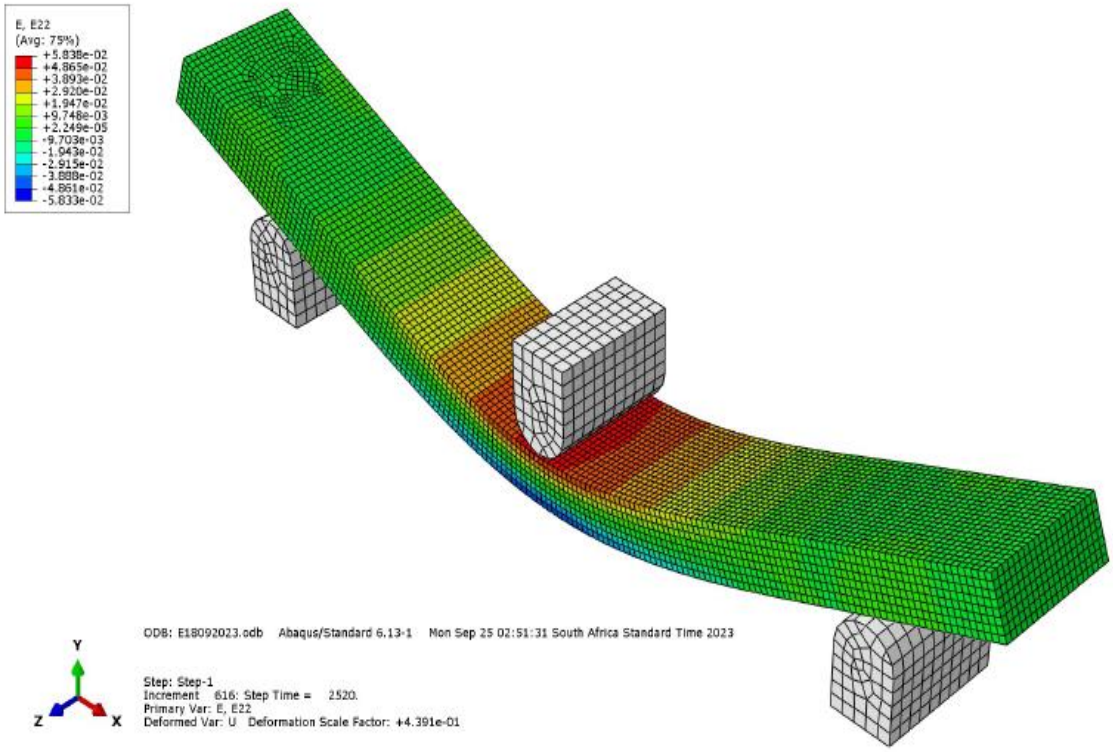

Figure 8.4: Flexural sample bending process

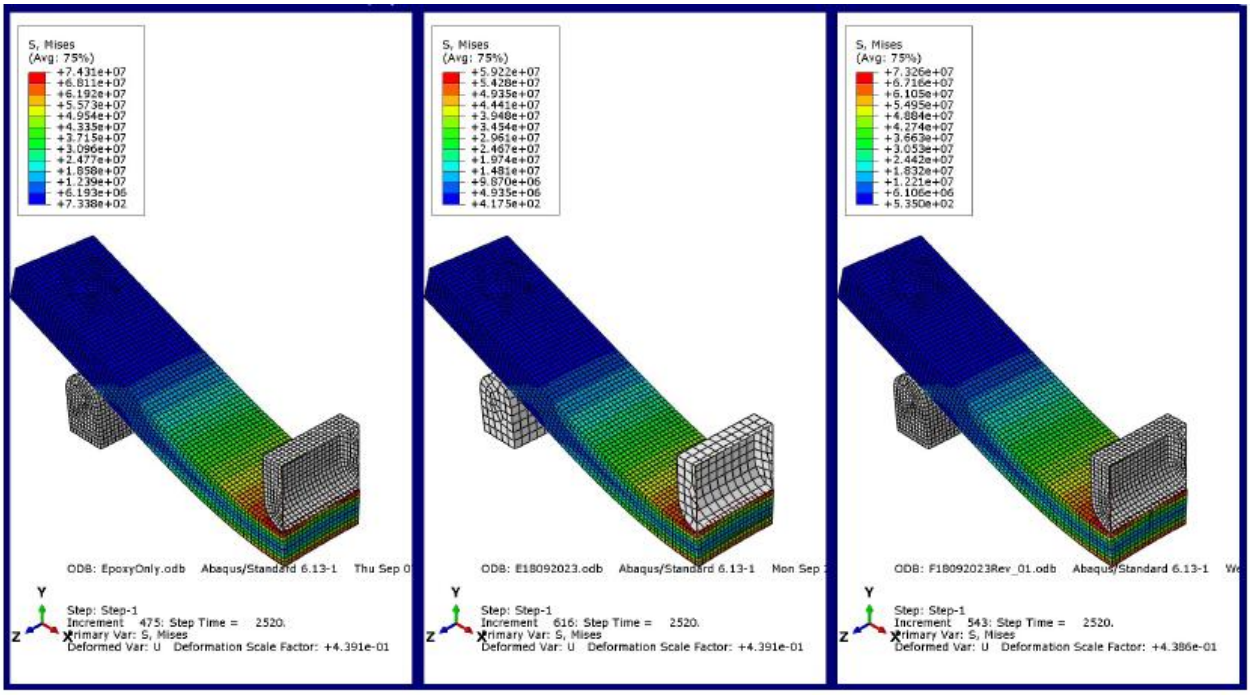

Figure 8.5: Modelled of flexural samples after failure

8.3 Discussion of Modelling results obtained

This model was employed to study the efficiency of using the 3D model for design of hybrid filled foam composite panel and the effect of hybrid fillers on the tensile and flexural strength of the foam panel. Firstly, from Figure 8.6 and 8.7, it was observed that the addition of filler increased the tensile strength at 3%wt.HGM+1%wt.Clay which indicate that there is a good synergy between the matrix and filler interface so the tensile strength of the foam composite was increased. Nevertheless, due to the higher loading of fillers which could not effectively withstand stress delivered from the matrix because of the decrease in matrix material, this later bring about a lower thickness of the interfacial layer [254, 321]. In addition, Figure 8.6 shows that the foam composite's elongation at the breaking load decreased as the filler content increased. This occurred because adding the filler particles increased the hardness of the foam composite panel. Furthermore, the material broke before it yielded at rapid tensile loading rates. While for that of flexural strength, it was observed that some specimens are brittle and crack after getting to the highest yield stress. The hybrid-filled foam composite panels possess better bending capacity than the neat epoxy except some few samples which has lower stress values. This occurrence is possible because of the weak interaction of fillers with the matrix during the process of mixing, causing early cracks and lowering the strain of the samples. The highest stress value was achieved at 1wt.%HGM+1wt.%Clay due to low filler concentration. This can

be related to adding a smaller quantity of HGM and nanoclay, giving better matrix dispersion during the mixing process, and resulting in high strength and stiffness[322, 323]. It was also observed that even though the tension experiments indicated that the unfilled Neat epoxy would have much better ductility than the filled epoxies, the bending tests indicated that the 3wt.%HGM+1wt.%Clay would have the best ductility (strain to failure). This may be due to the formation of a solid epoxy skin on the surfaces of the foam samples.

8.4 Comparison Between Experimental data and Numerical simulation

As can be seen from graphs in Figures 8.6, 8.7, 8.8 and 8.9 that were achieved from the comparative of experimental and Numerical analysis in which Abaqus was used. The results varied from Tensile and Flexural tests as compared to each other.

In all points of tensile in the sample formulation of composites they have similar trend, but overall results show that the numerical results are higher than experimental results because of an experimental working on the real contact and interface occur and a rigid bond between fillers and epoxy resin takes place while in finite element analysis way this contact has not taken place. Also, from flexural test results, numerical results obtained shows that the flexural strength and experimental results are very close to each other but the numerical results are higher than experimental results while experimental results have higher values in some samples, because of the sufficient and complete interaction between the fillers and matrix[324, 325]. Also, effect of unavoidable voids during the sample preparation in the experiment was not taking into consideration in the numerical model which caused numerical values to be higher than obtained experimental values.

Table 8.1: Comparison between Experimental and Numerical Tensile strength

Samples Name	Experimental Tensile Strength (MPa)	FEM Tensile Strength (MPa)
Neat epoxy	21.23	22.69
1wt.%HGM	19.71	17.25
1wt.%HGM+1wt.%Nanoclay	14.73	13.57
1wt.%HGM+3wt.%Nanoclay	21.59	22.90
1wt.%HGM+5wt.%Nanoclay	11.93	12.79
3wt.%HGM	19.67	20.33

3wt.%HGM+1wt.%Nanoclay	23.77	24.68
3wt.%HGM+3wt.%Nanoclay	13.64	6.57
3wt.%HGM+5wt.%Nanoclay	19.61	19.93

Table 8.2: Comparison between Experimental and Numerical Flexural Strength

Samples Name	Experimental Flexural Strength (MPa)	FEM Flexural Strength (MPa)
Neat epoxy	54.1	56.48
1wt.%HGM	61.61	64.00
1wt.%HGM+1wt.%Nanoclay	66.21	67.57
1wt.%HGM+3wt.%Nanoclay	42.53	36.40
1wt.%HGM+5wt.%Nanoclay	57.25	61.76
3wt.%HGM	31.50	36.58
3wt.%HGM+1wt.%Nanoclay	55.48	51.47
3wt.%HGM+3wt.%Nanoclay	38.50	39.71
3wt.%HGM+5wt.%Nanoclay	34.30	39.53

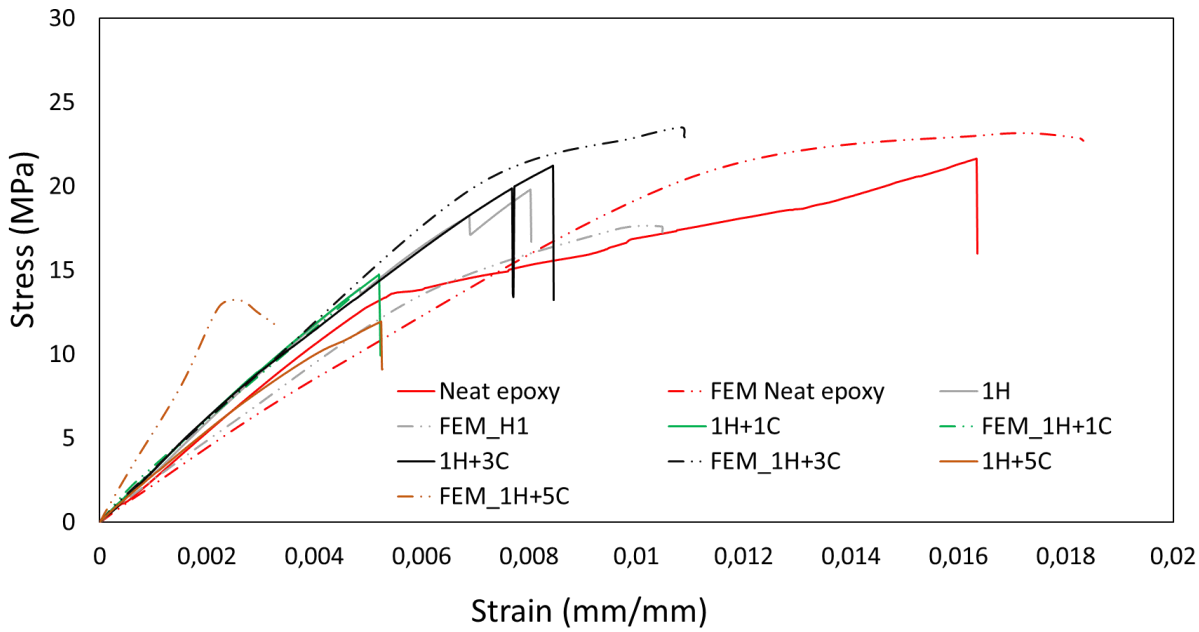

Figure 8.6:Tensile Stress-strain graph for 1%HGM filled series

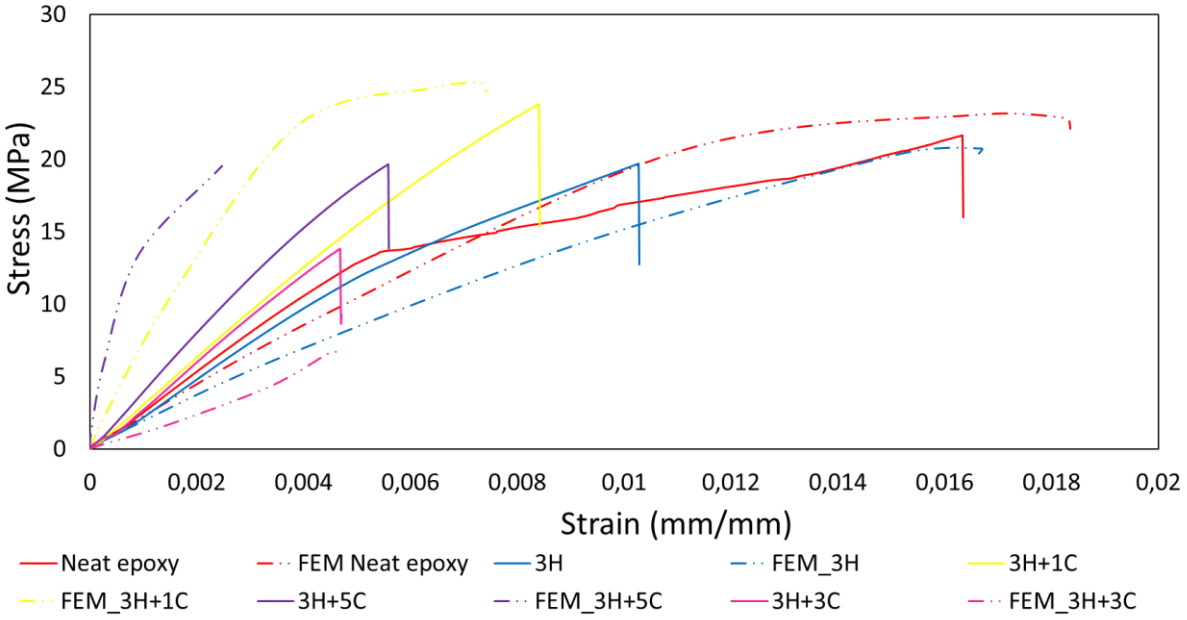

Figure 8.7:Tensile Stress-strain graph for 3%HGM filled series

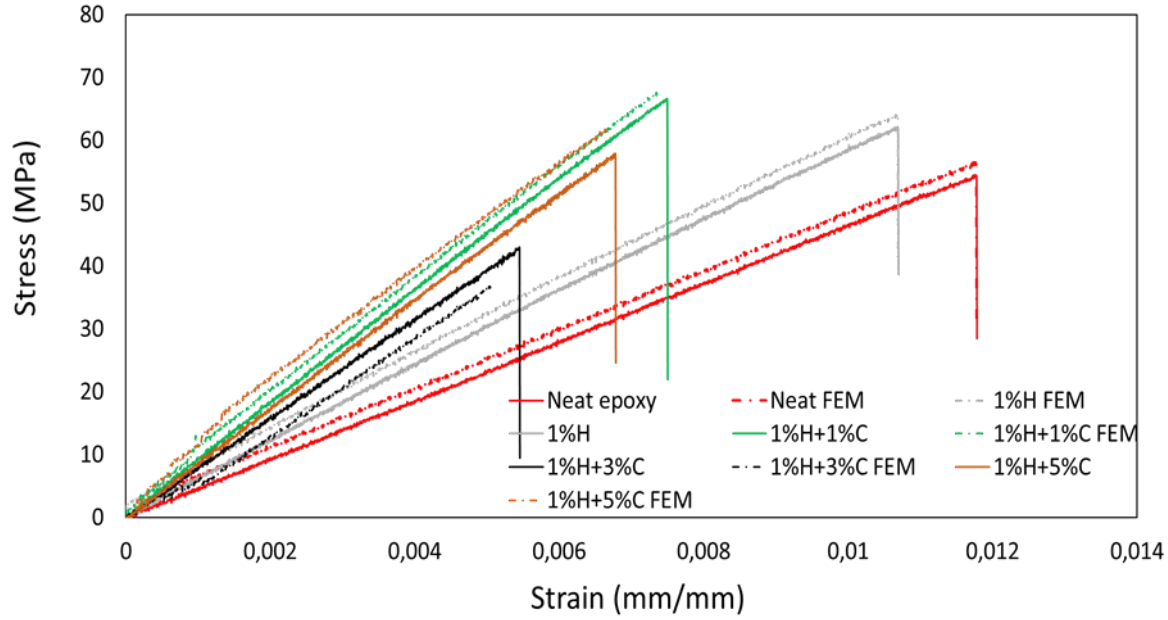

Figure 8.8: Flexural Stress-strain graph for 1%HGM filled series

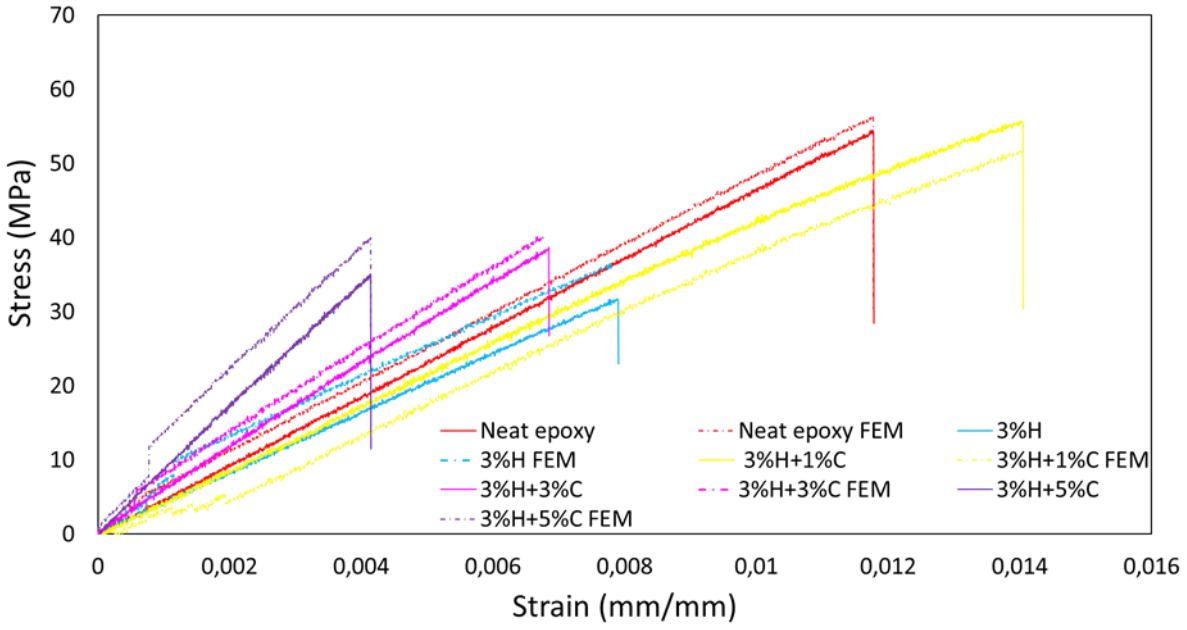

Figure 8.9: Flexural Stress-strain graph for 3%HGM filled series

The decision made in this study to model the foam composite panel situations and then forecast their structural performance using the Abaqus computer programme, which is based on the Finite Element Model (FEM). Using the Abaqus computer software packages, foam composite panel simulation was accomplished while taking static loading into account[326]. Additionally, the 3D and asymmetric geometric model, together with the nonlinear and viscoelastic material properties, were taken into consideration for the foam composite panel simulation[327, 328].
The overall FE model's loading and boundary conditions for the tested foam composite matting were applied in line with the results of the experimental testing (basically support conditions) as demonstrated in Figure 8.2 and 8.3

8.5 Theoretical Modelling

The mechanical behaviours of foam core and sandwich composites can be determined using a variety of mathematical models and experimental verifications. When predicting experimental outcomes, mathematical modelling is employed; it is more economical and time-efficient than conducting experimental research. Modelling helps engineers feel less stressed when creating composites[224, 329, 330]. In areas like sandwich composite panels, where various materials were employed in the design process, the mathematical model can be used to anticipate the optimal mix of constituent materials to be used in composites manufacturing. These models can provide

insights into the basic workings of reinforcement. In this investigation, two pre-existing mathematical models were utilized to validate the experimental data.

The properties of the individual sandwich composite components and their configuration are the basis for the development of micromechanical composites models. These consist of the matrix component materials, the modulus, the tensile strength, and the volume percentages of the constituent materials (which were determined using the rule of mixture).

The following theories were used to model the mechanical properties of sandwich composites:

(i) Series and parallel model: According to these models, the tensile strength and tensile modulus was calculated using Equation. 8.1-8.4. [224].

For series model:

$$M_{SC} = M_H V_H + M_c V_c + M_f V_f + M_m V_m \quad 8.1$$

$$T_{SC} = T_H V_H + T_c V_c + T_f V_f + T_m V_m \quad 8.2$$

For parallel model:

$$M_{SC} = \frac{M_m M_H M_C M_F M_H}{M_m V_C + M_H V_F + M_c V_m + M_F V_H} \quad 8.3$$

$$T_{SC} = \frac{T_m T_H T_C T_F}{T_m V_C + T_H V_F + T_c V_m + T_F V_H} \quad 8.4$$

The volume fractions of all the component parameters used in the fabrication of each sandwich composite panel are the functions of the series and parallel model equations employed in the modelling.

M_m is tensile modulus of matrix

M_{SC} is tensile modulus of sandwich composite

M_H is tensile modulus of HGM

M_C is tensile modulus of nanoclay

M_F is tensile modulus of banana fiber

T_m is tensile strength of matrix

T_{SC} is tensile strength of sandwich composite

T_H is tensile strength of HGM

T_C is tensile strength of nanoclay

T_f is tensile strength of banana fiber

Table 8.3: Volume fractions of fiber, matrix,HGM and nanoclay foam composite used for the model.

Sandwich	V_{matrix}	V_{HGM}	V_{Clay}	V_{fiber}
EPF	0.92	0	0	0.08
1HF	0.94	0.006	0	0.08
1H1CF	0.908	0.006	0.006	0.08
1H3CF	0.896	0.006	0.018	0.08
1H5CF	0.884	0.006	0.03	0.08
3HF	0.902	0.018	0	0.08
3H1CF	0.896	0.018	0.006	0.08
3H3CF	0.884	0.018	0.018	0.08
3H5CF	0.872	0.018	0.03	0.08

Table 8.4: Experimental and theoretical modulus(GPa) values for sandwich composites model

Sandwich	M_{matrix}	M_{HGM}	M_{Clay}	M_{fiber}	$M_{expt.}$	M_{series}	$M_{parallel}$
EPF	1.108	3.590	4.66	0.45	1.63	2.03	3.14
1HF	1.108	3.590	4.66	0.45	2.39	2.44	3.49
1H1CF	1.108	3.590	4.66	0.45	3.07	3.16	3.86
1H3CF	1.108	3.590	4.66	0.45	2.54	2.69	3.65
1H5CF	1.108	3.590	4.66	0.45	2.65	2.91	3.65
3HF	1.108	3.590	4.66	0.45	2.30	2.66	3.61
3H1CF	1.108	3.590	4.66	0.45	3.10	3.27	3.93
3H3CF	1.108	3.590	4.66	0.45	2.87	3.10	3.87
3H5CF	1.108	3.590	4.66	0.45	2.60	2.90	3.80

Table 8.5: Experimental and theoretical strength(MPa) for sandwich composite model

Sandwich	T_{matrix}	T_{HGM}	T_{Clay}	T_{fiber}	$T_{expt.}$	T_{series}	$T_{parallel}$
EPF	34.23	86	101	28	23.38	30.28	37.72
1HF	34.23	86	101	28	28.58	31.97	38.08
1H1CF	34.23	86	101	28	27.20	32.31	40.71
1H3CF	34.23	86	101	28	29.57	33.01	40.82
1H5CF	34.23	86	101	28	28.74	33.68	40.91
3HF	34.23	86	101	28	24.82	31.48	41.93
3H1CF	34.23	86	101	28	30.10	32.82	43.11
3H3CF	34.23	86	101	28	23.60	30.50	38.16
3H5CF	34.23	86	101	28	24.61	31.17	41.49

Table 8.3 shows the values of the volume fractions of fiber, matrix, HGM and nanoclay used for the theoretical calculations of the model. Also, Table 8.4 and Table 8.5 shows the theoretical modulus values (GPa) and theoretical tensile strength of sandwich composites in series and parallel compared with the experimental values. While Table 8.8 shows the theoretical tensile values (MPa) of sandwich composites in series and parallel compared with the experimental values used for the model.

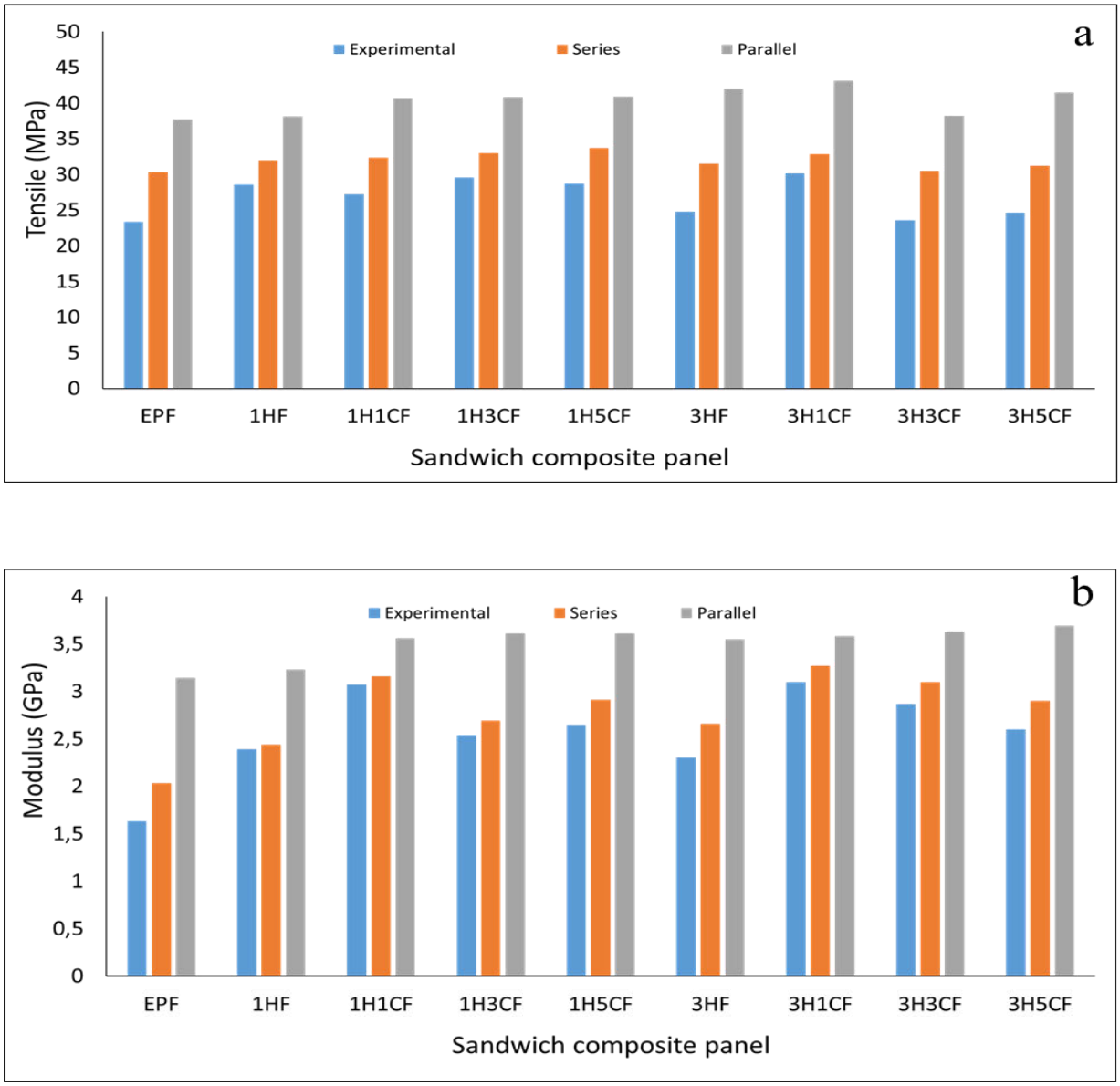

Figure 8.10:Variation of (a) experimental versus theoretical tensile strength and (b) experimental versus theoretical modulus values obtained for sandwich composite panel.

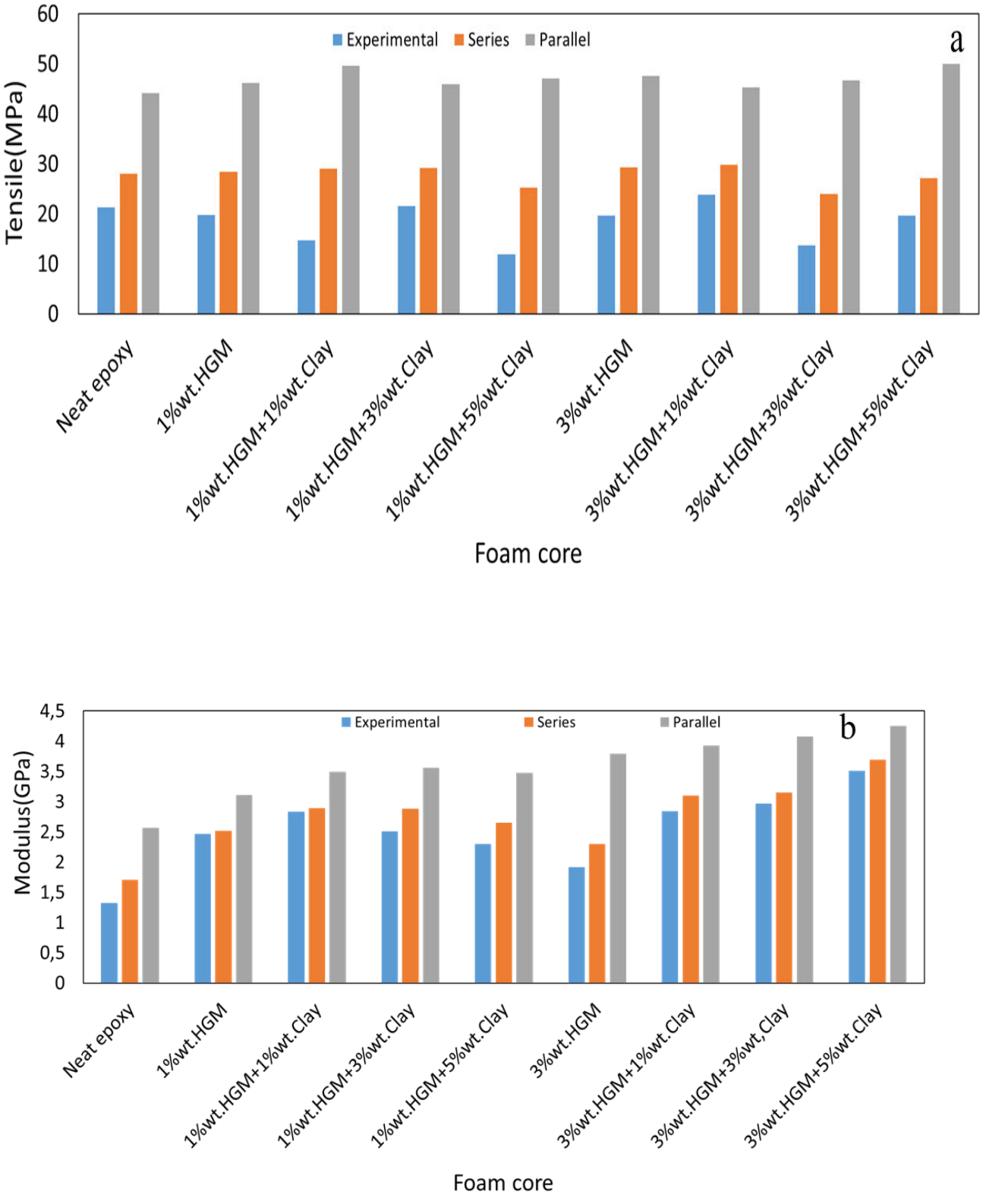

Figure 8.11:Variation of (a)experimental versus theoretical tensile strength and (b) experimental versus theoretical modulus values obtained for foam core

Figure 8.10 (a, and b) shows the variation of the theoretical models (tensile strength, and tensile modulus) as a function of sandwich composite compared with the experimental results. From Figure 8.10a and 8.10b, the two models show an increase of theoretical tensile strength values compared to the experimental result, the highest tensile strength (MPa) values for the models are at 3H1CF and 1%wt.HGM+1%wt.clay, which shows that the model predicted better result for the combination of HGM and nanoclay fillers with banana fibers reinforcement in sandwich composites as well as combination of HGM and nanoclay fillers reinforcement in foam core. From Figure 8.10b and 8.11b, because the parallel model takes into account more parameters than the series model, the theoretical tensile modulus values for that model are larger than those of the series model, which displays a narrower range of results when compared with experimental values. This showed that, generally speaking, the tensile and tensile modulus values in the series model are closer to the results of the experimental results than those in the parallel model.

CHAPTER 9: CONCLUSION AND RECOMMENDATION

9.1 Introduction

This chapter presents the overall conclusions gleaned from this research work of enhancing the properties of hybrid filled HGM/nanoclay foam composites and sandwich foam composites and also the recommendations. A novel hybrid foam composites and sandwich foam composites that is lightweight and with positive buoyancy was developed in this research work and its properties enhanced by HGM/clay and banana fibers. Section 9.2 present detailed conclusions about the novel HGM/nanoclay foam composites and sandwich foam composites and recommendations. HGM loadings of 0 wt%, 3 wt%, 5wt% were used while nanoclay loading of 0 wt%,1 wt%, 3 wt%, 5wt% were also used in this work. 3wt%HGM+1%wt.Clay was optimum and hence the conclusions discussed in the next sections focus on 3wt%HGM+1%wt.Clay hybrid filler loading.

9.2 Conclusions

This research resulted into development of novel, sustainable, lightweight and buoyant hybrid filled sandwich composite panel. The sandwich panels made had enhanced the basic mechanical, thermal and physical properties making them suitable for use in some high-performance marine applications replacing the conventional synthetic fibre-reinforced composites. The hybrid filled core of the sandwich panel developed in this research work has an average density of 0.903 g/cm^3.This clearly shows that the sandwich panels developed are lightweight and buoyant since their density is lower than density of water. In addition, this has addressed the research gaps regarding the limitation of previously fabricated sandwich composites for marine applications.

Materials selection for composite design is very crucial in critical engineering applications such as aerospace, marine and automobile industries.

Hybrid fillers were used to manufacture the foam composite panel. The foam core's fillers were nanoclay and hollow glass microspheres (HGM). These foam composite panels were created using a traditional resin casting process. The HGM content was adjusted from 1 weight percent to 3 weight percent in the foam composites panel, and the nanoclay content was adjusted from 1 weight percent to 5 weight percent in each of the HGM-filled series of foam composites panels. The hybrid-filled foam composite fabricated was also used as the core material for the

sandwich foam composites (SFC) and banana fibre was used as the facesheet at upper and lower-layer face-sheets reinforcement. Hand lay-up method was used for the fabrication of the SFC. Comprehensive characterization was carried out on the foam composite panels, this involve investigating their physical (density, water absorption, water contact angle, buoyancy) properties, mechanical (hardness, tensile, flexural, and impact) properties and thermal (thermal conductivity, thermal expansion, coefficient of thermal expansion and specific heat capacity, Thermo-gravimetric Analysis) properties. The results obtained showed that tensile and flexural strength improved by 12% and 23.1% respectively while the infusion of hybrid fillers content of 3%wt.HGM+1%wt.clay and 1%wt.HGM+1%wt.clay into the epoxy when compared to neat epoxy. Also an enhanced young modulus and flexural modulus by 165% and 78% respectively were observed with filler content of 3%wt.HGM+5%wt.clay and 1% wt.HGM+1%wt.clay when compared with neat epoxy. Likewise, it was observed that impact and hardness improved by 28.7% and 41.9% respectively with filler content of 3wt.%HGM+3wt.%clay and 3%wt. HGM+5%wt.clay when compared with neat epoxy. This improvement indicates that when this foam composite panel rubs or comes into contact with another surface, it is less likely to wear down, fracture, or display other symptoms of wear. This feature is very useful in applications where parts are frequently under mechanical stress.

Addition of nanoclay particles at 5%wt. as the second filler enhanced the resistance of the foam composite panels to water absorption rate by 16.2% while the thermal stability also improved as evidence in the results obtained from thermal properties when compared with neat epoxy. The buoyancy results revealed that the sample with 3%wt. hollow glass microspheres concentration has the highest buoyancy due to hollow spheres nature of the hollow glass microspheres.

The strength of each SFC material was determined by their mechanical (impact, tensile, flexural, and hardness) properties and discussed in chapter 6. The SFC tensile strength and modulus are highest at 3H1CF and 3H3CF with an increase of 28.2% and 86.4% respectively when compared with EPF.

Also the flexural strength and modulus are highest at 1H1CF and 1H5CF with an increase of 20.5% and 17.9% when compared with EPF. It could be noted that in all the SFC, that 3HF and 3H3CF showed lowest tensile stress values due to low level of interaction of fillers with fiber at that volume fraction of hybrid fillers. Likewise, 1HF and 3HF revealed low flexural values due to single filler which couldn't bear much load. However, it is worthy to note that impact energy was highest at 3H3CF with 32.3% increase when compared with EPF.

Generally, it can be observed that hybrid core can better perform as reinforcement in SFC than using single filler in the core.

Also, the densities (experimental and theoretical) of hybrid-filled foam composites and sandwich foam composites were investigated. The experimental densities were calculated manually, while the theoretical density was determined by the rule of mixture and were more than the measured density. The difference was calculated in percentage as the void or porosity fraction values. The porosity of the HFFC and SFC increased with increase in the concentration of the fillers. The water absorption rate decrease as the concentration of nanoclay particles increases in the composite due to nano silicate layers in the nanoclay.

The buoyancy was highest with 3HF concentration due to hollow sphere nature of HGM which means it can float effortlessly on a liquid surface better than other samples. Thus, a substance with a high buoyancy value displaces a significant volume of fluid relative to its own weight, exerting a strong upward force. As a result, instead of sinking, the material would usually float effortlessly on the fluid's surface. When buoyancy is required, such as in the design of boats, flotation devices, and even some types of building materials used in construction on water, this feature is helpful in such application.

Finally, the tensile and flexural results was validated numerically by using finite element method and abaqus® 6.13 software and this revealed that most of the modelled samples are stronger than the experimental tested samples with up to 9% increase from experimental values obtained due to incomplete interface interactions between the fillers and matrix as a result of hand lay-up method employed for the fabrication of the samples during the experimental process.

9.3 Limitation of the work and future recommendations

Considering the contributions this study has added to the body of knowledge, more research can still be done in the future. As a result, additional study can be conducted in the areas listed below.

- The banana fibres used in this study were in unidirectional layer and mercinarized, further research can be done on the woven mat to produce sandwich foam composite panel.
- This research work focused on the hybrid core and single face-sheets. For a more useful implementation of the research, future study should concentrate on the use of hybrid faces-sheets and hybrid cores.

- The numerical analysis carried out was to Tensile and flexural strength, further study can consider numerical analysis of the thermal properties.
- The surface modification of HGM filler was carried out while surface modification of nanoclay was not done. Hence, future study can focus on surface modification of nanoclay so as to improve the performance of the sandwich panel.
- Peel strength which measures the adhesion between face skins and core can be evaluated in the future study

APPENDIX

A-1: Influence of hybridizing fillers on mechanical properties of foam composite panel

Received: 30 March 2023 | Revised: 11 May 2023 | Accepted: 1 June 2023
DOI: 10.1002/pen.26396

RESEARCH ARTICLE

POLYMER ENGINEERING AND SCIENCE WILEY

Influence of hybridizing fillers on mechanical properties of foam composite panel

Ayodele Abraham Ajayi | **Mohan Turup Pandurangan** | **Krishnan Kanny**

Composite Research Group, Department of Mechanical Engineering, Durban University of Technology, Durban, South Africa

Correspondence
Mohan Turup Pandurangan, Composite Research Group, Mechanical Engineering Department, Durban University of Technology, S3-10 (CIM Lab), Durban, South Africa.
Email: mohanp@dut.ac.za

Funding information
Durban University of Technology

Abstract

Foam composite panels made from hybrid fillers are materials developed to have low density with high mechanical properties. This work focuses on improving the mechanical properties of epoxy-based foam composite panels with hybridized fillers by combining hollow glass microspheres (HGM) and nanoclay. The HGM content was varied from 1 wt.% to 3 wt.% in foam composites panel, while nanoclay content was varied from 1 wt.% to 5 wt.% in each of the HGM-filled series of foam composites panel, these foam composite panels were fabricated using a conventional resin casting method. The mechanical properties such as tensile strength, impact strength, hardness, flexural strength of the prepared hybrid-filled foam composite panels were determined and compared with the neat epoxy. It was found that the hybrid-filled foam composite panels exhibited improved mechanical properties than the neat epoxy. These improved properties were because of excellent interfacial adhesion between the hybrid fillers and the matrix. The improved mechanical properties could suggest that this material may be suitable for application in industries where lightweight materials with good mechanical properties are required. This study showed a new area of synthetic foam development research by enhancing mechanical properties using hybrid-filled.

KEYWORDS
fillers, foam composite panels, hollow glass microspheres, mechanical properties, Nanoclay

1 | INTRODUCTION

Epoxy-based foam composites are lightweight materials with attractive mechanical properties, hollow structures, very good adhesion, good chemical properties, heat resistance, low shrinkage, corrosion resistance, and excellent electrical properties.[1–8] This foam composite can be developed by mixing hollow particles in a matrix material.[9,10] The hollow particles give foam composite benefits of low density and low moisture absorption.[11–14] These properties give rise to its wide range of applications, including but not limited to insulation material, adhesives in power equipment and electronic packaging, and automotive and aircraft components.[15] At present, hollow glass microspheres (HGM) filler is one of the most suitable fillers being used in epoxy-based foam composite because HGM has resistant to high temperatures, high strength-to-weight ratio, and has stable chemical compositions which can effectively reduce the density of the material.[16–18] Despite the improved properties of epoxy-based foam composites,

This is an open access article under the terms of the Creative Commons Attribution License, which permits use, distribution and reproduction in any medium, provided the original work is properly cited.
© 2023 The Authors. *Polymer Engineering & Science* published by Wiley Periodicals LLC on behalf of Society of Plastics Engineers.

A-2: Thermal and Wettability properties of Nanoclay-filled epoxy-based foam composite as lightweight material

Materials Performance and Characterization

doi:10.1520/MPC20230085 / Vol. 12 / No. 1 / 2023 / available online at www.astm.org

Ayodele Abraham Ajayi,[1] Mohan Turup Pandurangan,[2] Krishnan Kanny,[1] and Velmurugan Ramachandran[3]

Thermal and Wettability Properties of Nanoclay-Filled Epoxy-Based Foam Composite as Lightweight Material

Reference

A. A. Ajayi, M. Turup Pandurangan, K. Kanny, and V. Ramachandran, "Thermal and Wettability Properties of Nanoclay-Filled Epoxy-Based Foam Composite as Lightweight Material," *Materials Performance and Characterization* 12, no. 1 (2023): 293–306. https://doi.org/10.1520/MPC20230085

ABSTRACT

Epoxy-based foam composite (EBFC) materials have received considerable attention recently because of their wide range of applications in the aerospace and marine industries. EBFC materials made from hybrid fillers are materials generated to have improved thermal properties. This work focuses on improving the thermal properties and wettability of EBFC materials with hybridized fillers by infusing hollow glass microspheres (HGM) and clay. The HGM content varied between 1 weight percent (wt.%) and 5 wt.% in foam composite materials while clay content varied between 1 wt.% and 5 wt.% in each of the HGM-filled series of foam composite materials. These foam composite materials were fabricated using a conventional resin casting method. The thermal properties, such as thermal conductivity, thermal expansion, coefficient of thermal expansion, as well as specific heat capacity, water contact angles, and percentage of water absorption of hybrid-filled foam composite materials were investigated and compared with neat epoxy and epoxy foam materials. It was found that hybrid-filled foam composite materials exhibited improved thermal properties over neat epoxy material because of good chemical reactions and excellent interfacial adhesion between the fillers and matrix. These improved thermal properties may suggest that this material may be suitable for application in industries where lightweight materials with good thermal properties are required. This reveals a new area in foam composite manufacturing research by enhancing thermal properties with hybrid fillers.

Keywords

hollow glass microspheres, clay, fillers, foam composite, wettability, thermal properties

Manuscript received August 1, 2023; accepted for publication November 2, 2023; published online December 13, 2023. Issue published December 13, 2023.

[1] Composite Research Group, Department of Mechanical Engineering, Steve Biko Campus, Durban University of Technology, Durban 4000, South Africa, https://orcid.org/0000-0002-3011-3466 (A.A.A.), https://orcid.org/0000-0001-8631-119X (K.K.)

[2] Composite Research Group, Department of Mechanical Engineering, Steve Biko Campus, Durban University of Technology, Durban 4000, South Africa (Corresponding author), mohanp@dut.ac.za, https://orcid.org/0000-0001-7577-8405

[3] Department of Aerospace Engineering, Indian Institute of Technology, Madras 600036, India

Copyright © 2023 by ASTM International, 100 Barr Harbor Drive, PO Box C700, West Conshohocken, PA 19428-2959

ASTM International is not responsible, as a body, for the statements and opinions expressed in this paper. ASTM International does not endorse any products represented in this paper.

A-3: Development of epoxy-based sandwich composite panel with hollow glass microspheres/clay hybrid core and banana fiber facesheet for structural applications

Heliyon 10 (2024) e30428

Contents lists available at ScienceDirect

Heliyon

journal homepage: www.cell.com/heliyon

Research article

Development of epoxy-based sandwich composite panel with hollow glass microspheres/clay hybrid core and banana fiber facesheet for structural applications

Ayodele Abraham Ajayi, Mohan Turup Pandurangan *, Kanny Krishnan

Composite Research Group, Department of Mechanical Engineering, Durban University of Technology, South Africa

ARTICLE INFO

Keywords:
Sandwich
Composites
Core
Facesheet
HGM
Nanoclay
Epoxy

ABSTRACT

This study focuses on improving the mechanical properties of sandwich composites by developing epoxy-based sandwich composite panels with hollow glass microspheres/nanoclay hybrid core and banana fiber facesheets for structural applications. The mechanical performance of sandwich composite panels made with hollow glass microspheres (HGM)/nanoclay hybrid core with banana fibers face-sheet composites panel is investigated in this work. The HGM content of the core was varied from 1 wt% to 3 wt% in the sandwich composites panel, while the nanoclay content of the core was varied from 1 wt% to 5 wt% in each of the HGM-filled series of the sandwich composite panel, these sandwich composite panels were fabricated using a conventional resin casting method. In this investigation, the mechanical, water absorption, and buoyancy behavior are thoroughly studied and the findings revealed better improvement at the sandwich composites with hybrid core formulation with banana fiber facesheets than the sandwich composites without hybrid core formulation. This demonstrates that banana fiber with epoxy resin has a limited amount of strength when used without a hybrid core but delivers better performance when HGM and clay particles are mixed as the hybrid core because of excellent interfacial adhesion between the hybrid core and the matrix. The improved mechanical properties could suggest that this material may be suitable for application in industries where sandwich structures that are lightweight with good mechanical properties are required. This study showed a new area of sandwich structure development by enhancing mechanical properties using hybrid core and banana fibers.

1. Introduction

Sandwich composite structures (SCS) are structures made up of three layers: a low-density core, a thin skin, or a facesheet layer bonded to each side of the core. SCS are employed in applications that require a high structural rigidity while remaining lightweight and they are important materials in a wide range of engineering applications, including aerospace, automotive, marine, and wind energy [1–4]. Due to their unique design, lightweight, high strength, and stiffness of the sandwich core composite structure, as well as their significance in the engineering technological fields of aerospace, automotive, marine, and construction, sandwich composite material structures are highly important to study. Sandwich structure principles have been used for more than two decades using

* Corresponding author. Composite research group, Mechanical Engineering Department, Durban University of Technology, S3-L0 (CIM Lab), Durban. South Africa.
E-mail address: mohanp@dut.ac.za (M. Turup Pandurangan).

https://doi.org/10.1016/j.heliyon.2024.e30428
Received 2 January 2024; Received in revised form 23 March 2024; Accepted 25 April 2024
Available online 27 April 2024
2405-8440/© 2024 The Authors. Published by Elsevier Ltd. This is an open access article under the CC BY license (http://creativecommons.org/licenses/by/4.0/).

REFRENCES

1. John B, Nair CR. Syntactic foams. *Handbook of thermoset plastics*: Elsevier; 2014: 511-554.
2. Huang C, Huang Z, Qin Y, Ding J, Lv X. Mechanical and dynamic mechanical properties of epoxy syntactic foams reinforced by short carbon fiber. *Polymer Composites.* 2016;37(7):1960-1970.
3. Gupta N, Zeltmann SE, Shunmugasamy VC, Pinisetty D. Applications of polymer matrix syntactic foams. *Jom.* 2014;66:245-254.
4. Wu X, Gao Y, Wang Y, et al. Recent developments on epoxy-based syntactic foams for deep sea exploration. *Journal of Materials Science.* 2021;56:2037-2076.
5. Cao S, Ma N, Zhang Y, Bo R, Lu Y. Fabrication, mechanical properties, and multifunctionalities of particle reinforced foams: A review. *Thin-Walled Structures.* 2023;186:110678.
6. Kausar A. Polyurethane composite foams in high-performance applications: A review. *Polymer-Plastics Technology and Engineering.* 2018;57(4):346-369.
7. Bajpai PK, Singh I, Madaan J. Comparative studies of mechanical and morphological properties of polylactic acid and polypropylene based natural fiber composites. *Journal of Reinforced Plastics and Composites.* 2012;31(24):1712-1724.
8. Hashim AF, Alghuthaymi MA, Vasil'kov AY, Abd-Elsalam KA. Polymer inorganic nanocomposites: A sustainable antimicrobial agents. *Advances and Applications Through Fungal Nanobiotechnology.* 2016:265-289.
9. Rajak DK, Pagar DD, Kumar R, Pruncu CI. Recent progress of reinforcement materials: A comprehensive overview of composite materials. *Journal of Materials Research and Technology.* 2019;8(6):6354-6374.
10. Bienvenu Y. Application and future of solid foams. *Comptes Rendus Physique.* 2014;15(8-9):719-730.
11. Suriani M, Ilyas R, Zuhri M, et al. Critical review of natural fiber reinforced hybrid composites: Processing, properties, applications and cost. *Polymers.* 2021;13(20):3514.
12. Atmakuri A, Palevicius A, Vilkauskas A, Janusas G. Review of hybrid fiber based composites with nano particles—material properties and applications. *Polymers.* 2020;12(9):2088.
13. Khan T, Acar V, Aydin MR, Hülagü B, Akbulut H, Seydibeyoğlu MÖ. A review on recent advances in sandwich structures based on polyurethane foam cores. *Polymer Composites.* 2020;41(6):2355-2400.
14. Önder A. *Harmonised method to validate the impact resistance performance of composite passenger railway carbodies*, Newcastle University; 2017.
15. Zabihi O, Ahmadi M, Liu C, et al. A sustainable approach to the low-cost recycling of waste glass fibres composites towards circular economy. *Sustainability.* 2020;12(2):641.
16. Naqvi S, Prabhakara HM, Bramer E, Dierkes W, Akkerman R, Brem G. A critical review on recycling of end-of-life carbon fibre/glass fibre reinforced composites waste using pyrolysis towards a circular economy. *Resources, conservation and recycling.* 2018;136:118-129.
17. Dong PAV, Azzaro-Pantel C, Cadene A-L. Economic and environmental assessment of recovery and disposal pathways for CFRP waste management. *Resources, Conservation and Recycling.* 2018;133:63-75.
18. Alves SMC, da Silva FS, Donadon MV, Garcia RR, Corat EJ. Process and characterization of reclaimed carbon fiber composites by pyrolysis and oxidation, assisted by thermal plasma to avoid pollutants emissions. *Journal of Composite Materials.* 2018;52(10):1379-1398.
19. Shuaib NA, Mativenga PT. Carbon footprint analysis of fibre reinforced composite recycling processes. *Procedia Manufacturing.* 2017;7:183-190.

20. Oliveux G, Dandy LO, Leeke GA. Current status of recycling of fibre reinforced polymers: Review of technologies, reuse and resulting properties. *Progress in materials science.* 2015;72:61-99.
21. Alsubari S, Zuhri M, Sapuan S, Ishak M, Ilyas R, Asyraf M. Potential of natural fiber reinforced polymer composites in sandwich structures: A review on its mechanical properties. *Polymers.* 2021;13(3):423.
22. Ma W, Elkin R. Application of sandwich structural composites. *Sandwich Structural Composites.* 2021:333-424.
23. Fajrin J. *Sustainable hybrid composite sandwich panel with natural fibre composites as intermediate layer*, University of Southern Queensland; 2013.
24. Ma W, Elkin R. Sandwich structural core materials and properties. *Sandwich Structural Composites*: CRC Press; 2021: 1-72.
25. Yung KC, Zhu B, Yue TM, Xie C. Preparation and properties of hollow glass microsphere-filled epoxy-matrix composites. *Composites science and technology.* 2009;69(2):260-264.
26. Qiao Y, Li Q, Li Q, et al. Lightweight epoxy foams prepared with arranged hollow-glass-microspheres/epoxy hollow spheres. *Composites Communications.* 2022;33:101197.
27. Awad ZK, Aravinthan T, Zhuge Y. Experimental and numerical analysis of an innovative GFRP sandwich floor panel under point load. *Engineering Structures.* 2012;41:126-135.
28. Kumar SA, Ahmed KS. Compression behavior and energy absorption capacity of stiffened syntactic foam core sandwich composites. *Journal of Reinforced Plastics and Composites.* 2013;32(18):1370-1379.
29. Balıkoğlu F, Demircioğlu TK, İnal O, Arslan N, Ataş A. Compression after low velocity impact tests of marine sandwich composites: effect of intermediate wooden layers. *Composite Structures.* 2018;183:636-642.
30. Alias A, Nor NAA, Said MR. The Behaviour Of Square Sandwich. *Jurnal Teknologi.* 2007;47(A):1-18.
31. Zhang J, Chaisombat K, He S, Wang CH. Hybrid composite laminates reinforced with glass/carbon woven fabrics for lightweight load bearing structures. *Materials & Design (1980-2015).* 2012;36:75-80.
32. Prabhakaran S, Krishnaraj V, Sharma S, Senthilkumar M, Jegathishkumar R, Zitoune R. Experimental study on thermal and morphological analyses of green composite sandwich made of flax and agglomerated cork. *Journal of Thermal Analysis and Calorimetry.* 2020;139:3003-3012.
33. Wang S, Meng W, Lv H, Wang Z, Pu J. Thermal insulating, light-weight and conductive cellulose/aramid nanofibers composite aerogel for pressure sensing. *Carbohydrate Polymers.* 2021;270:118414.
34. Zaini E, Azaman M, Jamali M, Ismail K. Synthesis and characterization of natural fiber reinforced polymer composites as core for honeycomb core structure: A review. *Journal of Sandwich Structures & Materials.* 2020;22(3):525-550.
35. Cao H, Qian K, Wei Q, Li H. Low-velocity impact behaviour of 3-D glass fibre hollow integrated core sandwich composites. *Polymers and Polymer Composites.* 2010;18(4):175-180.
36. Mohit H, Arul Mozhi Selvan V. A comprehensive review on surface modification, structure interface and bonding mechanism of plant cellulose fiber reinforced polymer based composites. *Composite Interfaces.* 2018;25(5-7):629-667.
37. Kalia S, Kaith B, Kaur I. Pretreatments of natural fibers and their application as reinforcing material in polymer composites—a review. *Polymer Engineering & Science.* 2009;49(7):1253-1272.
38. Mohammed M, Rahman R, Mohammed AM, et al. Surface treatment to improve water repellence and compatibility of natural fiber with polymer matrix: Recent advancement. *Polymer Testing.* 2022;115:107707.

39. Sharma PK, Singh S, Syed N, et al. Value Addition/Biorefinery Approaches Towards Biolubricants Production. *Lubricants from Renewable Feedstocks.* 2024:407-443.
40. Yi X-S, Du S, Zhang L. *Composite materials engineering, volume 1: fundamentals of composite materials*: Springer; 2018.
41. Barbero EJ. *Introduction to composite materials design*: CRC press; 2010.
42. Gay D. *Composite materials: design and applications*: CRC press; 2022.
43. Watt JP, Davies GF, O'Connell RJ. The elastic properties of composite materials. *Reviews of Geophysics.* 1976;14(4):541-563.
44. Clyne TW, Hull D. *An introduction to composite materials*: Cambridge university press; 2019.
45. Ferreira J, Capela C, Costa J. A study of the mechanical behaviour on fibre reinforced hollow microspheres hybrid composites. *Composites Part A: Applied Science and Manufacturing.* 2010;41(3):345-352.
46. Maharsia R, Gupta N, Jerro HD. Investigation of flexural strength properties of rubber and nanoclay reinforced hybrid syntactic foams. *Materials Science and Engineering: A.* 2006;417(1-2):249-258.
47. Harris B. Engineering composite materials. 1999.
48. Balaguru P, Nanni A, Giancaspro J. *FRP composites for reinforced and prestressed concrete structures: a guide to fundamentals and design for repair and retrofit*: CRC Press; 2008.
49. Kar KK. *Composite materials: processing, applications, characterizations*: Springer; 2016.
50. Garay AC, Souza JA, Amico SC. Evaluation of mechanical properties of sandwich structures with polyethylene terephthalate and polyvinyl chloride core. *Journal of sandwich structures & materials.* 2016;18(2):229-241.
51. Najafi M, Eslami-Farsani R. Design and characterization of a multilayered hybrid cored-sandwich panel stiffened by thin-walled lattice structure. *Thin-Walled Structures.* 2021;161:107514.
52. Vitale JP, Francucci G, Xiong J, Stocchi A. Failure mode maps of natural and synthetic fiber reinforced composite sandwich panels. *Composites Part A: Applied Science and Manufacturing.* 2017;94:217-225.
53. Kanny K, Mahfuz H. Flexural fatigue characteristics of sandwich structures at different loading frequencies. *Composite Structures.* 2005;67(4):403-410.
54. Gupta N. *Characterization of syntactic foams and their sandwich composites: modeling and experimental approaches*: Louisiana State University and Agricultural & Mechanical College; 2003.
55. Salleh Z, Islam MM, Epaarachchi JA, Su H. Mechanical properties of sandwich composite made of syntactic foam core and GFRP skins. *AIMS Material Science.* 2016;3(4):1704-1727.
56. Wouterson EM, Boey FY, Hu X, Wong S-C. Specific properties and fracture toughness of syntactic foam: Effect of foam microstructures. *Composites science and technology.* 2005;65(11-12):1840-1850.
57. Gupta N, Pinisetty D, Shunmugasamy VC. *Reinforced polymer matrix syntactic foams: effect of nano and micro-scale reinforcement*: Springer Science & Business Media; 2013.
58. Zhi C, Long H. Compressive properties of syntactic foam reinforced by warp-knitted spacer fabric. *Cellular Polymers.* 2015;34(4):173-188.
59. Omar MY, Xiang C, Gupta N, Strbik III OM, Cho K. Syntactic foam core metal matrix sandwich composite: Compressive properties and strain rate effects. *Materials Science and Engineering: A.* 2015;643:156-168.
60. Lamanna E, Gupta N, Cappa P, Strbik III OM, Cho K. Evaluation of the dynamic properties of an aluminum syntactic foam core sandwich. *Journal of Alloys and Compounds.* 2017;695:2987-2994.
61. Poveda RL, Dorogokupets G, Gupta N. Carbon nanofiber reinforced syntactic foams: Degradation mechanism for long term moisture exposure and residual compressive properties. *Polymer degradation and stability.* 2013;98(10):2041-2053.

62. Corigliano A, Rizzi E, Papa E. Experimental characterization and numerical simulations of a syntactic-foam/glass-fibre composite sandwich. *Composites Science and Technology.* 2000;60(11):2169-2180.
63. Bardella L, Genna F. Elastic design of syntactic foamed sandwiches obtained by filling of three-dimensional sandwich-fabric panels. *International Journal of Solids and Structures.* 2001;38(2):307-333.
64. Sankaran S, Sekhar KR, Raju G, Kumar MJ. Characterization of epoxy syntactic foams by dynamic mechanical analysis. *Journal of materials science.* 2006;41(13):4041-4046.
65. Paul D, Velmurugan R, Jayaganthan R, Gupta N, Manzhirov A. Analysis of syntactic foam–GFRP sandwich composites for flexural loads. Paper presented at: Journal of Physics: Conference Series, 2018.
66. Gupta N, Nagorny R. Tensile properties of glass microballoon-epoxy resin syntactic foams. *Journal of Applied Polymer Science.* 2006;102(2):1254-1261.
67. Ghamsari AK, Zegeye E, Woldesenbet E. Viscoelastic properties of syntactic foam reinforced with short sisal fibers. *Journal of Composite Materials.* 2015;49(1):27-34.
68. Shams A, Zhao S, Porfiri M. Water impact of syntactic foams. *Materials.* 2017;10(3):224.
69. Anbuchezhiyan G, Mohan B, Sathianarayanan D, Muthuramalingam T. Synthesis and characterization of hollow glass microspheres reinforced magnesium alloy matrix syntactic foam. *Journal of Alloys and Compounds.* 2017;719:125-132.
70. John B, Nair CR, Ninan K. Effect of nanoclay on the mechanical, dynamic mechanical and thermal properties of cyanate ester syntactic foams. *Materials Science and Engineering: A.* 2010;527(21-22):5435-5443.
71. Bharath Kumar B, Doddamani M, Zeltmann SE, et al. Effect of particle surface treatment and blending method on flexural properties of injection-molded cenosphere/HDPE syntactic foams. *Journal of materials science.* 2016;51:3793-3805.
72. Taherishargh M, Sulong M, Belova I, Murch G, Fiedler T. On the particle size effect in expanded perlite aluminium syntactic foam. *Materials & Design (1980-2015).* 2015;66:294-303.
73. Shunmugasamy VC, Mansoor B. Flexural response of an aluminum foam core/stainless steel facesheet sandwich composite. *JOM.* 2019;71(11):4024-4033.
74. Yousaf Z, Smith M, Potluri P, Parnell W. Compression properties of polymeric syntactic foam composites under cyclic loading. *Composites Part B: Engineering.* 2020;186:107764.
75. Salleh Z. *Characterisation of syntactic foams for marine applications*, University of Southern Queensland; 2017.
76. Kim HS, Khamis MA. Fracture and impact behaviours of hollow micro-sphere/epoxy resin composites. *Composites Part A: Applied Science and Manufacturing.* 2001;32(9):1311-1317.
77. Kim HS, Plubrai P. Manufacturing and failure mechanisms of syntactic foam under compression☆. *Composites Part A: Applied Science and Manufacturing.* 2004;35(9):1009-1015.
78. Wouterson EM, Boey FY, Hu X, Wong S-C. Effect of fiber reinforcement on the tensile, fracture and thermal properties of syntactic foam. *Polymer.* 2007;48(11):3183-3191.
79. Salleh Z, Islam MM, Epaarachchi JA. Compressive Behaviour of Low Density Polymeric Syntactic Foams. *Applied Mechanics and Materials.* 2015;799:135-139.
80. Vasiliev VV, Morozov EV. *Advanced mechanics of composite materials and structures*: Elsevier; 2018.
81. Potter K. *Introduction to composite products: design, development and manufacture*: Springer Science & Business Media; 1996.
82. Nurazzi N, Asyraf M, Fatimah Athiyah S, et al. A review on mechanical performance of hybrid natural fiber polymer composites for structural applications. *Polymers.* 2021;13(13):2170.
83. Manakari V, Parande G, Doddamani M, Gupta M. Enhancing the ignition, hardness and compressive response of magnesium by reinforcing with hollow glass microballoons. *Materials.* 2017;10(9):997.

84. Yalkin HE, Icten BM, Alpyildiz T. Tensile and compressive performances of foam core sandwich composites with various core modifications. *Journal of Sandwich Structures & Materials.* 2017;19(1):49-65.
85. Young P. *Fracture analysis of glass microsphere filled epoxy resin syntactic foam*, UNSW Sydney; 2008.
86. Ahmadi H, Liaghat G, Hadavinia H. Investigation on tensile properties of plain and nanoclay reinforced syntactic foams. *International Journal of Composite Materials.* 2016;6(1):34-41.
87. Dimchev M, Caeti R, Gupta N. Effect of carbon nanofibers on tensile and compressive characteristics of hollow particle filled composites. *Materials & Design.* 2010;31(3):1332-1337.
88. Colloca M, Gupta N, Porfiri M. Tensile properties of carbon nanofiber reinforced multiscale syntactic foams. *Composites Part B: Engineering.* 2013;44(1):584-591.
89. Doddamani M, Kishore, Shunmugasamy VC, Gupta N, Vijayakumar H. Compressive and flexural properties of functionally graded fly ash cenosphere–epoxy resin syntactic foams. *Polymer composites.* 2015;36(4):685-693.
90. Karthikeyan CS, Sankaran S, Kishore. Flexural Behaviour of Fibre-Reinforced Syntactic Foams. *Macromolecular Materials and Engineering.* 2005;290(1):60-65.
91. Liang J-Z. Tensile and flexural properties of hollow glass bead-filled ABS composites. *Journal of Elastomers & Plastics.* 2005;37(4):361-370.
92. Patil AN, Kubade PR, Kulkarni HB. Effect of composition on impact and flexural properties of hybrid glass microballoons/fly ash cenosphere filled vinyl ester matrix syntactic foams. IJRTE; 2020.
93. Andrew JJ, Arumugam V, Saravanakumar K, Dhakal HN, Santulli C. Compression after impact strength of repaired GFRP composite laminates under repeated impact loading. *Composite structures.* 2015;133:911-920.
94. Davies G, Hitchings D, Besant T, Clarke A, Morgan C. Compression after impact strength of composite sandwich panels. *Composite Structures.* 2004;63(1):1-9.
95. Burger N, Laachachi A, Ferriol M, Lutz M, Toniazzo V, Ruch D. Review of thermal conductivity in composites: Mechanisms, parameters and theory. *Progress in Polymer Science.* 2016;61:1-28.
96. James J, Spittle J, Brown S, Evans R. A review of measurement techniques for the thermal expansion coefficient of metals and alloys at elevated temperatures. *Measurement science and technology.* 2001;12(3):R1.
97. Menard KP, Menard N. *Dynamic mechanical analysis*: CRC press; 2020.
98. Plante AF, Fernández JM, Leifeld J. Application of thermal analysis techniques in soil science. *Geoderma.* 2009;153(1-2):1-10.
99. Akhtar K, Khan SA, Khan SB, Asiri AM. *Scanning electron microscopy: Principle and applications in nanomaterials characterization*: Springer; 2018.
100. Reve M. *Understanding of buoyancy in drill pipe and risers*, University of Stavanger, Norway; 2013.
101. Ren S, Hu X, Ren H, et al. Development of a buoyancy material of hollow glass microspheres/SiO2 for high-temperature application. *Journal of Alloys and Compounds.* 2017;721:213-219.
102. Zou L, Zhao Y. High-Performance Ship. *Encyclopedia of Ocean Engineering*: Springer; 2022: 699-707.
103. Mortensen A. *Concise encyclopedia of composite materials*: Elsevier; 2006.
104. Tagliavia G, Porfiri M, Gupta N. Influence of moisture absorption on flexural properties of syntactic foams. *Composites Part B: Engineering.* 2012;43(2):115-123.
105. Gupta N, Woldesenbet E. Hygrothermal studies on syntactic foams and compressive strength determination. *Composite Structures.* 2003;61(4):311-320.
106. Erikson R. A survey of current technology. 5th Aerospace Materials. *Von Braun Center, Huntsville, Alabama.* 2002.

107. Lee MY, Tan J, Heng JY, Cheeseman C. A comparative study of production of glass microspheres by using thermal process. Paper presented at: IOP Conference Series: Materials Science and Engineering, 2017.
108. Watkins IG, Prado M. Mechanical properties of glass microspheres. *Procedia Materials Science.* 2015;8:1057-1065.
109. Bobkova NM, Trusova E, Savchin V, Sabadakha E, Pavlyukevich YG. Obtaining Hollow Glass Microspheres and Their Use in the Production of Water-Dispersion Coatings. *Glass and Ceramics.* 2020;76:401-405.
110. Shira S, Buller C. Mixing and dispersion of hollow glass microsphere products. *Hollow glass microspheres for plastics, elastomers, and adhesives compounds*: Elsevier; 2015: 241-271.
111. Freitas S, Merkle HP, Gander B. Microencapsulation by solvent extraction/evaporation: reviewing the state of the art of microsphere preparation process technology. *Journal of controlled release.* 2005;102(2):313-332.
112. Aird F. *Fiberglass & composite materials: an enthusiast's guide to high performance non-metallic materials for automotive racing and marine use*: Penguin; 1996.
113. Nazir MS, Mohamad Kassim MH, Mohapatra L, Gilani MA, Raza MR, Majeed K. Characteristic properties of nanoclays and characterization of nanoparticulates and nanocomposites. *Nanoclay reinforced polymer composites: Nanocomposites and bionanocomposites.* 2016:35-55.
114. Nagaraju K, Prasad T, Munaswamy V, Ramu YR. Nanoclay and Its Importance. *Current Journal of Applied Science and Technology.* 2021;40(13):71-81.
115. Deorukhkar OA, Radhakrishnan S, Munde YS, Kulkarni M. Polymer Nanocomposites: Polymer Composites: Design, Manufacturing, and Applications. *Polymer-Based Composites.* 2021:73-95.
116. Cui Y, Kumar S, Kona BR, van Houcke D. Gas barrier properties of polymer/clay nanocomposites. *Rsc Advances.* 2015;5(78):63669-63690.
117. Martinez VS. Thermal and transport properties of layered silicate nanomaterials subjected to extreme thermal cycling. 2007.
118. Masini JC, Abate G. Guidelines to Study the Adsorption of Pesticides onto Clay Minerals Aiming at a Straightforward Evaluation of Their Removal Performance. *Minerals.* 2021;11(11):1282.
119. Perelomov L, Mandzhieva S, Minkina T, et al. The synthesis of organoclays based on clay minerals with different structural expansion capacities. *Minerals.* 2021;11(7):707.
120. Undabeytia T, Shuali U, Nir S, Rubin B. Applications of chemically modified clay minerals and clays to water purification and slow release formulations of herbicides. *Minerals.* 2020;11(1):9.
121. Jacquet A, Geatches DL, Clark SJ, Greenwell HC. Understanding cationic polymer adsorption on mineral surfaces: Kaolinite in cement aggregates. *Minerals.* 2018;8(4):130.
122. Lazorenko G, Kasprzhitskii A, Yavna V. Comparative study of the hydrophobicity of organo-montmorillonite modified with cationic, amphoteric and nonionic surfactants. *Minerals.* 2020;10(9):732.
123. Bergaya F, Lagaly G. Introduction to clay science: techniques and applications. *Developments in Clay Science.* Vol 5: Elsevier; 2013: 1-7.
124. Murugesan S, Scheibel T. Copolymer/clay nanocomposites for biomedical applications. *Advanced Functional Materials.* 2020;30(17):1908101.
125. Zhou Y, LaChance AM, Smith AT, Cheng H, Liu Q, Sun L. Strategic Design of Clay-Based Multifunctional Materials: From Natural Minerals to Nanostructured Membranes. *Advanced functional materials.* 2019;29(16):1807611.
126. Valapa RB, Loganathan S, Pugazhenthi G, Thomas S, Varghese T. An overview of polymer–clay nanocomposites. *Clay-Polymer Nanocomposites.* 2017:29-81.
127. Vo V-S, Mahouche-Chergui S, Babinot J, Nguyen V-H, Naili S, Carbonnier B. Photo-induced SI-ATRP for the synthesis of photoclickable intercalated clay nanofillers. *RSC advances.* 2016;6(92):89322-89327.

128. Müller K, Bugnicourt E, Latorre M, et al. Review on the processing and properties of polymer nanocomposites and nanocoatings and their applications in the packaging, automotive and solar energy fields. *Nanomaterials.* 2017;7(4):74.
129. Guo F, Aryana S, Han Y, Jiao Y. A review of the synthesis and applications of polymer–nanoclay composites. *Applied Sciences.* 2018;8(9):1696.
130. Bajpai PK, Singh I. *Reinforced polymer composites: Processing, characterization and post life cycle assessment*: John Wiley & Sons; 2019.
131. Deshmukh A, Pai Y. Compression after impact & vibrational analysis of aramid-basalt/epoxy interply composites under hygrothermal conditions. *Cogent Engineering.* 2023;10(2):2262812.
132. Seyedin S, Carey T, Arbab A, et al. Fibre electronics: towards scaled-up manufacturing of integrated e-textile systems. *Nanoscale.* 2021;13(30):12818-12847.
133. Barbero EJ. Fabric-Reinforced Composites. *Introduction to Composite Materials Design*: CRC Press; 2017: 303-350.
134. Prashanth S, Subbaya K, Nithin K, Sachhidananda S. Fiber reinforced composites-a review. *J Mater Sci Eng.* 2017;6(03):2-6.
135. Bunsell AR, Joannès S, Thionnet A. *Fundamentals of fibre reinforced composite materials*: CRC Press; 2021.
136. Begum K, Islam M. Natural fiber as a substitute to synthetic fiber in polymer composites: a review. *Res J Eng Sci.* 2013;2278:9472.
137. Cruz J, Fangueiro R. Surface modification of natural fibers: a review. *Procedia Engineering.* 2016;155:285-288.
138. Saba N, Paridah M, Jawaid M. Mechanical properties of kenaf fibre reinforced polymer composite: A review. *Construction and Building materials.* 2015;76:87-96.
139. Cheung H-y, Ho M-p, Lau K-t, Cardona F, Hui D. Natural fibre-reinforced composites for bioengineering and environmental engineering applications. *Composites Part B: Engineering.* 2009;40(7):655-663.
140. Lotfi A, Li H, Dao DV, Prusty G. Natural fiber–reinforced composites: A review on material, manufacturing, and machinability. *Journal of Thermoplastic Composite Materials.* 2021;34(2):238-284.
141. Pickering KL, Efendy MA, Le TM. A review of recent developments in natural fibre composites and their mechanical performance. *Composites Part A: Applied Science and Manufacturing.* 2016;83:98-112.
142. Lau K-t, Hung P-y, Zhu M-H, Hui D. Properties of natural fibre composites for structural engineering applications. *Composites Part B: Engineering.* 2018;136:222-233.
143. Väisänen T, Das O, Tomppo L. A review on new bio-based constituents for natural fiber-polymer composites. *Journal of Cleaner Production.* 2017;149:582-596.
144. Sanjay M, Madhu P, Jawaid M, Senthamaraikannan P, Senthil S, Pradeep S. Characterization and properties of natural fiber polymer composites: A comprehensive review. *Journal of Cleaner Production.* 2018;172:566-581.
145. Siakeng R, Jawaid M, Ariffin H, Sapuan S, Asim M, Saba N. Natural fiber reinforced polylactic acid composites: A review. *Polymer Composites.* 2019;40(2):446-463.
146. Mochane M, Mokhena TC, Mokhothu T, et al. Recent progress on natural fiber hybrid composites for advanced applications: A review. 2019.
147. Asim M, Abdan K, Jawaid M, et al. A review on pineapple leaves fibre and its composites. *International Journal of Polymer Science.* 2015;2015.
148. Antov P, Savov V, Neykov N. Utilization of agricultural waste and wood industry residues in the production of natural fiber-reinforced composite materials. *International Journal–Wood, Design, and Technology.* 2017;6:64-71.
149. Dunne R, Desai D, Sadiku R, Jayaramudu J. A review of natural fibres, their sustainability and automotive applications. *Journal of Reinforced Plastics and Composites.* 2016;35(13):1041-1050.

150. Adekomaya O, Jamiru T, Sadiku R, Huan Z. A review on the sustainability of natural fiber in matrix reinforcement–A practical perspective. *Journal of Reinforced Plastics and Composites.* 2016;35(1):3-7.
151. Mohanty A, Misra M, Drzal LT. Surface modifications of natural fibers and performance of the resulting biocomposites: An overview. *Composite interfaces.* 2001;8(5):313-343.
152. Buragohain MK. *Composite structures: design, mechanics, analysis, manufacturing, and testing*: CRC press; 2017.
153. John MJ, Thomas S. Biofibres and biocomposites. *Carbohydrate polymers.* 2008;71(3):343-364.
154. Sahu P, Gupta M. A review on the properties of natural fibres and its bio-composites: Effect of alkali treatment. *Proceedings of the Institution of Mechanical Engineers, Part L: Journal of Materials: Design and Applications.* 2020;234(1):198-217.
155. Thakur VK, Thakur MK. Processing and characterization of natural cellulose fibers/thermoset polymer composites. *Carbohydrate polymers.* 2014;109:102-117.
156. Tavares TD, Antunes JC, Ferreira F, Felgueiras HP. Biofunctionalization of natural fiber-reinforced biocomposites for biomedical applications. *Biomolecules.* 2020;10(1):148.
157. Webo W, Maringa M, Masu L. The combined effect of mercerisation, silane treatment and acid hydrolysis on the mechanical properties of sisal fibre/epoxy resin composites. *MRS Advances.* 2020;5:1225-1233.
158. Bhatia JK, Kaith BS, Kalia S. Recent developments in surface modification of natural fibers for their use in biocomposites. *Biodegradable Green Composites.* 2016:80-117.
159. Adekomaya O, Majozi T. Sustainability of surface treatment of natural fibre in composite formation: challenges of environment-friendly option. *The International Journal of Advanced Manufacturing Technology.* 2019;105(7):3183-3195.
160. Godara S. Effect of chemical modification of fiber surface on natural fiber composites: A review. *Materials Today: Proceedings.* 2019;18:3428-3434.
161. Latif R, Wakeel S, Zaman Khan N, Noor Siddiquee A, Lal Verma S, Akhtar Khan Z. Surface treatments of plant fibers and their effects on mechanical properties of fiber-reinforced composites: A review. *Journal of Reinforced Plastics and Composites.* 2019;38(1):15-30.
162. Koronis G, Silva A, Fontul M. Green composites: A review of adequate materials for automotive applications. *Composites Part B: Engineering.* 2013;44(1):120-127.
163. Li K, Fu S, Zhan H, Zhan Y, Lucia L. Analysis of the chemical composition and morphological structure of banana pseudo-stem. *BioResources.* 2010;5(2):576-585.
164. Sango T, Yona AMC, Duchatel L, et al. Step–wise multi–scale deconstruction of banana pseudo–stem (Musa acuminata) biomass and morpho–mechanical characterization of extracted long fibres for sustainable applications. *Industrial Crops and Products.* 2018;122:657-668.
165. Subagyo A, Chafidz A. Banana pseudo-stem fiber: Preparation, characteristics, and applications. *Banana nutrition-function and processing kinetics.* 2018:1-19.
166. Padam BS, Tin HS, Chye FY, Abdullah MI. Banana by-products: an under-utilized renewable food biomass with great potential. *Journal of food science and technology.* 2014;51:3527-3545.
167. Paul SA, Boudenne A, Ibos L, Candau Y, Joseph K, Thomas S. Effect of fiber loading and chemical treatments on thermophysical properties of banana fiber/polypropylene commingled composite materials. *Composites Part A: Applied Science and Manufacturing.* 2008;39(9):1582-1588.
168. Bilba K, Arsene M-A, Ouensanga A. Study of banana and coconut fibers: Botanical composition, thermal degradation and textural observations. *Bioresource technology.* 2007;98(1):58-68.
169. Cherian BM, Pothan LA, Nguyen-Chung T, Mennig Gn, Kottaisamy M, Thomas S. A novel method for the synthesis of cellulose nanofibril whiskers from banana fibers and characterization. *Journal of agricultural and food chemistry.* 2008;56(14):5617-5627.

170. Tock JY, Lai CL, Lee KT, Tan KT, Bhatia S. Banana biomass as potential renewable energy resource: A Malaysian case study. *Renewable and sustainable energy reviews.* 2010;14(2):798-805.
171. Kumar KS, Bhowmik D, Duraivel S, Umadevi M. Traditional and medicinal uses of banana. *Journal of pharmacognosy and phytochemistry.* 2012;1(3):51-63.
172. Vu HT, Scarlett CJ, Vuong QV. Phenolic compounds within banana peel and their potential uses: A review. *Journal of Functional Foods.* 2018;40:238-248.
173. Abdullah N, Sulaiman F, Miskam MA, Taib RM. Characterization of banana (Musa spp.) pseudo-stem and fruit-bunch-stem as a potential renewable energy resource. *International Journal of Energy and Power Engineering.* 2014;8(8):815-819.
174. Ahmad T, Danish M. Prospects of banana waste utilization in wastewater treatment: A review. *Journal of environmental management.* 2018;206:330-348.
175. Cordeiro N, Belgacem M, Torres I, Moura J. Chemical composition and pulping of banana pseudo-stems. *Industrial Crops and Products.* 2004;19(2):147-154.
176. Franck RR. *Bast and other plant fibres.* Vol 39: Crc Press; 2005.
177. Pappu A, Patil V, Jain S, Mahindrakar A, Haque R, Thakur VK. Advances in industrial prospective of cellulosic macromolecules enriched banana biofibre resources: A review. *International journal of biological macromolecules.* 2015;79:449-458.
178. Jayaprabha J, Brahmakumar M, Manilal V. Banana pseudostem characterization and its fiber property evaluation on physical and bioextraction. *Journal of Natural Fibers.* 2011;8(3):149-160.
179. Das H, Kalita D. Recent development of fiber reinforced composite materials. *Biosensors Nanotechnology.* 2014:441-496.
180. Chandramohan D, Marimuthu K. A review on natural fibers. *International Journal of Research and Reviews in Applied Sciences.* 2011;8(2):194-206.
181. Doshi A. *Banana fiber to fabric: Process optimization for improving its spinnability and hand*, Maharaja Sayajirao University of Baroda (India); 2017.
182. Gupta V, Gupta S. Cotton Fiber and Its Sustainable Alternatives. *Novel Sustainable Raw Material Alternatives for the Textiles and Fashion Industry*: Springer; 2023: 139-160.
183. Ray D, Nayak L, Ammayappan L, Shambhu V, Nag D. Energy conservation drives for efficient extraction and utilization of banana fibre. *International Journal of Emerging Technology and Advanced Engineering.* 2013;3(8):296-310.
184. Komal UK, Verma V, Ashwani T, Verma N, Singh I. Effect of chemical treatment on thermal, mechanical and degradation behavior of banana fiber reinforced polymer composites. *Journal of Natural Fibers.* 2020.
185. Komal UK, Verma V, Aswani T, Verma N, Singh I. Effect of chemical treatment on mechanical behavior of banana fiber reinforced polymer composites. *Materials Today: Proceedings.* 2018;5(9):16983-16989.
186. Santhanam V, Chandrasekaran M. Effect of surface treatment on the mechanical properties of banana-glass fibre hybrid composites. *Applied Mechanics and Materials.* 2014;591:7-10.
187. Kumar R, Haq MIU, Raina A, Sharma SM, Anand A, Abdollah MFB. Tribological behaviour of natural fibre based polymer composites. *Tribology of Polymer and Polymer Composites for Industry 40.* 2021:55-69.
188. Wang B, Panigrahi S, Tabil L, Crerar W. Pre-treatment of flax fibers for use in rotationally molded biocomposites. *Journal of reinforced plastics and composites.* 2007;26(5):447-463.
189. Adekunle K, Åkesson D, Skrifvars M. Biobased composites prepared by compression molding with a novel thermoset resin from soybean oil and a natural-fiber reinforcement. *Journal of applied polymer science.* 2010;116(3):1759-1765.
190. Mukhopadhyay S, Fangueiro R. Physical modification of natural fibers and thermoplastic films for composites—a review. *Journal of Thermoplastic Composite Materials.* 2009;22(2):135-162.

191. Lee SG, Choi SS, Park WH, Cho D. Characterization of surface modified flax fibers and their biocomposites with PHB. Paper presented at: Macromolecular symposia, 2003.
192. Sun D. Surface modification of natural fibers using plasma treatment. *Biodegradable green composites.* 2016:18-39.
193. Wang W, Chen W, Zou M, et al. Applications of power ultrasound in oriented modification and degradation of pectin: A review. *Journal of Food Engineering.* 2018;234:98-107.
194. Islam M, Beg M, Gupta A, Mina M. Optimal performances of ultrasound treated kenaf fiber reinforced recycled polypropylene composites as demonstrated by response surface method. *Journal of Applied Polymer Science.* 2013;128(5):2847-2856.
195. Chang W-P, Kim K-J, Gupta RK. Ultrasound-assisted surface-modification of wood particulates for improved wood/plastic composites. *Composite Interfaces.* 2009;16(7-9):687-709.
196. Benedetto RMD, Gelfuso MV, Thomazini D. Influence of UV radiation on the physical-chemical and mechanical properties of banana fiber. *Materials Research.* 2015;18(suppl 2):265-272.
197. Abdullah-Al-Kafi, Abedin M, Beg M, Pickering K, Khan MA. Study on the mechanical properties of jute/glass fiber-reinforced unsaturated polyester hybrid composites: Effect of surface modification by ultraviolet radiation. *Journal of Reinforced Plastics and Composites.* 2006;25(6):575-588.
198. Rahman MM, Khan MA. Surface treatment of coir (Cocos nucifera) fibers and its influence on the fibers' physico-mechanical properties. *Composites science and technology.* 2007;67(11-12):2369-2376.
199. Hamidon MH, Sultan MT, Ariffin AH, Shah AU. Effects of fibre treatment on mechanical properties of kenaf fibre reinforced composites: a review. *Journal of Materials Research and Technology.* 2019;8(3):3327-3337.
200. Li X, Tabil LG, Panigrahi S. Chemical treatments of natural fiber for use in natural fiber-reinforced composites: a review. *Journal of Polymers and the Environment.* 2007;15:25-33.
201. Lu N, Oza S, Tajabadi MG. Surface modification of natural fibers for reinforcement in polymeric composites. *Surface modification of biopolymers.* 2015:224-237.
202. Paul SA, Pothan LA, Thomas S. Advances in the characterization of interfaces of lignocellulosic fiber reinforced composites. *Characterization of Lignocellulosic Materials.* 2008:249-274.
203. Bledzki A, Reihmane S, Gassan J. Properties and modification methods for vegetable fibers for natural fiber composites. *Journal of applied polymer science.* 1996;59(8):1329-1336.
204. Valadez-Gonzalez A, Cervantes-Uc J, Olayo R, Herrera-Franco P. Effect of fiber surface treatment on the fiber–matrix bond strength of natural fiber reinforced composites. *Composites Part B: Engineering.* 1999;30(3):309-320.
205. Sreekala M, Kumaran M, Joseph S, Jacob M, Thomas S. Oil palm fibre reinforced phenol formaldehyde composites: influence of fibre surface modifications on the mechanical performance. *Applied Composite Materials.* 2000;7:295-329.
206. Zhou Y, Fan M, Chen L. Interface and bonding mechanisms of plant fibre composites: An overview. *Composites Part B: Engineering.* 2016;101:31-45.
207. Jacob M, Joseph S, Pothan LA, Thomas S. A study of advances in characterization of interfaces and fiber surfaces in lignocellulosic fiber-reinforced composites. *Composite interfaces.* 2005;12(1-2):95-124.
208. Maldas D, Kokta B. Interfacial adhesion of lignocellulosic materials in polymer composites: an overview. *Composite interfaces.* 1993;1(1):87-108.
209. Farahani GN, Ahmad I, Mosadeghzad Z. Effect of fiber content, fiber length and alkali treatment on properties of kenaf fiber/UPR composites based on recycled PET wastes. *Polymer-Plastics Technology and Engineering.* 2012;51(6):634-639.
210. Fiore V, Di Bella G, Valenza A. The effect of alkaline treatment on mechanical properties of kenaf fibers and their epoxy composites. *Composites Part B: Engineering.* 2015;68:14-21.
211. Oushabi A, Sair S, Hassani FO, Abboud Y, Tanane O, El Bouari A. The effect of alkali treatment on mechanical, morphological and thermal properties of date palm fibers (DPFs): Study of the

interface of DPF–Polyurethane composite. *South African Journal of Chemical Engineering.* 2017;23:116-123.
212. Faruk O, Bledzki AK, Fink H-P, Sain M. Biocomposites reinforced with natural fibers: 2000–2010. *Progress in polymer science.* 2012;37(11):1552-1596.
213. Mwaikambo LY, Tucker N, Clark AJ. Mechanical properties of hemp-fibre-reinforced euphorbia composites. *Macromolecular Materials and Engineering.* 2007;292(9):993-1000.
214. Ray D, Sarkar BK, Rana A, Bose NR. Effect of alkali treated jute fibres on composite properties. *Bulletin of materials science.* 2001;24:129-135.
215. Paul A, Joseph K, Thomas S. Effect of surface treatments on the electrical properties of low-density polyethylene composites reinforced with short sisal fibers. *Composites Science and Technology.* 1997;57(1):67-79.
216. Gupta US, Dhamarikar M, Dharkar A, Chaturvedi S, Tiwari S, Namdeo R. Surface modification of banana fiber: a review. *Materials Today: Proceedings.* 2021;43:904-915.
217. Hari Sankar P, Hemacahndra Reddy K, Mohana Reddy Y, Ashok Kumar M, Ramesh A. The effect of fiber length on tensile properties of polyester resin composites reinforced by the fibers of Sansevieria trifasciata. *International Letters of Natural Sciences.* 2014;3.
218. Biswal M, Mohanty S, Nayak SK. Effect of mercerized banana fiber on the mechanical and morphological characteristics of organically modified fiber-reinforced polypropylene nanocomposites. *Polymer-Plastics Technology and Engineering.* 2011;50(14):1458-1469.
219. Mittal KL. *Silanes and other coupling agents.* Vol 4: CRC Press; 2007.
220. Sreekala M, Kumaran M, Thomas S. Water sorption in oil palm fiber reinforced phenol formaldehyde composites. *Composites Part A: Applied science and manufacturing.* 2002;33(6):763-777.
221. Seki Y. Innovative multifunctional siloxane treatment of jute fiber surface and its effect on the mechanical properties of jute/thermoset composites. *Materials Science and Engineering: A.* 2009;508(1-2):247-252.
222. Khalil HA, Rozman H, Ahmad M, Ismail H. Acetylated plant-fiber-reinforced polyester composites: A study of mechanical, hygrothermal, and aging characteristics. *Polymer-plastics technology and engineering.* 2000;39(4):757-781.
223. Fabrice PKR, Abejide SO, Adedeji JA, Mostafa MMH. Evaluating the performance of warm mix asphalt incorporating recycled asphalt pavement treated bases. *Transportation Research Procedia.* 2020;45:716-723.
224. Munde YS, Ingle RB. Theoretical modeling and experimental verification of mechanical properties of natural fiber reinforced thermoplastics. *Procedia technology.* 2015;19:320-326.
225. Habal A, Singh D. Effects of warm mix asphalt additives on bonding potential and failure pattern of asphalt-aggregate systems using strength and energy parameters. *International Journal of Pavement Engineering.* 2021;22(4):467-479.
226. Hubert P, Vaziri R, Poursartip A. A two-dimensional flow model for the process simulation of complex shape composite laminates. *International Journal for Numerical Methods in Engineering.* 1999;44(1):1-26.
227. Abrate S. Modeling of impacts on composite structures. *Composite structures.* 2001;51(2):129-138.
228. Madke RR, Chowdhury R. A multiscale continuum model for inelastic behavior of woven composite. *Composite Structures.* 2019;226:111267.
229. Lisle TJ, Shaw BA, Frazer RC. External spur gear root bending stress: A comparison of ISO 6336: 2006, AGMA 2101-D04, ANSYS finite element analysis and strain gauge techniques. *Mechanism and Machine Theory.* 2017;111:1-9.
230. Noman AA, Shohel SM, Riyad SH, Gupta SS. Investigate the mechanical strength of laminated composite carbon fiber with different fiber orientations by numerically using finite element analysis. *Materials Today: Proceedings.* 2023.

231. Faizan M, Gangwar S. Tensile behaviour of carbon fiber reinforced polymer composite using ANSYS 21. *Materials Today: Proceedings.* 2021;46:6519-6526.
232. Norman DA, Robertson RE. The effect of fiber orientation on the toughening of short fiber-reinforced polymers. *Journal of applied polymer science.* 2003;90(10):2740-2751.
233. Fu S-Y, Hu X, Yue C-Y. Effects of fiber length and orientation distributions on the mechanical properties of short-fiber-reinforced polymers a review. *Journal of the Society of Materials Science, Japan.* 1999;48(6Appendix):74-83.
234. Jakob M, Mahendran AR, Gindl-Altmutter W, et al. The strength and stiffness of oriented wood and cellulose-fibre materials: A review. *Progress in Materials Science.* 2022;125:100916.
235. Masoumy E, Kacir L, Kardos J. Effect of fiber-aspect ratio and orientation on the stress-strain behavior of aligned, short-fiber-reinforced, ductile epoxy. *Polymer composites.* 1983;4(1):64-72.
236. Zwawi M. A review on natural fiber bio-composites, surface modifications and applications. *molecules.* 2021;26(2):404.
237. Khoathane MC, Sadiku ER, Agwuncha CS. Surface modification of natural fiber composites and their potential applications. *Surface modification of biopolymers.* 2015:370-400.
238. Shah I, Jing L, Fei ZM, Yuan YS, Farooq MU, Kanjana N. A review on chemical modification by using sodium hydroxide (NaOH) to investigate the mechanical properties of sisal, coir and hemp fiber reinforced concrete composites. *Journal of Natural Fibers.* 2022;19(13):5133-5151.
239. Olonisakin K, Fan M, Xin-Xiang Z, et al. Key improvements in interfacial adhesion and dispersion of fibers/fillers in polymer matrix composites; focus on pla matrix composites. *Composite Interfaces.* 2022;29(10):1071-1120.
240. Murawski A, Diaz R, Inglesby S, Delabar K, Quirino RL. Synthesis of bio-based polymer composites: fabrication, fillers, properties, and challenges. *Polymer nanocomposites in biomedical engineering.* 2019:29-55.
241. Jayabal S, Sathiyamurthy S, Loganathan K, Kalyanasundaram S. Effect of soaking time and concentration of NaOH solution on mechanical properties of coir–polyester composites. *Bulletin of Materials Science.* 2012;35(4):567-574.
242. Nasidi IN, Ismail LH, Samsudin EM. Effect of Sodium Hydroxide (NaOH) Treatment on Coconut Coir Fibre and its Effectiveness on Enhancing Sound Absorption Properties. *Pertanika Journal of Science & Technology.* 2021;29(1).
243. Khan M, Rahamathbaba S, Mateen M, Ravi Shankar D, Manzoor Hussain M. Effect of NaOH treatment on mechanical strength of banana/epoxy laminates. *Polymers from Renewable Resources.* 2019;10(1-3):19-26.
244. Hashim MY, Amin AM, Marwah OMF, Othman MH, Yunus MRM, Huat NC. The effect of alkali treatment under various conditions on physical properties of kenaf fiber. Paper presented at: Journal of Physics: Conference Series, 2017.
245. Karthikeyan A, Balamurugan K, Kalpana A. The effect of sodium hydroxide treatment and fiber length on the tensile property of coir fiber-reinforced epoxy composites. *Science and Engineering of Composite Materials.* 2014;21(3):315-321.
246. Simon M-O, Li C-J. Green chemistry oriented organic synthesis in water. *Chemical Society Reviews.* 2012;41(4):1415-1427.
247. Butler RN, Coyne AG. Water: Nature's Reaction Enforcer· Comparative Effects for Organic Synthesis "In-Water" and "On-Water". *Chemical reviews.* 2010;110(10):6302-6337.
248. Saavedra J, Doan HA, Pursell CJ, Grabow LC, Chandler BD. The critical role of water at the gold-titania interface in catalytic CO oxidation. *Science.* 2014;345(6204):1599-1602.
249. Biedermann F, Nau WM, Schneider HJ. The hydrophobic effect revisited—studies with supramolecular complexes imply high-energy water as a noncovalent driving force. *Angewandte Chemie International Edition.* 2014;53(42):11158-11171.
250. Butler RN, Coyne AG. Organic synthesis reactions on-water at the organic–liquid water interface. *Organic & biomolecular chemistry.* 2016;14(42):9945-9960.

251. Asim M, Jawaid M, Saba N, Nasir M, Sultan MTH. Processing of hybrid polymer composites—a review. *Hybrid polymer composite materials.* 2017:1-22.
252. Ajayi AA, Turup Pandurangan M, Kanny K. Influence of hybridizing fillers on mechanical properties of foam composite panel. *Polymer Engineering & Science.* 2023.
253. Afolabi OA, Kanny K, Mohan T. Loading Effect of Hollow Glass Microsphere (HGM) and Foam Microstructure on the Specific Mechanical Properties and Water Absorption of Syntactic Foam Composite. *International Journal of Engineering Research in Africa.* 2021;56:34-50.
254. Ajayi AA, Turup Pandurangan M, Kanny K. Influence of hybridizing fillers on mechanical properties of foam composite panel. *Polymer Engineering & Science.* 2023;63(8):2565-2577.
255. Mahmoudian S, Wahit MU, Imran M, Ismail A, Balakrishnan H. A facile approach to prepare regenerated cellulose/graphene nanoplatelets nanocomposite using room-temperature ionic liquid. *Journal of nanoscience and nanotechnology.* 2012;12(7):5233-5239.
256. Afolabi OA. *Hybrid syntactic foam core cased natural-glass fibre sandwich composite*; 2023.
257. Nergaard A, Architect N, Engineer P. The Magic of Buoyancy and Hydrostatics–Buoyancy and Effective Forces. *Modern Applied Science.* 2017;11(12):77-83.
258. Ajayi AA, Pandurangan MT, Krishnan K. Development of Epoxy-based sandwich composite panel with Hollow glass microspheres/Clay hybrid core and banana fiber facesheet for structural applications. *Heliyon.* 2024.
259. Ajayi AA, Turup Pandurangan M, Kanny K, Ramachandran V. Thermal and Wettability Properties of Nanoclay-Filled Epoxy-Based Foam Composite as Lightweight Material. *Materials Performance and Characterization.* 2023;12(1):293-306.
260. International A. *Standard test method for compositional analysis by thermogravimetry*: ASTM International; 2003.
261. ASTM D I. Standard practice for plastics: Dynamic mechanical properties: Determination and report of procedures. ASTM International West Conshohocken, PA; 2012.
262. Stark W. Investigation of the curing behaviour of carbon fibre epoxy prepreg by Dynamic Mechanical Analysis DMA. *Polymer Testing.* 2013;32(2):231-239.
263. Gostynska NE. Investigation of Different Crosslinking Strategies to Develop 3D Polymer Scaffolds for Cartilage Tissue Engineering. 2017.
264. Gracia-Fernández C, Gómez-Barreiro S, López-Beceiro J, Saavedra JT, Naya S, Artiaga R. Comparative study of the dynamic glass transition temperature by DMA and TMDSC. *Polymer Testing.* 2010;29(8):1002-1006.
265. Toader G, Ginghina RE, Diacon A, et al. Design and Application of Photocrosslinkable Hydrogel Films for Fast and Efficient Decontamination of Chemical Warfare Agents. *ACS Applied Polymer Materials.* 2022;5(1):877-891.
266. Ribeiro Junior AH, Ribeiro Filho SLM, Ribeiro FJV, et al. Statistical and numerical approaches of particulate reinforced polymers and their effect on the interlocking effect of hybrid composite joints. *Journal of Composite Materials.* 2022;56(8):1267-1285.
267. Kootsookos A, Burchill P. The effect of the degree of cure on the corrosion resistance of vinyl ester/glass fibre composites. *Composites Part A: Applied Science and Manufacturing.* 2004;35(4):501-508.
268. Grujić A, Talijan N, Stojanović D, et al. Mechanical and magnetic properties of composite materials with polymer matrix. *Journal of mining and metallurgy, Section B: Metallurgy.* 2010;46(1):25-32.
269. Standard A. Standard test methods for flexural properties of unreinforced and reinforced plastics and electrical insulating materials. ASTM D790. *Annual book of ASTM standards.* 1997.
270. Afolabi OA, Kanny K, Mohan TP. Investigation of mechanical characterization of hybrid sandwich composites with syntactic foam core for structural applications. *Composites and Advanced Materials.* 2023;32:26349833221147539.
271. Pagano N. Exact moduli of anisotropic laminates. *Mechanics of Composite Materials: Selected Works of Nicholas J. Pagano*: Springer; 1994: 210-231.

272. Böhm HJ. Micromechanics. *Encyclopedia of Continuum Mechanics.* 2020:1621-1628.
273. Ibrahim AH, Yigit AS. Accuracy and Computational Efficiency of Finite Element Models for Low Velocity Impact on Composite Structures Subject to Progressive Damage and Delamination. *Journal of Computational and Nonlinear Dynamics.* 2015;10(6):061009.
274. Liang J, Wu C. Effects of the glass bead content and the surface treatment on the mechanical properties of polypropylene composites. *Journal of applied polymer science.* 2012;123(5):3054-3063.
275. Barbosa A, Da Silva L, Abenojar J, Figueiredo M, Öchsner A. Toughness of a brittle epoxy resin reinforced with micro cork particles: Effect of size, amount and surface treatment. *Composites Part B: Engineering.* 2017;114:299-310.
276. Raju B, Suresha B, Swamy R, Bharath K. The effect of silicon dioxide filler on the wear resistance of glass fabric reinforced epoxy composites. *polymer composites.* 2012;18:20.
277. Qiao Y, Wang X, Zhang X, Xing Z. Investigation of flexural properties of hollow glass microsphere filled resin-matrix composites. *Pigment & Resin Technology.* 2016;45(6):426-430.
278. Tian Q, Yu D. Preparation and properties of polymer microspheres filled epoxy composite films by UV-curable polymerization. *Materials & Design.* 2016;107:221-229.
279. Bensadoun F, Kchit N, Billotte C, Trochu F, Ruiz E. A comparative study of dispersion techniques for nanocomposite made with nanoclays and an unsaturated polyester resin. *Journal of Nanomaterials.* 2011;2011:6-6.
280. Nzioka Mutua F, Omollo E, Khamala E, Igadwa Mwasiagi J, Ciera L, Wang Y. A study of the characteristics of hollow glassmicrospheres reinforced thermoplastic polyurethane composite foam. 2015.
281. Li J, Luo X, Lin X. Preparation and characterization of hollow glass microsphere reinforced poly (butylene succinate) composites. *Materials & Design (1980-2015).* 2013;46:902-909.
282. Gupta N, Ye R, Porfiri M. Comparison of tensile and compressive characteristics of vinyl ester/glass microballoon syntactic foams. *Composites Part B: Engineering.* 2010;41(3):236-245.
283. He H, Li K. Silane coupling agent modification on interlaminar shear strength of carbon fiber/epoxy/nano-caco3 composites. *Polymer composites.* 2012;33(10):1755-1758.
284. Chen J-S, Poliks MD, Ober CK, Zhang Y, Wiesner U, Giannelis E. Study of the interlayer expansion mechanism and thermal–mechanical properties of surface-initiated epoxy nanocomposites. *Polymer.* 2002;43(18):4895-4904.
285. Ulus H, Kaybal HB, Cacık F, Eskizeybek V, Avcı A. Effect of long-term stress aging on aluminum-BFRP hybrid adhesive joint's mechanical performance: Static and dynamic loading scenarios. *Polymer Composites.* 2022;43(8):5301-5318.
286. Messersmith PB, Giannelis EP. Synthesis and characterization of layered silicate-epoxy nanocomposites. *Chemistry of materials.* 1994;6(10):1719-1725.
287. Latsuzbaya V, Middendorf P, Völkle D, Weber C. Improving the thermal properties of aircraft cabin interiors with the integration of vacuum insulation panels. *CEAS Aeronautical Journal.* 2022;13(3):705-718.
288. Vahtrus M, Oras S, Antsov M, et al. Mechanical and thermal properties of epoxy composite thermal insulators filled with silica aerogel and hollow glass microspheres. *Proceedings of the Estonian Academy of Sciences.* 2017;66(4).
289. He Z-Q, Yang Y, Yu B, et al. Research on properties of hollow glass microspheres/epoxy resin composites applied in deep rock in-situ temperature-preserved coring. *Petroleum Science.* 2022;19(2):720-730.
290. Ma B, Zhou X-y, Liu J, You Z, Wei K, Huang X-f. Determination of specific heat capacity on composite shape-stabilized phase change materials and asphalt mixtures by heat exchange system. *Materials.* 2016;9(5):389.

291. Guo K-Y, Wu Q, Mao M, et al. Water-based hybrid coatings toward mechanically flexible, super-hydrophobic and flame-retardant polyurethane foam nanocomposites with high-efficiency and reliable fire alarm response. *Composites Part B: Engineering.* 2020;193:108017.
292. Xiong B, Li J, He C, et al. Effect of pore morphology and surface roughness on wettability of porous titania films. *Materials Research Express.* 2020;7(11):115013.
293. Klein NS, Bachmann J, Aguado A, Toralles-Carbonari B. Evaluation of the wettability of mortar component granular materials through contact angle measurements. *Cement and concrete research.* 2012;42(12):1611-1620.
294. Zhao H, Li RK. Effect of water absorption on the mechanical and dielectric properties of nano-alumina filled epoxy nanocomposites. *Composites Part A: Applied Science and Manufacturing.* 2008;39(4):602-611.
295. Ibrahim ID, Jamiru T, Sadiku ER, Kupolati WK, Agwuncha SC. Impact of surface modification and nanoparticle on sisal fiber reinforced polypropylene nanocomposites. *Journal of Nanotechnology.* 2016;2016.
296. Nimbagal V, Banapurmath N, Umarfarooq M, et al. Mechanical and fracture properties of carbon nano fibers/short carbon fiber epoxy composites. *Polymer Composites.* 2023.
297. Shahapurkar K. Tensile behavior of environmental pollutant crumb rubber filled epoxy composites. *Materials Research Express.* 2021;8(9):095505.
298. Dhal JP, Mishra SC. Processing and properties of natural fiber-reinforced polymer composite. *Journal of Materials.* 2013;2013.
299. Rahman R, Putra SZFS. Tensile properties of natural and synthetic fiber-reinforced polymer composites. *Mechanical and physical testing of biocomposites, fibre-reinforced composites and hybrid composites.* 2019:81-102.
300. Alshammari BA, Alenad AM, Al-Mubaddel FS, et al. Impact of Hybrid Fillers on the Properties of High Density Polyethylene Based Composites. *Polymers.* 2022;14(16):3427.
301. Boopalan M, Niranjanaa M, Umapathy M. Study on the mechanical properties and thermal properties of jute and banana fiber reinforced epoxy hybrid composites. *Composites Part B: Engineering.* 2013;51:54-57.
302. Pandey A, Muchhala D, Kumar R, Sriram S, Venkat AC, Mondal D. Flexural deformation behavior of carbon fiber reinforced aluminium hybrid foam sandwich structure. *Composites Part B: Engineering.* 2020;183:107729.
303. Burianek DA, Spearing SM. Fatigue damage in titanium-graphite hybrid laminates. *Composites science and technology.* 2002;62(5):607-617.
304. Leguillon D, Martin É, Lafarie-Frenot M-C. Flexural vs. tensile strength in brittle materials. *Comptes Rendus Mécanique.* 2015;343(4):275-281.
305. Cabral H, Cisneros M, Kenny J, Vazquez A, Bernal C. Structure–properties relationship of short jute fiber-reinforced polypropylene composites. *Journal of Composite Materials.* 2005;39(1):51-65.
306. Kumar SS, Raja VM. Processing and determination of mechanical properties of Prosopis juliflora bark, banana and coconut fiber reinforced hybrid bio composites for an engineering field. *Composites Science and Technology.* 2021;208:108695.
307. Eyvazian A, Taghizadeh SA, Hamouda AM, Tarlochan F, Moeinifard M, Gobbi M. Buckling and crushing behavior of foam-core hybrid composite sandwich columns under quasi-static edgewise compression. *Journal of Sandwich Structures & Materials.* 2021;23(7):2643-2670.
308. Radzi F, Suriani M, Bakar AA, et al. Effect of reinforcement of Alkaline-treated sugar palm/bamboo/kenaf and fibreglass/Kevlar with polyester hybrid biocomposites: mechanical, morphological, and water absorption properties. *Journal of Materials Research and Technology.* 2023;24:4190-4202.
309. Sharba MJ, Leman Z, Sultan M, Ishak M, Hanim M. Tensile and compressive properties of woven kenaf/glass sandwich hybrid composites. *International Journal of Polymer Science.* 2016;2016.

310. Nemati Giv A, Rastegar S, Özcan M. Influence of nanoclays on water uptake and flexural strength of glass–polyester composites. *Journal of applied biomaterials & functional materials.* 2020;18:2280800020930180.
311. Ajayi AA, Kanny K, Pandurangan MT, Ramachandran V. Thermal and Wettability Properties of Nanoclay-Filled Epoxy-Based Foam Composite as Lightweight Material. *Materials Performance and Characterization.* 2023;12(1):293-306.
312. Eker Gümüş B. Effect of MA-g-PP addition on mechanical properties of polypropylene/hollow glass spheres/nanoclay composites. *Polymer Bulletin.* 2023;80(3):3405-3422.
313. Qiu W, Zhang F, Endo T, Hirotsu T. Effect of maleated polypropylene on the performance of polypropylene/cellulose composite. *Polymer Composites.* 2005;26(4):448-453.
314. Svoboda P, Zeng C, Wang H, Lee LJ, Tomasko DL. Morphology and mechanical properties of polypropylene/organoclay nanocomposites. *Journal of Applied polymer science.* 2002;85(7):1562-1570.
315. Nourbakhsh A, Ashori A. Influence of nanoclay and coupling agent on the physical and mechanical properties of polypropylene/bagasse nanocomposite. *Journal of applied polymer science.* 2009;112(3):1386-1390.
316. Risite H, Oualid HA, Mabrouk KE. Effects of Vinyltriethoxysilane and Maleic Anhydride Grafted Polypropylenes on the Morphological, Thermal, Rheological, and Mechanical Properties of Polypropylene/Clay Nanocomposites. *Multidisciplinary Digital Publishing Institute Proceedings.* 2018;3(1):6.
317. Sombatsompop N, Yotinwattanakumtorn C, Thongpin C. Influence of type and concentration of maleic anhydride grafted polypropylene and impact modifiers on mechanical properties of PP/wood sawdust composites. *Journal of Applied Polymer Science.* 2005;97(2):475-484.
318. Yalcin B, Amos SE. Hollow glass microspheres in thermoplastics. *Hollow glass microspheres for plastics, elastomers, and adhesives compounds*: Elsevier; 2015: 35-105.
319. Amos SE, Yalcin B. *Hollow glass microspheres for plastics, elastomers, and adhesives compounds*: Elsevier; 2015.
320. Gupta G. *A Study on Using Glass Micro-Spheres in Erosion Resistant Coatings and Polymer Composites*; 2015.
321. Das PP, Chaudhary V, Ahmad F, Manral A. Effect of nanotoxicity and enhancement in performance of polymer composites using nanofillers: A state-of-the-art review. *Polymer Composites.* 2021;42(5):2152-2170.
322. Anirudh S, Jayalakshmi C, Anand A, Kandasubramanian B, Ismail SO. Epoxy/hollow glass microsphere syntactic foams for structural and functional application-A review. *European Polymer Journal.* 2022;171:111163.
323. Jung BN, Kang D, Cheon S, Shim JK, Hwang SW. The addition effect of hollow glass microsphere on the dispersion behavior and physical properties of polypropylene/clay nanocomposites. *Journal of Applied Polymer Science.* 2019;136(14):47476.
324. Yu M, Zhu P, Ma Y. Experimental study and numerical prediction of tensile strength properties and failure modes of hollow spheres filled syntactic foams. *Computational materials science.* 2012;63:232-243.
325. Boussès Y, Brulat-Bouchard N, Bouchard P-O, Tillier Y. A numerical, theoretical and experimental study of the effect of thermocycling on the matrix-filler interface of dental restorative materials. *Dental Materials.* 2021;37(5):772-782.
326. Liu H, Liu J, Kaboglu C, et al. Modelling the quasi-static flexural behaviour of composite sandwich structures with uniform-and graded-density foam cores. *Engineering Fracture Mechanics.* 2022;259:108121.
327. Safarabadi M, Haghighi-Yazdi M, Sorkhi M, Yousefi A. Experimental and numerical study of buckling behavior of foam-filled honeycomb core sandwich panels considering viscoelastic effects. *Journal of Sandwich Structures & Materials.* 2021;23(8):3985-4015.

328. Hössinger-Kalteis A, Reiter M, Jerabek M, Major Z. Overview and comparison of modelling methods for foams. *Journal of Cellular Plastics.* 2021;57(6):951-1001.
329. Kalaprasad G, Joseph K, Thomas S, Pavithran C. Theoretical modelling of tensile properties of short sisal fibre-reinforced low-density polyethylene composites. *Journal of materials science.* 1997;32:4261-4267.
330. Dong C, Davies IJ. Effect of stacking sequence on the flexural properties of carbon and glass fibre-reinforced hybrid composites. *Advanced Composites and Hybrid Materials.* 2018;1:530-540.